

Evolution of the Western Newfoundland Appalachian Orogen and its Foreland Basin

by

Shawna Elizabeth White

A thesis submitted in partial fulfillment of the requirements for the degree of

Doctor of Philosophy

Department of Earth and Atmospheric Sciences
University of Alberta

© Shawna Elizabeth White, 2018

Abstract

The northern Appalachian Orogen was built during multiple orogenic episodes resulting from Cambrian through Devonian accretion of microcontinents and/or crustal ribbons to the eastern margin of Laurentia. Orogenic loading formed a foreland basin on the Laurentian craton. Orogen-derived sediments were deposited into the basin on top of a Cambrian through Early Ordovician passive margin, formed prior to the closure of the Iapetus Ocean. This study combines geophysical interpretation, geologic mapping, and geochronology to study the geologic history of deformed Paleozoic rocks of Laurentian affinity and the Appalachian foreland basin in the western Newfoundland Appalachians.

Interpreted seismic reflection profiles and offshore aeromagnetic maps enable recognition of structure of the foreland basin, largely hidden beneath the Gulf of St. Lawrence. Isochron maps of the Middle Ordovician Goose Tickle Group demonstrate eastward thickening, suggesting loading by the Newfoundland segment of the orogen. A fast subsidence rate of ~ 0.17 km/Myr implies deposition in a pro-arc basin, formed on the eastward subducting Laurentian plate. Major fault-scarp units within the Goose Tickle Group indicate subsidence was controlled by large faults, in addition to distributed flexure resulting from orogenic loading and slab pull. Tectonic models indicate that subduction reversed polarity from east to west-dipping by the Late Ordovician, implying the Upper Ordovician Long Point Group was deposited in a retro-arc basin, on the upper plate. However, a fast subsidence rate of 0.17 km/Myr is consistent with deposition in a pro-arc basin. Isochron maps also demonstrate southward thickening of the Long Point Group, suggesting the basin was generated by loading from the Québec segment of the orogen. These observations indicate subduction polarity reversal was delayed in the Québec embayment, placing the Upper Ordovician basin in a hybrid retro/pro-arc setting. The hybrid setting, resulting from the irregular margin shape, is analogous to the modern plate boundary configuration along the northern Australian Plate. The record of Silurian activity is largely

removed in the foreland basin at the latest Silurian Clam Bank unconformity which likely records uplift and erosion associated with slab break-off of the west-dipping subducting slab during the trailing end of (~ 440 – 420 Ma) Salinian orogenesis. Early Devonian (~ 420 – 400 Ma) Acadian orogenesis resulted in deposition of the latest Silurian to Early Devonian Clam Bank-Red Island Road succession.

New mapping, aeromagnetic, and seismic interpretation at Parsons Pond allow recognition of structure in poorly exposed areas. The Humber Arm Allochthon contains a series of stacked and folded duplexes, typical of thrust belts. To the east, the Parsons Pond thrust transported basement, shelf and foreland-basin units westward above the allochthon. The Long Range thrust, farther east, shows less offset. Stratigraphic relationships indicate that basement-involved thrusts originated as normal faults, active during Neoproterozoic rifting and Taconian flexure. Devonian (Acadian) continental collision inverted the Parsons Pond and Long Range thrusts generating basement-cored fault-propagation folds, structurally analogous to uplifts of the Laramide Orogen in western USA. Similar deep-seated inversion structures may extend through the northern Appalachians, explaining enigmatic map patterns in New England.

U-Pb ages of detrital zircon within the foreland basin are consistent with derivation from Laurentian sources. The Goose Tickle Group has abundant Mesoproterozoic and Archean grains. Paleoproterozoic ages are predominantly 1.85 Ga, indicating derivation from units within the Humber Arm Allochthon, which contain abundant zircons at 1.85 Ga. An abundance of Mesoproterozoic grains and conspicuous lack of 1.85 Ga zircons in the Long Point Group indicates a major provenance shift, whereby sediments were not derived from the Humber Arm Allochthon. Probability density plots of continental margin units in the Québec/New England segment of the orogen demonstrate a similar strong Mesoproterozoic and weak Paleoproterozoic signature, suggesting derivation of the Long Point Group from the Québec segment of the orogen. Similar provenance shifts in other foreland basins, formed at promontory to embayment

transitions, may indicate a similar delay in subduction polarity reversal at the embayment. The absence of 2.0 – 2.2 Ga and 550 – 650 Ma Gondwanan zircons, and abundant 1.0 Ga grains within the Clam Bank-Red Island Road succession, is consistent with underthrusting of Ganderia and Avalonia during Salinian and Acadian orogenesis. Only Mesoproterozoic zircons were found in the Early Devonian Red Island Road Formation, consistent with derivation from Mesoproterozoic Grenville massifs uplifted during Devonian Acadian inversion.

Preface

This thesis is the original work of Shawna White, carried out under the supervision of Dr. John Waldron. All field work, data interpretation, figure construction and original manuscript writing was carried out by White.

A version of Chapter 2 is to be submitted to the Geological Society of America Bulletin under the authorship White, Shawna E; Waldron, John WF; Harris, Nicholas. White was responsible for all interpretation and data compilations as well as manuscript composition. Waldron contributed to manuscript edits. Harris reviewed the final manuscript. Chapter 3 has been submitted and is in revision with the Geological Society of London, Special Publications, vol. 470. Tectonic Evolution: 50 Years of the Wilson Cycle Concept. Authorship of paper is White, Shawna E and Waldron, John WF. White carried out all field work, geophysical interpretation, and writing of original manuscript. Waldron contributed to editing original manuscript. Both authors contributed to revisions before resubmission to the journal. A version of Chapter 4 will be submitted to the American Journal of Science under the authorship White, Shawna E; Waldron, John WF; Dunning, Greg R; DuFrane, Andrew S. White carried out field work, sample collection, mount making, laser operation and writing of original manuscript. Waldron contributed to editing the manuscript. DuFrane carried out initial set-up and calibration of the laser ablation inductively coupled plasma mass spectrometer (LA-ICP-MS). Dunning carried out U/Pb analyses of zircons from a rhyolite boulder using thermal ionization mass spectrometry (TIMS). The final chapter, Chapter 5, will be submitted to a special issue of Tectonics in honour of the career of C. van Staal under the authorship White, Shawna E and Waldron, John WF. The original manuscript was written by White; Waldron contributed by editing.

Acknowledgments

First and foremost, I'd like to thank my supervisor Dr. John Waldron. As a supervisor he has always gone above and beyond. Not only did he provide me with funding, a fantastic project, guidance, and his time, but he has always treated me like a colleague. I could not have gotten through this process with the confidence I have without his support.

I'd like to acknowledge the support of the Petroleum Exploration Enhancement Program, a joint initiative of both the Newfoundland and Labrador Provincial Government and Nalcor Energy, which provided funding for this research. I thank Ian Atkinson at Nalcor and Wes Foote at the Newfoundland Department of Natural Resources for their support. I also thank Henry Williams for graptolite identification and photos. I acknowledge John and Doug Mahar of Leprechaun resources for access to seismic data. I'd also like to acknowledge Lori Cook, Larry Hicks and Karen Waterman, from the Newfoundland and Labrador Department of Natural Resources, for field visits and important discussions regarding the project and data.

I'd also like to thank members of my committee, faculty, and staff in the department who have been an integral part of my degree. I'd like to thank Dr. Tom Chacko, who has always been one of the graduate students' biggest supporters.

I'd also like to express my sincere gratitude to the people of western Newfoundland. To Jenny and Peter, thank you for your hospitality, kindness, and raspberry pie which made the wet cold days seem sunny. Thanks to Earl Keough for always getting us there, offering your house, and the wonderful stories.

I'd like to acknowledge the amazing field assistants I've had throughout the years. Thank you to Tiffany Miller for sunny personality and ability to work through anything, Nicole Roberts for her meticulous organizational skills (which I lacked at time!), and Ryan Lacombe for saving me from drowning in a bog (and for your terrible yet uplifting puns).

To my best bud Diana White, you are the best. To all the friends that have made me feel like I've always had family in Edmonton. I'd like to thank Faye Wyatt, Janina Czas, Merilie Reynolds, Morgan Snyder, Hilary Corlett, Jody Reimer, Kurt Borth, Michelle Speta, Dave Dockman, Wafa Veljee Margo Regier and Lauren Eggleston. You've all made Edmonton my home, gave me amazing memories and helped me get through the "dark days" of my PhD. I'll never forget your awesomeness

Finally, I'd like to thank my parents, Marilyn and Noel White. No matter what I chose to do with my life you have always been behind me. I know now just how important that was.

Table of Contents

Chapter 1: Introduction	1
1.1. Appalachian Orogen	1
1.1.1. Appalachian Subdivisions	1
1.1.2. The Foreland Basin	3
1.1.3. Appalachian Events	6
1.2. Thesis Objectives	7
1.3. Methods	7
1.3.1. Field Work and Mapping	7
1.3.2. Geophysics	8
1.3.3. Detrital Zircon Geochronology	10
1.4. Roadmap of Thesis and Main Objectives	10
1.4.1. Chapter 2	10
1.4.2. Chapter 3	11
1.4.3. Chapter 4	11
1.4.4. Chapter 5	11
1.4.5. Chapter 6	12
1.4.6. Conventions and Nomenclature	12
1.5. References	12
Chapter 2: Anticosti Foreland Basin Offshore of Western Newfoundland: Concealed Record of Northern Appalachian Orogen Development	16
2.1. Introduction	17
2.2. Geologic Setting and Tectonics	17
2.2.1. Taconian Collision of Peri-Laurentian Fragments	19
2.2.2. Laurentian-Gondwanan Suture	20
2.2.3. Salinian Arrival of Ganderia	21
2.2.4. Acadian Orogenesis	21
2.2.5. Neo-Acadian Arrival of Meguma Terrane and Opening of Maritimes Basin	21
2.3. Regional Geology	22
2.3.1. The St. Lawrence Platform and Basement	22
2.3.2. Foreland Basin Successions	22
2.3.3. Deformation Front	27

2.4.	Data Sources	27
2.4.1.	2D Seismic Reflection Data	28
2.4.2.	Airborne Magnetic Data	28
2.5.	Methods	30
2.6.	Observations and Interpretation of Aeromagnetic Data	30
2.7.	Seismic Characteristics	33
2.7.1.	Seismic Horizons and Events	33
2.7.2.	Seismic Reflection Packages	36
2.8.	Discussion	40
2.8.1.	Foreland Basin Types	40
2.8.2.	Dapingian to Early Darriwilian (470-465 Ma)	41
2.8.3.	Later Darriwilian Events (465-458 Ma)	41
2.8.4.	Sandbian to Katian (~458-445 Ma)	45
2.8.5.	Katian-Pridoli Events	47
2.8.6.	Lokhovian to Emsian	49
2.9.	Conclusions	50
2.10.	References	51
Chapter 3: Inversion of Taconian Extensional Structures during Palaeozoic Orogenesis in Eastern Newfoundland		61
3.1.	Introduction	61
3.2.	Regional Geological Setting	63
3.2.1.	Stratigraphy	63
3.2.2.	Tectonic and Structural History	66
3.3.	Methods and Data	68
3.3.1.	Geological Mapping	68
3.3.2.	Orientation Data	68
3.3.3.	Aeromagnetic Data	68
3.3.4.	Seismic Data	71
3.4.	Results	71
3.4.1.	Distribution of Units	71
3.4.2.	Mapped Faults and Folds	75
3.4.3.	Outcrop-scale Structures	75
3.4.4.	Aeromagnetic Interpretation	81

3.4.5.	Seismic Interpretation	84
3.5.	Discussion	85
3.5.1.	Structure in the Humber Arm Allochthon	85
3.5.2.	Structure in Autochthonous Platform	86
3.5.3.	Structure of the Parautochthonous Parsons Pond Thrust Sheet	86
3.5.4.	Fault History	90
3.5.5.	Regional Correlations	92
3.5.6.	Analogues in Other Orogens	93
3.5.7.	A Laramide-Type Orogen	94
3.6.	Conclusions	94
3.7.	References	95
Chapter 4: Provenance of the Newfoundland Appalachian Foreland Basins		102
4.1.	Introduction	102
4.2.	Tectonic Setting and Source Regions	103
4.2.1.	Laurentian Basement	103
4.2.2.	Rift and Passive Margin Units	105
4.2.3.	Ordovician Taconian Orogeny and Foreland Basin	111
4.2.4.	Late Ordovician Long Point Group	112
4.2.5.	Silurian to Early Devonian Clam Bank Formation	113
4.2.6.	Early Devonian Red Island Road Formation	113
4.3.	Sampled Units	114
4.3.1.	Lourdes Formation	114
4.3.2.	Winterhouse Formation	115
4.3.3.	Clam Bank Formation	115
4.3.4.	Red Island Road Formation	115
4.4.	U/Pb Geochronology of Detritus	117
4.4.1.	Sample Preparation	117
4.4.2.	Analysis	117
4.4.3.	Data Reduction	118
4.4.4.	Data Presentation	118
4.5.	TIMS analysis	119
4.5.1.	Sample Preparation and Analysis	119

4.6.	Results	122
4.6.1.	Lourdes Formation	122
4.6.2.	Winterhouse Formation	122
4.6.3.	Clam Bank Formation	123
4.6.4.	Red Island Road Formation	123
4.6.5.	K-S Test	123
4.7.	Discussion	124
4.8.	Conclusions	127
4.9.	References	128
Chapter 5: Along-Strike Variations in Foreland Provenance and Orogenesis in the Northern Appalachians: Inherited Geometry of Rifted Margins and Arcs		134
5.1.	Introduction	135
5.1.1.	Objectives of this paper	135
5.1.2.	Previous syntheses of the margin	135
5.2.	Cambrian to Early Ordovician Evolution of the Laurentian Margin in Newfoundland	136
5.2.1.	Laurentian Basement	138
5.2.2.	Rift-Related Rocks	140
5.2.3.	Passive Margin	149
5.3.	Ordovician Orogenic Record along Eastern Laurentian Margin	150
5.3.1.	Foreland Basins Successions in Western Newfoundland	150
5.3.2.	Foreland Basin Successions in Québec and New England	152
5.4.	Later Paleozoic Orogenic Record	155
5.4.1.	Newfoundland	155
5.4.2.	Québec and New England	157
5.5.	Discussion: History of the Laurentian margin	157
5.5.1.	Rifted Margin of Laurentia	157
5.5.2.	Provenance of Eastern Laurentian Continental Margin in Newfoundland	159
5.5.3.	Taconian Arc-Continent Collision along the Margin	163
5.5.4.	Subduction Polarity Reversal	169
5.5.5.	Salinian Accretion of Ganderia	171
5.5.6.	Acadian Collision of Avalonia	172

5.5.7.	Diachronism in Collisions	176
5.6.	Conclusions	178
5.7.	References	180
Chapter 6: Conclusions		191
6.1.	Chapter 2	191
6.2.	Chapter 3	191
6.3.	Chapter 4	192
6.4.	Chapter 5	193
6.5.	Future Work	194
6.6.	References	194
Bibliography		196
Appendix: Detrital zircon U-Pb geochronology data		217

List of Figures

Figure 1.1: Map of present day tectonostratigraphic realms in the northern Appalachians.....	2
Figure 1.2: Geologic map of western Newfoundland showing important zones, realms, and study locations.....	4
Figure 1.3: Schematic cross-section of retro-arc and pro-arc basins.....	5
Figure 2.1: Map of present day tectonostratigraphic realms in the Northern Appalachians.	18
Figure 2.2: Regional stratigraphic column for the Anticosti Basin including Anticosti Island and the Mingan Islands, western Newfoundland and Québec.	23
Figure 2.3: Map of second vertical derivative of the residual magnetic field (modified from Dumont & Jones 2013) and interpreted geologic boundaries.	26
Figure 2.4: Interpreted dip-direction seismic profiles displaying the geometry of seismic reflections offshore western Newfoundland.	31
Figure 2.5: (a) Google Earth satellite imagery and bathymetry data offshore Long Point, Port au Port Peninsula. (b) Interpreted geologic boundaries offshore and onshore.	32
Figure 2.6: Interpreted strike-direction seismic profiles displaying the geometry of seismic reflections offshore western Newfoundland.	34
Figure 2.7: TWT (ms) maps of seismic horizons.	35
Figure 2.8: TWT (ms) isochron maps.....	38
Figure 2.9: Tectonic configuration of Laurentian and Gondwanan components in the northern Appalachians and associated foreland basin development.....	42
Figure 2.10: (a) Plate boundary configuration of the eastern Laurentian margin in the Lpper Ordovician. (b) Mirror image of Australia demonstrating the present day plate boundary configuration along the Timor and New Guinea trench.....	48
Figure 3.1: (a) Geological map of western Newfoundland showing major locations, tectonic units and Acadian thrust faults. (b) Map of northern Appalachians showing locations of major inversion related basement structures in Newfoundland and interpreted analogs to the south. ...	62
Figure 3.2: (a) Stratigraphic column of western Newfoundland. (b) Structural relationships of units (onshore and offshore) in the Parsons Pond region of western Newfoundland.	64
Figure 3.3: Geological map of the Parsons Pond area.	69
Figure 3.4: Map of the second vertical derivative of the residual magnetic field in the Parsons Pond map area.	70

Figure 3.5: (a) Seismic profile 96069 (position shown on Figure 3.4) (b) Interpreted geological cross-section. (c) Restored section.	72
Figure 3.6: (a) Seismic profile 92067 (position shown on Figure 3.4). (b) Interpreted geological cross-section. (c) Restored section.	73
Figure 3.7: (a) Geological cross-section along line C-C' on Figure 3.3. (b) Restored section C- C' prior to Acadian thrusting.	76
Figure 3.8: (a) Geological cross-section along line D-D' on Figure 3.3. (b) Restored section D-D' prior to Acadian thrusting.	77
Figure 3.9: (a) Geological cross-section along line E-E' on Figure 3.3. (b) Restored section E-E' prior to Acadian thrusting.	78
Figure 3.10: Field and sample photographs from the Parsons Pond map area.	80
Figure 3.11: Equal-area projections of structures in the Humber Arm Allochthon.	82
Figure 3.12: Equal-area projections of poles to bedding in the Parsons Pond thrust sheet.	83
Figure 3.13: (a) Isochron map of the top of platform in the footwall of the Parsons Pond Thrust (Location shown on Figure 3.1). (b) Rose plot of fault strikes in the autochthonous platform offshore and onshore. Bin size is 15° and number of measurements is 77.	87
Figure 3.14: Summary of faulting history of Parsons Pond area.	91
Figure 4.1: Geological map of western Newfoundland showing important place names.	104
Figure 4.2: Map showing major structural provinces which make up eastern Laurentia.	106
Figure 4.3: Detrital zircon probability density functions for data from this study and previously published data.	107
Figure 4.4: Stratigraphic column of western Newfoundland including autochthonous and allochthonous successions.	110
Figure 4.5: Photomicrographs of sampled foreland basin units.	116
Figure 4.6: U-Pb concordia plots for detrital zircon data.	120
Figure 4.7: Detrital zircon cumulative density plots.	121
Figure 5.1: Map of present day tectonostratigraphic realms in the Northern Appalachians. ...	137
Figure 5.2: Map of eastern Laurentia after Neoproterozoic and Cambrian rifting episodes. ...	139
Figure 5.3: Stratigraphic columns of western Newfoundland, Quebec and New England autochthonous and allochthonous passive margin and foreland successions.	141
Figure 5.4: Detrital zircon probability density functions for data from this study and previously	

published data.143

Figure 5.5: Geologic map of western Newfoundland.147

Figure 5.6: Detrital zircon probability density functions for units along the eastern Laurentian margin in Quebec and New England.161

Figure 5.7: Schematic diagram demonstrating how inherited shape of rifted margin and arc cause diachronous collision along a cratons margin at various times174

Chapter 1: Introduction

The Appalachian Orogen is an extensive belt of Mesoproterozoic to Paleozoic rocks which extends along the eastern Laurentian margin of North America from Alabama to its most northern portion in Newfoundland. The orogen was built during multiple orogenic events which involved various phases of ocean closure associated with the accretion of microcontinents and/or crustal ribbons to the eastern margin of Laurentia. In the northern Appalachians (Figure 1.1) these continental fragments include the Dashwoods block of peri-Laurentian origin, together with Ganderia, Avalonia and the Meguma Terrane, all of peri-Gondwanan origin (van Staal et al. 1998, 2007, Waldron & van Staal 2001, Hibbard et al. 2006).

This study is based in western Newfoundland and is focused on the deformed Paleozoic rocks of Laurentian affinity and the adjacent Appalachian foreland basin (Figure 1.1). Although extensive work has been carried out in western Newfoundland (Williams & Stevens 1974, Williams & Hatcher 1983, Waldron 1985, Cawood & Williams 1987, Williams & Cawood 1989, Cawood 1993, Waldron et al. 1993, Stockmal et al. 1998) many of the maps (Cawood & Williams 1987, Williams & Cawood 1989) and interpretations of the offshore geology (Stockmal & Waldron 1990, Stockmal et al. 1998) are outdated. The foreland basin in western Newfoundland, largely underlying the Gulf of St. Lawrence, is also relatively unexplored and little work has been done regarding the structural history of the basin. This thesis combines detailed field-based mapping, geophysical interpretation, and geochronology to provide a model of foreland basin evolution which explains aspects of Appalachian orogenesis which are currently not well understood or remain unexplained by current tectonic models such as the relationship of deformation to the kinematics of subduction, variations in the timing of foreland basin development along the length of the orogen, and the distribution of basement massifs which are major contributors to the topography of western Newfoundland.

1.1. Appalachian Orogen

1.1.1. Appalachian Subdivisions

The northern Appalachian Orogen has been divided into tectonostratigraphic zones (Williams & Hatcher 1983), and more recently realms (Hibbard et al. 2006), based on the nature of basement crust (either belonging to Laurentia or Gondwana) and the pre-Silurian geologic history of the zones or realms.

The most westerly region within the northern Appalachians, comprising deformed rocks of Paleozoic Laurentian affinity, has been termed the Laurentian realm (Hibbard et al. 2006) and includes the Humber Zone of (Williams & Hatcher 1983) (Figure 1.1). This thesis focuses

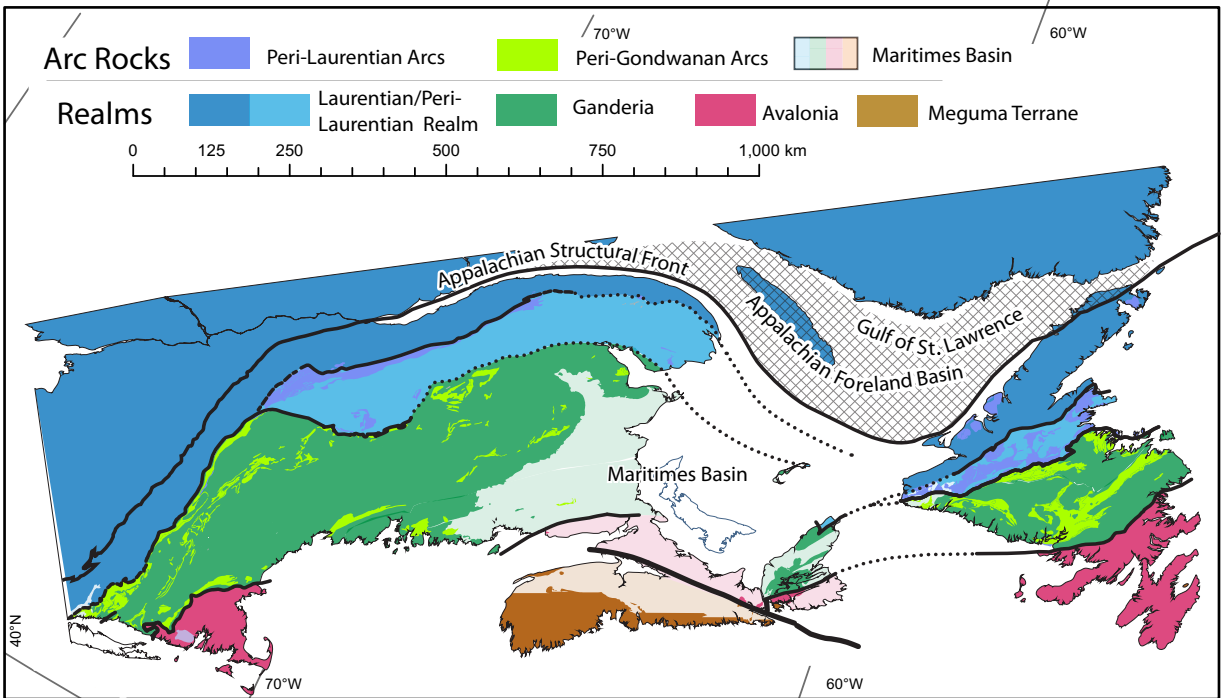


Figure 1.1: Map of present day tectonostratigraphic realms in the Northern Appalachians (after Hibbard et al. 2006).

on the Laurentian realm of western Newfoundland (Figure 1.2). In western Newfoundland, the oldest rocks are Mesoproterozoic basement units exposed in the Long Range inlier (Heaman et al. 2002). Unconformably overlying the basement is a predominantly carbonate rift-to-drift succession formed on the western margin of the Iapetus Ocean during the Cambrian through Early Ordovician. The Humber Arm Allochthon, containing deep-water equivalents of the rift-drift succession, lies structurally above the carbonate shelf as a result of Middle Ordovician west-directed transport. The youngest rocks in the Humber zone (or Laurentian realm) are Middle Ordovician to Early Devonian foreland basin units (Figure 1.2).

East of the Humber zone are the Notre Dame and Dashwoods subzones (Figure 1.2), more recently referred to as the peri-Laurentian realm (Hibbard et al. 2006) of the Appalachians. This realm contains metasediments which are correlated with the rift-drift succession in the Laurentian realm and intruded by Cambrian through Early Ordovician arc rocks. East of the peri-Laurentian realm are arc-related rocks of the peri-Gondwanan realm. The boundary between the two is an important boundary in Newfoundland, termed the Red Indian Line, marking the juxtaposition of Laurentian and Gondwanan realms (Figure 1.1). Farther east are terranes of exotic, Gondwanan affinity that include Ganderia and Avalonia in Newfoundland. The most easterly exotic terrane in the northern Appalachians is the Meguma Terrane, which is exposed in Nova Scotia (Figure 1.1).

1.1.2. The Foreland Basin

Foreland basins, elongate troughs of sediment formed on continental crust between an orogenic belt and adjacent craton (DeCelles & Giles 1996), are largely formed as a result of orogenic loading. Sediments that fill the developing basin are predominantly derived from the advancing orogen. Due to this intrinsic link between basin and orogen (Ettensohn & Brett 2002, Ettensohn 2005), foreland basins provide one of the best records of tectonic events associated with orogenesis.

The geometry and subsidence history of foreland basins are largely controlled by the position of the orogenic load in the orogen and position of the developing basin. Basins atop the subducting plate are described as pro-arc basins whereas basins on the overriding lithospheric plate are retro-arc basins (Figure 1.3). In a pro-arc basin, lithospheric flexure and associated subsidence are largely controlled by the tectonic load of the orogen (Beaumont, 1981; Jordan, 1981) and subsidence rates are high (> 0.05 km/Myr) (Sinclair & Naylor 2012). In retro-arc settings dynamic effects, related to both subduction-induced corner flows and gravitational pull of the down-going slab (Catuneanu 2004), modify flexure due to orogenic loading (Catuneanu 2004) and subsidence rates are generally much slower, typically < 0.05 km/Myr (Sinclair & Naylor 2012).

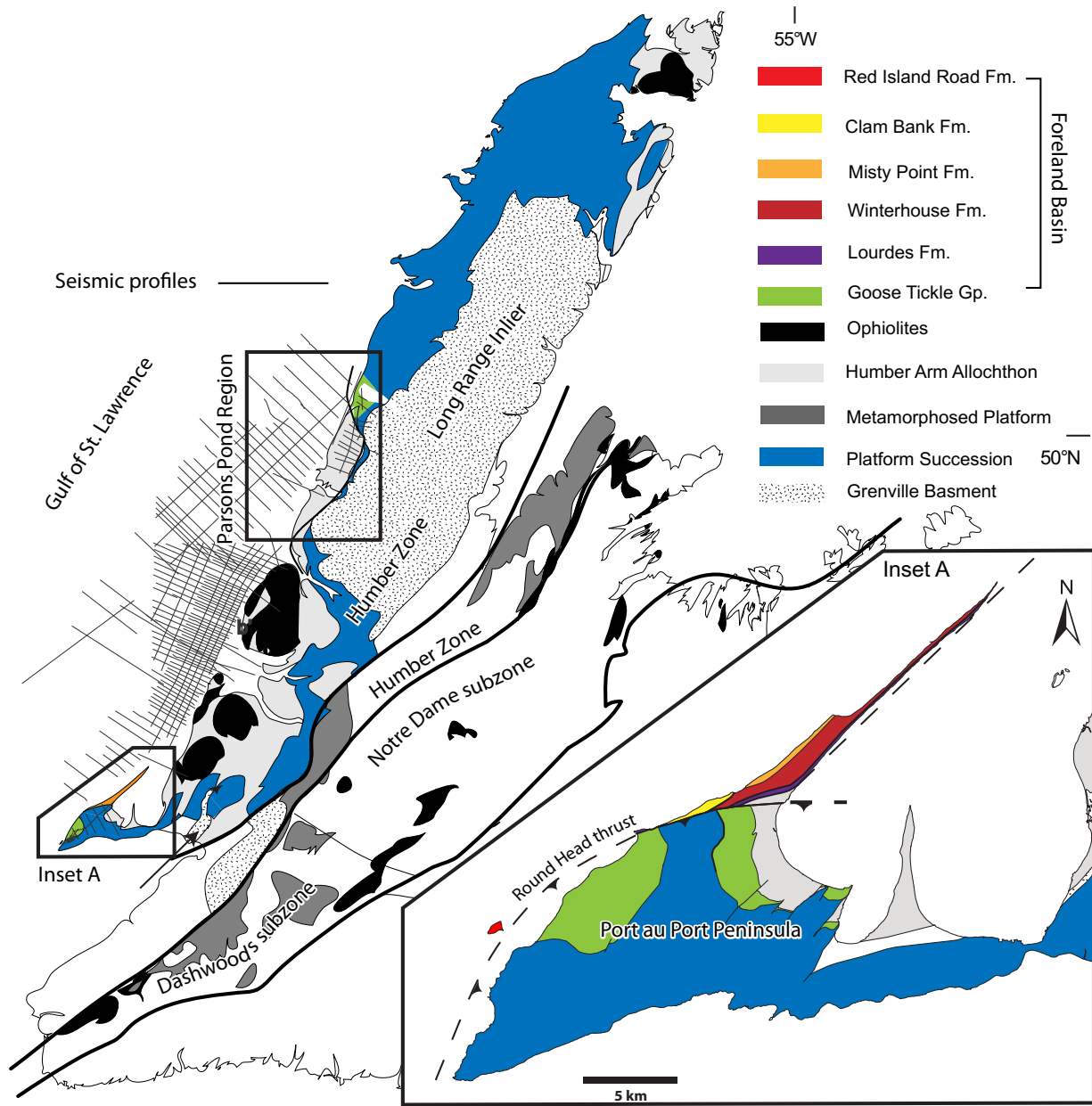


Figure 1.2: Geologic map of western Newfoundland showing important zones, realms, and study locations (modified from Waldron & van Staal 2001).

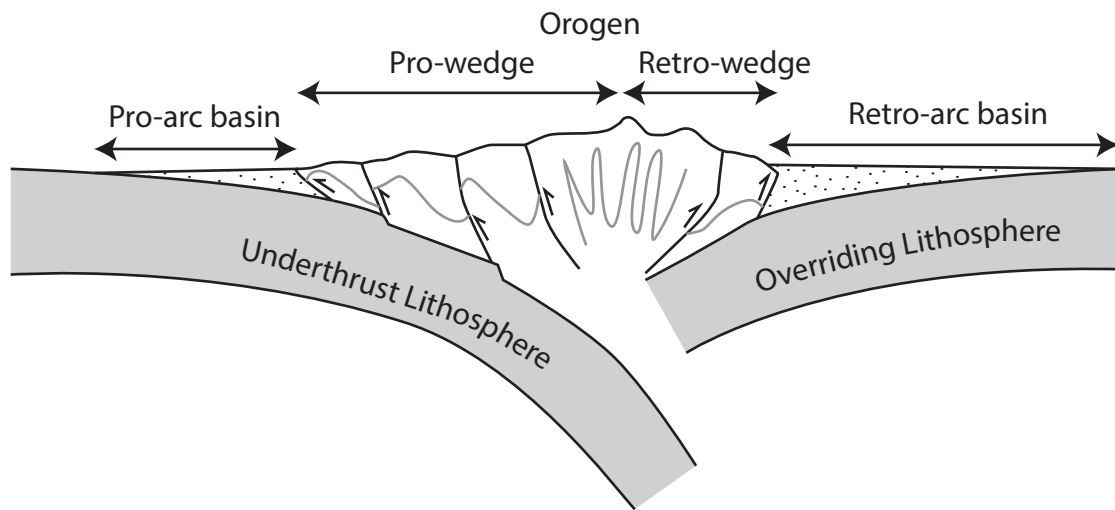


Figure 1.3: Schematic cross-section demonstrating the position (on the overriding or underthrusting lithospheric plate) in which a retro-arc and pro-arc basin develop between a developing orogen and stable craton (modified from Sinclair & Naylor 2012).

The Appalachian foreland basin, largely hidden beneath the Gulf of St. Lawrence, lies west of the Humber zone (Figure 1.1). A Middle Ordovician to Early Devonian foreland basin succession, overlying Cambrian through Early Ordovician carbonate shelf units, was deposited during multiple episodes of uplift and erosion associated with orogenesis. The oldest siliciclastic flysch units of the Middle Ordovician Goose Tickle Group (Quinn 1992) have been incorporated into thrust sheets of the orogen and are exposed along the length of the Laurentian realm in Newfoundland (Figure 1.1). Younger, Upper Ordovician to Devonian foreland successions are only exposed in a small region on the Port au Port Peninsula in western Newfoundland (Quinn et al. 1999, 2004) (Figure 1.2).

1.1.3. Appalachian Events

In Newfoundland, three main orogenic episodes are traditionally recognized: an Early to Middle Ordovician Taconian episode (Williams & Stevens 1974, St. Julien & Hubert 1975), a Silurian Salinian episode (Dunning et al. 1990, Cawood et al. 1994) and an Early Devonian Acadian episode (Cawood & Williams 1988, Cawood 1993, Williams 1993).

In Newfoundland, the Taconian Orogeny involved the emplacement of the thin-skinned Humber Arm Allochthon (Williams 1975, Stanley & Ratcliffe 1985), comprising structural stacks of slope/rise rocks, mélangé, and ophiolitic rocks (Williams 1975, Williams & Hatcher 1983) and collision of the peri-Laurentian Dashwoods microcontinent (Waldron & van Staal 2001, van Staal et al. 2009) onto Laurentia's eastern margin (Williams & Stevens 1974, Williams 1975, Williams & Hatcher 1983, Waldron 1985, Bosworth 1989) above an east-dipping subduction zone (Jacobi, 1981).

A distinct Silurian (440-422 Ma) orogenic episode, involving magmatism, metamorphism, and deformation, is recognized in central Newfoundland as the Salinian Orogeny (Dunning et al. 1990, Cawood et al. 1994, van Staal et al. 2009). This orogenic episode has been attributed to westward subduction of an Iapetan seaway and collision of a Ganderian microcontinent with Laurentia (van Staal et al. 2009).

The Acadian Orogeny (423-400 Ma) is conventionally attributed to the accretion of Avalonia to Laurentia (Bird & Dewey 1970, Bradley 1983, van Staal et al. 2009), involving the westward subduction of Avalonia beneath the Laurentian margin (Waldron et al. 1996, Murphy et al. 1999). Timing of related magmatism (423-416 Ma) and subduction-related metamorphism (420 – 416 Ma) demonstrate that the Acadian Orogeny began shortly after or during the waning stages of the Salinian Orogeny (van Staal et al. 2009). This orogenic episode involved the generation of deep-seated thrust faults (Cawood & Williams 1988) which cross-cut earlier-formed thin-skinned structures formed during the Taconian Orogeny, including the Humber Arm Allochthon.

A prolonged record of Late Devonian to Pennsylvanian dextral transtension and transpression is observed in the northern Appalachians (van Staal et al. 2009, Hibbard et al. 2010, Waldron et al. 2015). Late Devonian transtension led to dextral motion along major northeast-directed faults which initiated the opening of the Maritimes Basin (Figure 1.1) which currently overlies older terranes that were accreted to the Laurentian margin during earlier orogenesis (Waldron et al. 2015). Continued Appalachian-trend strike-slip faulting led to Mississippian to Pennsylvanian juxtaposition of the Meguma Terrane in approximately its present position with respect to Avalonia (Figure 1.1).

1.2. Thesis Objectives

This thesis aims to answer the following questions relating to the Newfoundland Appalachians and their foreland basins.

- 1) What are the controls on subsidence and accommodation in the western Newfoundland foreland basin and how do they relate to the position and variability of loads in the northern Appalachian Orogen?
- 2) What was the provenance of the sedimentary successions which fill the foreland basin in western Newfoundland?
- 3) Were these basins pro-arc or retro-arc basins and when did transitions occur between these styles?
- 4) How did the opening and closing of the Iapetus Ocean lead to the reactivation of earlier basement structures during later continental collision?
- 5) Did similar processes occur in Québec and New England and what was their timing?
- 6) What are the major controls on the diachronous nature of collisions, subduction polarity reversal, and retro-arc basin development along the Laurentian margin?

The following sections describe the methods used to achieve the above objectives and the major components of the thesis.

1.3. Methods

1.3.1. Field Work and Mapping

Field work was carried out during four summers, from 2011 to 2014, during which time mapping and sample collection took place. The first two summers focused on mapping the Humber Arm Allochthon in the Parsons Pond region of western Newfoundland (Figure 1.2) and the collection of fault/fracture data and samples for detrital zircon geochronology

from the Port au Port Peninsula (Figure 1.2). Before mapping, type sections for the Humber Arm Allochthon units were visited. Traverses were planned and executed each day to cover the majority of the Humber Arm Allochthon in the Parsons Pond region (Figure 1.2). On the Port au Port Peninsula, faults, associated slickenlines, and fractures in the vicinity of the Round Head thrust were measured and cross-cutting relationships documented. Lithologic and structural data were collected in regions where foreland basin units were exposed. Samples for detrital zircon geochronology were collected from coarse-grained clastic units at locations where depositional age was well constrained.

The last two summers involved detailed back country mapping of a deep-seated basement-involved thrust sheet near the Long Range Mountains. Multiple five-day traverses were planned well in advance to cover all logistics. All collected field data were compiled into an ArcGIS database.

1.3.2. Geophysics

1.3.2.1. Aeromagnetic Interpretation

When a magnetic material is placed in a magnetic field the material becomes magnetized and induces its own magnetic field, reinforcing the external field into which it was placed. This process is known as induced magnetisation. If this external field is shut off, the induced magnetisation will cease; however, some materials will retain a permanent magnetisation in the direction of the external field that was removed. This is known as remanent magnetisation. Minerals within rocks are affected by the Earth's magnetic field and can exhibit induced and/or remanent magnetization. The induced and remanent magnetisation (the latter being a function of magnetite content) of the rocks in the crust adds to, or offsets, the magnetic dipole field of the Earth, producing magnetic anomalies. Aeromagnetic surveys take advantage of this physical process and produce magnetic anomaly maps which are a useful aid in geologic mapping as it can give subsurface information for regions which have poor outcrop exposure.

Offshore and onshore (Parsons Pond region, figure 1.2) aeromagnetic maps were available through the Department of Natural Resources, Government of Newfoundland and Labrador. We imported these maps into the ArcGIS database with our field data and interpreted geologic maps. In our interpretations we used the second vertical derivative of the residual magnetic field because it emphasizes the effects of the near-surface magnetic sources and gives a better resolution of closely-spaced features.

Magnetic anomalies of the onshore aeromagnetic data were correlated with mapped geology in the ArcGIS database. Orogen derived siliciclastic units produced strong magnetic

anomalies while carbonate units produced relatively weak anomalies. Using the correlation of anomalies to known geology, geologic units and boundaries were extended into regions covered by bogs, brush, and vegetation.

A pair of offshore magnetic anomalies, the Odd-Twins magnetic anomaly (Ruffman & Woodside 1970), has been interpreted to parallel stratigraphy by (Waldron et al. 2002). (Waldron et al. 2002) traced the offshore anomalies onshore and demonstrated that they were generated by detrital magnetite within stratigraphic horizons of the foreland basin succession. These anomalies also parallel stratigraphy close to the coast, visible using Google Earth imagery. In order to interpret their geologic significance, we traced the anomalies along strike to where they intersect the shoreline and matched them with mapped geologic units.

1.3.2.2. Seismic Interpretation

Both offshore and onshore 2D seismic reflection data were provided by Leprechaun Resources and Black Spruce Corp. 2D seismic data image the subsurface in a discrete vertical plane whereas 3D data are obtained from continuous volumes in the subsurface. The dataset consisted of several thousand kilometres of 2D seismic reflection data spanning an area of over 13 000 km² (Figure 1.2). These data were imported into Petrel™ seismic interpretation software, along with geologic maps and interpreted aeromagnetic maps from this study, to create a database for 3D interpretation.

Seismic reflections are generated when a seismic (or acoustic) wave, propagating through the subsurface, meets a boundary between two units with contrasting velocities and densities. Some of the seismic energy is refracted, while some is reflected off the boundary and returned to the surface receiver and recorded. Six major seismic reflections were picked in this study based on their relative amplitude and continuity. Only horizons which showed strong impedance contrasts and were laterally extensive were chosen. These horizons were picked across the entire survey using crossing seismic profiles. Time-structure and isochron thickness maps were generated in Petrel™.

In order to give seismic reflections any geologic significance they need to be tied to geologic boundaries. This is best done by using well ties but no wells were drilled in the offshore region; therefore, we traced seismic reflections to where they intersected the seafloor/offshore aeromagnetic map (where anomalies were determined to parallel stratigraphy). Then, we followed each anomaly along strike to outcropping geology onshore on the Port au Peninsula (Figure 1.2). Details of this methodology are provided in Chapter 2.

1.3.3. Detrital Zircon Geochronology

Since zircon is highly refractory at the surface of the Earth it occurs in virtually all siliciclastic deposits, and the presence of U, and therefore of radiogenic Pb, in zircon allows dating using U-Pb geochronology. The existence of two independent U-Pb decay systems, ^{238}U to ^{206}Pb and ^{235}U to ^{207}Pb , allows two independent estimates of age. Recent advancements in U-Pb dating techniques, using inductively coupled plasma mass spectrometry (ICP-MS), have allowed relatively inexpensive and fast acquisition of large quantities of data for statistical analysis. The above features have made detrital zircon geochronology one of the best methods for determining basin sediment provenance.

Detrital zircon samples were sent to Dalhousie University for crushing and mineral separation. Zircons were picked from the heavy mineral separates. Mounts were prepared using the facilities at the University of Alberta. Before analyzing, zircons were imaged using the scanning electron microscope in the Canadian Center for Isotope Microanalysis (CCIM) facility at the University of Alberta. U-Pb analyses (of at least 100 zircons for each sample) were carried out in the ICP-MS facility at the University of Alberta, using the Nu Plasma U-Pb laser ablation multicollector inductively coupled plasma mass spectrometer (LA-MC-ICP-MS). Data were later reduced using the software Excel. Concordia and probability density functions were generated in Isoplot (Ludwig 2012). A rhyolite boulder from the youngest foreland succession was sent to Memorial University for U-Pb dating of zircon using thermal ionization mass spectrometry (TIMS).

1.4. Roadmap of Thesis and Main Objectives

1.4.1. Chapter 2

Chapter 2 is a detailed study of the foreland basin successions in western Newfoundland. The foreland basin is largely submerged beneath the Gulf of St. Lawrence; therefore, the majority of this work depended on interpretation of geophysical information, including 2D seismic reflection profiles and offshore aeromagnetic data. Using these interpretations, we generated a model of basin evolution which recorded events in the orogen's history which were previously not defined. This chapter is to be submitted to the Geological Society of America Bulletin under the authorship White, Shawna E; Waldron, John WF; Harris, Nick. White was responsible for all interpretation and data compilations as well as manuscript composition. Waldron contributed to manuscript edits. Harris reviewed final manuscript before thesis submission making recommendations to aid in accessibility of ideas to a broader audience.

1.4.2. Chapter 3

Chapter 3 documents the protracted history of motion along deep-seated faults in western Newfoundland. Detailed mapping and seismic interpretation allowed interpretations regarding generation, reactivation, and inversion of basement-involved structures during multiple orogenic episodes. This paper was resubmitted to the Geological Society of London, Special Publications, vol. 470. Tectonic Evolution: 50 Years of the Wilson Cycle Concept. Authorship of paper is White, Shawna E; Waldron, John WF. White carried out all field work and seismic interpretation and writing of original manuscript. Waldron contributed to editing original manuscript. Both authors contributed to revisions before resubmission to the Journal.

1.4.3. Chapter 4

Chapter 4 is a provenance study of the western Newfoundland foreland basin successions using detrital zircon geochronology. Four samples from four foreland basin successions were analysed and compared with previously published results of analyses from earlier continental margin units now exposed in the adjacent orogen. Results allowed for the identification of major shifts in provenance which correlated with important periods of uplift and erosion within the orogen. This paper will be submitted to the American Journal of Science under the authorship White, Shawna E; Waldron, John WF; Dunning, Greg R; DuFrane, S. Andrew. White carried out field work, sample collection, mount making, laser operation and writing of original manuscript. Waldron contributed to editing the manuscript. DuFrane did initial set-up and calibration of LA-ICP-MS and guided the analytical process. Dunning carried out U-Pb analyses of zircons from rhyolite boulder using TIMS.

1.4.4. Chapter 5

Chapter 5 is a detailed study on the Neoproterozoic through Paleozoic evolution of the eastern margin of Laurentia, based on new data and interpretations from this thesis and previously published work. In this chapter we provide new interpretations regarding initial structure of the margin following Iapetan ocean opening and explanations as to how the inherited irregular shapes of both the rifted Laurentian margin and arcs strongly control the timing of collisions along the northern Appalachian orogenic belt and lead to non-orthogonal collisions. This paper will be submitted to a special issue of Tectonics in honour of the career of C. van Staal under the authorship White, Shawna E; Waldron, John WF. The original manuscript was written by White; Waldron contributed later by editing.

1.4.5. Chapter 6

Chapter 6 outlines the main conclusions and outcomes of this thesis.

1.4.6. Conventions and Nomenclature

All chapters, with the exception of Chapter 3, use American spelling conventions. Chapter 3 uses British conventions as it will be published with the Geological Survey of London. We only capitalize series (e.g. lower, middle, and upper) which have been formally defined by the International Commission on Stratigraphy. For example, we would write “Upper” Ordovician. Because the Cambrian Period (Peng et al. 2012) contains series which are not formally defined we use lowercase letters to describe the lower and middle Cambrian.

1.5. References

- BEAUMONT C. 1981. Foreland basins. *Geophysical Journal International* 65: 291–329.
- BIRD J. M. & DEWEY J. F. 1970. Lithosphere plate-continental margin tectonics and the evolution of the Appalachian orogen. *Geological Society of America Bulletin* 81: 1031–1060.
- BOSWORTH W. 1989. Mélange fabrics in the unmetamorphosed external terranes of the northern Appalachians. In: *Melanges and Olistostromes of the U.S. Appalachians* (Ed. by J. W. Horton & N. Rast), pp. 65–92. Geological Society of America.
- BRADLEY D. C. 1983. Tectonics of the Acadian orogeny in New England and adjacent Canada. *The Journal of Geology* 91: 381–400.
- CATUNEANU O. 2004. Retroarc foreland systems-evolution through time. *Journal of African Earth Science* 38: 225–242.
- CAWOOD P. A. 1993. Acadian orogeny in west Newfoundland: Definition, character, and significance. *Geological Society of America Special Papers* 275: 135–152.
- CAWOOD P. A., DUNNING G. R., LUX D. & VAN GOOL J. A. M. 1994. Timing of peak metamorphism and deformation along the Appalachian margin of Laurentia in Newfoundland: Silurian, not Ordovician. *Geology* 22: 399–402.
- CAWOOD P. A. & WILLIAMS H. 1987. Geology of Portland Creek Area (12I/4) Western Newfoundland. Geologic Survey of Canada.
- CAWOOD P. A. & WILLIAMS H. 1988. Acadian basement thrusting, crustal delamination, and structural styles in and around the Humber Arm allochthon, western Newfoundland. *Geology* 16: 370.
- DECELLES P. G. & GILES K. A. 1996. Foreland basin systems. *Basin research* 8: 105–123.

- DUNNING G. R., O'BRIEN S. J., COLMAN-SADD S. P., BLACKWOOD R. F., DICKSON W. L., O'NEILL P. P. & KROGH T. E. 1990. Silurian Orogeny in the Newfoundland Appalachians. *The Journal of Geology* 98: 895–913.
- ETTENSOHN F. R. 2005. 5. The sedimentary record of foreland-basin, tectophase cycles: Examples from the Appalachian Basin, USA. In: *Developments in Sedimentology* pp. 139–172. Elsevier.
- ETTENSOHN F. R. & BRETT C. E. 2002. Stratigraphic evidence from the Appalachian basin for the continuation of the taconian orogeny into the Early Silurian time. *Physics and Chemistry of the Earth* 27: 279–288.
- HEAMAN L. M., ERDMER P. & OWEN J. V. 2002. U–Pb geochronologic constraints on the crustal evolution of the Long Range Inlier, Newfoundland. *Canadian Journal of Earth Sciences* 39: 845–865.
- HIBBARD J. P., VAN STAAL C. R. & RANKIN D. W. 2010. Comparative analysis of the geological evolution of the northern and southern Appalachian orogen: Late Ordovician-Permian. In: *From Rodinia to Pangea: The Lithotectonic Record of the Appalachian Region* (Ed. by R. P. Tollo, M. J. Bartholomew, J. P. Hibbard & P. M. Karabinos), pp. 51–69. Geological Society of America.
- HIBBARD J. P., VAN STAAL C. R., RANKIN D. W. & WILLIAMS H. 2006. Lithotectonic Map of the Appalachian Orogen, Canada- United States of America. Geological Survey of Canada.
- JACOBI R. D. 1981. Peripheral bulge—a causal mechanism for the Lower/Middle Ordovician unconformity along the western margin of the Northern Appalachians. *Earth and Planetary Science Letters* 51: 245–251.
- JORDAN T. E. 1981. Thrust loads and foreland basin evolution, Cretaceous, western United States. *AAPG bulletin* 65: 2506–2520.
- KNIGHT I., JAMES N. P. & LANE T. E. 1991. The Ordovician St. George Unconformity, northern Appalachians: The relationship of plate convergence at the St. Lawrence Promontory to the Sauk/Tippecanoe sequence boundary. *Geological Society of America Bulletin* 103: 1200–1225.
- LUDWIG K. R. 2012. User's manual for Isoplot 3.75. *Berkeley Geochronology Center Special Publication* 5: 75.
- MURPHY J. B., VAN STAAL C. R. & KEPPIE J. D. 1999. Middle to late Paleozoic Acadian orogeny in the northern Appalachians: A Laramide-style plume-modified orogeny?. *Geology* 27: 653–656.
- PENG S., BABCOCK L. E. & COOPER R. A. 2012. The Cambrian Period. In: *The Geologic Time Scale* (Ed. by F. M. Gradstein, J. G. Ogg, M. Schmitz & G. Ogg), pp. 437–488. Elsevier.

- QUINN L. A. 1992. Foreland and trench slope basin sandstones of the Goose Tickle group and Lower Head Formation, western Newfoundland. PhD Thesis, Memorial University of Newfoundland, St. John's Newfoundland.
- QUINN L., BASHFORTH A. R., BURDEN E. T., GILLESPIE H., SPRINGER R. K. & WILLIAMS S. H. 2004. The Red Island Road Formation: Early Devonian terrestrial fill in the Anticosti Foreland Basin, western Newfoundland. *Canadian Journal of Earth Sciences* 41: 587–602.
- QUINN L., WILLIAMS S. H., HARPER D. A. T. & CLARKSON E. N. K. 1999. Late Ordovician foreland basin fill: Long Point Group of onshore western Newfoundland. *Bulletin of Canadian Petroleum Geology* 47: 63–80.
- RUFFMAN A. & WOODSIDE J. 1970. The Odd-twins magnetic anomaly and its possible relationship to the Humber Arm Klippe of Western Newfoundland, Canada. *Canadian Journal of Earth Sciences* 7: 326–337.
- SINCLAIR H. D. & NAYLOR M. 2012. Foreland basin subsidence driven by topographic growth versus plate subduction. *Geological Society of America Bulletin* 124: 368–379.
- ST. JULIEN P. & HUBERT C. 1975. Evolution of the Taconic orogen in the Quebec Appalachians. *American Journal of Science* 275–A: 337–362.
- STANLEY R. S. & RATCLIFFE N. M. 1985. Tectonic synthesis of the Taconian orogeny in western New England. *Geological Society of America Bulletin* 96: 1227–1250.
- STOCKMAL G. S., SLINGSBY A. & WALDRON J. W. 1998. Deformation styles at the Appalachian structural front, western Newfoundland: implications of new industry seismic reflection data. *Canadian Journal of Earth Sciences* 35: 1288–1306.
- STOCKMAL G. S. & WALDRON J. W. F. 1990. Structure of the Appalachian deformation front in western Newfoundland: implications of multichannel seismic reflection data. *Geology* 18: 765–768.
- VAN STAAL C. R., WHALEN J. B., VALVERDE-VAQUERO P., ZAGOREVSKI A. & ROGERS N. 2009. Pre-Carboniferous, episodic accretion-related, orogenesis along the Laurentian margin of the northern Appalachians. In: *Ancient Orogens and Modern Analogues* (Ed. by J. B. Murphy, J. D. Keppie & A. J. Hynes), pp. 271–316. Geological Society, London, Special Publications.
- VAN STAAL C. R., WHALEN J. B., MCNICOLL V. J., PEHRSSON S., LISSEBERG C. J., ZAGOREVSKI A., VAN BREEMEN O. & JENNER G. A. 2007. The Notre Dame arc and the Taconic orogeny in Newfoundland. In: *4-D Framework of Continental Crust* (Ed. by R. D. Hatcher, M. P. Carlson, J. H. McBride & J. R. Martinez Catalan), pp. 511–552.
- VAN STAAL C. R., DEWEY J. F., NIOCAILL C. M. & MCKERROW W. S. 1998. The Cambrian-Silurian tectonic evolution of the northern Appalachians and British Caledonides: history

- of a complex, west and southwest Pacific-type segment of Iapetus. In: *Lyell, the Past is the Key to the Present* (Ed. by D. J. Blundell & A. C. Scott), pp. 197–242. Geological Society, London, Special Publications.
- WALDRON J. W. F. 1985. Structural history of continental margin sediments beneath the Bay of Islands Ophiolite, Newfoundland. *Canadian Journal of Earth Sciences* 22: 1618–1632.
- WALDRON J. W. F., BARR S. M., PARK A. F., WHITE C. E. & HIBBARD J. 2015. Late Paleozoic strike-slip faults in Maritime Canada and their role in the reconfiguration of the northern Appalachian orogen: STRIKE SLIP, NORTHERN APPALACHIANS. *Tectonics*: n/a-n/a.
- WALDRON J. W. F., DEWOLFE J., COURTNEY R. & FOX D. 2002. Origin of the Odd-twins anomaly: magnetic effect of a unique stratigraphic marker in the Appalachian foreland basin, Gulf of St. Lawrence. *Canadian Journal of Earth Sciences* 39: 1675–1687.
- WALDRON J. W. F., MURPHY J. B., MELCHIN M. J. & DAVIS G. 1996. Silurian tectonics of western Avalonia: strain-corrected subsidence history of the Arisaig Group, Nova Scotia. *The Journal of Geology*: 677–694.
- WALDRON J. W. F. & VAN STAAL C. R. 2001. Taconian orogeny and the accretion of the Dashwoods block: A peri-Laurentian microcontinent in the Iapetus Ocean. *Geology* 29: 811–814.
- WALDRON J. W. F., STOCKMAL G. S., CORNEY R. E. & STENZEL S. R. 1993. Basin development and inversion at the Appalachian structural front, Port au Port Peninsula, western Newfoundland Appalachians. *Canadian Journal of Earth Sciences* 30: 1759–1772.
- WILLIAMS H. 1975. Structural succession, nomenclature, and interpretation of transported rocks in western Newfoundland. *Canadian Journal of Earth Sciences* 12: 1874–1894.
- WILLIAMS H. 1993. Acadian orogeny in Newfoundland. *Geological Society of America Special Papers* 275: 123–134.
- WILLIAMS H. & CAWOOD P. A. 1989. Geology of Humber Arm Allochthon, Newfoundland. Geologic Survey of Canada, western Newfoundland.
- WILLIAMS H. & HATCHER R. D. 1983. Appalachian suspect terranes. In: *Geological Society of America Memoirs* pp. 33–53. Geological Society of America.
- WILLIAMS H. & STEVENS R. K. 1974. Taconic Orogeny and the development of the ancient continental margin of eastern North American in Newfoundland. *Journal of the Geological Association of Canada* 1: 31–33.

Chapter 2: Anticosti Foreland Basin Offshore of Western Newfoundland: Concealed Record of Northern Appalachian Orogen Development

The Anticosti Basin, largely hidden beneath the Gulf of St. Lawrence, includes foreland basin successions that record four distinct tectonic events associated with the Middle Ordovician to Early Devonian evolution of the northern Appalachian Orogen. Due to the lack of well ties and minimal onshore exposure, geophysical data must be used in mapping the offshore stratigraphy. By combining aeromagnetic and 2D seismic data, we create a 3D basin model for the Anticosti Basin offshore of western Newfoundland. The overall basin is divided into stratigraphic packages, which represent distinct episodes of foreland basin development, by tying outcropping geologic boundaries to magnetic lineaments that parallel offshore foreland basin stratigraphy. These lineaments are then correlated with reflections on seismic profiles in order to interpret the subsurface. Seismic isochron maps for each basin display differences in geometry, implying that orogenic loading varied through time in amount, distribution, and location. The geometry and subsidence rates of the first foreland basin succession, the Middle Ordovician Goose Tickle Group, imply that it formed in a pro-arc setting associated with loading from the Newfoundland portion of the Appalachians. Facies variations in this basin imply diachronous collision of arcs and Laurentian microcontinents during the Taconian Orogeny. The geometry and subsidence rate of the overlying Long Point Group suggest that loading of the Laurentian margin by Taconian allochthons along the Québec segment of the Appalachians was responsible for generating this second foreland basin succession. The geometry and subsidence rate of the Long Point Group reflect diachronous subduction polarity reversal along the margin which resulted in the unique tectonic setting of the Long Point Group in a combined retro-arc and pro-arc setting. The latest Silurian to Early Devonian Clam Bank Formation and Early Devonian Red Island Road Formation represent retro-arc foreland basin successions associated with the Salinian and Acadian orogenies respectively. The consistent thickness of the dominantly terrestrial Clam Bank Formation suggests a broad, shallow basin, probably due to lithosphere cooling and strengthening below the basin. The combination of structural, stratigraphic and geophysical data from the foreland basin of the Newfoundland Appalachians improves our understanding of the diachronous tectonic events within the orogen.

2.1. Introduction

Foreland basins, elongate troughs of sediment formed on continental crust between an orogenic belt and adjacent craton (DeCelles & Giles 1996), provide some of the best records of tectonic events associated with orogenesis. The Middle Ordovician through Early Devonian successions of the Anticosti Basin, which extends over 50,000 km² from southern Québec to western Newfoundland (Figure 2.1) (Quinn 1992, Stockmal et al. 1995, Quinn et al. 1999, 2004), were deposited in a foreland basin along the eastern margin of Laurentia, providing a hidden record of Appalachian orogenesis. The Anticosti Basin largely underlies the Gulf of St. Lawrence, precluding direct geological mapping, except on islands and coastal sections (Figure 2.1). This study aims to combine offshore geophysical interpretation with onshore geologic mapping to determine the structure and tectonic history of the basin and, in particular, the relationship of the foreland basin to the evolution of the western Newfoundland Appalachian Orogen, for which isotopic evidence providing age information is relatively scarce.

2.2. Geologic Setting and Tectonics

The oldest stratified rocks in the Anticosti Basin were deposited during several episodes of Neoproterozoic to early Cambrian rifting (Cawood et al. 2001). These events led to the opening of an ocean basin (the Iapetus), the development of conjugate margins of Laurentia and Amazonia (Cawood & Williams 1988, Cawood et al. 2001), and the rifting of crustal ribbons from both Laurentian and Amazonian margins (van Staal et al. 1998, Waldron & van Staal 2001, van Staal et al. 2009). The overall sinuous trend of promontories and embayments along the Appalachian Orogen has been interpreted to be inherited from this early rifted margin (Thomas 1977, Allen et al. 2010) and to have played a crucial role in the tectono-sedimentary evolution of the margin (Lavoie 1994, Allen et al. 2010).

In Newfoundland, three main orogenic episodes are traditionally recognized: an Early to Middle Ordovician Taconian episode (Williams & Stevens 1974, St. Julien & Hubert 1975), a Silurian Salinian episode (Dunning et al. 1990, Cawood et al. 1994) and an Early Devonian Acadian episode (Cawood & Williams 1988, Cawood 1993, Williams 1993). These orogenic events involved various phases of ocean closure associated with the accretion of microcontinents and/or crustal ribbons to the eastern margin of Laurentia. In the northern Appalachians (Figure 2.1) these continental fragments include: the Dashwoods block of peri-Laurentian origin, together with Ganderia, Avalonia and the Meguma terrane, all of Peri-Gondwanan origin (van Staal et al. 1998, Waldron & van Staal 2001, Hibbard et al. 2006, van Staal et al. 2007).

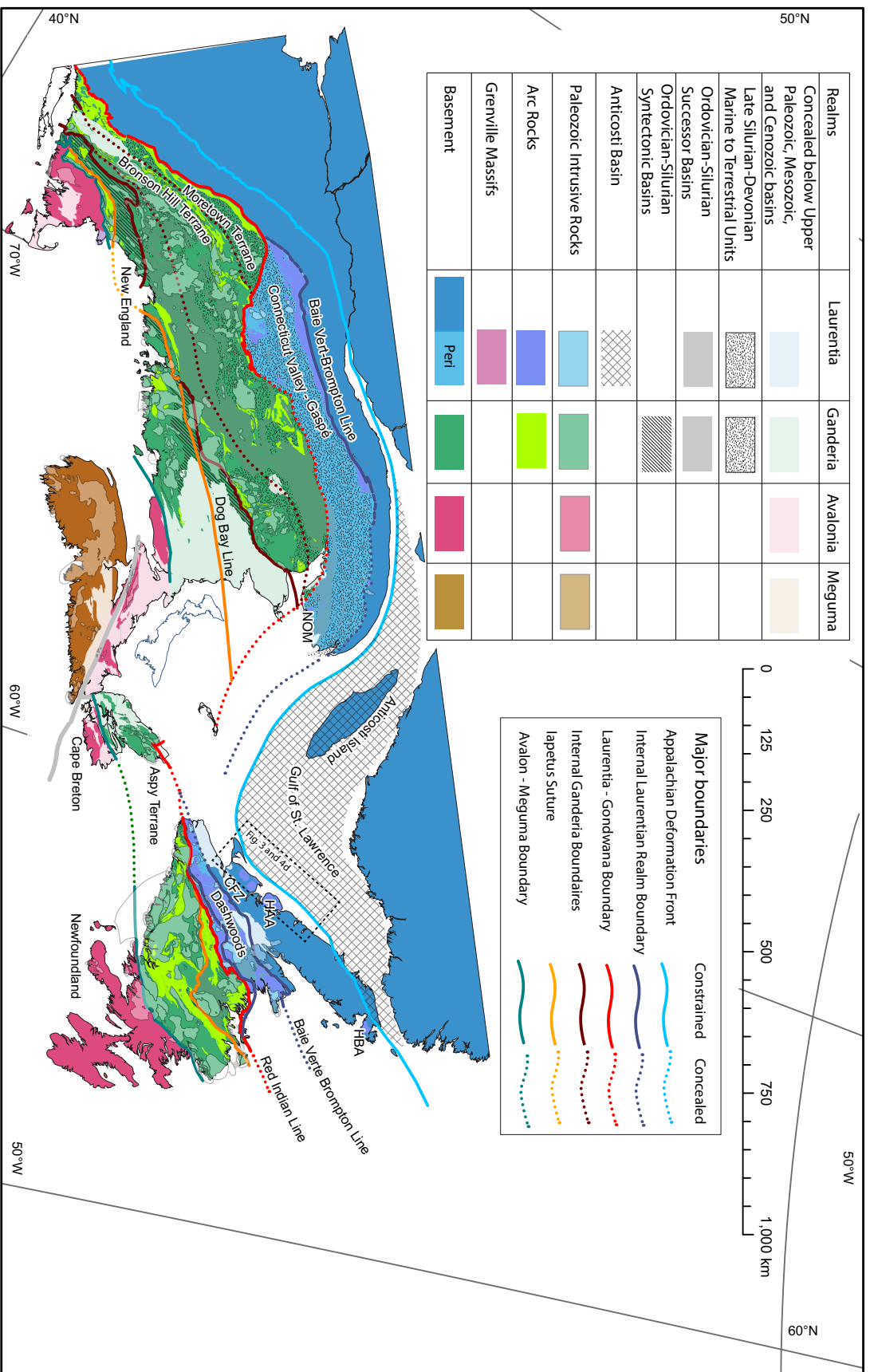


Figure 2.1: Map of present day tectonostratigraphic realms in the Northern Appalachians. CFZ, Cabot Fault Zone; CL, Chain Lakes; CD, Chester Dome; HAA, Humber Arm Allochthon; HB, Hare Bay Allochthon; MM, Maqueran-Mictaw inlier; NOM, Nadeau Ophiolite. (Modified from Waldron et al. 2017, in press).

2.2.1. Taconian Collision of Peri-Laurentian Fragments

The earliest orogenic episode, the Taconian Orogeny, is recognized along the length of the Appalachians and involves the emplacement of allochthons (Williams 1975, Stanley & Ratcliffe 1985) and collision of peri-Laurentian microcontinents (Waldron & van Staal 2001, van Staal et al. 2009) onto Laurentia's eastern margin (Williams & Stevens 1974, Williams 1975, Williams & Hatcher 1983, Waldron 1985, Bosworth 1989) above an east-dipping subduction zone (Jacobi, 1981). These accreted rocks can be traced along western portions of the northern Appalachians from Newfoundland to New England (Figure 2.1).

In Newfoundland, the collision of the Dashwoods microcontinent with the Laurentian margin (~ 470 Ma: Waldron & van Staal 2001) led to the closure of a small seaway within the Iapetus Ocean and obduction of oceanic rocks along the suture zone. The Humber Arm and Hare Bay allochthons (Figure 2.1), comprising structural stacks of slope/rise rocks, mélangé, and ophiolitic rocks (Williams 1975, Williams & Hatcher 1983) (Figure 2.1), were thrust atop passive margin sedimentary rocks during Taconian orogenesis. Middle Ordovician foreland basin clastic rocks containing ophiolitic detritus (Hiscott 1978, Quinn 1992) lie stratigraphically above the Laurentian carbonate shelf (Stevens 1970, Quinn 1992) and constrain the (~470 Ma) arrival of allochthons at the margin (Botsford 1987).

In Newfoundland, $^{39}\text{Ar}/^{40}\text{Ar}$ and U-Pb metamorphic ages associated with Taconian orogenesis and ophiolite obduction are scarce (van Staal et al. 2009, Castonguay et al. 2014). Isotopic dating of metamorphic rocks has mainly yielded Silurian (or younger) ages (Dunning et al. 1990, Cawood et al. 1994, Castonguay et al. 2014). More recently however, Castonguay et al. (2014) obtained 481-465 Ma Ar-Ar ages from amphiboles at the structural base of obducted ophiolites, interpreting this to confirm underthrusting of the leading edge of Laurentia by at least 480 Ma.

In southern Québec, the earliest stages of deformation and metamorphism are also associated with the obduction of ophiolites (Pinet & Tremblay 1995) along the Baie Vert-Brompton Line (Figure 2.1). In this region, $^{40}\text{Ar}/^{39}\text{Ar}$ amphibole ages from metamorphosed ophiolite soles suggest obduction between ~ 479 – 466 Ma (De Souza et al. 2012). Farther north in Québec, a muscovite cooling age of 470 +/- 0.4 Ma from an amphibolite at the sole of the Nadeau Ophiolitic mélangé (De Souza et al. 2012) (Figure 2.1) has been interpreted to reflect earliest interactions of ophiolites (between ca. 480 and 475 Ma) with the Laurentian margin at the promontory (De Souza et al. 2012) (Figure 2.1). Radiometric $^{40}\text{Ar}/^{39}\text{Ar}$ ages (469-461 Ma) of metamorphosed Laurentian rocks from the eastern Humber Zone in Québec have been interpreted to record Middle Ordovician Taconian metamorphism associated with crustal thickening and nappe emplacement (Castonguay et al. 2001). De Souza et al. (2012) suggested

that ophiolitic nappes were translated onto the margin until ~ 460 – 457 Ma (as suggested by $^{40}\text{Ar}/^{39}\text{Ar}$ muscovite and amphibole ages associated with latest recrystallization and cooling).

A west-dipping subduction zone was initiated outboard of Laurentia and the Dashwoods block by at least ~ 464 Ma, as recorded by U-Pb ages from the Pierre's Plutonic suite stitching the fault zone between the Dashwoods block and the Annieopsquotch Accretionary Tract (van Staal et al. 2009, Zagorevski et al. 2009). This west-dipping subduction and slab break-off of the east-dipping Laurentian plate led to reversal in subduction polarity at the Newfoundland Laurentian margin by ~ 460 Ma (van Staal et al. 2009).

2.2.2. Laurentian-Gondwanan Suture

The Red Indian Line (Figure 2.1) represents an important boundary in the Newfoundland Appalachians, separating rocks of peri-Laurentian affinity (in Newfoundland the Annieopsquotch oceanic tract) from those formed in the Gondwanan realm (Williams et al. 1988, Williams 1991). In Newfoundland, several lines of evidence suggest that the first accretion of peri-Gondwanan crust occurred by 455-450 Ma (van Staal et al. 1991, Rodgers & Van Staal 2002, O'brian 2003, Waldron et al. 2012). Structural data (Zagorevski et al. 2007) and interpretations of seismic reflection data (van der Velden et al. 2004) suggest underthrusting of the peri-Gondwanan Victoria Arc beneath the Laurentian margin (Zagorevski et al. 2007). After collision, there was another phase of slab break-off and re-initiation of west-dipping subduction east of the Laurentian-Gondwanan boundary (Zagorevski et al. 2007), along the Dog Bay Line (Reusch & van Staal 2012).

In New England, the boundary between the Laurentian and Gondwanan realms has been interpreted to lie west of the Bronson Hill terrane (Figure 2.1) under Silurian-Devonian cover successions of the Connecticut Valley Trough (Figure 2.1) (van Staal et al. 1998, Hibbard et al. 2006, Dorais et al. 2011, Macdonald et al. 2014). Macdonald et al. (2014) observed that 475 Ma plutons intrude the Gondwanan Moretown terrane (Figure 2.1) and overlying Laurentia-derived sediments. This implies initial accretion of peri-Gondwanan material to Laurentia by at least 475 Ma, 20 Myr earlier than the recorded timing of peri-Gondwanan collisions to the north. These earlier interactions in New England are interpreted to have taken place outboard of the Laurentian margin (Macdonald et al. 2014), and to have involved the obduction of the Moretown terrane above another peri-Laurentian continental fragment. Karabinos et al. (1998) and Moench and Aleinikoff (2003) interpreted that subduction polarity reversal in New England occurred by 454 Ma and 458 Ma respectively, constrained by the age of units within the Bronson Hill Arc, which the authors interpret to have formed above a west-dipping subduction zone (Karabinos et al. 1998, Moench & Aleinikoff 2003).

2.2.3. Salinian Arrival of Ganderia

A distinct Silurian (440-422 Ma) orogenic episode, involving magmatism, metamorphism and deformation, has been recognized in central Newfoundland as the Salinian Orogeny (Dunning et al. 1990, Cawood et al. 1994, van Staal et al. 2009). Orogenesis has been attributed to mid-Silurian collision of a Ganderian microcontinent with Laurentia, resulting in the closure of an intervening Iapetan seaway (van Staal et al. 2009). Although subduction and accretion of peri-Gondwanan terranes within this seaway were active since the Late Ordovician (van Staal et al. 2009), the final collision of Ganderian fragments did not occur until the Wenlock (Pollock et al. 2007).

Silurian orogenesis can be recognized elsewhere in the northern Appalachians. On Cape Breton Island (Figure 2.1), the majority of the volcanism, plutonism, metamorphism and deformation in the Aspy Terrane (Figure 2.1) is Silurian (Jamieson et al. 1986). In New Brunswick (van Staal & De Roo 1995) and Maine (West et al. 1992), structural studies, conjoined with isotopic age dating, have also demonstrated the importance of a Silurian event.

2.2.4. Acadian Orogenesis

The Acadian Orogeny (423-400 Ma) is conventionally attributed to the accretion of Avalonia to Laurentia (Bird & Dewey 1970, Bradley 1983, van Staal et al. 2009), involving the westward subduction of Avalonia beneath Laurentia (Waldron et al. 1996, Murphy et al. 1999) and closure of the easternmost segment of the Iapetus Ocean. Timing of related magmatism (423-416 Ma), subduction-related metamorphism (420 – 416 Ma) (van Staal et al. 2009), and deposition of latest Silurian – Early Devonian foreland basin deposits atop Avalonia (Waldron et al. 1996) demonstrate that the Acadian Orogeny began shortly after or during the waning stages of the Salinian Orogeny (van Staal et al. 2009). Acadian orogenesis continued into the Early Devonian (~400 Ma: van Staal et al., 2009) in Newfoundland, but lasted until about 380 Ma in Québec (Bradley et al. 2000).

2.2.5. Neo-Acadian Arrival of Meguma Terrane and Opening of Maritimes Basin

The collision of the Meguma Terrane with Laurentia has commonly been interpreted to be the cause of the Neo-Acadian Orogeny (van Staal 2007), which was defined by Robinson et al. (1998) to encompass strong Late Devonian to Early Carboniferous (366-350 Ma) magmatism, deformation and granulite facies metamorphism in the southern New England Appalachians. Middle Devonian to Early Mississippian magmatism along the length of the orogen (Hibbard et al. 2010) is synchronous with the Neo-Acadian Orogeny. However, these magmatic and metamorphic events overlap in time with the opening of the Maritimes Basin, interpreted

by Waldron et al. (2015) as recording prolonged Late Devonian to Pennsylvanian dextral transtension and transpression (van Staal et al. 2009, Hibbard et al. 2010, Waldron et al. 2015). In Newfoundland, Waldron et al. (2015) interpreted that this motion was carried on the Cabot fault zone (CFZ on Figure 2.1), with as much as 250 km right-lateral offset interpreted. An important implication of this deformation is that all Laurentian and Gondwanan fragments east of the fault were actually accreted ~ 250 km north of their present day position (Figure 2.1).

2.3. Regional Geology

2.3.1. *The St. Lawrence Platform and Basement*

The stratigraphy of the Anticosti Basin is summarized in Figure 2.2. The oldest rocks in the region are Mesoproterozoic crystalline basement units of the Grenville and associated Mesoproterozoic orogens (~ 1 Ga). Overlying these basement rocks is an extensive succession of synrift to passive margin sediments (Williams & Hiscott 1987, Chow & James 1987, Knight & James 1987). In the Newfoundland portion of the basin, lower portions of the Cambrian Labrador Group represent the rift phase of basin development (Williams & Hiscott 1987) and upper portions of the Labrador Group represent the earliest post-rift deposits on the continental margin (Williams & Hiscott 1987). The Labrador Group is overlain by thinly bedded high-energy carbonates of the middle to upper Cambrian Port au Port Group (Chow & James 1987). These units are overlain by massive, thick-bedded lower-energy limestone and dolostone of the Lower Ordovician St. George Group (Knight & James 1987).

2.3.2. *Foreland Basin Successions*

2.3.2.1. *Ordovician Units*

In western Newfoundland, the St. George unconformity (Figure 2.2) marks an ~ 3 Myr hiatus between the St. George Group and the overlying Table Head Group which comprises middle to upper Darriwilian carbonates that represent the basal unit of the earliest foreland basin (Stenzel et al. 1990). The Table Head Group is characterized by major lateral thickness and facies variations, attributed to draping over a karstic and faulted topography (Stenzel et al. 1990, Knight et al. 1991). The youngest unit within the group, the Cape Cormorant Formation, is mainly limestone cobble to boulder conglomerate composed of clasts derived from the platform along submarine fault scarps (Stenzel et al. 1990). A transition to orogen-derived clastic sediments is recorded by overlying turbiditic sandstone of the Goose Tickle Group (Quinn 1992), also Darriwilian. These siliciclastic rocks also vary in thickness, thicker deposits filling grabens and

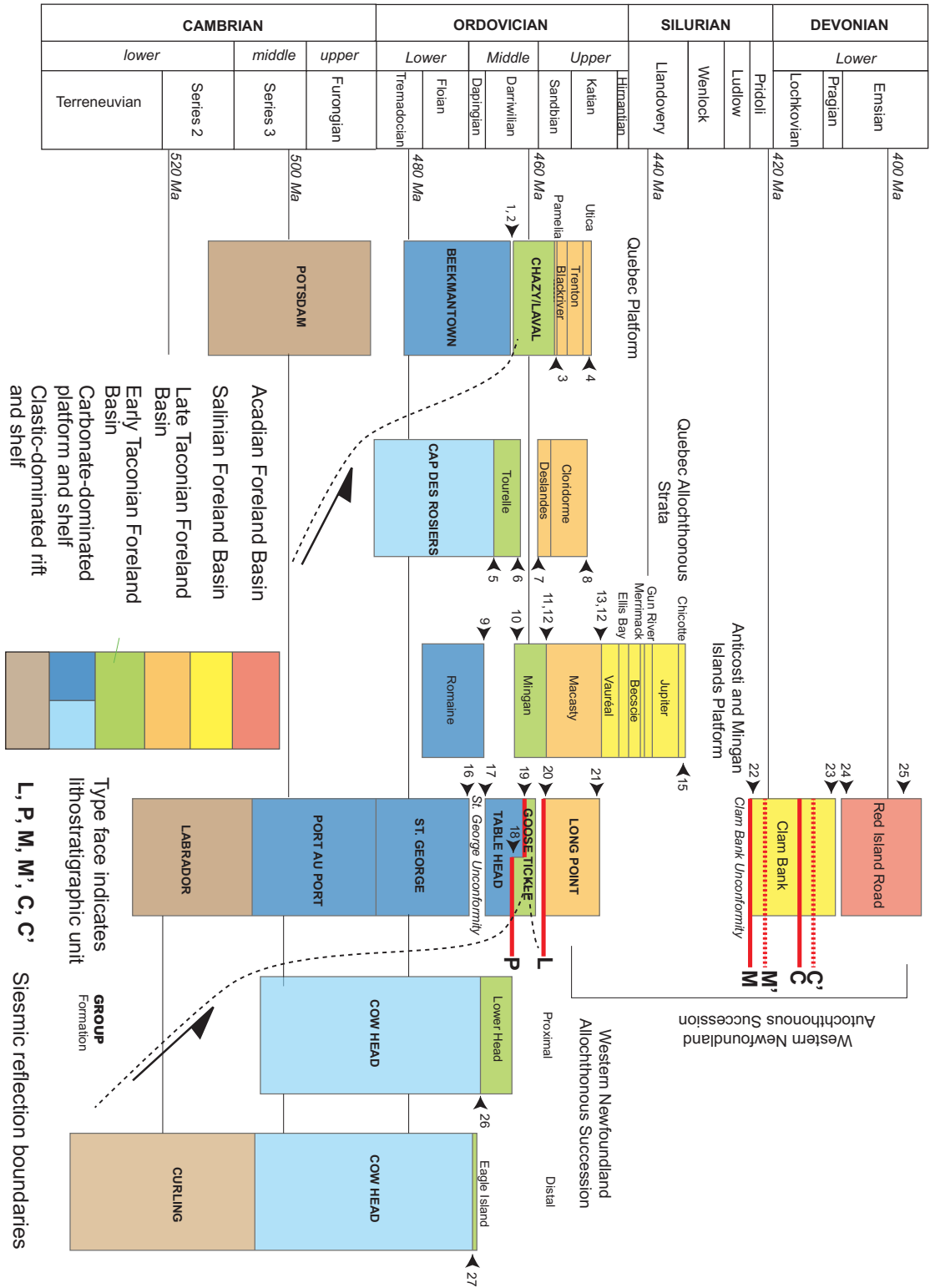


Figure 2.2: Regional stratigraphic column for the Anticosti Basin including Anticosti Island and the Mingan Islands, western Newfoundland and Québec.

Numbers along the columns correspond to specific fossils that were used to place boundary at proper age. Biostratigraphic correlation was only done for the top of platform and boundaries of younger foreland basin units. A list follows of the fossils and corresponding publications in which the data were found. 1 = *H. holodentata* zone (Dix et al., 2013) & *E. suceicus* zone (Salad Hersi et al. 2003); 2 = *E. suceicus* zone (Dix et al., 2013); 3 = Top of *C. sweeti* conodont zone (Dix et al. 2013); 4 = *O. robustus* (Goldman et al. 1994); 5 = *D. "Bifidus"* (Prave et al. 2000); 6 = *D. murchisoni* (Prave et al. 2000); 7 = *N. gracilis* (Prave et al. 2000); 8 = *C. spiniferus* (Prave et al. 2000); 9 = *Acidiphorus*, *Pseudomera* (Shaw and Bolton, 2011); 10 = *C. friendsvillensis* (Graptolite zone based on trilobite assemblage of Shaw and Bolton (2011); 11 = *C. sweeti* (Graptolite zone based on trilobite assemblage of Shaw and Bolton (2011); 12 = *C. spiniferus* (Rudolf Ruedeman, 1947) correlated with *C. bicornis* (Goldman et al., 2007); 13 = *D. complanatus* (Riva 1988, Achab et al. 2011); 14 = *P. manitoulinensis* (Jacobson & Achab 1985) correlated with *linearis* (Eriksson & Mitchell 2006); 15 = *A. Bullatus-Ou.? Expansus* (Zhang and Barnes, 2002); 16 = *I.v. lunatus* zone (Zhang & Barnes 2004); 17 = upper part of the *Undulograptus dentatis* zone (Maletz 2011); 18 = top part of *H. lentus* zone (Maletz et al. 2011); 19 = *P. elegans* (Maletz et al. 2011); 20 = *Amorphognathus tvaerensis* (Batten Hender 2008); 21 = *Isotelus walcotti* (Quinn et al. 1999); 22 = *Ozarkodina eosteinhornensis* s.l interval Zone (Burden et al. 2002); 23 = Palynomorph assemblage detailed in Burden et al. (2002); 24, 25 = *Emphanisporites annulatus* – *Camarozonotriletes sexantii* Assemblage Zone (Quinn et al., 2004); 26, = *Isograptus victoriae maximus* to *U. austroduntatus* biozone (Botsford 1987; James & Stevens 1986); 27 = *I. v. lunatus*, *I. v. victoriae* (Botsford 1987).

thinner units occurring atop horsts. The Goose Tickle sandstone and siltstone units are locally interbedded with limestone conglomerate (Daniels Harbour Member), interpreted to be derived from exposures of the Table Head Group on local uplifts within the basin (Stenzel et al. 1990).

The Upper Ordovician (Sandbian to Katian) Long Point Group is interpreted to unconformably overlie the Goose Tickle Group (Burden & Williams 1995, Quinn et al. 1999, Cooper et al. 2001, Batten Hender & Dix 2008). This contact is nowhere preserved on land; however, information from Port au Port No. 1 well (Figure 2.3) demonstrates a dramatic downward increase in the thermal alteration index across the Goose Tickle - Long Point contact, and this increase has been interpreted to indicate a disconformity (Burden & Williams 1995). Biostratigraphic studies suggest a small time gap across the boundary (Burden & Williams 1995, Batten Hender & Dix 2008) of only ~ 1.5 Myr, when correlated with the timescale of Cooper et al. (2012) (Figure 2.2). The Long Point Group directly overlies the Humber Arm Allochthon on the Port au Port Peninsula (Figure 2.3). Although Rodgers (1965) and Stait & Barnes (1991) interpreted this contact as an unconformity, Stockmal & Waldron (1990) reinterpreted the boundary as a thrust contact, based on field relationships and offshore seismic data that show a tectonically thickened wedge of Humber Arm Allochthon below the contact. The basal unit of the Long Point Group is the Lourdes Formation, a 75 m thick unit of shallow-marine limestone in outcrop. However, Burden & Williams (1995) observed a significantly thicker (180 m) Lourdes Formation in the Port au Port No. 1 well (Figure 2.3). Cooper et al. (2001) interpret this eastward thinning to represent an original regional onlap of the Lourdes Formation onto the Humber Arm Allochthon.

Shallow-marine siliciclastic rocks of the Upper Ordovician Winterhouse Formation gradationally overlie the Lourdes Formation (Quinn et al. 1999) and record the demise of the Lourdes platform (Quinn et al. 1999, Batten Hender 2007, Batten Hender & Dix 2008). This succession of sandstone and shale is overlain by red beds of the Upper Ordovician Misty Point Formation (Quinn et al. 1999). The measured thickness of the Long Point Group is 1260 m (Quinn et al. 1999) and is interpreted to represent important subsidence (Stockmal et al. 1995, Quinn et al. 1999), not obviously related to an orogenic episode. Waldron et al. (1993) suggested that the Long Point – Clam Bank succession was deposited during a period of quiescence between the Taconian and Acadian orogenies, whereas Stockmal et al. (1995) identified this succession as Salinian. Quinn et al. (1999) noted that the composition of the Long Point Group suggests renewed erosion of Taconian sources during the Late Ordovician and conclude that the tectonic activity suggested by Stockmal et al. (1995) may have been a late or second phase of the Taconian Orogeny.

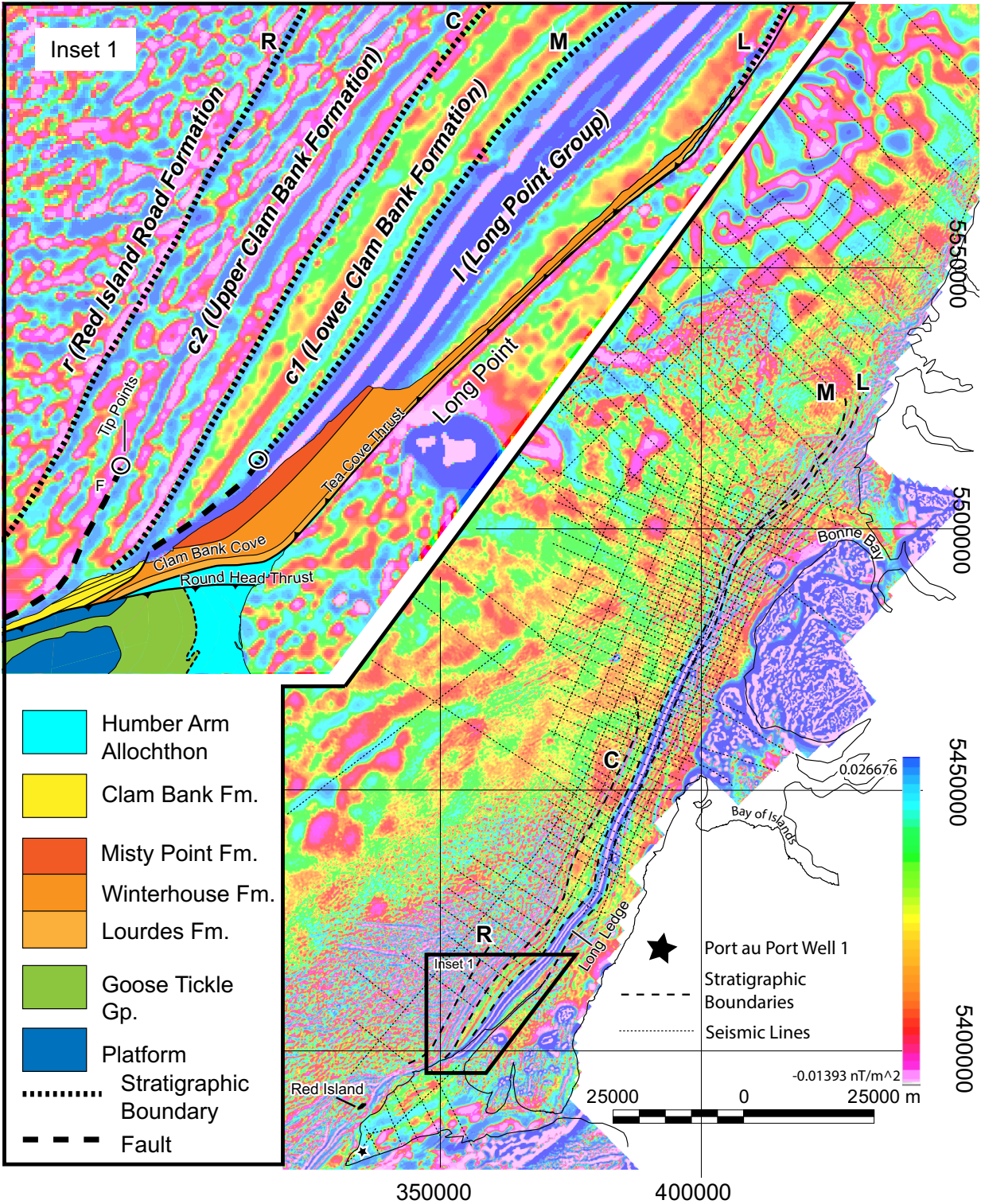


Figure 2.3: Map of second vertical derivative of the residual magnetic field (modified from Dumont & Jones 2013) and interpreted geologic boundaries. Location of map on figure 2.1. **Inset 1** shows the geology along Long Point on the Port au port Peninsula and interpreted geologic boundaries offshore.

2.3.2.2. Post-Ordovician Units

In the Newfoundland portion of the Anticosti Basin, the Silurian record of deposition is highly incomplete because a major hiatus of ~ 25 Myr (Figure 2.2) occurs below the Pridoli through Early Devonian (Lochkovian) Clam Bank Formation (Burden et al. 2002). The inferred unconformity, herein referred to as the Clam Bank unconformity, is nowhere observed on land but is faulted at Clam Bank Cove (Figure 2.3: inset 1). The lowest portion of the Clam Bank Formation is a mixed carbonate and clastic unit; a second unconformity above this mixed lower portion is interpreted to mark the transition to a dominantly siliciclastic succession, deposited in a terrestrial environment (Burden et al. 2002).

Clast-supported conglomerate and sandstone of the Emsian Red Island Road Formation are interpreted to overlie the Clam Bank Formation (Quinn et al. 2004), but the contact is concealed beneath the Gulf of St. Lawrence just offshore of the Port au Port Peninsula. This unit is only exposed on Red Island (Figure 2.3, 2.4d). These strata, including cobbles and boulders derived from mixed volcanic and low-grade metamorphic sources (Quinn et al. 2004), represent the uppermost division of the post-Taconian foreland succession inferred by Stockmal et al. (1995) to exist offshore. Earlier workers had mapped a large portion of the offshore regions as Carboniferous (Sandford & Grant 1990); however with recognition of the Red Island Road Formation as Devonian (Quinn et al. 2004), much of this region is now understood to be underlain by the youngest rocks of the Appalachian foreland basin (Quinn et al. 2004), represented onshore by the Red Island Road Formation.

2.3.3. Deformation Front

Stratigraphy of the foreland basins is deformed at the structural front of the Newfoundland Appalachians by the Devonian emplacement age (Waldron & Stockmal 1991, Stockmal et al. 1998) of a tectonic wedge (Stockmal & Waldron 1990). This wedge was interpreted to contain rocks of the Humber Arm Allochthon inserted into the foreland basin between oppositely-vergent thrust faults (Stockmal & Waldron 1990). The tectonic wedge is in turn cut by the deep-seated Round Head thrust (Figure 2.3); folds associated with this structure are truncated unconformably by flat-lying Visean strata. These relationships bracket both insertion and cross-cutting of the wedge by the Round Head thrust between the Emsian and Visean (Stockmal et al. 1998).

2.4. Data Sources

Knowledge of the offshore stratigraphy of the Anticosti Basin has been based dominantly on geophysical surveys acquired from the 1970's through the early 90's (Lamb 1976, Sandford &

Grant 1990, Sinclair 1990, Stockmal & Waldron 1990, Dietrich et al. 2011, Pinet et al. 2012). We therefore rely on geophysical data to map the subsurface beneath the Gulf of St. Lawrence.

2.4.1. 2D Seismic Reflection Data

Stockmal & Waldron (1990) interpreted a tectonic wedge, of Acadian (Devonian) age (Waldron & Stockmal 1991, Stockmal et al. 1998) at the structural front of the Newfoundland Appalachians using three marine seismic reflection profiles shot by Shell Canada Resources Limited (Lamb 1976) (Figure 2.4d). Subsequent offshore seismic surveys were undertaken by Mobil Oil Company Canada Ltd and BHP Petroleum in the 1990's. On land (Port au Port Peninsula) surveys were carried out by Hunt Oil Company and Canadian Imperial Venture Corporation (CIVC) in 1993 and 2001 respectively. The surveys span an area of over 13 000 km². 2D seismic profiles dominantly trend northeast (sub-parallel to the dominant strike-direction of mapped geologic boundaries) and northwest (sub-parallel to the dip-direction of major geologic boundaries) (Figure 2.4d). These data entered the public domain as printed copies and were scanned and converted commercially using a proprietary process back to SEG Y format. These data have been made available to us by Leprechaun Resources and input into Petrel™, a software package for seismic interpretation.

The surveys shot by Mobil, Hunt and CIVC are of good quality (Figure 2.4a, b: lines a-a' and b-b'), and the reflections observed are mainly interpreted to represent real geologic boundaries. The quality of the BHP survey is poorer, because seafloor multiples interfere with principal reflections, making the interpretation of some geologic boundaries speculative (Figure 2.4c: line c-c').

2.4.2. Airborne Magnetic Data

Figure 2.3 shows the results of an aeromagnetic survey which was carried out in 2012 by Goldak Airborne Surveys and Terraquest Airborne Geophysics Ltd. under the Offshore Geoscience Data Program, an initiative of the Department of Natural Resources, Government of Newfoundland and Labrador (Dumont & Jones 2013). These maps are publicly available as a joint Open File distributed by the Geological Survey Division (Newfoundland and Labrador Department of Natural Resources) and the Geological Survey of Canada (Natural Resources Canada) (Dumont & Jones 2013). Figure 2.3 shows a compilation of 32 1:100 000-scale aeromagnetic maps for 16 National Topographic System (NTS) map areas, covering a portion of the offshore and onshore area in western Newfoundland. We chose to use the second vertical derivative of the residual magnetic field in our interpretations because it emphasizes the effects of the near-surface magnetic sources.

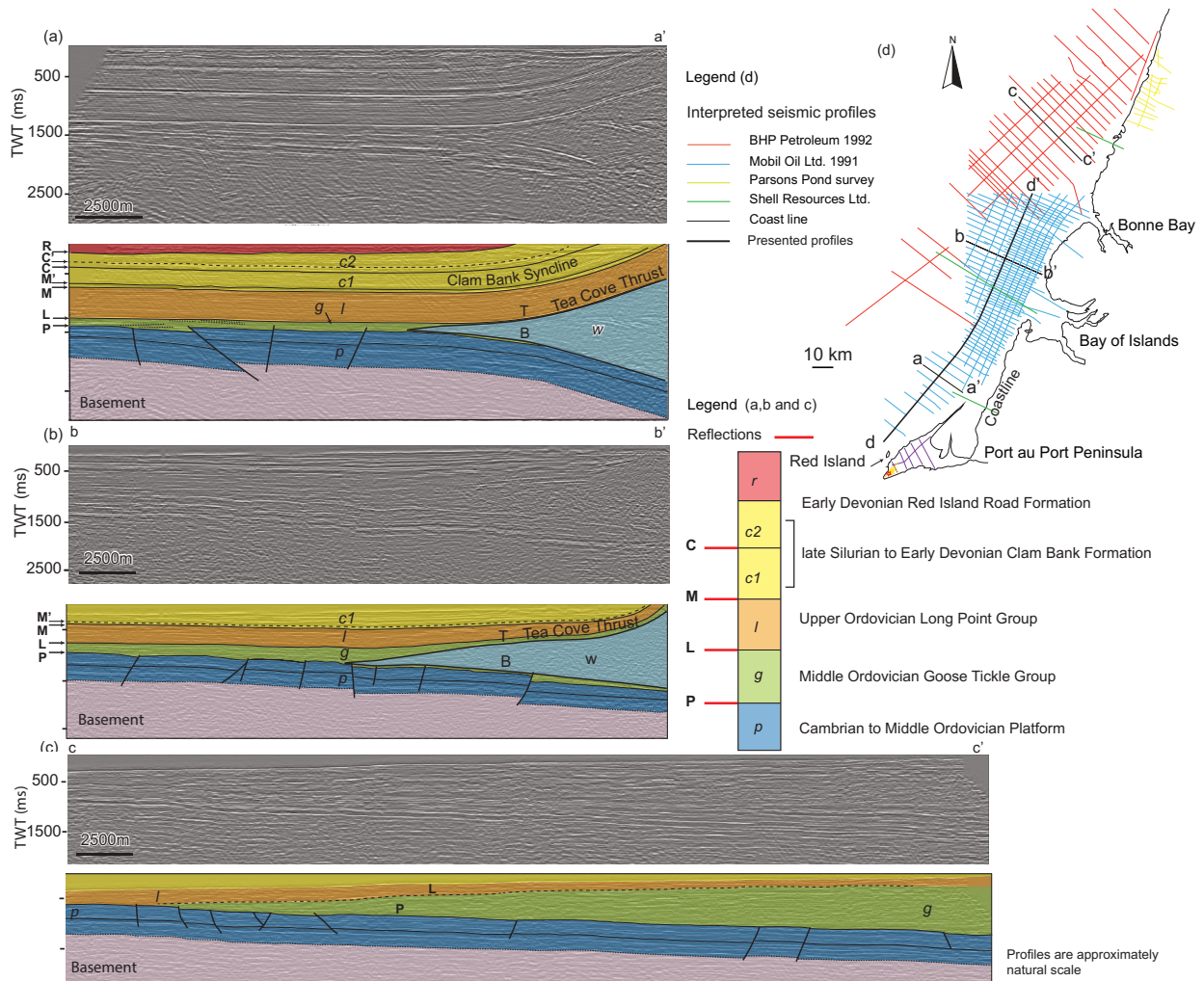


Figure 2.4: Interpreted dip-direction seismic profiles (a), (b) and (c) displaying the geometry of seismic reflections offshore western Newfoundland. (d) shows the location of all seismic profiles in the offshore region. See figure 2.1 for location of (d). See text for details.

2.5. Methods

Seismic reflections need to be tied to specific geologic boundaries in order to make subsurface interpretations; however, no wells have been drilled in the offshore region of interest, making this difficult. Onshore, the Port au Port No. 1 well (Burden & Williams 1995) lies within 200 m of the CIVC seismic survey (Figure 2.4d). A synthetic seismogram was generated using geophysical data from the well. However, the CIVC survey does not tie directly to the offshore seismic surveys. Only seismic reflections with identifiable and consistent characteristics, which can be correlated with reasonable certainty, are tied across the 3.7 km gap.

We use aeromagnetic data (Figure 2.3), higher resolution Google Earth imagery, and multibeam bathymetry data (Figure 2.5) (Shaw et al. 1997, Courtney 2013) to link the majority of seismic reflections to outcrop. Waldron et al. (2002) observed that the “Odd-Twins” magnetic anomaly, reported by Ruffman & Woodside (1970) offshore of the Port au Port Peninsula, correlated to the position of two magnetic units within the Winterhouse/Misty Point succession onshore. Their observations show that the variations in magnetic susceptibility are controlled by variations in the amount of detrital magnetite within the siliciclastic units and is largely stratigraphically controlled. Sea-floor exposures of strata observed on the Google Earth imagery also parallel the magnetic anomalies (Figures 2.3 and 2.5). The linear magnetic anomalies in Figure 2.3 are therefore considered to represent stratigraphy (i.e. units within the foreland basin). Ties are made by tracing seismic reflections to their point of intersection with the aeromagnetic map, and then along strike (parallel to anomalies) to onshore geology (Figure 2.3). Geophysical features identified in this study that represent geologic boundaries are labelled using bold capital letters (e.g. **L**, **P**, **M**, **C** and **R**). Intervening groups of anomalies, inferred to represent lithostratigraphic units, are labelled with lowercase italic letters (e.g. *p*, *g*, *l*, *c1*, *c2*, and *r*).

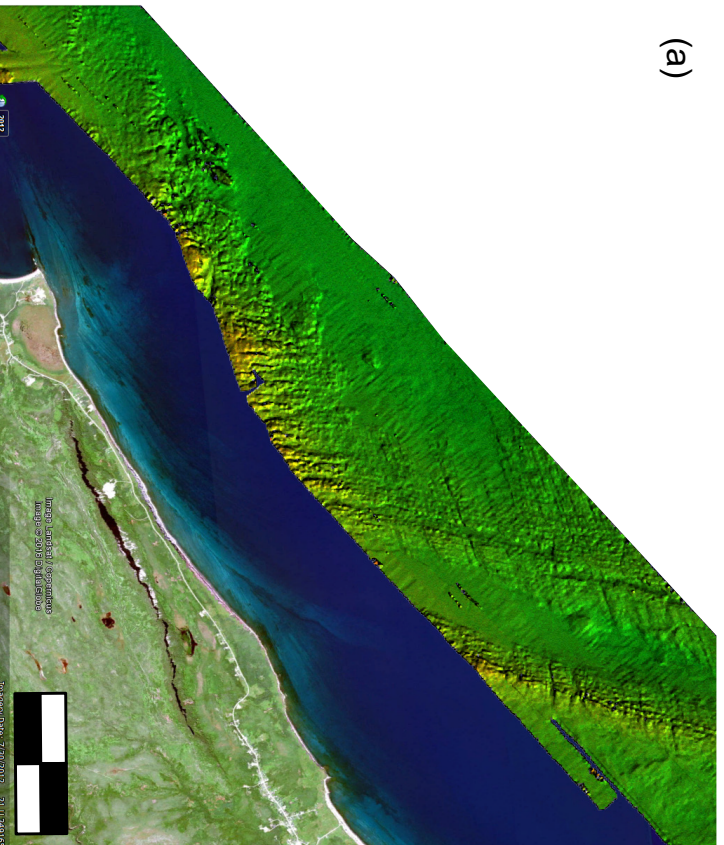
When converting from the time to depth domain an average velocity of 4.45 km/s is used, following Stockmal et (1995). This velocity is appropriate for the lithologies present and estimates of thicknesses from seismic profiles directly offshore of the Port au Port Peninsula correlate well with thickness measurements made onshore.

2.6. Observations and Interpretation of Aeromagnetic Data

Anomalies on the aeromagnetic map (Figure 2.3) are divided into 4 groups representing stratigraphic units, *l*, *c1*, *c2*, and *r*, which are sub-parallel to each other.

The most conspicuous feature on the aeromagnetic map is a pair of northeast-trending, positive magnetic anomalies (group *l* in Figure 2.3), extending from Long Point to a position north of Bonne Bay (Figure 2.3), corresponding to the “Odd-Twins” anomalies of Ruffman and

(a)



(b) See Figure 3 for geology legend

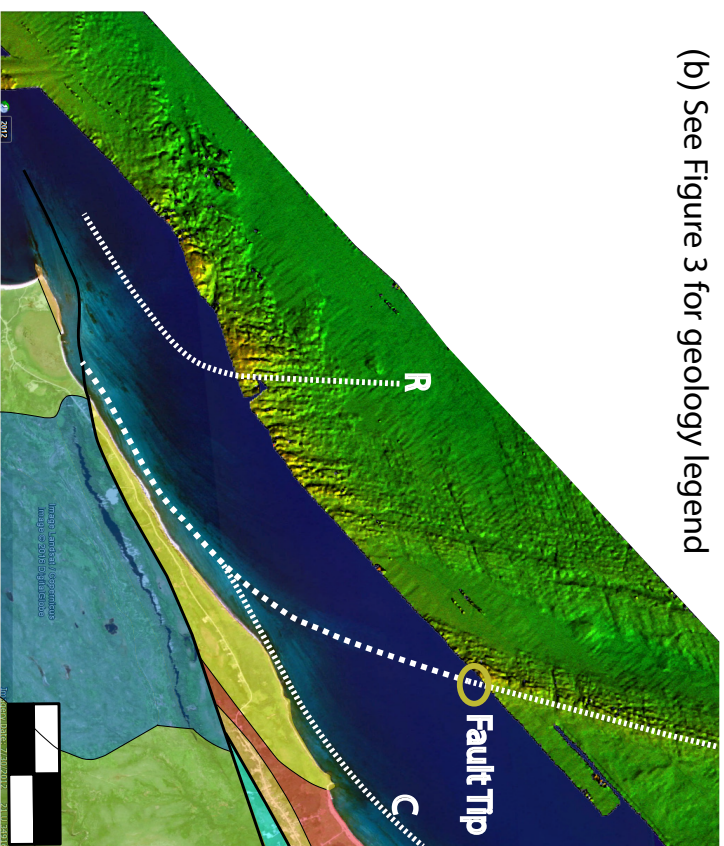


Figure 2.5: (a) Google Earth satellite imagery and bathymetry data offshore Long Point, Port au Port Peninsula. (b) Interpreted geologic boundaries offshore and onshore.

Woodside (1970) and Waldron et al. (2002). Group *l* is bounded to the east by **L** and west by **M**. The amplitude of the magnetic anomalies within group *l* is the greatest of all groupings identified (Figure 2.3). The anomalies within group *l* are sub-parallel to one another and boundary **M**. These anomalies coincide exactly with the onshore position of two magnetic units within the Long Point Group (Waldron et al. 2002). We therefore correlate *l* with Long Point Group strata.

Group *c1* lies adjacent to and west of *l*, and is bounded to the east and west by **M** and **C** respectively. Individual anomalies within *c1* are oblique to **M**. Anomaly amplitudes within *c1* are stronger and more continuous in the south relative to the north. Group *c1* can be traced to the north only as far as the Bay of Islands (Figure 2.3) where its component anomalies curve west and become untraceable. To the south group *c1* is traced to Clam Bank Cove where it rapidly thins and terminates. **C** correlates with the highest mapped unit of the west-dipping Clam Bank Formation on land (Figures 2.3 and 2.4). It is therefore likely that anomaly group *c1* represents the Clam Bank Formation. The widths of both *l* and *c1* are not constant along their length suggesting changes in inclination and/or thickness of these units.

Group *c2* lies adjacent and west of *c1*. Westward younging in on-land exposures of Clam Bank Formation indicates that *c2* lies stratigraphically higher than *c1* and is a previously unrecognized portion of foreland basin stratigraphy between the exposed Clam Bank and Red Island Road formations. Directly offshore of the Port au Port Peninsula, *c2* is divided by boundary **F**, separating it into an eastern and western portion. Anomalies within the eastern part of *c2* curve sharply and are truncated by boundary **F** while anomalies in the western part parallel **F** everywhere (Figure 2.3 and 2.4). The angular discordance between **F** and *c2* (east) is $\sim 20^\circ$; however, farther north anomalies within *c2* (east) parallel boundary **F**. We interpret **F** as a fault, possibly a splay of the Round Head thrust, which cuts out a large portion of *c2* and ends to the north at a tip point where displacement on the fault decreases to zero (Figure 2.3).

Boundary **R** separates regions *c2* and *r*. Although the magnetic character of these regions is similar, *r* can be picked using bathymetry data (Shaw et al. 1997, Courtney 2013). The region underlain by *r* is characterised by a knobby and irregular seafloor, and contrasts with the regularly lineated and smooth seafloor associated with *c2* (Figure 2.3). The bathymetric signature to the west of **R** continues into the area surrounding Red Island (Figure 2.3) and *r* is therefore interpreted as seafloor outcrop of Red Island Road Formation. The lack of magnetic lineation in the area corresponding to *r* most likely reflects the shallow dip of bedding, similar to that on Red Island where the measured dip is $\sim 07^\circ$.

The geophysical signatures of *l*, *c1*, and *c2* abruptly end in the south near the interpreted position of the Round Head thrust (Figure 2.3), suggesting that all these units are cut by the thrust. Towards the north all anomaly groups curve west and lose coherence. We interpret (in the following discussion) that this curvature is produced by a gently south-plunging syncline, herein

named the Clam Bank syncline, previously interpreted from seismic profiles by Shearer (1973) and Stockmal & Waldron (1990).

2.7. Seismic Characteristics

2.7.1. Seismic Horizons and Events

The horizons picked on 2D seismic reflection profiles are chosen here based on relative amplitude, continuity and geographic extent of reflections. Ties to stratigraphy are made by tracing reflections to the seafloor or, where possible, to wells. Other major geologic boundaries, such as faults, are picked based on discontinuities and breaks in lateral continuity of seismic reflections. Only major, basin-scale faults are individually discussed, but figures 2.4 and 2.6 show the distribution of minor faults (predominantly affecting platform and basement rocks).

The deepest and most laterally extensive reflection picked for interpretation is a high amplitude, positive reflection **P** (Figures 2.4 and 2.6). The phase and amplitude of **P** are consistent along the majority of profiles, suggesting that the physical characteristics of the geology are consistent across the basin. A time-structure map of **P** (Figure 2.7a) demonstrates a dominant SE-dip, where **P** steepens towards the coastline. Along the majority of profiles, **P** shows multiple small offsets in two-way travel time (TWT) (Figures 2.4 and 2.6). These offsets are discussed in the following section. **P** is nowhere traceable to surface but can be traced to line GH-1 CIVC 2001 (Figure 2.4d) where it correlates to the top of the Table Point Formation picked in Port au Port No. 1 well (Figure 2.4d). We herein refer to **P** as the “top of platform reflection”.

Reflection **L** lies above **P** and is also a high amplitude, positive reflection (Figure 2.4). South of the Bay of Islands, **L** has the highest amplitude of all interpreted reflections (Figure 2.4a, b). North of the Bay of Islands, however, the amplitude of reflection **L** decreases significantly and it becomes difficult to trace (Figures 2.4c and 2.6). The position of **L** north of Bonne Bay is speculative due to the poor quality of the BHP seismic data (Figure 2.4c, d line c-c'). Along dip-direction profiles, **L** is observed to be folded into the Clam Bank syncline (Figure 2.4a, b). Within the hinge zone of this fold small faults offset **L** with minor contractional separation. Elsewhere, it does not show any major offsets. Reflection **L** is projected to surface and along strike to outcrops of Lourdes Formation on Long Ledge (Figure 2.3). It corresponds to the eastern boundary of magnetic package *l* identified on Figure 2.3. Reflection **L** is also correlated to a high amplitude peak above a strong trough on the synthetic seismogram generated for Port au Port No. 1 well (Figure 2.3). Based on these observations, we interpret **L** as a reflection close to the top of the thin (~75 m) Lourdes Formation and refer to it as the “Lourdes Formation reflection”.

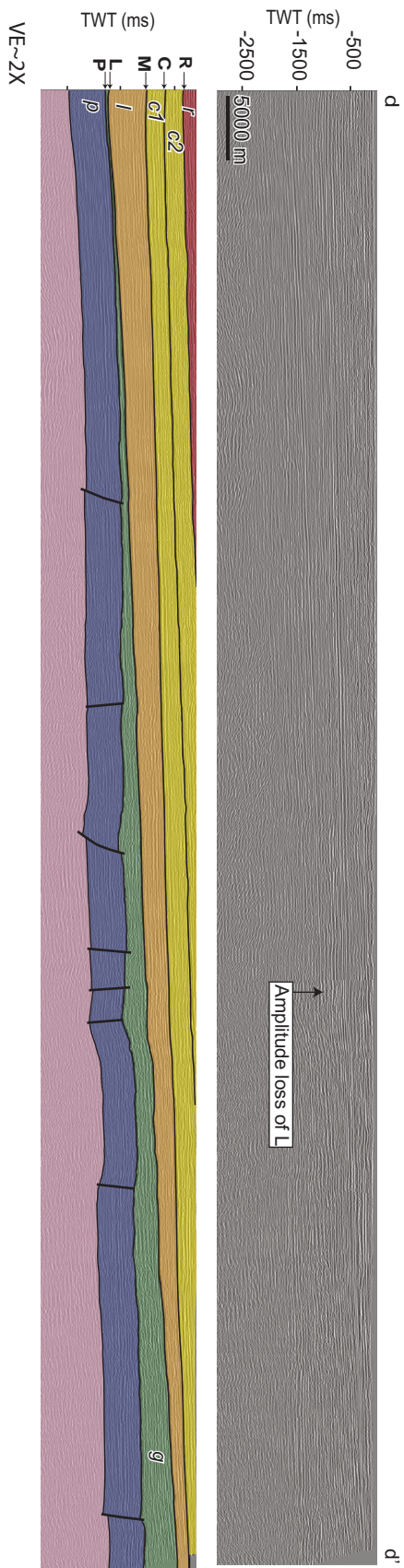


Figure 2.6: Interpreted strike-direction seismic profiles displaying the geometry of seismic reflections offshore western Newfoundland. See figure 5(d) for location of line and text for details.

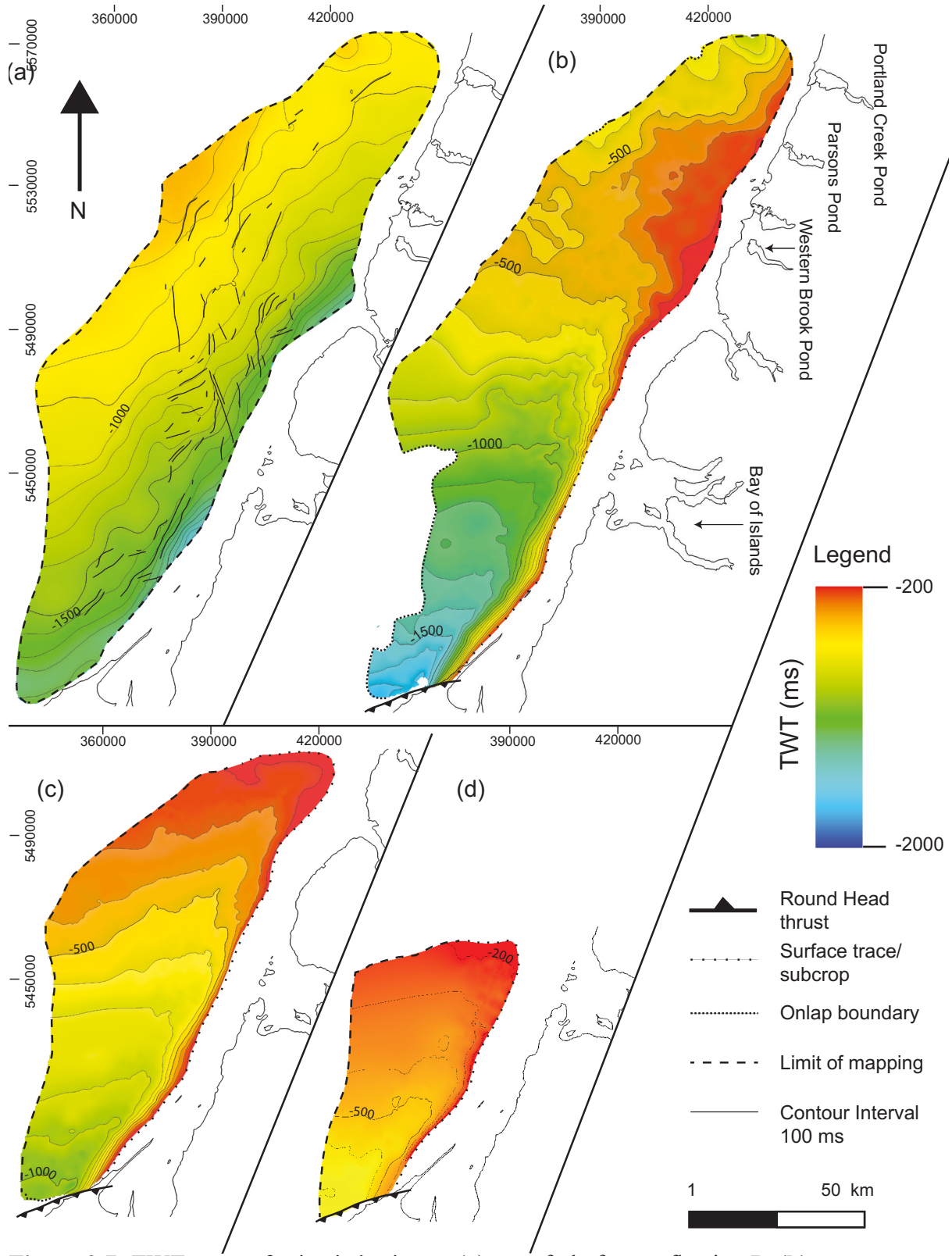


Figure 2.7: TWT maps of seismic horizons. (a) top of platform reflection P, (b) near-top Lourdes Formation reflection L, (c) near-top Misty Point Formation reflection M, (d) near-top Clam-Bank Formation reflection C.

Reflections **M** and **M'** are strong, positive reflections above **L**, forming an easily recognizable doublet (Figure 2.4). The amplitude of **M** is constantly higher than surrounding reflections (Figure 2.4). This reflection is laterally continuous and not fragmented or offset in TWT. Its mapped extent is shown in figure 2.7c. Like reflection **L**, **M** and **M'** are also folded by the Clam Bank syncline (Figure 2.4a, b). **M** is projected to surface and intersects the aeromagnetic map along the entire western boundary of *l* (Figure 2.3) and corresponds to a stratigraphic position close to the top of the mapped succession of Misty Point Formation. It is referred herein as the “near-top Misty Point Formation reflection” (Figure 2.7). **M'** is a distinctive reflection above **M** but cannot be correlated with any major geological boundary on land.

Reflections **C** and **C'** are observed as the base and top of a set of four mutually parallel peak reflections (Figure 2.4a, b). Both reflections are also folded into the same open, west-facing synform as **M** and **L**. Projected to the aeromagnetic map, **C** correlates everywhere with the western boundary of *c1* (Figure 2.3), near the top of the exposed Clam Bank succession mapped onshore (Quinn et al. 1999). We therefore refer to **C** as the “near-top Clam-Bank Formation reflection”. **C'** is a distinctive reflection that sits stratigraphically above **C**, but because it does not correlate to any onshore geologic contact, we cannot correlate it with a specific formation or lithologic boundary.

Along the western parts of all profiles reflections are dominantly sub-parallel and continuous, reflecting the stratified nature of the geology. On the eastern portion of the Mobil dip-direction profiles, however, this stratified character breaks down (Figure 2.4). Boundaries **T** and **B** separate a region of discontinuous reflections from stratified reflections (Figure 2.4a, b). **T** is parallel to and below **L**. Boundary **B** is sub-parallel to and above **P**. **T** and **B** converge westward to a tip-point, forming an overall wedge shape. This structure is the “triangle zone” or tectonic wedge identified by Stockmal and Waldron (1990).

2.7.2. Seismic Reflection Packages

The geologic boundaries (**P**, **L**, **M**, **C**, **R**, **T** and **B**) described above bound six distinct seismic reflection packages: *p*, *g*, *w*, *l*, *c1*, *c2* (Figure 2.4). Three boundaries, **L**, **M** and **C** (Figure 2.4) are correlated to the boundaries previously identified on the aeromagnetic map (Figure 2.3) and they bound reflection packages (*l*, *c1* and *c2*) also identified on Figure 2.3.

2.7.2.1. Package *p*: Platform Reflections

Below **P** is reflection package *p* (Figures 2.4 and 2.6), a set of mutually parallel (to **P**) reflections which generally dip to the southeast (at about 1-3°), increasing in inclination towards the coastline. The thickness of package *p* in two-way travel time (TWT) is relatively constant.

The reflections however, are repeatedly offset in TWT, disrupting lateral continuity. The offsets occur along lineaments which we interpret as faults that have steep apparent dips (Figures 2.4 and 2.6). Offset is dominantly in a normal sense, but reverse faults are also observed. Offset (or apparent dip-slip) amounts range from tens to hundreds of meters, with greater offset towards the tectonic wedge. Despite the difficulty in correlating faults between 2D profiles which are spaced kilometres apart, some correlations were able to be made. Faults are observed more frequently along dip-direction profiles and more rarely along strike-lines, indicating that faults are dominantly oriented at a low angle to the trend of the basin. The majority of faults strike NE and fewer strike NW (Figure 2.7a). NW-striking faults cross-cut the more numerous NE-striking structures.

2.7.2.2. Packages *w* and *g*: Tectonic Wedge and Goose Tickle Group

Reflection package *w* is a distinct set of discontinuous, poorly defined reflections bounded by faults **T** and **B** (Figure 2.4a, b). Package *w* has an overall wedge shape, thickest in the east and thinning westward to a tip (Figure 2.4a,b). Variable dips and cross-cutting relationships of reflections within *w* suggest structural complexity. It is interpreted as the tectonic wedge recognized by Stockmal and Waldron (1990) which contains rocks of the Humber Arm Allochthon.

Reflections in package *g* are sub-parallel to **L** (the Lourdes Formation reflection) and onlap **P** (the top of platform reflection) to the west and south (Figures 2.4 and 2.6). We interpret *g* as the Goose Tickle Group.

Offshore of the Port au Port Peninsula, we trace *g* east to where it pinches out above the wedge, near the tip (Figure 2.4b). In this region, **T** represents the Tea Cove thrust (Stockmal & Waldron 1990) and sits directly below the Lourdes Formation (Figure 2.4a). However, north of the Port au Port Peninsula, we can trace reflections *g* atop the wedge, where they are bounded by **T** at the base and **L** at the top (Figure 2.4b). Goose Tickle Group reflections thin to the east above the wedge. Below the wedge, it is evident that package *g* lies atop down-dropped blocks of the platform *p* (Figure 2.4b).

The isochron map for *g* (Figure 2.8a) is generated by subtracting the wedge from the total thickness of *g* calculated between **P** and **L**. The map demonstrates thickness variations along and across the trend of the basin (Figure 2.8a). West of the tip of the wedge, the Goose Tickle Group generally thins westward (Figure 2.4a, b). Offshore of Port au Port Peninsula the unit is relatively thin, at about 200 m (~100 ms TWT: Figure 2.8a), reaching a zero net thickness where **L** onlaps the platform (Figure 2.8a). The thickness increases northeastward to ~ 670 m offshore of the Bay of Islands (~ 300 ms TWT: Figure 2.8) but may reach thicknesses of ~2000 m north of Bonne Bay (~900 ms TWT: Figure 2.8). However, there is uncertainty in thickness estimates north

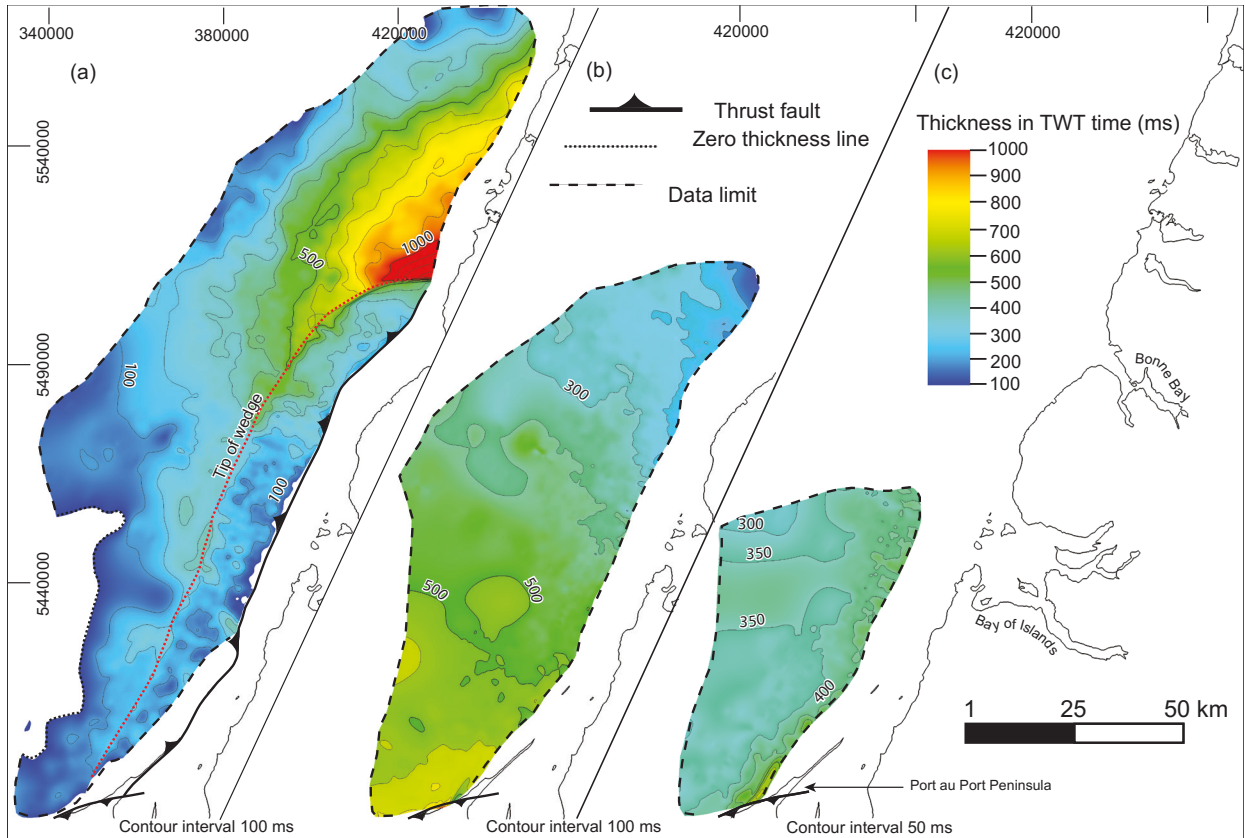


Figure 2.8: TWT isochron maps. (a) Goose Tickle Group *g* (minus tectonic wedge), (b) Long Point Group *l* and (c) basal portion of the Clam Bank Formation *cI*.

of Bonne Bay, as picks for **L** are speculative in this region. Estimates south of Bonne Bay are consistent with previous thickness estimates for the Goose Tickle Group strata in the Port au Port region which range from < 225 m, based on seismic interpretations (Stockmal et al. 1995), to 622 m, based on outcrop studies (Quinn 1992). This northward thickening trend has previously not been recognized. Offshore of Bonne Bay, a thickness of ~ 680 m over a period of 4 Myr (Figure 2.2) implies an average sedimentation rate for the Goose Tickle Group of at least 0.17 km/Myr, which may have reached 0.50 km/Myr (as indicated by possible thicknesses of ~ 2000 m north of Bonne Bay). Because these units were deposited below sea level, in a succession that began in shallow water, subsidence rates must have been at least this fast.

To the north of Bonne Bay, poor seismic quality leads to poor control on horizon picks. Reflections above **P** are relatively continuous and stratified, dipping and tapering westward (Figure 2.4c: line c-c'); no tectonic wedge is imaged. Reflections are folded (into low amplitude, open to gentle folds) and progressively steepen eastward from 01° to 06° (Figure 2.4c).

2.7.2.3. Package l: Long Point Group

Reflection package *l* is a sub-parallel package of reflections bounded by **L** and **M** (Figure 2.4) that corresponds to the Upper Ordovician Long Point Group. The most conspicuous thickness variations occur north to south (Figure 2.8). In the south, the thickness of the Long Point Group is estimated at about 1500 m (TWT ~ 680 ms), consistent with Quinn et al. (1999) who estimate a minimum thickness of 1325 m from outcrop. Offshore of Bonne Bay, the thickness decreases to less than 450 m (TWT ~ 200 ms) (Figure 2.8). Because the Long Point Group is dominantly shallow marine, we can use sedimentation rate as a proxy for subsidence rate and estimate a subsidence rate of ~ 0.17 km/Myr based on 1500 m of sediment over an estimated depositional period of 9 Myr (Figure 2.2). Offshore of the Port au Port Peninsula, *l* is folded into the Clam Bank syncline. The thickness of *l* remains constant along both limbs of the fold (Figure 2.4). North of the Bay of Islands, *l* appears to thin eastward above the Tea Cove thrust (Figures 2.4b).

2.7.2.4. Packages c1, c2 and r: Clam Bank and Red Island Road Formations

Package *c1* is bounded at its base by **M** and at its top by **C**. Internal reflections in *c1* are sub-parallel (Figure 2.4), indicating that these rocks are also stratified. These reflections are also folded by the Clam Bank syncline. Reflections *c1* are interpreted to represent the Clam Bank Formation. The thickness of reflection package *c1* is approximately 780 m (TWT ~ 350 ms) offshore of the Port au Port Peninsula (Figure 2.8), which is reasonably consistent with previous estimates of at least 620 m for the Clam Bank Formation (Williams et al. 1996) using outcrop

measurements. An isochron map of *c1* suggests that minor thickness variations occur east to west (Figure 2.8).

Above **C** is reflection package *c2* (Figure 2.4). Using bathymetric data (Figure 2.5) the upper boundary of *c2* is placed at boundary **R**, the near-base Red Island Road Formation anomaly (Figure 2.3). **R** does not correlate with a mappable reflection on seismic profiles; therefore, an isochron map was not made for *c2*. However, a position for **R** is estimated by following the apparent dip of deeper reflections on seismic profiles (Figure 2.4a and 2.6). Geologic units represented by *c2* do not correlate with any onshore strata but must lie between Clam Bank Formation and exposed Red Island Road Formation offshore. These strata therefore represent a thick succession of foreland basin sediments, ~ 550 m thick offshore of the Port au Port Peninsula (TWT~ 250 ms), which has previously not been recognized. Imagery and seismic observations suggest that *c2* is in stratigraphic contact with underlying *c1* with no angular unconformity. Reflections within *c2* are also folded into the Clam Bank syncline. We speculate that *c2* may represent a stratigraphically higher portion of the Clam Bank Formation that does not crop out anywhere on land. Together, thicknesses of *c1* and *c2* correspond to a total thickness of ~1275 m, almost twice the previous thickness estimate.

Above **R** is the stratified reflection package *r*, though interference from seafloor multiples make it difficult to resolve its reflection characteristics (Figure 2.4a). It is correlated with the Red Island Road Formation. The top of the Red Island Road Formation coincides with the present erosion surface. An estimated minimum thickness for the Red Island Road Formation is ~ 670 m (TWT ~ 300 ms), much greater than a previous minimum estimate of 100 m (Quinn et al. 2004). Reflections *r* may be folded and occupy the core of the Clam Bank syncline (Figure 2.4a).

2.8. Discussion

2.8.1. Foreland Basin Types

The earliest collisions along the length of the northern Appalachians involve east-dipping subduction of the Laurentian margin beneath obducted allochthons (Williams 1975, Stanley & Ratcliffe 1985), implying that the Goose Tickle Group was deposited in a pro-arc setting. Tectonic models of Appalachian evolution in Newfoundland indicate that subduction polarity reversal at ~ 460 Ma (van Staal 2007, Zagorevski et al. 2009) placed the Laurentian craton on the upper plate by the Late Ordovician, implying the Long Point Group was deposited in retro-arc basin.

The geometry and subsidence history of foreland basins provide detailed information regarding the tectonic history of an orogen. These variables are largely controlled by the position of the orogenic load along the orogen and position of the developing basin atop either the

subducting (pro-arc basin) or overriding lithospheric plate (retro-arc basin). In a pro-arc basin, lithospheric flexure and associated subsidence is largely controlled by the tectonic load of the orogen (Beaumont, 1981; Jordan, 1981) and subsidence rates are high (> 0.05 km/Myr) (Sinclair & Naylor 2012). In retro-arc settings dynamic subsidence, related to both subduction-induced corner flows and gravitational pull of the down-going slab (Catuneanu 2004), counteracts flexural effects of orogenic loading (Catuneanu 2004) and subsidence rates are generally much slower at < 0.05 km/Myr (Sinclair & Naylor 2012). Regardless of current tectonic models of Appalachian evolution, our results indicate that the geometry and subsidence history of the Upper Ordovician Long Point Group are not consistent with development as a retro-arc basin developed as a result of loading from the Newfoundland segment of the orogen to the east.

2.8.2. Dapingian to Early Darriwilian (470-465 Ma)

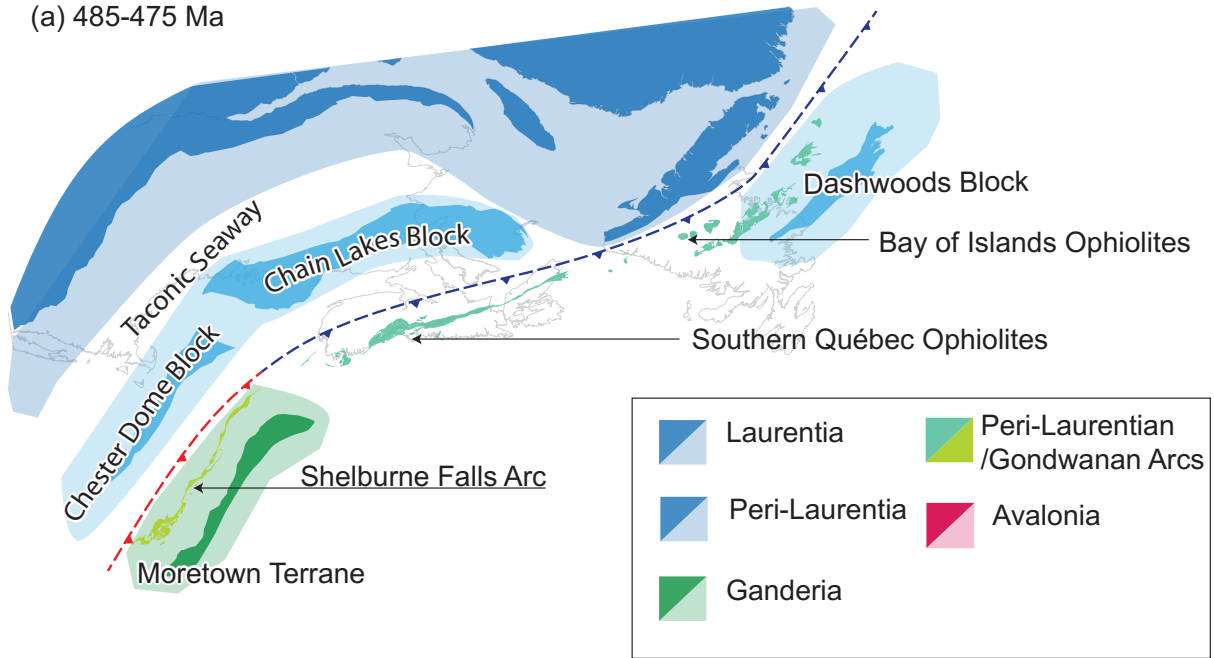
The base of the foreland succession in Newfoundland is defined by an extensive unconformity interpreted to result from a regional uplift due to the passage of a peripheral bulge (Jacobi 1981). Westward propagation of the peripheral bulge, associated with east-dipping subduction, has been inferred by previous workers (Knight et al. 1991, Dix et al. 1998, Salad Hersi et al. 2003). This study compiles biostratigraphic data from previously published sources (Figure 2.2) and suggests northwestward (with respect to present day coordinates) migration of the Taconian peripheral bulge. For example, in Québec, the Beekmantown and post-Romaine unconformities are the same age, ~ 462.5 Ma, and slightly younger than the ~ 465 Ma St. George unconformity in Newfoundland (Figure 2.2) implying that the axis of the bulge at 462.5 Ma trended northeast-southwest with respect to present day coordinates (Figure 2.9).

2.8.3. Later Darriwilian Events (465-458 Ma)

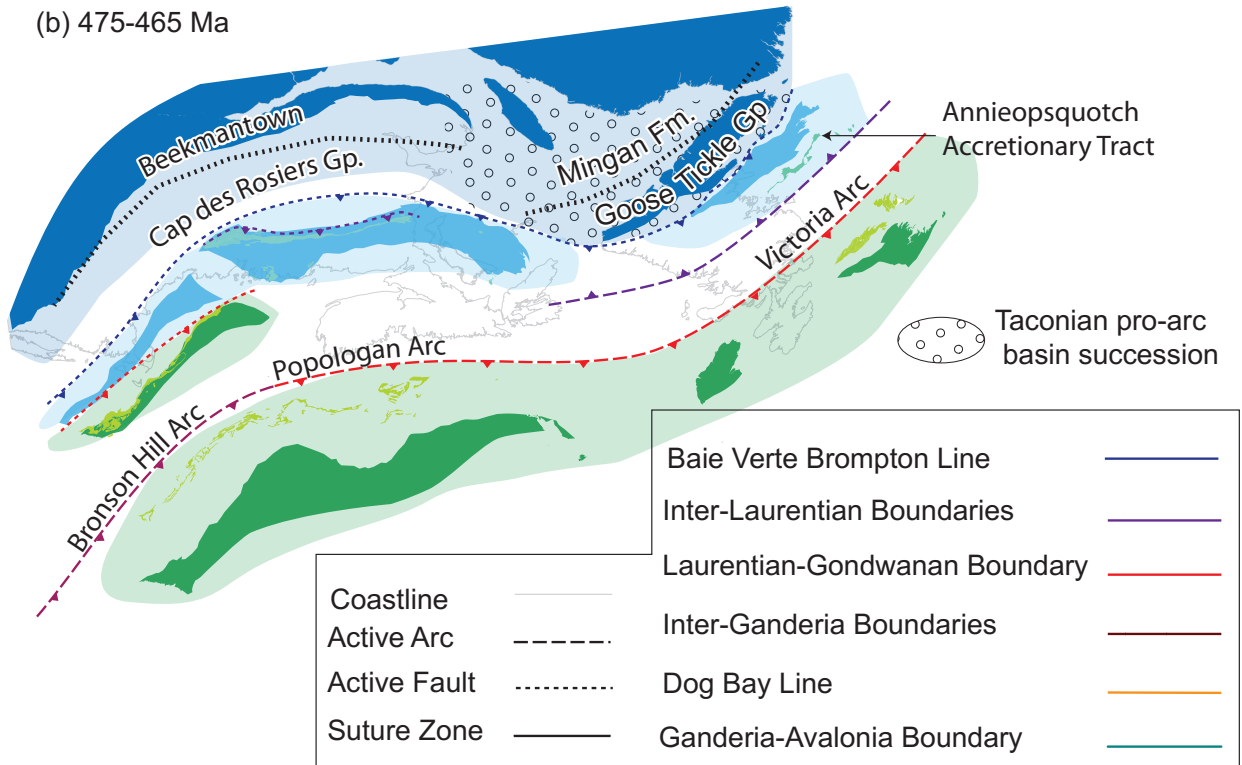
2.8.3.1. Geometry and Facies Variations of the Goose Tickle Group

Our observations of the overall geometry of the Goose Tickle Group – the orogen-parallel nature of the basin, and the general westward thinning and onlap of reflection package *g* atop the platform – support the interpretations of Stevens (1970) and Quinn (1992) that the Goose Tickle Group represents the foredeep of a foreland basin filled by sediments that were derived from the Newfoundland portion of the orogen. Our new observations demonstrate that the Goose Tickle Group also displays along-strike variability, thinning dramatically southwards (Figure 2.8a). The thinning trend was not generated by post-deposition differential uplift and erosion because reflections *g* are not visibly truncated at **L**. Along-strike thickness variations therefore most likely indicate greater orogenic loading in northern portions of the Newfoundland Appalachians. Dominant southwest-directed paleocurrent indicators reported by Quinn (1992) and Batten

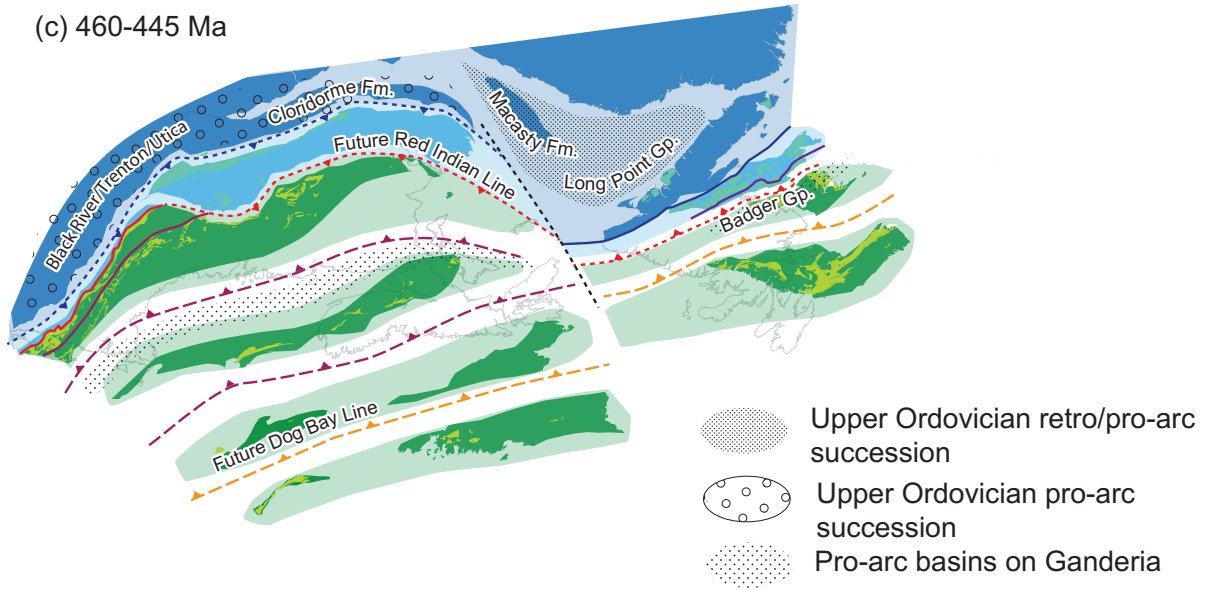
(a) 485-475 Ma



(b) 475-465 Ma



(c) 460-445 Ma



(d) 430-420 Ma

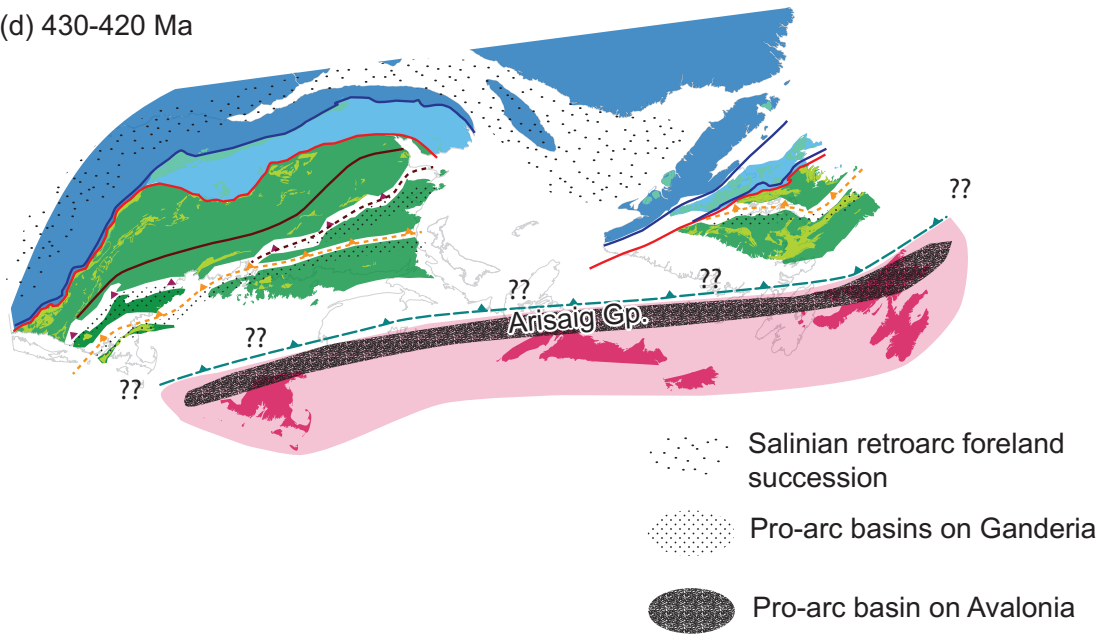


Figure 2.9: Tectonic configuration of Laurentian and Gondwanan components in the northern Appalachians and associated foreland basin development at (a) 485-475 Ma, (b) 475-465 Ma, (c) 460-445 Ma, and (d) 430-420 Ma.

Hender and Dix (2008) also imply that sediments were sourced from the orogenic load which lay to the north.

However, to fully understand the position of tectonic loads during basin development, we must consider the effects of late Paleozoic strike-slip faults. A palinspastic reconstruction of the northern Appalachians by Waldron et al. (2015) shows the inferred positions of northern Appalachian terranes at ~370 Ma. The restoration places the Dashwoods block ~250 km north of its present-day position (Figure 2.9). The Dashwoods block could therefore have been both a source of Goose Tickle sediments and a cause of the north-directed tilt of the foredeep.

Facies variations within the Goose Tickle Group indicate that subsidence was controlled by large faults, in addition to distributed flexure. The most obvious indication of faulting is a distinctive limestone conglomerate facies (Daniels Harbour Member), with clasts derived almost entirely from the Table Head Group (Stenzel et al. 1990) exposed mainly in the immediate hanging walls of steep deep-seated faults (Stockmal et al. 2004). Middle Ordovician extension on these faults played a role in generating accommodation space for the earliest foredeep deposits (Palmer et al. 2002, Stockmal et al. 2004).

Orientations (and cross-cutting relationships) of the Middle Ordovician faults measured in this study (Figure 2.7a) match those of the St. Lawrence rift system in Québec (Tremblay et al. 2003) and mimic an even larger scale geometry of promontories and embayments on the Laurentian margin defined by northeast-trending rifts, offset by northwest-striking transfer faults (Thomas 1977, Allen et al. 2010). We interpret that these faults, which offset basement and platform rocks, are reactivated faults that were originally related to Neoproterozoic to Cambrian opening of the Iapetus.

Facies stratigraphically higher in the Goose Tickle Group reflect the variability of sources in the foreland basin system. On the Port au Port Peninsula, a succession ~ 250 m thick (Lacombe 2017) of the Goose Tickle Group partly overlies rocks of the Humber Arm Allochthon. Within this succession are compositionally and texturally immature shale-chip conglomerates, a rare facies within the Goose Tickle Group, indicating deposition close to the leading edge of the allochthon. Combined with observations from seismic (Figure 2.4b), that indicate that the Goose Tickle Group lies on top of the tectonic wedge, we interpret that portions of the Goose Tickle Group may have been deposited in the wedge-top depozone (DeCelles & Giles 1996).

2.8.3.2. Regional Tectonic Setting of the Foreland Basin

In Québec, the Darriwilian Tourelle Formation (Figure 2.2), the upper portion of which is time-correlative with the Goose Tickle Group, contains detritus sourced from allochthons (Hiscott 1978), and represents the oldest Middle Ordovician foreland basin fill (Figure 2.2). However, the unit lies conformably above deeper-water strata now structurally incorporated

into allochthons on the Gaspé Peninsula (Hiscott 1978). This implies that a deep-water seaway (Taconic Seaway), overlying the Laurentian slope and rise, must have been open during the Middle Ordovician (at least until ~ 461 Ma) in Québec (Figure 2.9b) while in Newfoundland stratigraphic relationships indicate closure of the equivalent seaway by this time (Figure 2.9b). This also implies that obduction of the southern Québec ophiolites at approximately 477 Ma (Tremblay & Castonguay 2002) occurred outboard of the Laurentian margin, onto a Laurentian microcontinental block, here referred to as the Chain Lakes block (Figure 2.9b). Diachronous, non-orthogonal collisions along the margin (Waldron et al. 2014) may also explain the very early (~475 Ma) interaction of Laurentian and Gondwanan components observed in New England (Macdonald et al. 2014). In our interpretation, these interactions occurred outboard of the Laurentian margin before closure of the Taconic Seaway (Figure 2.9a).

2.8.4. Sandbian to Katian (~458-445 Ma)

2.8.4.1. Geometry and Facies Variations in the Long Point Group

Previous work on the Long Point Group by Stockmal et al. (1995) and Quinn et al. (1999) implies that Late Ordovician subsidence was due to loading by the Newfoundland Appalachians; however, our observations suggest that the Late Ordovician foreland basin had a very different geometry from the Middle Ordovician basin in which the Table Head and Goose Tickle groups accumulated.

Within the Long Point Group, only the basal Lourdes Formation shows onlap onto the platform to the west, in addition to possible eastward onlap onto the Goose Tickle Group and/or Humber Arm Allochthon (Figure 2.4). The Lourdes Formation is interpreted to have been deposited during a period of quiescence, in which facies variations and geometry reflected eustatic changes (Batten Hender & Dix 2008). Batten Hender & Dix (2006) describe coral bioherms, with approximate NNW-SSE orientations, within a restricted interval of the Lourdes Formation, and interpret this to represent progradational bioherm growth to the northwest. Those onlap relationships and bioherm orientations suggest that the paleo-shoreline, at the time of Lourdes deposition, trended NE, sub-parallel to the present-day coastline. However, the significant amplitude decrease in reflection L, north of the Bay of Islands (Figure 2.4b and 2.6), implies that the carbonate facies of the Lourdes Formation may pass northwards into clastic rocks, which suggests that the southern portion of the basin was shallower than the north, similar to the earlier Goose Tickle basin. Therefore, the basal Lourdes Formation possibly filled residual topography left after Middle Ordovician development of the Goose Tickle basin, which was flooded as a result of Late Ordovician sea-level rise.

Bioherm trends change up-section within the Lourdes Formation, from a dominant NW-trend to an approximate N-trend (George Dix, Carlton University, personal communication, May 2012), suggesting a change in basin geometry, consistent with shallowing to the north. Figure 2.8b shows that dominant thickness variations in the overlying Winterhouse and Misty Point formations, the bulk of the Long Point Group, occur along the trend of the basin, not perpendicular to it. Southward thickening implies that the load generating accommodation for the siliciclastic units was to the south, not east of the basin. Prominent NE-directed unidirectional paleocurrents (Batten Hender & Dix 2008) suggest a southern source for Winterhouse/Misty Point detritus. Quinn et al. (1999) suggest that Long Point Group detritus is compositionally similar to that of the Goose Tickle Group and may also be sourced from Taconian allochthons; however, Taconian allochthons in Newfoundland and Québec have similar overall compositions and could equally have been the source of the Long Point Group detritus. In combination, the geometry and provenance of the Long Point Group is consistent with derivation from allochthons farther south, potentially as distant as the Gaspé Peninsula. Therefore, the allochthons in the Québec Appalachians could have provided both the flexural load and source of detritus for the Long Point basin.

Minor thinning of the Long Point Group above the wedge is observed north of the Bay of Islands (Figure 2.4b) but suggests syntectonic deposition or onlap of Upper Ordovician strata during wedge emplacement. Therefore, like the Goose Tickle Group, portions of the Long Point Group may also have been deposited in the wedge-top depozone and the Tea Cove thrust (Figure 2.4) may represent a thrust-modified unconformity.

2.8.4.2. Regional Tectonic Setting of the Foreland Basin

Previous Late Ordovician tectonic reconstructions of the Newfoundland Appalachians (Zagorevski et al. 2007, van Staal et al. 2009) imply that the Long Point Group was deposited, after subduction polarity reversed, in a retro-arc setting. However, our estimated subsidence rate of ~ 0.17 km/Myr for the Upper Ordovician foreland basin is more comparable to subsidence rates of pro-arc basins (Sinclair & Naylor 2012).

Previous workers have suggested that the autochthonous Upper Ordovician foreland basin in Québec (Laval/ Chazy groups: Dix et al. 2013) was also deposited in a retro-arc setting based on tectonic models of Karabinos et al. (1998) and Moench and Aleinkoff (2003) who interpreted a west-dipping subduction zone beneath the Laurentian margin at this time. However, Upper Ordovician foredeep strata (Deslandes and Cloridome formations, Figure 2.2, Figure 2.9c) are incorporated into thrust sheets of the overriding allochthon in Québec, suggesting that east-dipping subduction of the Laurentian plate continued until ~ 450 Ma, the age of the Cloridome Formation. Oldest units of the unconformably overlying fore-arc basin (Matapédia basin)

contain graptolites of the *Climacograptus spiniferus* biozone, the same zone as those in the Cloridorme Formation, effectively constraining subduction polarity reversal at ~ 450 Ma in the timescale of Cooper et al. (2012). Because allochthons were still loading the Laurentian margin until ~450 Ma, the Upper Ordovician foreland succession in Québec was deposited in a pro-arc setting. The Québec allochthons also loaded the Upper Ordovician basin in Newfoundland along its southern margin, placing the Long Point Group in a hybrid pro-arc and retro-arc setting (Figure 2.9c).

The combined retro and pro-arc setting of the Long Point Group, shown in Figure 2.9c, is interpreted as a consequence of the irregular margin shape, analogous to the present-day plate boundary configuration in northern Australia near Papua New Guinea. The Indo-Australian Plate is simultaneously being subducted beneath the Sunda Plate along the Timor Trough (Tate et al. 2015) and overthrust above the Pacific Plate along the New Guinea Trench (Haddad & Watts 1999), placing the Australian plate in a combined pro-arc and retro-arc setting in this region (Figure 2.10). Figure 2.10 demonstrates that the northwestern margin of the Australian plate resembles a mirror image of the Laurentian margin and that the present tectonic configuration along this portion of the Australian margin (Figure 2.10b) is much like that proposed for the Late Ordovician in Newfoundland (Figure 2.10a). The foreland basin developing on the Australian plate is in a hybrid retro and pro-arc setting (Figure 2.10b), similar to the hybrid setting proposed for the Long Point Group in Newfoundland (Figure 2.10a).

2.8.5. Katian-Pridoli Events

The Katian to Pridoli Clam Bank unconformity suggests either an extensive period of non-deposition or major uplift and erosion prior to deposition of the Clam Bank succession. The Late Ordovician was a tectonically complex time, during which subduction polarity reversal (Zagorevski et al. 2009) eventually placed the Anticosti Basin in an upper-plate retro-arc setting. Closure of a seaway between composite Laurentia and Ganderia also began at ~ 450 Ma and continued until the Wenlock suturing of Ganderia with Laurentia (Pollock et al. 2007) along the Dog Bay Line (Williams et al. 1993) in Newfoundland. Following accretion of the final Ganderian fragment to the Laurentian margin, break-off of the west-dipping subducting slab occurred (Whalen et al. 2006, van Staal et al. 2009). Whalen et al. (2006) use temporal and compositional variations in magmatism to constrain break-off at ~ 433 – 425 Ma. It is likely that the Clam Bank unconformity represents a period of uplift and erosion following slab break off of the west-dipping subducting slab that was associated with Salinian orogenesis.

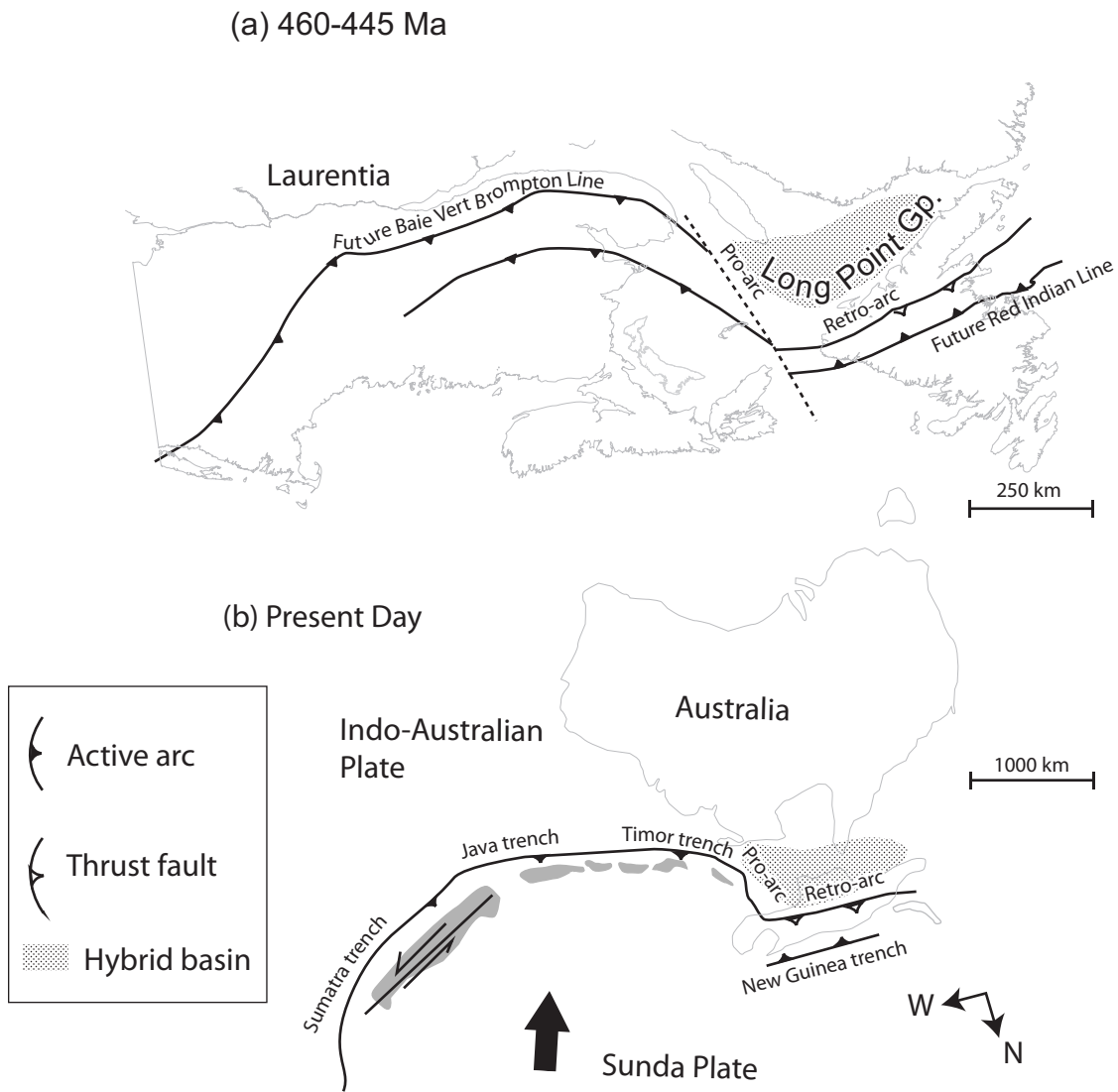


Figure 2.10: (a) Plate boundary configuration of the eastern Laurentian margin in the Late Ordovician. (b) Mirror image of Australia demonstrating the present day plate boundary configuration along the Timor and New Guinea trench.

2.8.6. Likhovian to Emsian

2.8.6.1. Geometry and Facies Variations in the Clam Bank-Red Island Road Formations

The Clam Bank – Red Island Road succession of the foreland basin transitions from shallow-marine to dominantly terrestrial, indicating the basin was in an overfilled stage, where sediment supply outpaced accommodation. Slow subsidence and/or rapid supply could account for the observed facies. The constant thickness (i.e.: lack of asymmetry) observed indicates that the Clam Bank Formation was deposited as an extensive siliciclastic blanket. Together, the geometry and facies imply that the basin was broad and its fill was approximately tabular. By the time the Clam Bank – Red Island Road succession was deposited, the lithosphere below the basin was likely cooler and stronger than it was in the Ordovician, the orogenic load was spread out over a great area, and the locus of tectonism was far removed from the developing basin. All these factors likely contributed to the development of the shallow, broad basin observed.

There are no local sources for the volcanic clasts within the Red Island Road Formation, implying either the source region has been eroded away or displaced by later fault movement. Limited paleocurrent data (Quinn et al. 2004) also suggest that the source region was east of the present-day position of the basin. The source of these clasts will be considered in Chapter 4.

2.8.6.2. Tectonic Setting of the Foreland Basin

The onset of sedimentation of the Clam Bank Formation (~ 423 Ma) follows final collision of Ganderia with Laurentia (Pollock et al. 2007) and overlaps in time only with the trailing end of Salinian orogenesis (440-420 Ma) and the first half of the 421-400 Ma Acadian Orogeny. It is therefore likely that these sediments were sourced from erosion of the orogen formed during the collision of Avalonia with Laurentia and represent the early part of the Acadian foreland basin. The Acadian Orogeny involved west-dipping subduction of Avalonia beneath the Laurentian margin (van Staal et al. 1998) placing the foreland basin in a retro-arc setting, where subsidence rates are predicted to have been slow compared to pro-arc settings . This may explain the absence of a deep-marine facies at the base of the Clam Bank Formation. The marginal marine to terrestrial Red Island Road Formation, overlapping in time with the second half of the Acadian Orogeny, represents the overfilled stage of the Acadian retro-arc basin. A restoration of Appalachian terranes prior to Carboniferous movements by Waldron et al. (2015) suggests the Aspy terrane of Cape Breton Island lay directly east of the present day position of the Port au Port Peninsula. This terrane contains abundant 430-375 Ma plutons (Lin et al. 2007) that are age equivalent and compositionally similar to rhyolitic cobbles within rocks

of the Red Island Road Formation (G. Dunning, Memorial University, personal communication, 2013). In Chapter 4 we will investigate whether these plutons could be the roots or feeders to the volcanic rocks which were eroded into the Acadian foreland basin.

The folding and constant thickness of foreland basin sediments above the wedge offshore of the Port au Port Peninsula indicate that sedimentation occurred prior to insertion of the tectonic wedge to its current structural position (i.e. Emsian or later). It is therefore likely that emplacement of the tectonic wedge, offshore of the Port au Port Peninsula, occurred later than it did in the Bonne Bay region, and is associated with the Acadian Orogeny.

2.9. Conclusions

The foreland basin in western Newfoundland developed as a pro-arc basin above an east-dipping subduction zone during Taconian continent-arc collision (Figure 2.9b). Taconian collision was diachronous, as suggested by facies variations along the length of the pro-arc basin. The earliest non-orthogonal collisions along the margin occurred in the south, explaining the very early (~475 Ma) interaction of Laurentian and Gondwanan components observed in New England. During this time, Taconian (~ 477 Ma) obduction of the southern Québec ophiolites occurred outboard of the Laurentian margin, on the Chain Lakes block. In Newfoundland, the collision of the Dashwoods microcontinent with the Laurentian margin (~ 470 Ma: Waldron & van Staal 2001) led to the closure of a small seaway within the Iapetus and obduction of oceanic rocks along the suture zone. The Humber Arm and Hare Bay allochthons were thrust atop passive margin sedimentary rocks during the Taconian Orogeny. The seaway separating the Chain Lakes block from the Laurentian margin existed until ~461 Ma. However, Taconian orogenesis, involving the obduction of allochthonous slices, continued until ~450 Ma in Québec.

Diachronous subduction polarity reversal led to the unique tectonic setting in which the Upper Ordovician Long Point Group was deposited, which has combined aspects of both retro and pro-arc settings, similar to that of the present day tectonic scenario of parts of the northeastern Australian continental margin. The Upper Ordovician basin was generated from loading in the Québec Appalachians, where allochthons on the Gaspé Peninsula provided both the orogenic load and source of detritus. Therefore, pro-arc processes related to the continuing arc-continent obduction until ~450 Ma in the Québec Appalachians were more important than retro-arc processes in generating subsidence and accommodation in the Long Point Group basin.

The Clam Bank unconformity occurred following, and likely results from, slab break-off of the west-dipping Salinian subducting slab. The (440-422 Ma) Salinian Orogeny was immediately followed by the Late Silurian to Early Devonian (421-400 Ma) Acadian Orogeny which overlapped in time with deposition of both the Clam Bank and Red Island Road

formations. It is therefore interpreted that this succession represents the Acadian retro-arc foreland basin in Newfoundland.

2.10. References

- ALLEN J. S., THOMAS W. A. & LAVOIE D. 2010. The Laurentian margin of northeastern North America. In: *From Rodinia to Pangea: The Lithotectonic Record of the Appalachian Region* (Ed. by R. P. Tollo, M. J. Bartholomew, J. P. Hibbard & P. M. Karabinos), pp. 71–90.
- BATTEN HENDER K. L. 2007. Mixed siliciclastic-carbonate ramp sediments and coral bioherms of the Late Ordovician Lourdes Formation, western Newfoundland: Sedimentology, stratigraphy, and tectonic significance. PhD Thesis, Carleton University, Ottawa.
- BATTEN HENDER K. L. & DIX G. R. 2006. Facies, geometry and geological significance of Late Ordovician (early Caradocian) coral bioherms: Lourdes Formation, western Newfoundland. *Sedimentology* 53: 1361–1379.
- BATTEN HENDER K. L. & DIX G. R. 2008. Facies development of a Late Ordovician mixed carbonate-siliciclastic ramp proximal to the developing Taconic orogen: Lourdes Formation, Newfoundland, Canada. *Facies* 54: 121–149.
- BEAUMONT C. 1981. Foreland basins. *Geophysical Journal International* 65: 291–329.
- BIRD J. M. & DEWEY J. F. 1970. Lithosphere plate-continental margin tectonics and the evolution of the Appalachian orogen. *Geological Society of America Bulletin* 81: 1031–1060.
- BOSWORTH W. 1989. Mélange fabrics in the unmetamorphosed external terranes of the northern Appalachians. In: *Melanges and Olistostromes of the U.S. Appalachians* (Ed. by J. W. Horton & N. Rast), pp. 65–92. Geological Society of America.
- BOTSFORD J. W. 1987. Depositional history of Middle Cambrian to Lower Ordovician deep water sediments, Bay of Islands, western Newfoundland. PhD Thesis, Memorial University of Newfoundland.
- BRADLEY D. C. 1983. Tectonics of the Acadian orogeny in New England and adjacent Canada. *The Journal of Geology* 91: 381–400.
- BRADLEY D. C., TUCKER R. D., LUX D. R., HARRIS A. G. & MCGREGOR D. C. 2000. Migration of the Acadian orogen and foreland basin across the northern Appalachians of Maine and adjacent areas. *U.S. Geological Survey Professional paper* 1624: 49.
- BURDEN E. T., QUINN L., NOWLAN G. S. & BAILEY-NILL L. A. 2002. Palynology and micropaleontology of the Clam Bank Formation (Lower Devonian) of western Newfoundland, Canada. *Palynology* 26: 185–215.
- BURDEN E. T. & WILLIAMS S. H. 1995. Biostratigraphy and thermal maturity of strata in Hunt-Pan Canadian Port au Port well # 1. Hunt oil, St. John's Newfoundland.

- CASTONGUAY S., RUFFET G., TREMBLAY A. & FÉRAUD G. 2001. Tectonometamorphic evolution of the southern Quebec Appalachians: $^{40}\text{Ar}/^{39}\text{Ar}$ evidence for Middle Ordovician crustal thickening and Silurian–Early Devonian exhumation of the internal Humber zone. *Geological Society of America Bulletin* 113: 144–160.
- CASTONGUAY S., VAN STAAL C. R., JOYCE N., SKULSKI T. & HIBBARD J. P. 2014. Taconic Metamorphism Preserved in the Baie Verte Peninsula, Newfoundland Appalachians: Geochronological Evidence for Ophiolite Obduction and Subduction and Exhumation of the Leading Edge of the Laurentian (Humber) Margin During Closure of the Taconic Seaway. *Geoscience Canada* 41: 459.
- CATUNEANU O. 2004. Retroarc foreland systems-evolution through time. *Journal of African Earth Science* 38: 225–242.
- CAWOOD P. A. 1993. Acadian orogeny in west Newfoundland: Definition, character, and significance. In: *The Acadian Orogeny: Recent studies in New England, maritime Canada, and the autochthonous foreland* (Ed. by D. C. Roy, J. W. Skehan), Geological Society of America Special Papers 275: 135–152.
- CAWOOD P. A., DUNNING G. R., LUX D. & VAN GOOL J. A. M. 1994. Timing of peak metamorphism and deformation along the Appalachian margin of Laurentia in Newfoundland: Silurian, not Ordovician. *Geology* 22: 399–402.
- CAWOOD P. A., MCCAUSLAND P. J. & DUNNING G. R. 2001. Opening Iapetus: Constraints from the Laurentian margin in Newfoundland. *Geological Society of America Bulletin* 113: 443–453.
- CAWOOD P. A. & WILLIAMS H. 1988. Acadian basement thrusting, crustal delamination, and structural styles in and around the Humber Arm allochthon, western Newfoundland. *Geology* 16: 370.
- CHOW N. & JAMES N. P. 1987. Cambrian Grand Cycles: A northern Appalachian perspective. *Geological Society of America Bulletin* 98: 418.
- COOPER M., WEISSENBERGER J., KNIGHT I., HOSTAD D., GILLESPIE D., WILLIAMS H., BURDEN E., PORTER-CHAUDHRY J., RAE D. & CLARK E. 2001. Basin evolution in western Newfoundland: new insights from hydrocarbon exploration. *AAPG bulletin* 85: 393–418.
- COOPER R. A., SADLER P. M., HAMMER O. & GRADSTEIN F. M. 2012. The Ordovician Period. In: *The Geologic Time Scale* (Ed. by F. M. Gradstein, J. G. Ogg, M. Schmitz & G. Ogg), pp. 489–523. Elsevier.
- COURTNEY R. C. 2013. Canada GEESE 2: Visualization of Integrated Marine Geoscience Data for Canadian and Proximal Waters. *Geoscience Canada* 40: 141.
- DE SOUZA S., TREMBLAY A., RUFFET G. & PINET N. 2012. Ophiolite obduction in the Quebec Appalachians, Canada. *Canadian Journal of Earth Sciences* 49: 91–110.

- DECELLES P. G. 2011. Foreland basin systems revisited: Variations in response to tectonic settings. *Tectonics of Sedimentary Basins: Recent Advances: New York, John Wiley & Sons*: 405–426.
- DECELLES P. G. & GILES K. A. 1996. Foreland basin systems. *Basin research* 8: 105–123.
- DIETRICH J., LAVOIE D., HANNIGAN P., PINET N., CASTONGUAY S., GILES P. & HAMBLIN A. 2011. Geological setting and resource potential of conventional petroleum plays in Paleozoic basins in eastern Canada 59: 54–84.
- DIX G. R., NEHZA O. & OKON I. 2013. Tectonostratigraphy of the Chazyan (Late Middle-Early Late Ordovician) Mixed Siliciclastic-Carbonate Platform, Quebec Embayment. *Journal of Sedimentary Research* 83: 451–474.
- DIX G. R., ROBINSON G. W. & MCGREGOR D. C. 1998. Paleokarst in the Lower Ordovician Beekmantown Group, Ottawa Embayment: structural control inboard of the Appalachian orogen. *Geological Society of America Bulletin* 110: 1046–1059.
- DORAIS M. J., ATKINSON M., KIM J., WEST D. P., KIRBY G. A. & MURPHY B. 2011. Where is the Iapetus suture in northern New England? A study of the Ammonoosuc Volcanics, Bronson Hill terrane, New Hampshire 1 1 This article is one of a series of papers published in this CJES Special Issue: In honour of Ward Neale on the theme of Appalachian and Grenvillian geology.. *Canadian Journal of Earth Sciences* 49: 189–205.
- DUMONT R. & JONES A. 2013. Aeromagnetic survey of offshore western Newfoundland, NTS 11, Newfoundland and Labrador / Levé aéromagnétique extracôtier de l'ouest de Terre-Neuve, SNRC 11, Terre-Neuve-et-Labrador. Newfoundland and Labrador Department of Natural Resources.
- DUNNING G. R., O'BRIEN S. J., COLMAN-SADD S. P., BLACKWOOD R. F., DICKSON W. L., O'NEILL P. P. & KROGH T. E. 1990. Silurian Orogeny in the Newfoundland Appalachians. *The Journal of Geology* 98: 895–913.
- GERBI C. C., JOHNSON S. E. & ALEINIKOFF J. N. 2006. Origin and orogenic role of the Chain Lakes massif, Maine and Quebec. *Canadian Journal of Earth Sciences* 43: 339–366.
- HADDAD D. & WATTS A. B. 1999. Subsidence history, gravity anomalies, and flexure of the northeast Australian margin in Papua New Guinea. *Tectonics* 18: 827–842.
- HIBBARD J. P., VAN STAAL C. R. & RANKIN D. W. 2010. Comparative analysis of the geological evolution of the northern and southern Appalachian orogen: Late Ordovician-Permian. In: *From Rodinia to Pangea: The Lithotectonic Record of the Appalachian Region* (Ed. by R. P. Tollo, M. J. Bartholomew, J. P. Hibbard & P. M. Karabinos), pp. 51–69. Geological Society of America.
- HIBBARD J. P., VAN STAAL C. R., RANKIN D. W. & WILLIAMS H. 2006. Lithotectonic Map of the Appalachian Orogen, Canada- United States of America. Geological Survey of Canada.

- HISCOTT R. N. 1978. Provenance of Ordovician deep-water sandstones, Tourelle Formation, Quebec, and implications for initiation of the Taconic orogeny. *Canadian Journal of Earth Sciences* 15: 1579–1597.
- JACOBI R. D. 1981. Peripheral bulge—a causal mechanism for the Lower/Middle Ordovician unconformity along the western margin of the Northern Appalachians. *Earth and Planetary Science Letters* 51: 245–251.
- JAMIESON R. A., BREEMEN O. VAN, SULLIVAN R. W. & CURRIE K. L. 1986. The age of igneous and metamorphic events in the western Cape Breton Highlands, Nova Scotia. *Canadian Journal of Earth Sciences* 23: 1891–1901.
- JORDAN T. E. 1981. Thrust loads and foreland basin evolution, Cretaceous, western United States. *AAPG bulletin* 65: 2506–2520.
- KARABINOS P., SAMSON S. D., HEPBURN J. C. & STOLL H. M. 1998. Taconian orogeny in the New England Appalachians: Collision between Laurentia and the Shelburne Falls arc. *Geology* 26: 215–218.
- KNIGHT I. & JAMES N. P. 1987. The stratigraphy of the Lower Ordovician St. George Group, western Newfoundland: the interaction between eustasy and tectonics. *Canadian Journal of Earth Sciences* 24: 1927–1951.
- KNIGHT I., JAMES N. P. & LANE T. E. 1991. The Ordovician St. George Unconformity, northern Appalachians: The relationship of plate convergence at the St. Lawrence Promontory to the Sauk/Tippecanoe sequence boundary. *Geological Society of America Bulletin* 103: 1200–1225.
- LACOMBE R. 2017. Stratigraphic and structural relationships in the foreland basin and Humber Arm Allochthon on Port au Port Peninsula, western Newfoundland. Masters Thesis, University of Alberta, Edmonton.
- LAMB A. T. 1976. Geophysical report on a seismic survey off western Newfoundland: Covering work done by Shell Canada Resources Limited with super long airgun (SLAG) and super long detector cable (SLDC) system during during October 1973.
- LAVOIE D. 1994. Diachronous tectonic collapse of the Ordovician continental margin, eastern Canada: comparison between the Quebec Reentrant and St. Lawrence Promontory. *Canadian Journal of Earth Sciences* 31: 1309–1319.
- LIN S., DAVIS D. W., BARR S. M., VAN STAAL C. R., CHEN Y. & CONSTANTIN M. 2007. U-Pb geochronological constraints on the evolution of the Aspy terrane, Cape Breton Island: implications for relationships between Aspy and Bras d’Or terranes and Ganderia in the Canadian Appalachians. *American Journal of Science* 307: 371–398.

- MACDONALD F. A., RYAN-DAVIS J., COISH R. A., CROWLEY J. L. & KARABINOS P. 2014. A newly identified Gondwanan terrane in the northern Appalachian Mountains: Implications for the Taconic orogeny and closure of the Iapetus Ocean. *Geology* 42: 539–542.
- MOENCH R. H. & ALEINIKOFF J. N. 2003. Stratigraphy, geochronology, and accretionary terrane settings of two Bronson Hill arc sequences, northern New England. *Physics and Chemistry of the Earth* 28: 113–160.
- MURPHY J. B., VAN STAAL C. R. & KEPPIE J. D. 1999. Middle to late Paleozoic Acadian orogeny in the northern Appalachians: A Laramide-style plume-modified orogeny?. *Geology* 27: 653–656.
- O'BRIAN B. 2003. Geology of the central Notre Dame Bay region (parts of NTS areas 2E/3,6,11), northeastern Newfoundland. Government of Newfoundland and Labrador, *Department of Mines and Energy, Geological Survey*, St. John's Newfoundland. p. 147.
- PALMER S. E., WALDRON J. W. F. & SKILLITER D. M. 2002. Post-Taconian shortening, inversion and strike slip in the Stephenville area, western Newfoundland Appalachians. *Canadian Journal of Earth Sciences* 39: 1393–1410.
- PINET N., KEATING P., LAVOIE D., DIETRICH J., DUCHESNE M. J. & BRAKE V. 2012. Revisiting the Appalachian structural front and offshore Anticosti Basin (northern Gulf of St. Lawrence, Canada) by integrating old and new geophysical datasets. *Marine and Petroleum Geology* 32: 50–62.
- PINET N. & TREMBLAY A. 1995. Tectonic evolution of the Quebec-Maine Appalachians: from oceanic spreading to obduction and collision in the northern Appalachians. *American Journal of Science* 295: 173–200.
- POLLOCK J. C., WILTON D. H. C., VAN STAAL C. R. & MORRISSEY K. D. 2007. U-Pb detrital zircon geochronological constraints on the Early Silurian collision of Ganderia and Laurentia along the Dog Bay Line: The terminal Iapetan suture in the Newfoundland Appalachians. *American Journal of Science* 307: 399–433.
- QUINN L. 1992. Diagenesis of the Goose Tickle Group, western Newfoundland. Mobil Oil. p. 26.
- QUINN L., BASHFORTH A. R., BURDEN E. T., GILLESPIE H., SPRINGER R. K. & WILLIAMS S. H. 2004. The Red Island Road Formation: Early Devonian terrestrial fill in the Anticosti Foreland Basin, western Newfoundland. *Canadian Journal of Earth Sciences* 41: 587–602.
- QUINN L., WILLIAMS S. H., HARPER D. A. T. & CLARKSON E. N. K. 1999. Late Ordovician foreland basin fill: Long Point Group of onshore western Newfoundland. *Bulletin of Canadian Petroleum Geology* 47: 63–80.

- REUSCH D. N. & VAN STAAL C. R. 2012. The Dog Bay–Liberty Line and its significance for Silurian tectonics of the northern Appalachian orogen. *Canadian Journal of Earth Sciences* 49: 239–258.
- ROBINSON P., TUCKER R. D., BRADLEY D., BERRY IV H. N. & OSBERG P. H. 1998. Paleozoic orogens in New England, USA. *GFF* 120: 119–148.
- RODGERS J. 1965. Long Point and Clam Bank formations, western Newfoundland. *Geological Association of Canada Proceedings* 16: 83–94.
- RODGERS N. & VAN STAAL C. R. 2002. Toward a Victoria Lake Supergroup: a provisional stratigraphic revision of the Red Indian to Victoria lakes area, central Newfoundland. *Newfoundland Department of Mines and Energy*. pp. 185–195.
- RUFFMAN A. & WOODSIDE J. 1970. The Odd-twins magnetic anomaly and its possible relationship to the Humber Arm Klippe of Western Newfoundland, Canada. *Canadian Journal of Earth Sciences* 7: 326–337.
- SALAD HERSI O., LAVOIE D. & NOWLAN G. S. 2003. Reappraisal of the Beekmantown Group sedimentology and stratigraphy, Montréal area, southwestern Quebec: implications for understanding the depositional evolution of the Lower-Middle Ordovician Laurentian passive margin of eastern Canada. *Canadian Journal of Earth Sciences* 40: 149–176.
- SANDFORD B. V. & GRANT A. C. 1990. Bedrock geological mapping and basin studies in the Gulf of St. Lawrence. *Geological Survey of Canada*. p. 33-42.
- SHAW J., COURTNEY R. C., CHRISTIAN H. & DEHLER S. 1997. Ground-truthing of multibeam bathymetry data in western Newfoundland: Bonne Bay, Bay of Islands, Port au Port region, and St. George's Bay. *Geologic Survey of Canada*. p. 25.
- SHEARER J. M. 1973. Bedrock and surficial geology of the northern Gulf of St. Lawrence as interpreted from continuous seismic reflection profiles. In: *Earth Science Symposium of Offshore Eastern Canada* (Ed. by J. D. Hood), pp. 285–303. Geologic Survey of Canada, Ottawa, ON, Canada.
- SINCLAIR H. D. & NAYLOR M. 2012. Foreland basin subsidence driven by topographic growth versus plate subduction. *Geological Society of America Bulletin* 124: 368–379.
- SINCLAIR I. K. 1990. A Review of the Upper Precambrian and Lower Paleozoic geology of western Newfoundland and the hydrocarbon potential of the adjacent offshore area of the Gulf of St. Lawrence. Canada-Newfoundland Offshore Petroleum Board.
- ST. JULIEN P. & HUBERT C. 1975. Evolution of the Taconic orogen in the Quebec Appalachians. *American Journal of Science* 275–A: 337–362.
- VAN STAAL C. R. 2007. Pre-Carboniferous Tectonic Evolution and Metallogeny of the Canadian Appalachians. In: *Mineral Deposits of Canada: A Synthesis of Major Deposit-Types, District Metallogeny, the Evolution of Geological Provinces, and Exploration*

- Methods* (Ed. by W. D. Goodfellow), pp. 793–818. Geological Association of Canada, Mineral Deposits Division.
- VAN STAAL C. R. & DE ROO J. A. 1995. Mid-Paeozoic tectonic evolution of the Appalachian Central Mobile Belt in northern New Brunswick. In: *Current Perspectives in the Appalachian-Caledonian Orogen* (Ed. by J. Hibbard, C. R. Van Staal & P. A. Cawood), pp. 367–389. Geological Association of Canada.
- VAN STAAL C. R., DEWEY J. F., NIOCAILL C. M. & MCKERROW W. S. 1998. The Cambrian-Silurian tectonic evolution of the northern Appalachians and British Caledonides: history of a complex, west and southwest Pacific-type segment of Iapetus. In: *Lyell, the Past is the Key to the Present* (Ed. by D. J. Blundell & A. C. Scott), pp. 197–242. Geological Society, London, Special Publications.
- VAN STAAL C. R., WHALEN J. B., MCNICOLL V. J., PEHRSSON S., LISSEBERG C. J., ZAGOREVSKI A., VAN BREEMEN O. & JENNER G. A. 2007. The Notre Dame arc and the Taconic orogeny in Newfoundland. In: *4-D Framework of Continental Crust* (Ed. by R. D. Hatcher, M. P. Carlson, J. H. McBride & J. R. Martinez Catalan), pp. 511–552.
- VAN STAAL C. R., WHALEN J. B., VALVERDE-VAQUERO P., ZAGOREVSKI A. & ROGERS N. 2009. Pre-Carboniferous, episodic accretion-related, orogenesis along the Laurentian margin of the northern Appalachians. In: *Ancient Orogens and Modern Analogues* (Ed. by J. B. Murphy, J. D. Keppie & A. J. Hynes), pp. 271–316. Geological Society, London, Special Publications.
- VAN STAAL C. R., WINCHESTER J. A. & BEDARD J. H. 1991. Geochemical variations in Middle Ordovician volcanic rocks of the northern Miramichi Highlands and their tectonic significance. *Canadian Journal of Earth Sciences* 28: 1031–1049.
- STAIT B. A. & BARNES C. R. 1991. Stratigraphy of the Middle Ordovician Long Point Group, western Newfoundland. In: *Advances in Ordovician Geology* (Ed. by C. R. Barnes & S. H. Williams), pp. 235–244. Geological Survey of Canada.
- STANLEY R. S. & RATCLIFFE N. M. 1985. Tectonic synthesis of the Taconian orogeny in western New England. *Geological Society of America Bulletin* 96: 1227–1250.
- STENZEL S. R., KNIGHT I. & JAMES N. P. 1990. Carbonate platform to foreland basin: revised stratigraphy of the Table Head Group (Middle Ordovician), western Newfoundland. *Canadian Journal of Earth Sciences* 27: 14–26.
- STEVENS R. K. 1970. Cambro-Ordovician flysch sedimentation and tectonics in west Newfoundland and their possible bearing on a proto-Atlantic Ocean. In: *Flysch Sedimentology in North America* (Ed. by P. Lajoie), pp. 165–177. Geological Association of Canada.

- STOCKMAL G. S., SLINGSBY A. & WALDRON J. W. 1998. Deformation styles at the Appalachian structural front, western Newfoundland: implications of new industry seismic reflection data. *Canadian Journal of Earth Sciences* 35: 1288–1306.
- STOCKMAL G. S., SLINGSBY A. & WALDRON J. W. F. 2004. Basement-involved inversion at the Appalachian structural front, western Newfoundland: an interpretation of seismic reflection data with implications for petroleum prospectivity. *Bulletin of Canadian Petroleum Geology* 52: 215–233.
- STOCKMAL G. S. & WALDRON J. W. F. 1990. Structure of the Appalachian deformation front in western Newfoundland: implications of multichannel seismic reflection data. *Geology* 18: 765–768.
- STOCKMAL G. S., WALDRON J. W. F. & QUINLAN G. M. 1995. Flexural modeling of Paleozoic foreland basin subsidence, offshore western Newfoundland: Evidence for substantial post-Taconian thrust transport. *The Journal of Geology* 103: 653–671.
- TATE G. W., MCQUARRIE N., VAN HINSBERGEN D. J. J., BAKKER R. R., HARRIS R. & JIANG H. 2015. Australia going down under: Quantifying continental subduction during arc-continent accretion in Timor-Leste. *Geosphere* 11: 1860–1883.
- THOMAS W. A. 1977. Evolution of Appalachian-Ouachita salients and recesses from reentrants and promontories in the continental margin. *American Journal of Science* 277: 1233–1278.
- TREMBLAY A. & CASTONGUAY S. 2002. Structural evolution of the Laurentian margin revisited (southern Quebec Appalachians): Implications for the Salinian orogeny and successor basins. *Geology* 30: 79–82.
- TREMBLAY A., LONG B. & MASSÉ M. 2003. Supracrustal faults of the St. Lawrence rift system, Québec: kinematics and geometry as revealed by field mapping and marine seismic reflection data. *Tectonophysics* 369: 231–252.
- VAN STAAL C. R., WILSON R. A., KAMO S. L., MCCLELLAND W. C. & MCNICOLL V. 2015. Evolution of the Early to Middle Ordovician Popelogan arc in New Brunswick, Canada, and adjacent Maine, USA: Record of arc-trench migration and multiple phases of rifting. *Geological Society of America* 128: 122–146.
- VAN DER VELDEN A. J., VAN STAAL C. R. & COOK F. A. 2004. Crustal structure, fossil subduction, and the tectonic evolution of the Newfoundland Appalachians: Evidence from a reprocessed seismic reflection survey. *Geological Society of America Bulletin* 116: 1485–1498.
- WALDRON J. W. ., ANDERSON S. D., CAWOOD P. A., GOODWIN L. B., HALL J., JAMIESON R. A., PALMER S. E., STOCKMAL G. S. & WILLIAMS P. F. 1998. Evolution of the Appalachian

- Laurentian margin: Lithoprobe results in western Newfoundland. *Canadian Journal of Earth Sciences* 35: 1271–1287.
- WALDRON J. W. F. 1985. Structural history of continental margin sediments beneath the Bay of Islands Ophiolite, Newfoundland. *Canadian Journal of Earth Sciences* 22: 1618–1632.
- WALDRON J. W. F., BARR S. M., PARK A. F., WHITE C. E. & HIBBARD J. 2015. Late Paleozoic strike-slip faults in Maritime Canada and their role in the reconfiguration of the northern Appalachian orogen: *Tectonics*, **34**, 1661–1684.
- WALDRON J. W. F., DEWOLFE J., COURTNEY R. & FOX D. 2002. Origin of the Odd-twins anomaly: magnetic effect of a unique stratigraphic marker in the Appalachian foreland basin, Gulf of St. Lawrence. *Canadian Journal of Earth Sciences* 39: 1675–1687.
- WALDRON J. W. F., MCNICOLL V. J. & VAN STAAL C. R. 2012. Laurentia-derived detritus in the Badger Group of central Newfoundland: deposition during closing of the Iapetus Ocean. *Canadian Journal of Earth Sciences* 49: 207–221.
- WALDRON J. W. F., MURPHY J. B., MELCHIN M. J. & DAVIS G. 1996. Silurian tectonics of western Avalonia: strain-corrected subsidence history of the Arisaig Group, Nova Scotia. *The Journal of Geology*: 677–694.
- Waldron, J.W.F., Schofield, D.I. & Murphy, J.B. 2017. Diachronous Palaeozoic accretion of peri-Gondwanan terranes at the Laurentian margin. In: Wilson, R. W., Houseman, G. A., McCaffrey, K. J. W., Dore, A. G. & Buiter, S. J. H. (eds) *Fifty Years of the Wilson Cycle*. 470.
- WALDRON J. W. F., SCHOFIELD D. I., MURPHY J. B. & THOMAS C. W. 2014. How was the Iapetus Ocean infected with subduction?. *Geology* 42: 1095–1098.
- WALDRON J. W. F. & VAN STAAL C. R. 2001. Taconian orogeny and the accretion of the Dashwoods block: A peri-Laurentian microcontinent in the Iapetus Ocean. *Geology* 29: 811–814.
- WALDRON J. W. F. & STOCKMAL G. S. 1991. Mid-Paleozoic thrusting at the Appalachian deformation front: Port au Port Peninsula, western Newfoundland. *Canadian Journal of Earth Sciences* 28: 1992–2002.
- WALDRON J. W. F., STOCKMAL G. S., CORNEY R. E. & STENZEL S. R. 1993. Basin development and inversion at the Appalachian structural front, Port au Port Peninsula, western Newfoundland Appalachians. *Canadian Journal of Earth Sciences* 30: 1759–1772.
- WEST D. P., LUDMAN A. & LUX D. R. 1992. Silurian age for the Pocomoonshine gabbro-diorite, southeastern Maine and its regional tectonic implications. *American Journal of Science* 292: 253–273.
- WHALEN J. B., MCNICOLL V. J., VAN STAAL C. R., LISSENBERG C. J., LONGSTAFFE F. J., JENNER G. A. & VAN BREEMAN O. 2006. Spatial, temporal and geochemical characteristics of

- Silurian collision-zone magmatism, Newfoundland Appalachians: An example of a rapidly evolving magmatic system related to slab break-off. *Lithos* 89: 377–404.
- WILLIAMS H. 1975. Structural succession, nomenclature, and interpretation of transported rocks in western Newfoundland. *Canadian Journal of Earth Sciences* 12: 1874–1894.
- WILLIAMS H. 1993. Acadian orogeny in Newfoundland. *Geological Society of America Special Papers* 275: 123–134.
- WILLIAMS H., BURDEN E. T., QUINN L., VON BITTER P. & BASHFORTH A. 1996. Geology and Paleontology of the Port au Port Peninsula, Western Newfoundland. In: p. 74. Geological Association of Canada.
- WILLIAMS H., COLMAN-SADD S. P. & SWINDEN H. S. 1988. Tectonic-stratigraphic subdivisions of central Newfoundland. *Geological Survey of Canada*: 91–98.
- WILLIAMS H., CURRIE K. L. & PIASECKI M. A. J. 1993. The Dog Bay Line: a major Silurian tectonic boundary in northeast Newfoundland. *Canadian Journal of Earth Sciences* 30: 2481–2494.
- WILLIAMS H. & HATCHER R. D. 1983. Appalachian suspect terranes. In: *Geological Society of America Memoirs* pp. 33–53. Geological Society of America.
- WILLIAMS H. & HISCOTT R. N. 1987. Definition of the lapetus rift-drift transition in western Newfoundland. *Geology* 15: 1044–1047.
- WILLIAMS H. & STEVENS R. K. 1974. Taconic Orogeny and the development of the ancient continental margin of eastern North American in Newfoundland. *Journal of the Geological Association of Canada* 1: 31–33.
- WILLIAMS S. H. 1991. Stratigraphy and graptolites of the Upper Ordovician Point Leamington Formation, central Newfoundland. *Canadian Journal of Earth Sciences* 28: 581–600.
- ZAGOREVSKI A., LISSEBERG C. J. & VAN STAAL C. R. 2009. Dynamics of accretion of arc and backarc crust to continental margins: Inferences from the Annieopsquotch accretionary tract, Newfoundland Appalachians. *Tectonophysics* 479: 150–164.
- ZAGOREVSKI A., VAN STAAL C. R., MCNICOLL V., ROGERS N. & VALVERDE-VAQUERO P. 2007. Tectonic architecture of an arc-arc collision zone, Newfoundland Appalachians. In: *Formation and Applications of the Sedimentary Record in Arc Collision Zones* (Ed. by A. Draut, P. D. Clift & D. W. Scholl), pp. 309–333. The Geological Society of America.

Chapter 3: Inversion of Taconian Extensional Structures during Palaeozoic Orogenesis in Eastern Newfoundland

West Newfoundland was critical in the development of the Wilson Cycle concept. Neoproterozoic rifting established a passive margin adjacent to the Iapetus Ocean. Ordovician (Taconian) arc-continent collision emplaced ophiolites and the thin-skinned Humber Arm Allochthon. Subsequent Devonian (Acadian) ocean closure produced basement-involved thrust faults that dominate the present-day mapped distribution of units.

New mapping, aeromagnetic and seismic interpretation around Parsons Pond allow recognition of structure in poorly exposed areas. Following Cambrian to Middle Ordovician passive-margin deposition, Taconian deformation produced a flexural bulge unconformity. Subsequent extensional faults shed localized limestone conglomerate into the foreland basin. The Humber Arm Allochthon contains a series of stacked and folded duplexes, typical of thrust belts. To the east, the Parsons Pond Thrust has transported shelf and foreland-basin units westward above the allochthon. The Long Range Thrust, farther east, shows major topographic expression but less offset. Stratigraphic relationships indicate that most thrusts originated as normal faults, active during Neoproterozoic rifting, and subsequently during Taconian flexure. Devonian continental collision inverted the Parsons Pond and Long Range thrusts. Basement-cored fault-propagation folds are structurally analogous to uplifts of the Laramide Orogen in the western USA. Similar deep-seated inversion structures may extend through the northern Appalachians.

3.1. Introduction

The geology of Newfoundland was critical in shaping Tuzo Wilson's (1966) concept of an ocean that had closed and then reopened. The rocks exposed in western Newfoundland (Figure 3.1) provide a complete record of the Wilson Cycle (Wilson 1966). Cambrian through Early Ordovician strata represent a rift-to-drift succession developed along the western margin of Laurentia (Bird & Dewey 1970) following the Ediacaran opening of the Iapetus Ocean (Cawood et al. 2001) (Figure 3.1). Lower Ordovician ophiolites, preserved in the highest structural slices of obducted allochthons (Figure 3.1), are interpreted as remnants of arcs within this ocean (Dewey & Bird 1971; Dewey & Casey 2013), providing evidence of arc-continent collision during Taconian (Ordovician) orogenesis. Subsequently, collisions of Gondwanan components with Laurentia during the Silurian and Devonian resulted in Salinian and Acadian orogenic events which closed the Iapetus Ocean (e.g., Dunning et al. 1990, Van Staal et al. 2014, Waldron et al. 2017).

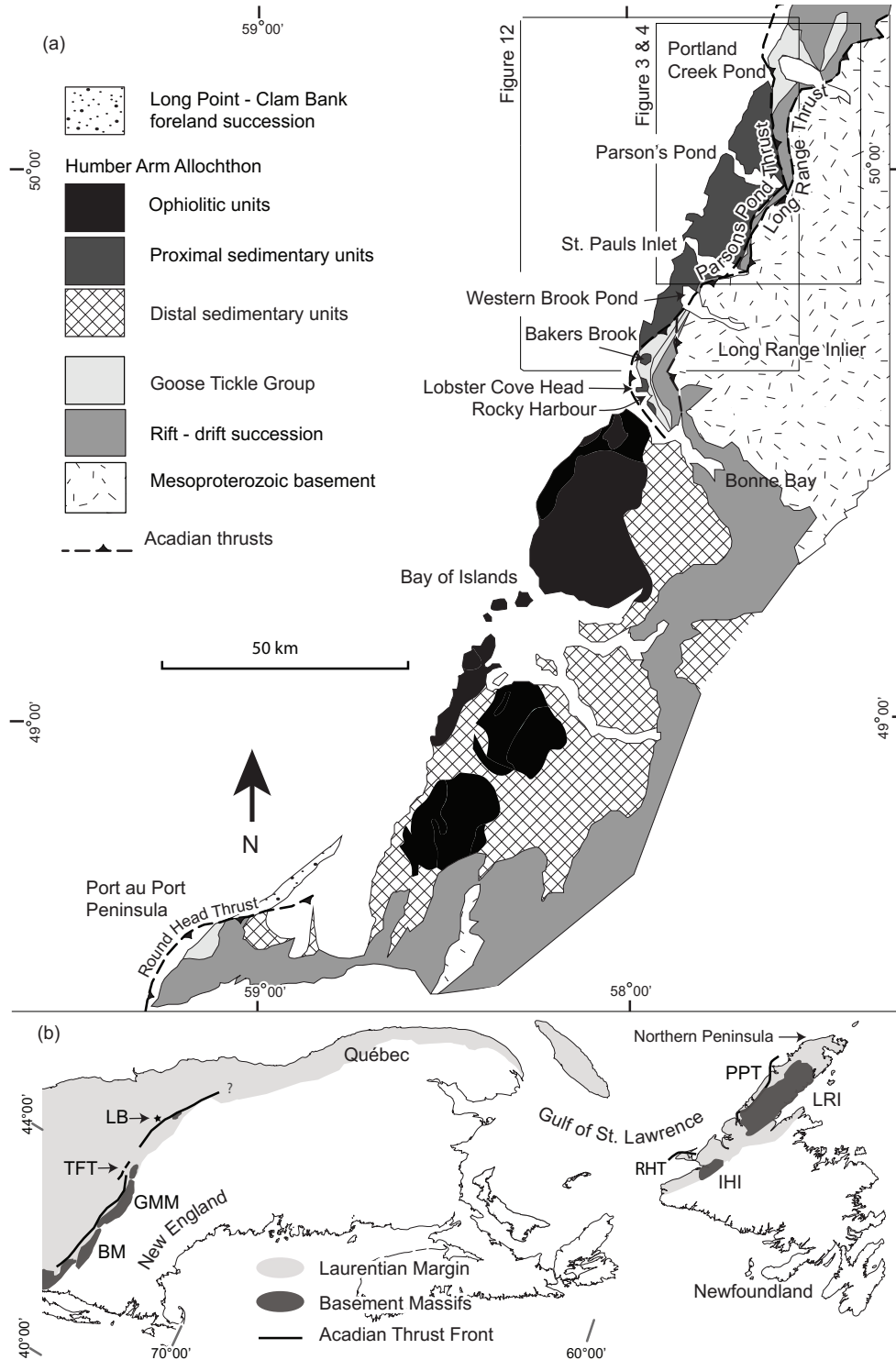


Figure 3.1: (a) Geological map of western Newfoundland showing major locations, tectonic units and Acadian thrust faults. (b) Map of northern Appalachians showing locations of major inversion related basement structures in Newfoundland and interpreted analogs to the south. Abbreviations: BM, Berkshire Massif; GMM, Green Mountain Massif; IHI, Indian Head Inlier; LB, Lacolle Breccia; LRI, Long Range Inlier; PPT, Parsons Pond Thrust; RHT, Round Head Thrust; TFT, Taconian Frontal Thrust.

The structural framework of geologic units in western Newfoundland is a direct result of this history of orogenesis and deformation associated with ocean closure. The Humber Arm Allochthon (Figure 3.1) involves a thin-skinned stack of structurally imbricated deep-water continental-margin successions that were assembled and emplaced over adjacent shelf rocks during the mid-Ordovician Taconian Orogeny. Deep-seated extensional faults, preserved in basement and shelf units, were also generated during Taconian orogenesis. It is interpreted that these faults formed as a result of flexure (Jacobi 1981; Bradley & Kidd 1991) of the down-going Laurentian plate during Taconian orogenic loading and slab pull; in some cases they reactivated earlier, rift-phase faults.

Later Palaeozoic deformation generated west-vergent thrusts which are also deep-seated. Unlike the Taconian thrusts, they extend into Mesoproterozoic crystalline basement units (Cawood & Williams 1988; Stockmal et al. 1998; Palmer et al. 2002). In this paper we use a combination of geological and geophysical data to focus on these later, out-of-sequence structures which formed during ocean closure, placing shelf and basement units structurally above the Humber Arm Allochthon (Figure 3.1) along its eastern margin. We show that the geometry of these structures is analogous to Laramide basement uplifts in northeastern Utah and northwestern Colorado (U.S.A.). We test the hypothesis that some of these thrusts reactivated earlier extensional structures that developed during rifting and/or Taconian orogenesis.

3.2. Regional Geological Setting

3.2.1. Stratigraphy

The oldest rocks in the western Newfoundland Appalachians are Mesoproterozoic basement units exposed as the Long Range Inlier (Figure 3.1). In the Parsons Pond region, the focus of this study (Figure 3.1), arkosic sandstone and conglomerate of the Bradore Formation (of the Labrador Group) unconformably overlie these crystalline basement rocks and have been interpreted to represent the rift portion (Williams & Hiscott 1987) of an extensive Cambrian to Lower Ordovician rift-drift succession (Figure 3.2). Upper portions of the Labrador Group, including marine limestone and shale of the Forteau Formation and shallow marine sandstone of the Hawke Bay Formation, overlie the Bradore Formation (Figure 3.2a) and represent the transition to a passive margin (Williams & Hiscott 1987). Thinly bedded, high energy carbonate rocks of the middle to upper Cambrian Port au Port Group (Chow & James 1987) and massive, thick-bedded, lower energy limestone and dolostone of the Lower Ordovician St. George Group (Knight & James 1987), form the top of the passive margin succession (Figure 3.2).

The transition from a passive margin to a tectonically active basin is marked by the St. George Unconformity (Knight et al. 1991), above which is the Middle Ordovician Table

Head Formation of the Table Head Group (Figure 3.2a). This carbonate foreland-basin unit is characterized by major lateral thickness and facies variations, attributed to draping over a rapidly subsiding karstic and faulted topography (Stenzel et al. 1990; Knight et al. 1991). The Table Point Formation shows strong similarities in composition, facies, and seismic response, to the underling shelf succession, and is difficult to distinguish in geophysical data. Therefore, we define all Palaeozoic stratified units below the top of the Table Point Formation as the “platform succession” and refer to the top surface of the Table Point Formation as the “top of platform”.

A transition to orogen-derived clastic sediments is recorded by upper parts of the Table Head Group and overlying turbiditic siliciclastic rocks (“flysch”) of the Middle Ordovician Goose Tickle Group (Figure 3.2) (Quinn 1992). Thinly bedded limestone, fine-grained sandstone, and siltstone are interbedded with localized lenses of limestone conglomerate (Cape Cormorant Formation and Daniels Harbour Member; Figure 3.2a). These conglomerates are interpreted to have been derived from submarine fault escarpments within the foreland basin which locally exposed as much as 1000 m of platform strata (Stenzel et al. 1990).

The Humber Arm Allochthon sits structurally above the autochthonous platform and Middle Ordovician foreland basin strata in western Newfoundland (Figure 3.2b). The allochthon mainly comprises sedimentary rocks deposited on the Laurentian slope and rise (James & Stevens 1986, Botsford 1988). In the Parsons Pond region, these are assigned to the middle Cambrian to Early Ordovician Cow Head Group (James & Stevens 1986) which is overlain by siliciclastic “flysch” of the Lower Head Formation (somewhat older than the Goose Tickle Group that overlies the platform succession; Figure 3.2). The Humber Arm Allochthon shows distinct lithological changes toward the south. In the Bay of Islands region (Figure 3.1, 2) the equivalents of the Cow Head Group show more distal facies, and overlie clastic rocks (Curling Group: Palmer et al. 2001) correlative with the early Cambrian Labrador Group (for which there are no equivalents in Parsons Pond). The Humber Arm Allochthon in the Bay of Islands area also includes, at the top of the thrust stack, ophiolitic rocks of the Bay of Islands and Little Port complexes (Dewey & Bird 1971; Dewey & Casey 2013). Although these units originated to the east of the platform succession, and were emplaced westwards during Taconian orogenesis (Figure 3.2b), their distribution was modified by later deformation, such that they are now mainly exposed in structural depressions to the west of the exposed platform (Figure 3.1).

Younger units that occur outside the area of this study help to constrain the history of deformation. In the Port au Port Peninsula area (Figure 3.1), and beneath the Gulf of St. Lawrence to the west, Upper Ordovician to Devonian strata (Long Point Group; Clam Bank and Red Island Road formations) record continued foreland basin development after the Taconian Orogeny. Unconformably overlying Carboniferous strata (Codroy Group) are largely flat-lying.

3.2.2. Tectonic and Structural History

3.2.2.1. Basement and rift history

The eastern Laurentian margin was developed above basement rocks of the Canadian Shield including the Mesoproterozoic Grenville Orogen, formed during the assembly of the supercontinent Rodinia (Rivers 2008). Neoproterozoic to Cambrian rifting (Cawood et al. 2001) marked the beginning of the Wilson Cycle in western Newfoundland. Extensional basement faults, preserved within the Appalachian foreland, typically parallel the orientation of the rifted margin of the Iapetus and have been interpreted as rift-related structures (Kumarapeli 1985, Tremblay et al. 2003). These faults generated a horst and graben topography, which ponded thick successions of rift-related coarse clastic rocks (Bradore Formation; Figure 3.2), and local mafic volcanic rocks (Lighthouse Cove Formation), in their hanging walls. However, at large scale the margin shows a sinuous geometry of embayments and promontories, interpreted to be inherited from this rift system (Thomas 1977, Allen et al. 2010). During the subsequent ocean opening, crustal ribbons, including the Dashwoods microcontinent, became separated as microcontinents within the Iapetus Ocean (Waldron & van Staal 2001).

3.2.2.2. Taconian Deformation

The first orogenic episode recorded by the Palaeozoic Laurentian rocks in western Newfoundland was the Early to Middle Ordovician Taconian Orogeny. This orogenic episode involved collision of the Dashwoods microcontinent, a rifted fragment of Laurentia (Waldron & van Staal 2001), and the westward emplacement of allochthons, including the Humber Arm Allochthon (Figure 3.1) (Williams & Stevens 1974; St. Julien & Hubert 1975) above the autochthonous platform.

Major structural differences occur within the Humber Arm Allochthon along the trend of the orogen and these differences geographically coincide with the observed lithological variation described above. In the study area of Parsons Pond, the Humber Arm Allochthon has been mapped as a series of imbricate thrust slices which interleave slope and rise sedimentary rocks of the Cow Head Group with east-derived flysch of the Lower Head Formation (Williams & Cawood 1989). South of Parsons Pond, in the Bay of Islands region (Figure 3.1), units are exposed in a series of stacked thrust sheets (Waldron et al. 2003), the structurally highest sheet comprising 485 Ma ophiolites (Dunning & Krogh 1985, Dewey & Casey 2013). Disrupted units and scaly *mélange* characteristically bound thrust sheets (Waldron et al. 2003) in the Bay of Islands, in contrast to the Parsons Pond region farther north where a scaly *mélange* is not typically observed.

Structurally below the Humber Arm Allochthon, the platform developed a series of deep-seated extensional normal faults in response to flexure as the lower-plate was loaded by the developing orogen (Bradley & Kidd 1991). During this episode of Middle Ordovician extension, limestone conglomerate units were shed from local highs along fault scarps which are now exposed in the hanging walls of steep basement faults (Stenzel et al. 1990). We suggest that the presence of these Middle Ordovician fault scarp deposits, exposed along the entire western margin of Newfoundland, indicates that extension played an important role during early phases of contractional deformation.

3.2.2.3. Post-Taconian (Acadian) Deformation

The Early Devonian Acadian Orogeny is conventionally attributed to the collision of Avalonia, a peri-Gondwanan terrane representing the eastern margin of the Iapetus Ocean, with Laurentia (Wilson 1966; Bird & Dewey 1970; Bradley 1983; van Staal et al. 2009). Contractional structures generated during the Acadian Orogeny have been interpreted to extend deeper than Taconian features, into platform and basement units (Cawood & Williams 1988; Stockmal et al. 1998; Palmer et al. 2002). Along the Northern Peninsula of Newfoundland (Figure 3.1), these features have been mapped as a narrow zone of thrusts, including the Long Range Thrust and the Parsons Pond Thrust, previously interpreted as a minor splay (Cawood & Williams 1988). Early maps (Cawood & Williams 1988) indicate that Mesoproterozoic rocks of the Grenville Orogen were thrust over platform units and rocks of the Humber Arm Allochthon along the Long Range Thrust. The Long Range Thrust has been mapped southward, curving from a dominant NE strike to a NW strike just south of Western Brook Pond (Figure 3.1). The fault loses offset and its mapped trace ends in the East Arm of Bonne Bay (Figure 3.1) (Cawood & Williams 1988).

The absence of younger, flat-lying stratigraphic units in the region disallows direct age control on these faults, but an Acadian age is inferred based on structures on the Port au Port Peninsula (Figure 3.1) where the analogous Round Head Thrust cross-cuts Silurian to Early Devonian rocks (Clam Bank Formation), and is unconformably overlain by Carboniferous strata Stockmal et al. (2004). Also on the Port au Port Peninsula, Middle Ordovician limestone conglomerates, localized in the immediate hanging wall of the thrust (Figure 3.2b), show that it inverted an earlier, Taconian, extensional fault (Stockmal et al. 2004).

3.3. Methods and Data

3.3.1. Geological Mapping

With the exception of coastline outcrops and the region near the Long Range Inlier, the Parsons Pond mapping area (Figures 3.1 and 3.3) is covered by dense foliage, bogs and wetlands, which limit exposure and access, particularly in areas underlain by shaly rocks of the Humber Arm Allochthon (Figure 3.3). Field data and a digital elevation model were compiled into a geographic information system (GIS) for map construction and interpretation. The map was then imported into seismic interpretation software, along with images from an on-land aeromagnetic survey (Cook & Kilfoil 2009) and 2D seismic reflection data, to assist in the interpretation of poorly exposed areas and subsurface geology.

3.3.2. Orientation Data

Spherical projections were plotted and statistics of oriented linear and planar data were calculated using Orient, a spherical projection and orientation data analysis software (Vollmer 2015). Within Orient we used the minimum eigenvector to estimate the orientation of fold axes for planar structures and the maximum eigenvector to estimate the mean orientations for clustered linear data (e.g. fold hinges), and C, the cylindricity index (Vollmer 1986, 1990), to gauge the cylindricity of folds.

3.3.3. Aeromagnetic Data

Figure 3.4 shows the results of a high resolution airborne magnetic survey, flown in 2008-2009 by Novatem Surveys Inc, for the Energy Branch of the Newfoundland and Labrador Department of Natural Resources and Nalcor Energy (available as an open file, with acquisition and processing details in Cook & Kilfoil, 2009). We used the second vertical derivative of the residual magnetic field in our interpretations because it emphasizes the effects of the near-surface magnetic sources and gives a better resolution of closely-spaced features; it is therefore most useful as an aid to geological mapping in poorly exposed areas. We used the process of zoning as described by Reeves (2005), outlining areas, patterns, shapes and amplitudes of anomalies. We then carried out qualitative interpretation by overlaying the aeromagnetic survey and its interpreted zones with the collected geological data in the ArcGIS platform.

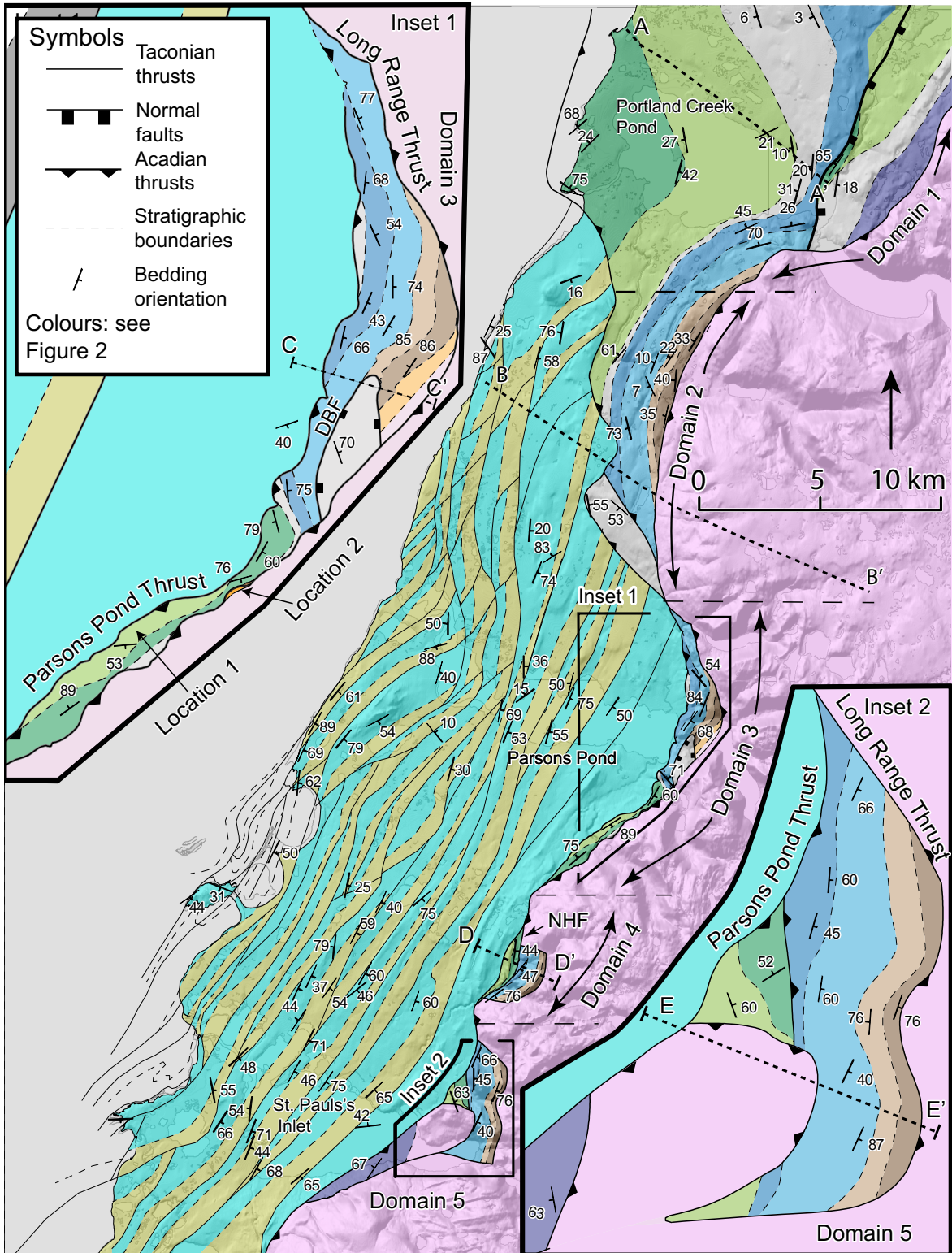


Figure 3.3: Geological map of the Parsons Pond area (Figure 3.1), underlain by digital elevation model acquired from Natural Resources Canada. Inset 1: Detailed geological map of the region near Parsons Pond. Inset 2: Detailed geological map of the St. Paul's Inlet region. Abbreviations: DBF, Devil's Bight Fault; NHF, Neddy's Hole Fault. See Figure 3.2 for colour legend.

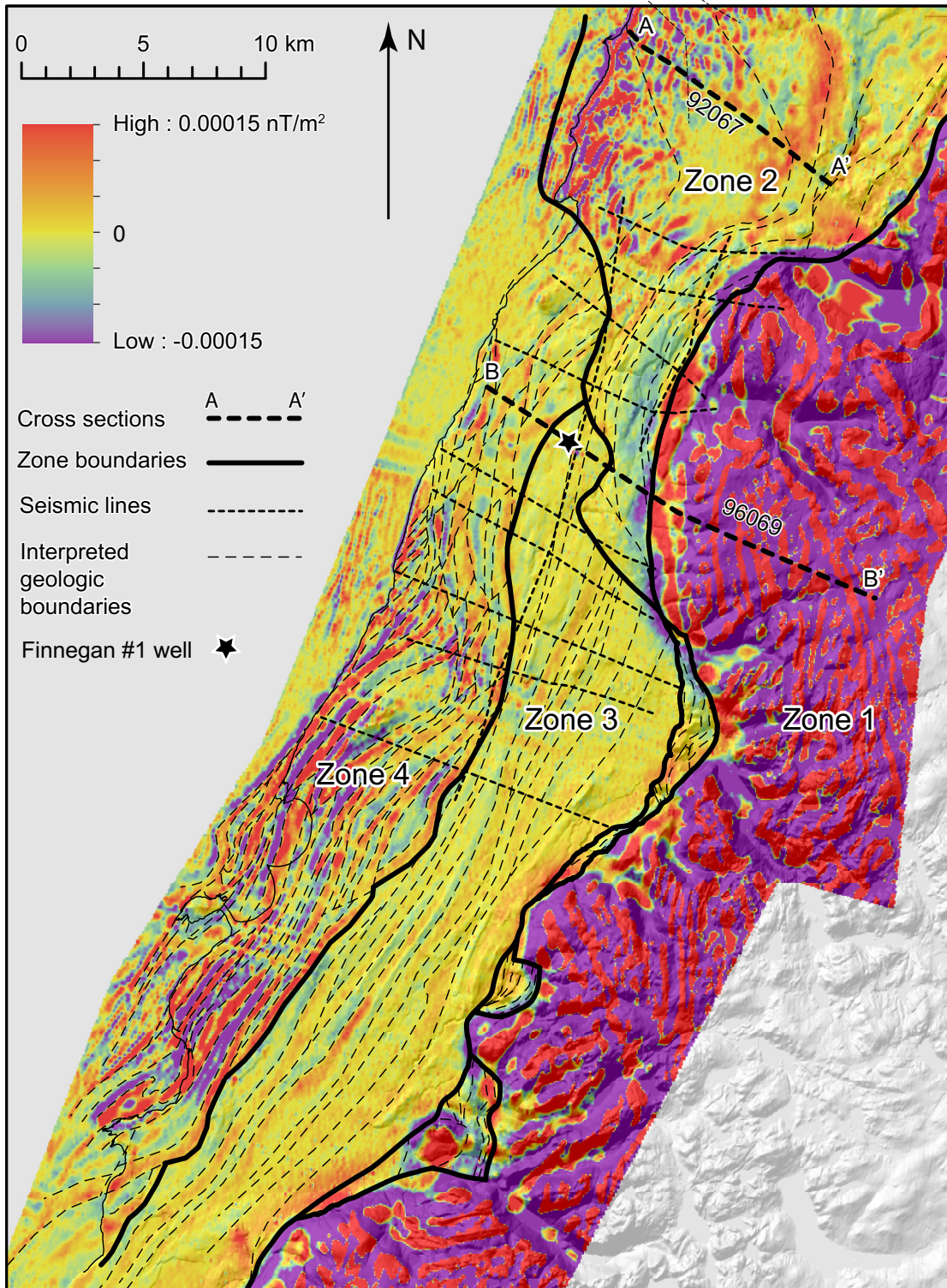


Figure 3.4: Map of the second vertical derivative of the residual magnetic field in the Parsons Pond map area. The aeromagnetic map overlies a digital elevation model for the region. The map also displays interpreted geological boundaries, magnetic anomaly zones (described in text), 2D seismic surveys, and the position of interpreted seismic profiles. Map area is the same as Figure 3.3 (location is shown on Figure 3.1).

3.3.4. Seismic Data

3.3.4.1. Acquisition

The available onshore seismic data include 250 km of 2D reflection data from two surveys conducted by Talisman Energy (Godlewski 1997) and Labrador Mining and Exploration Co. Ltd (Anonymous 1998) in 1996 and 1992 respectively (Figure 3.4). Detailed acquisition and processing information can be found in reports by Godlewski (1997) and Anonymous (1998). The surveys are of fair to good quality. The Talisman report indicates that data quality is most likely degraded by both thick glacial fill and structural complexity, resulting in a significant amount of off-line energy and complex shallow velocity variations which degrade images at depth (Godlewski 1997).

3.3.4.2. Well Data and Ties to Geological Boundaries

The Finnegan # 1 well, drilled by Nalcor Energy in 2012, is located in the Parsons Pond region (Figure 3.4), on seismic profile 96069 (Figure 3.5). The well penetrates a thick section of Humber Arm Allochthon before intersecting autochthonous platform at a depth of approximately 2250 m (Roberts 2011). Although Finnegan # 1 does not intersect the entire platform at depth, we were able to tie one strong and continuous reflection to the top of platform using a synthetic seismogram generated from sonic and density data collected along the well (Figure 3.4). We call this reflection **P** (Figure 3.5). Using a checkshot generated from the despiked sonic log we estimated the average velocity for the upper portion of the seismic profiles (above **P**) as 5.2 km/s and the lower portion of the profile as 6 km/s. Reflections below **P** were identified using this velocity and the known thicknesses of units from regional stratigraphic studies (e.g., Burden & Williams 1995). No well is located in the region east of the Parsons Pond Thrust; however, shallow reflections project to surface and can be tied to mapped geological boundaries.

3.4. Results

3.4.1. Distribution of Units

Western portions of the map area are occupied by rocks of the Humber Arm Allochthon (Figure 3.3). Mappable units include deep-water slope and rise sediments of the Cow Head Group and overlying siliciclastic flysch of the Lower Head Formation. Farther east these rocks are juxtaposed against platform and overlying Goose Tickle Group sedimentary rocks, along a major boundary which we interpret as the Parsons Pond Thrust (Figure 3.3).

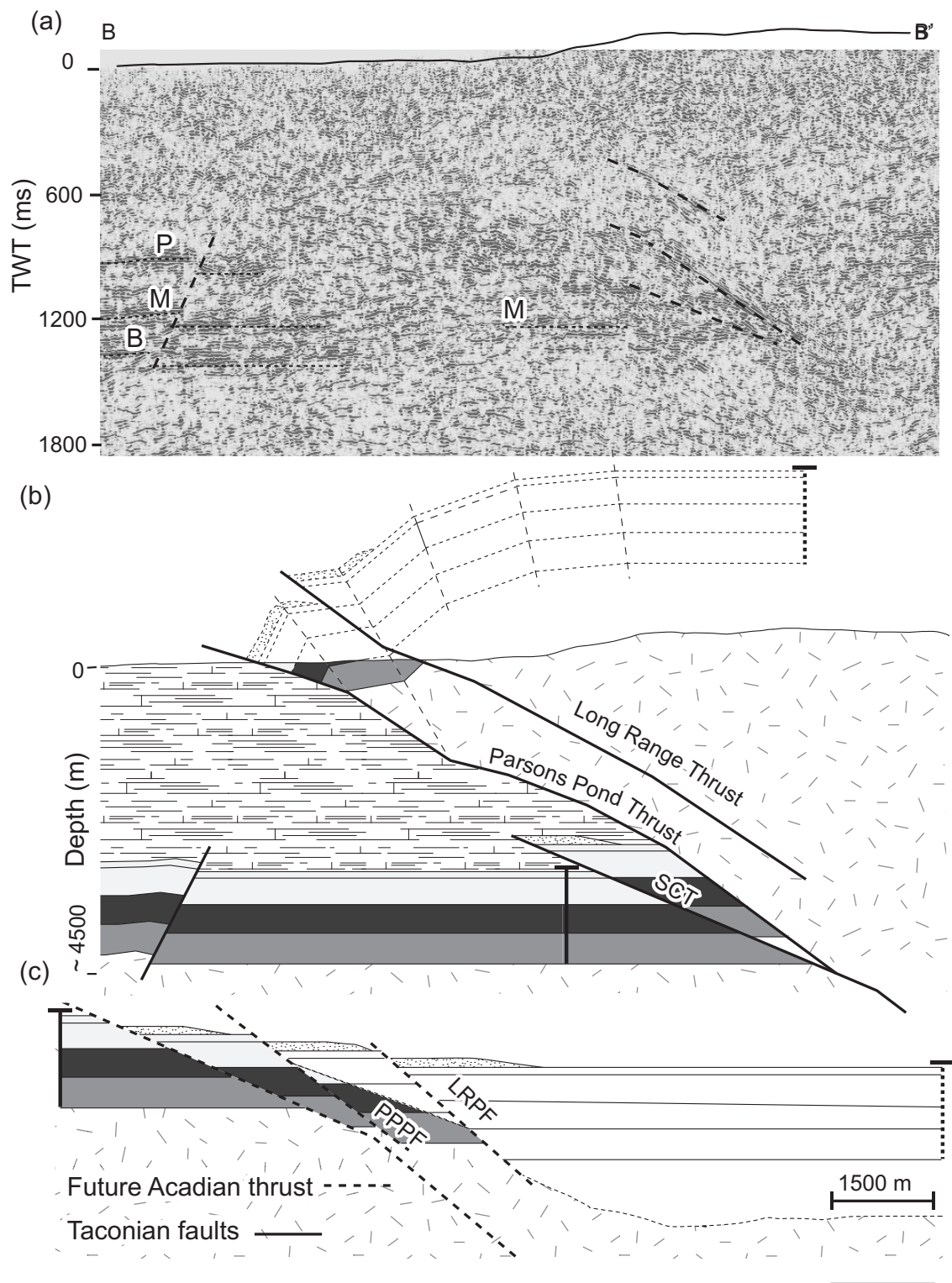


Figure 3.5: (a) Seismic profile 96069 (position shown on Figure 3.4) (b) Interpreted geological cross section. (c) Restored section. Abbreviations: B, near basement reflection; M, mid-platform reflection; NF, a normal fault; P, top-of-platform reflection; SCT, shortcut thrust.

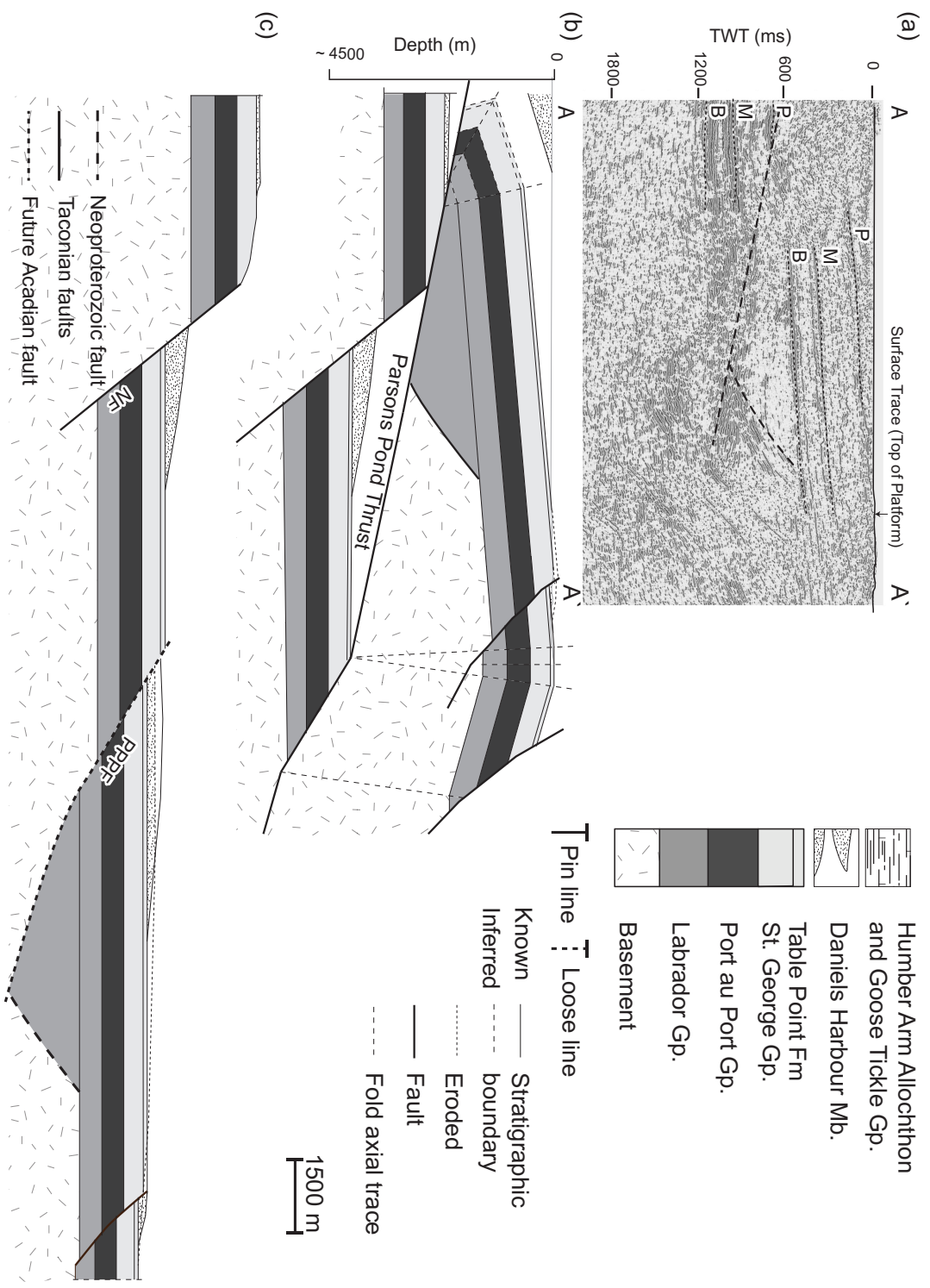


Figure 3.6: (a) Seismic profile 92067 (position shown on Figure 3.4). (b) Interpreted geological cross section. (c) Restored section (b) prior to Acadian thrusting. Abbreviations and legend as Figure 3.5.

In the region occupied by the Humber Arm Allochthon (Figure 3.3), the Cow Head - Lower Head succession is repeated, reflecting structural repetition related to thrusting (Figure 3.2b). Units of the Cow Head Group range from coarse conglomerate and calcarenite on the coast to dominantly fine-grained shale and ribbon limestone farther east. This lithological variation is interpreted to reflect a preserved proximal to distal facies transition on the slope and rise, although it has been modified through shortening during Humber Arm Allochthon assembly (James & Stevens 1986).

East of the Parsons Pond Thrust is a succession of platform and overlying Goose Tickle Group strata which generally young to the west. We refer to this succession as the Parsons Pond thrust sheet. In the north (Figure 3.3, along line A-A'), upright west-dipping beds show gentle dips (Figure 3.6); however, in the south (Figure 3.3, lines C-C', D-D' and E-E') bedding is generally steep to overturned closer to the Parsons Pond Thrust (Figures 3.7a, 3.8a and 3.9a). Mapping indicates that steep west-dipping to overturned platform strata are 10 to 20 % thinner than known platform thicknesses measured in relatively undeformed sections elsewhere in western Newfoundland. Overall thinning of the forelimb is commonly observed in fault propagation folds (Suppe & Medwedeff 1990). Thinning could result from a component of distributed simple shear or from closely spaced reverse faults along planes roughly parallel to the axial plane (e.g. figure 6 in Mitra & Mount 1998). Variable thicknesses are observed for the Goose Tickle Group, but local thickening could easily result from folding or internal thrusting. The Daniels Harbour Member (Figure 3.10a) of the Goose Tickle Group is observed only in the immediate hanging walls of the Parsons Pond Thrust and in the hanging walls of steep normal faults east of the Parsons Pond Thrust.

South of Parsons Pond (Figure 3.3: Inset 1: Location 1), the Goose Tickle Group transitions westward to a highly deformed broken formation with competent elongated blocks of medium to fine-grained sandstone surrounded by a scaly matrix of finer grained sandstone and siltstone (Figure 3.10b). Williams et al. (1985) refer to this unit as the Rocky Harbour *mélange* and they interpreted the unit as the structural base of the Humber Arm Allochthon (Williams et al. 1985; Williams & Cawood 1989). However, graptolites (Figure 3.10c), from broken beds south of Parsons Pond (Figure 3.3: Inset 1, Location 1) and two locations from Rocky Harbour (Figure 3.1), were collected and have been identified as *Archiclimacograptus* sp. (S.H. Williams, pers. comm., 2014) indicative of a Darriwilian 3 age, consistent with the Goose Tickle Group. The age, absence of exotic blocks (Raymond, 1975), stratigraphic position and lithological characteristics of the broken formation lead us to interpret that it is mainly deformed Goose Tickle Group.

Platform and Goose Tickle Group rocks are juxtaposed east of Mesoproterozoic basement rocks across another major boundary, the Long Range Thrust. Near Parsons Pond the basement

is stratigraphically overlain by quartz pebble conglomerate interpreted as the Bradore Formation of the Labrador Group (Figure 3.3: Inset 1: Location 2). Younger formations of the platform succession are interpreted to have been eroded from the hanging wall of the Parsons Pond Thrust.

3.4.2. Mapped Faults and Folds

In the Humber Arm Allochthon, extensive NE-striking map-scale thrust faults are interpreted where the older, east-dipping Cow Head Group lies east of (and therefore structurally above) younger Lower Head strata (Figure 3.3). These major faults are nowhere observed in outcrop.

The Parsons Pond Thrust, although also not directly observed in outcrop, is inferred to be located between the Humber Arm Allochthon to the west and platform overlain by Goose Tickle Group to the east. The mapped surface trace of the fault indicates it dips east and changes orientation along its length, from a dominant NE strike to a local NW strike, generating the conspicuously sinuous map pattern.

Thrust contacts are interpreted, east of the Parsons Pond Thrust, in places where Goose Tickle strata structurally underlie the St. George Group or older units (Figure 3.3). These faults connect to and broadly parallel the Parsons Pond Thrust, leading us to interpret that these are smaller splays which branch from the Parsons Pond Thrust.

Gently-dipping normal and thrust faults branch from the Long Range Thrust. At Parsons Pond, a gently east-dipping Neddy's Hole Fault places steeply dipping Table Head Group above older units in the platform (Figure 3.3: Inset 1). In the St. Paul's area (Figure 3.3: Inset 2) basement rocks lie structurally above younger platform sediments along a gently west-dipping fault which also branches from the Long Range Thrust. Some gently dipping normal faults are contractional (e.g. Devil's Bight Fault, DBF in Figure 3.3, 3.7a) and reverse faults are extensional (e.g. Neddy's Hole Fault, NHF in Figure 3.3, 3.8a).

The Long Range Thrust juxtaposes Mesoproterozoic basement rocks with platform and overlying Goose Tickle Group strata (Figure 3.3). Its trace is similar to the Parsons Pond Thrust, striking dominantly NE but curving along its length, showing NW strike in places.

3.4.3. Outcrop-scale Structures

Bedding in the Humber Arm Allochthon, west of the Parsons Pond Thrust, is folded at outcrop-scale into dominantly tight, overturned, asymmetric folds (Figure 3.10d). Locally, these have curved axial traces suggesting later refolding (Figure 3.11c). An equal-area projection of poles to bedding indicates that bedding is folded about a subhorizontal axis trending 210°. The dense clustering along the NW portion of the girdle indicates asymmetric folds that verge NW (Figure 3.11a).

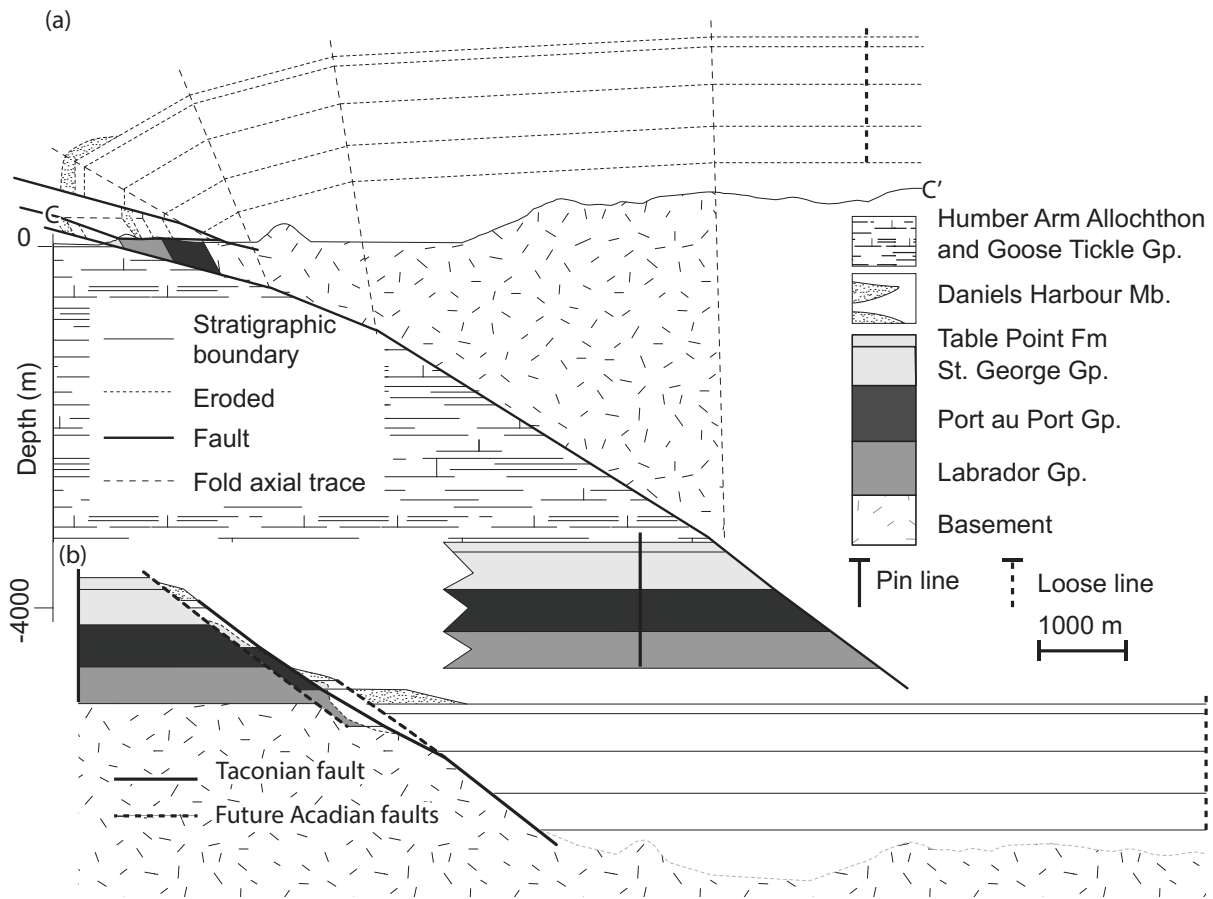


Figure 3.7: (a) Geological cross-section along line C-C' on Figure 3.3. (b) Restored section C-C' prior to Acadian thrusting. Abbreviations: DBF, Devil's Bight Fault; LRT, Long Range Thrust; LRPF, Long Range precursor fault; PPT, Parsons Pond Thrust; PPPF, Parsons Pond precursor fault.

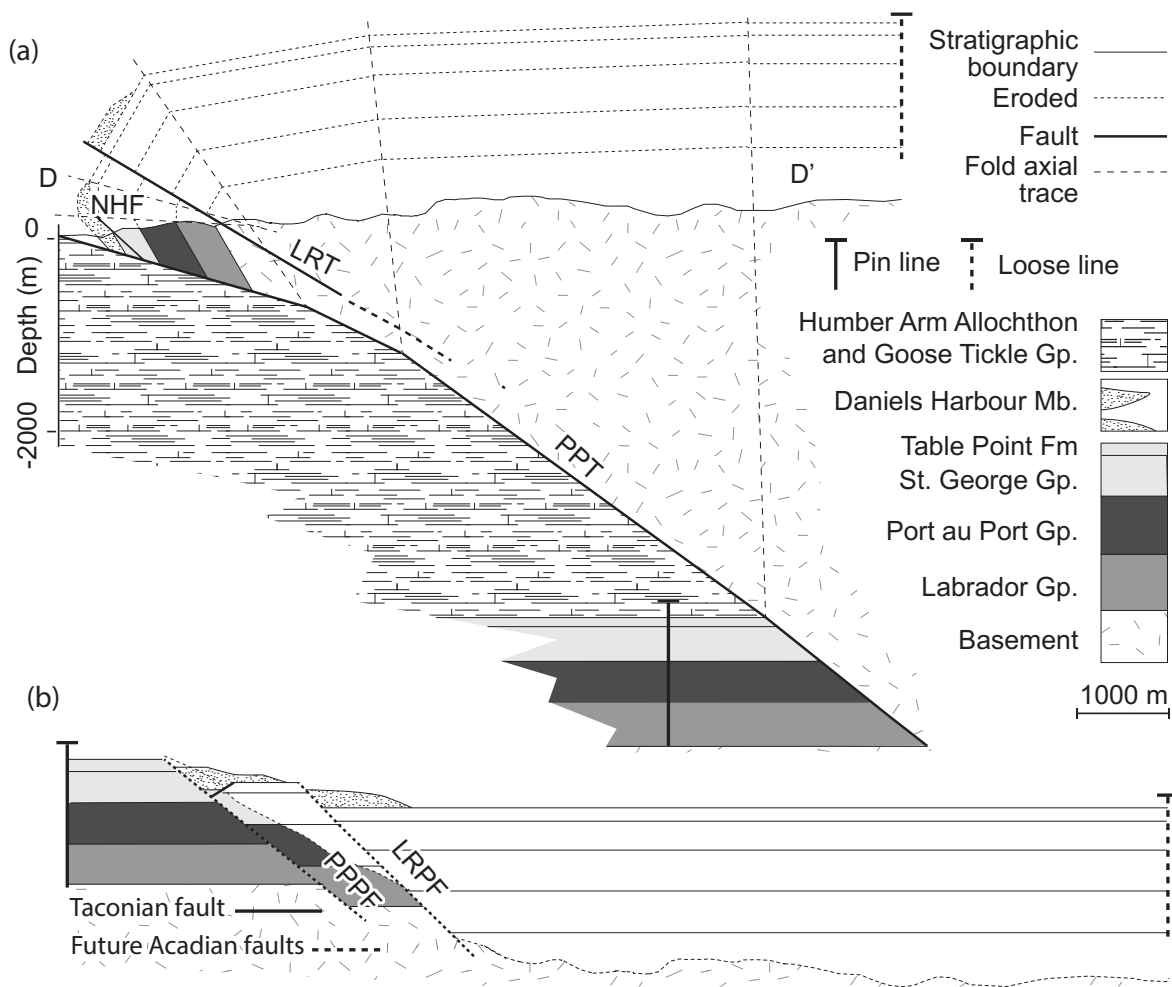


Figure 3.8: (a) Geological cross-section along line D-D' on Figure 3.3. (b) Restored section D-D' prior to Acadian thrusting. NHF, Neddy's Hole Fault; LRT, Long Range Thrust; LRPF, Long Range precursor fault; PPT, Parsons Pond Thrust; PPPF, Parsons Pond precursor fault.

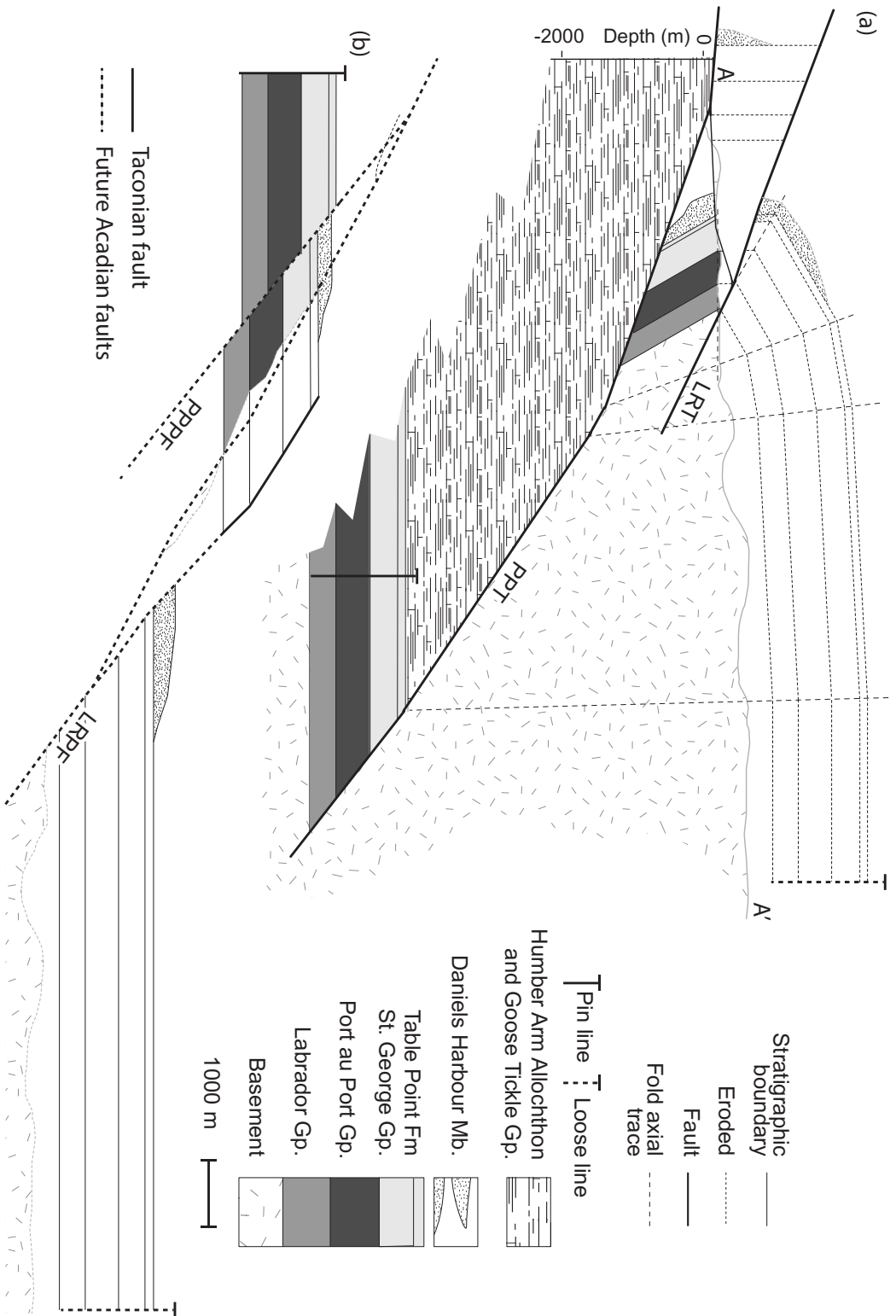


Figure 3.9: (a) Geological cross-section along line E-E' on Figure 3.3. (b) Restored section E-E' prior to Acadian thrusting. LRT, Long Range Thrust; LRP, Long Range precursor fault; PPT is the Parsons Pond Thrust; PPP is the Parsons Pond precursor fault.

Fold hinges, plotted on an equal-area projection in Figure 3.11b, have a maximum eigenvector orientation of 042° - 08° , indicating a dominant NE trend of fold axes. This mean orientation is close to the value determined from folded bedding (Figure 3.11a). Fold axial surfaces (Figure 3.11c) show a similar distribution. The large spread in fold hinge data ($C = 0.4797$; Figure 3.11b), together with the girdle distribution of axial surfaces, suggest fold overprinting during the progressive development of the thrust belt, although the overall curvilinear nature of the thrust belt may also contribute to the spread in the distributions.

Faults were measured in outcrops within the Humber Arm Allochthon (Figure 3.10e) but the sense of slip and timing relationships for many of these structures could not be determined. Where separation could be determined, the majority have a thrust sense of offset; however, in some cases where strata dip more steeply than the faults, the beds are extended, not shortened. Fault orientations plotted on an equal-area projection (Figure 3.11d) are highly variable. The minimum eigenvector orientation for the distribution of poles suggests the faults are generally folded about a NE-trending, shallow plunging axis. There is a large spread in the data yielding a cylindricity index (Vollmer 1990) of $C = 0.5147$ (Figure 3.11). Some spread is likely a function of different orientations associated with differences in timing and type of faulting, conjugate faults, branches and splays. However, this axis orientation agrees, within error, with fold axes calculated for folded beds and fold hinges (Figure 3.11a,b). It is therefore interpreted that the shortening direction was the same during the folding of both bedding and faults.

Outcrop-scale folds are less commonly observed in platform rocks east of the Parsons Pond Thrust. A few folds are overturned, with axial planes dipping eastward and westward. A locally developed cleavage is stylonitic where present in carbonate units of the platform; its orientation is variable. Where faults are observed in the Parsons Pond thrust sheet they typically have a thrust sense of offset (Figure 3.10e); however, in many cases where strata dip more steeply than the faults, the beds are extended, not shortened, analogous to relationships seen at map scale (e.g., Figure 3.8a).

Figure 3.12a shows an equal-area projection of all poles to bedding in the Parsons Pond thrust sheet, and indicates a subhorizontal fold axis trending approximately 200° . There is however, a large spread of data across the girdle with a cylindricity index (Vollmer 1990) of $C = 0.696$. The spread across the girdle is most likely a function of the large geographical distribution of bedding measurements which span an area of approximately 270 km^2 . Therefore, we divide the data into 5 domains based on geography (Figure 3.3). Figure 3.12b-f shows the resulting equal-area projections for each domain. Significant variations are seen between domains; these are discussed further below.

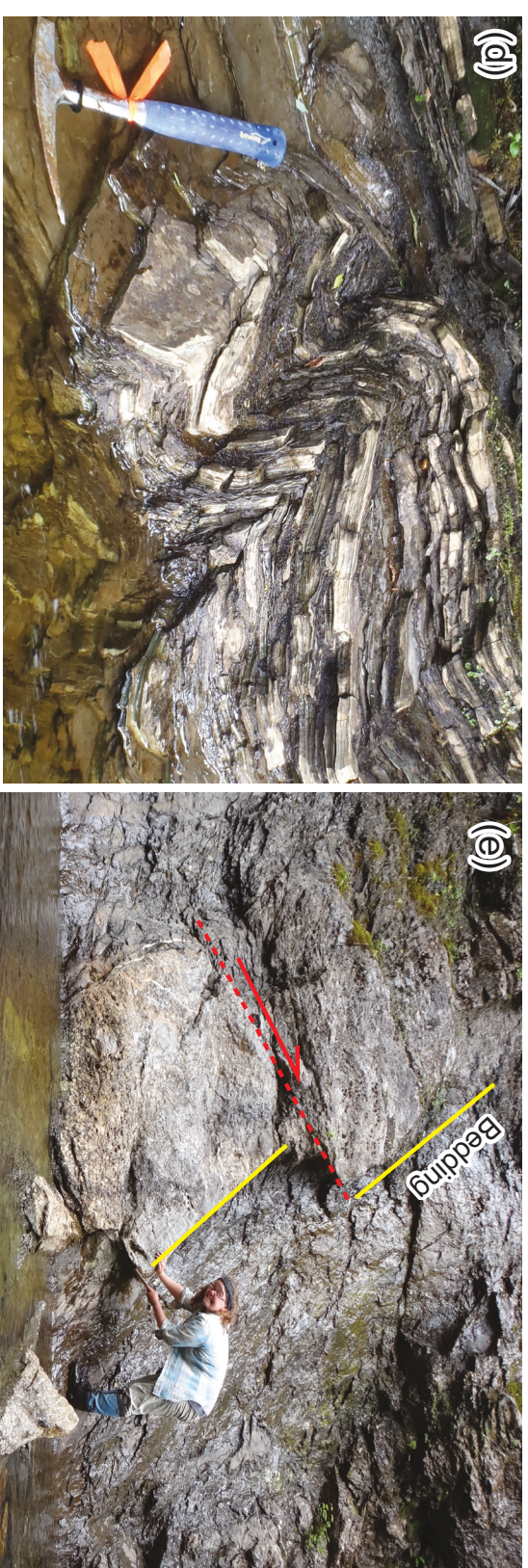


Figure 3.10: Field and sample photographs from the Parsons Pond map area. (a) Daniels Harbour conglomerate. (b) Goose Tickle broken formation found at location 1 on Figure 3.3. (c) Specimen of graptolite *Archiclimacograptus* sp. from location 1 on Figure 3.3. (d) Asymmetric tight folds in the Humber Arm Allochthon (e) Gently dipping thrust fault offsetting a bed of the Daniels Harbour Member.

3.4.4. Aeromagnetic Interpretation

The aeromagnetic map is divided into 4 zones (Zone 1, 2, 3 and 4: Figure 3.4) based on the characteristics of the anomalies. The most conspicuous boundary separates an extensive region of high-amplitude disorganized anomalies to the east (Zone 1) from a region of lower amplitude, aligned anomalies to the west (Zone 2). The boundary corresponds to the mapped position of the Long Range Thrust. East of the Long Range Thrust (in Zone 1) granitic and gneissic crystalline rocks of the Long Range Inlier likely contain a higher proportion of high-susceptibility minerals than the platform carbonate rocks (Zone 2) west of the fault, generating relatively higher amplitude anomalies. The anomalies in Zone 2 show no clear correlation with units seen on the ground which likely reflects a lack of high-susceptibility minerals in the carbonate units exposed at the surface. The weak anomalies present do not follow the stratigraphic trends; they may be generated from deeper basement units.

Outcrop is sparse in the region underlain by the Humber Arm Allochthon west of the Parsons Pond Thrust, but there is a strong relationship between observed outcrops and the anomaly patterns. Therefore, we strongly rely on aeromagnetic data to interpret unexposed geology and map-scale structures in this region. In the eastern region of the Humber Arm Allochthon (Zone 3), anomalies are more diffuse, less intense and straighter than those in the western region (Zone 4) which is defined by linear, curved anomalies which alternate systematically from high to medium values (Figure 3.4). Within Zone 4, anomalies with a positive gradient (displayed in reds in Figure 3.4), correlate with the Lower Head Formation. Anomalies with negative gradients correspond to rocks of the Cow Head Group (greens in Figure 3.4). We interpret that this relationship results from the abundance of chromite and other magnetic detrital grains (Stevens 1970) in the flysch units.

Boundaries between formations were traced and interpreted as either stratigraphic or structural boundaries. Field data indicate that bedding dips east; therefore we interpret faults wherever rocks of the younger Lower Head Formation lie west of the older Cow Head Group. These lineaments were traced until they terminated, generally by truncation with a cross-cutting lineament. The lineaments along which anomalies are truncated are also interpreted as faults.

Using these methods we interpret a sequence of NNE-striking, subparallel map-scale faults which are connected by networks of NE-striking branching faults in Zone 4. This is a pattern of duplexes which is typical in fold and thrust belts (e.g. Butler 1982). The pattern of folding observed is therefore interpreted as a result of fault-bend folding of the thrust sheets within Zone 4 (Figure 3.11).

In contrast to Zone 4, anomalies in Zone 3 are not folded and no branching or cross-cutting faults are observed. Faults in Zone 3 therefore formed after folding and faulting in Zone

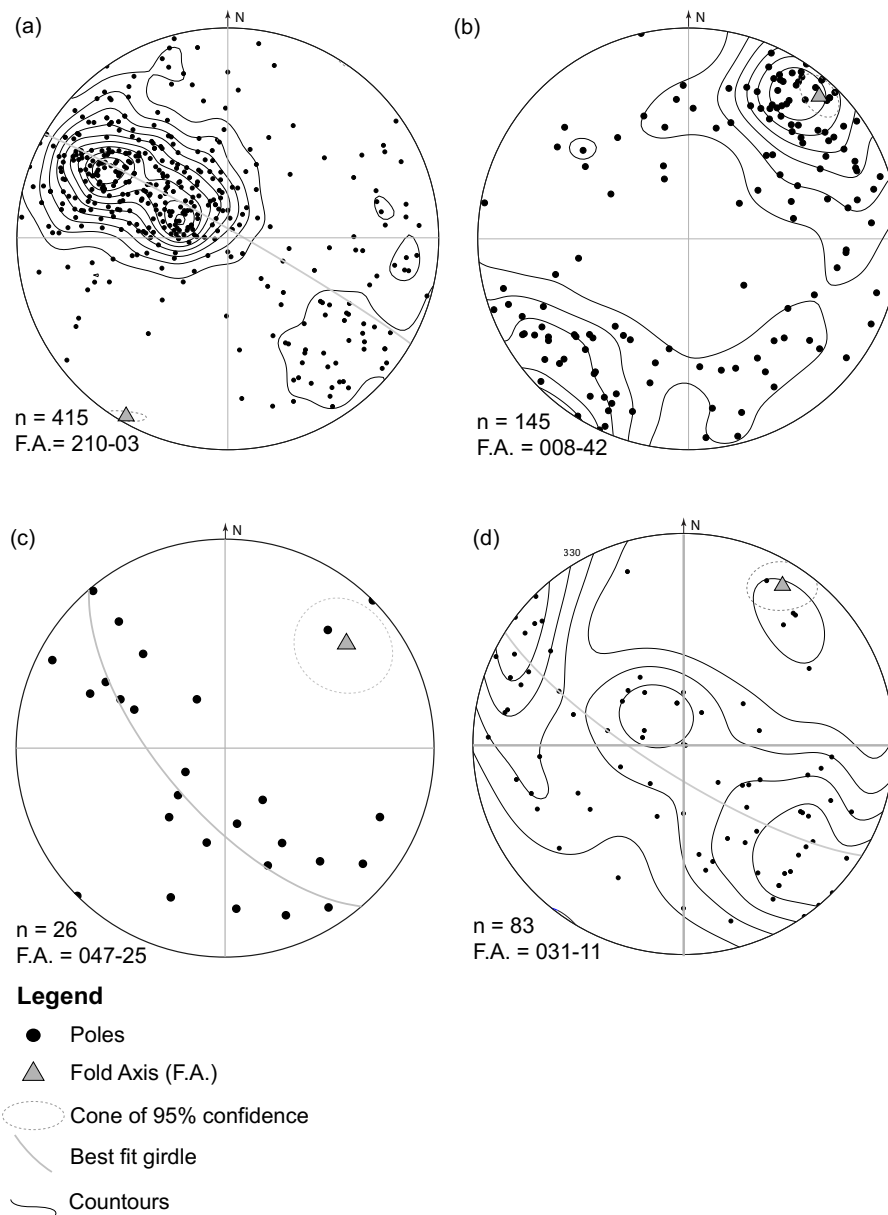
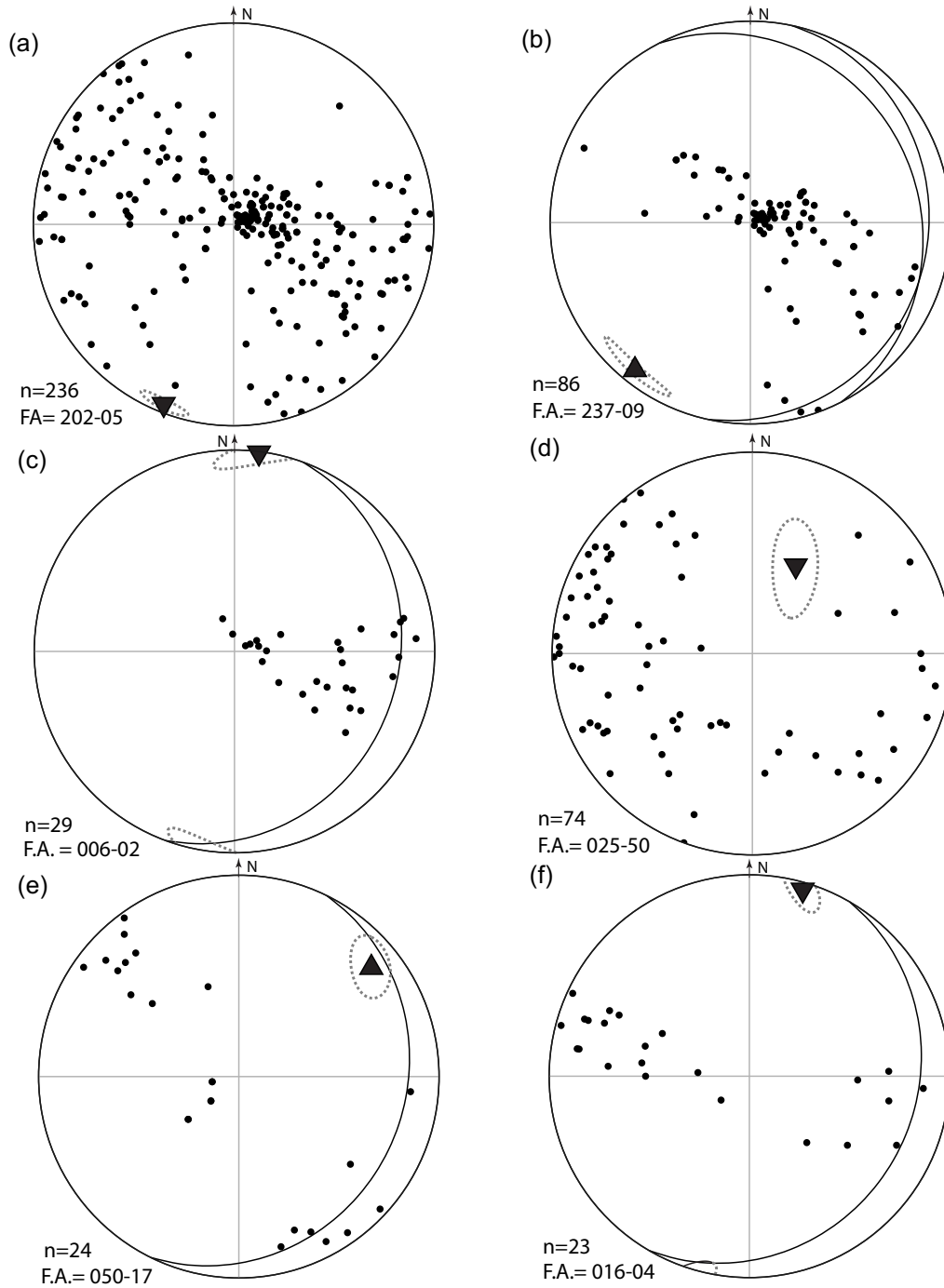


Figure 3.11: Equal-area projections of structures in the Humber Arm Allochthon. (a) Poles to bedding. (b) Fold hinges and intersection lineations (c) Poles to axial planes in the Humber Arm Allochthon. (d) Poles to faults.



- Poles to bedding ●
- Fold axis (F.A.) ▼
- 95% cone of confidence ○
- Fault —

Figure 3.12: Equal-area projections of poles to bedding in the Parsons Pond thrust sheet. Domains are labelled on Figure 3.3. Orientation of Parsons Pond Thrust is inferred from seismic profiles and mapped fault trace. (a) Entire Parsons Pond thrust sheet. (b) Domain 1. (c) Domain 2. (d) Domain 3. (e) Domain 4. (f) Domain 5.

4, suggesting that out-of-sequence thrusting affected rocks within Zone 3 of the Humber Arm Allochthon. All geological boundaries within Zones 3 and 4 are truncated by the Parsons Pond Thrust.

3.4.5. Seismic Interpretation

3.4.5.1. Line 96069: Section B-B'

The uppermost portion of seismic profile 96069 is characterized by discontinuous reflections with no lateral continuity (Figure 3.5). We primarily rely on field data and aeromagnetic interpretations to construct the upper portion of this section (line B-B', Figure 3.3). Using our geological map (Figure 3.3) we interpret that the Humber Arm allochthon crops out west of the Parsons Pond Thrust along line B-B' (Figure 3.3), while platform and flysch units crop out to the east. Steeply dipping strata in the Parsons Pond Thrust sheet and intense deformation in the allochthon account for the poor imaging at shallow levels (Figure 3.6). However, at 950 ms TWT (two-way-travel-time), corresponding to a depth of 2250 m, well Finnegan #1 intersects a peak reflection (**P**) that is both strong and laterally continuous. **P** bounds the top of a package of parallel continuous reflections approximately 450 ms thick in TWT. Picking **P** along all profiles, we generate a time-structure map of the top of platform (Figure 3.13).

Below **P**, continuous and parallel reflections represent platform stratigraphy, within which a strong peak overlies an easily identifiable doublet of trough reflections at 1100 ms (Figure 3.5). We identify the peak as **M**, the mid-platform reflection, due to its continuous and easily identifiable character. Based on an average velocity of 6 km/s and a TWT of 1100 ms, **M** sits 850 m below **P** and represents a surface within the Port au Port Group (Figure 3.2a). Although the well does not intersect these reflections, we suggest that the trough below **M** most likely represents the Big Cove Member, a shale unit bounded by dolostone on either side (Figure 3.2a).

We pick reflection **B** representing the base of platform, below which seismic reflections lose their parallel structure and coherence. The platform reflections **P**, **M** and **B**, although slightly offset by reverse faults, can be traced from west to east along the profile (Figure 3.5, B-B'). The reflections abruptly discontinue at an east-dipping boundary which, when traced to the surface, corresponds to the Parsons Pond Thrust along line B-B' (Figure 3.3). The fault dips slightly more steeply where it cuts the footwall platform than the Humber Arm Allochthon (Figure 3.5). The fault is likely steeper where it cuts through stronger platform units and shallows in strongly deformed, less competent rocks of the Humber Arm Allochthon (Figure 3.5). West of the Parsons Pond Thrust, an east-dipping boundary offsets the footwall platform reflections in a reverse

sense and is interpreted as a footwall shortcut thrust (SCT on Figure 3.5). East of the Parsons Pond Thrust, another reflection dips more steeply. Projected to the surface it corresponds to the mapped position of the Long Range Thrust.

3.4.5.2. *Line 92067: Section A-A'*

Seismic line 92067 corresponds to the position of line A-A' (Figure 3.3). Mapping (Figure 3.3) indicates that in the footwall of the Parsons Pond Thrust, poorly imaged Humber Arm Allochthon rocks likely occur above **P**. Reflection **P** is also identified in the hanging wall of the Parsons Pond Thrust as a high amplitude peak reflection, traced to surface at the mapped top of platform (Figure 3.6). Below **P**, platform reflections dip gently west and steepen before being cut off at a conspicuous boundary which correlates with the Parsons Pond Thrust (Figure 3.6). Its apparent dip in profile suggests that the Parsons Pond Thrust is relatively steep where it crosses the hanging wall platform and shallows as it cuts up section in the Humber Arm Allochthon (Figure 3.6), as in line B-B'.

Reflections **P**, **M**, and **B** in the footwall of the Parsons Pond Thrust, are cut off at a steep east-dipping boundary interpreted as a fault (Figure 3.6). This steep fault is overridden and cross-cut by the Parsons Pond Thrust and offsets the platform by 500 ms. It is likely that this second fault is an earlier normal fault which has been cross-cut by the younger Parsons Pond Thrust. In contrast to line B-B', no footwall shortcut thrust is present.

3.5. Discussion

3.5.1. *Structure in the Humber Arm Allochthon*

New observations in the Parsons Pond region demonstrate that structural styles within the Humber Arm Allochthon are more complex than previous mapping has shown. Although eastern portions of the allochthon are deformed by a series of simple imbricate thrusts, western portions demonstrate a more complicated structure of NNE-striking faults, connected by networks of NE-striking branching faults forming duplex structures. These duplexes are stacked, the highest stacks being exposed farther to the east. Curved traces of thrust faults and stratigraphic boundaries cannot be explained by topography in the flat terrane of Zone 4 (Figure 3.4). Therefore, these features must be folded in three dimensions. Because faults in Zone 3 (Figure 3.4) are not folded we interpret that later out-of-sequence faults formed after faulting and folding in Zone 4.

3.5.2. Structure in Autochthonous Platform

By combining local offshore data from White (Chapter 2) with our picks of the top of platform **P** in the footwall of the Parsons Pond Thrust (Figure 3.13a) we demonstrate that the platform is folded into a broad SW-plunging synform beneath the Humber Arm Allochthon. The steep normal and reverse faults that cut the platform beneath the Humber Arm Allochthon (Figure 3.5, 3.6) parallel offshore faults described by White (Chapter 2) (Figure 3.13b). Steep reverse faults bound a SW-plunging antiform, forming a pop-up structure (the target of drilling by Nalcor in 2012).

The NE and NW-striking normal and reverse basement faults from this study match orientations of rift-related faults which form the St. Lawrence rift system in Québec, described by (Tremblay et al. (2003). We also observe that the dominant NE-strike of the faults (Figure 3.13b) matches NE-striking rift-related dyke swarms in the northern Appalachians, including the Long Range dyke swarm in Newfoundland (Burton & Southworth 2010) and the Blair River Inlier dykes in Cape Breton (Miller & Barr 2004). These faults mimic the even larger-scale trend of promontories and embayments formed along the Laurentian margin, defined by NE-trending rifts which are offset by NW-trending transfer faults (Thomas 1977, Allen et al. 2010).

3.5.3. Structure of the Parautochthonous Parsons Pond Thrust Sheet

The Parsons Pond and Long Range thrusts bound the Parsons Pond thrust sheet (PPTS) (Figure 3.3). Mapping and seismic interpretation indicate that, although the Long Range Thrust (LRT) is the most conspicuous boundary in the mapping region, it is not the major structural boundary. The Long Range Thrust is a branch from the Parsons Pond Thrust (PPT) (Figure 3.3), which carried all platform, basement and flysch units, exposed in the area, in its hanging wall. This interpretation differs from previous interpretations (Williams et al. 1985a, Williams & Cawood 1989) that suggest the platform rocks in the Parsons Pond region were brought to surface by folding above basement duplexes and that the Long Range Thrust is the main thrust in the system (Williams & Cawood 1989).

3.5.3.1. Transport Direction

In thrust belts it is common practice to assume tectonic transport to be perpendicular to the trend of the average fold axis (Elliott & Johnson 1980). In order to make this assumption we must first determine if folding is related to faulting. Due to variable orientations of bedding in the PPTS (Figure 3.12a) and the PPT we compare the orientations of both for individual domains. We did not make a fault-orientation estimate for Domains 1 and 3 because the fault orientation is highly variable. Figures 3.12b - f show that the PPT passes through the cone of

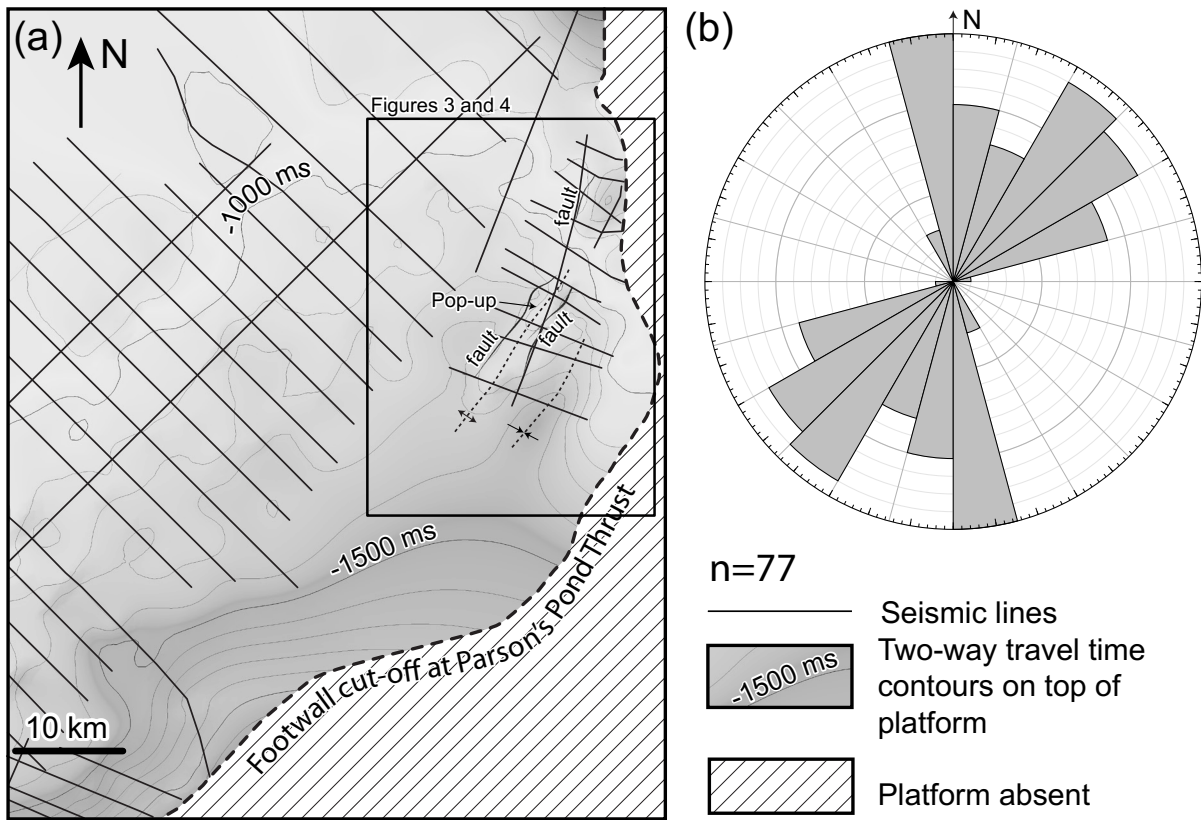


Figure 3.13: (a) Isochron map of the top of platform in the footwall of the Parsons Pond Thrust (Location shown on Figure 3.1). (b) Rose plot of fault strikes in the autochthonous platform offshore and onshore. Bin size is 15° and number of measurements is 77.

confidence for the mean fold axis for domains (2, 4 and 5) where the orientation of the thrust is well constrained. It is therefore likely that folds were generated as a result of transport along the Parsons Pond Thrust and variations in fold axis orientations are a reflection of changing strike along the fault. Fold axes calculated for all domains indicate a general NW-directed transport. Therefore, NE-striking segments along the Parsons Pond Thrust represent frontal ramps and lesser NW-striking portions are lateral ramps. Regions bounded by extensive lateral ramps, like Domain 1 (Figure 3.12b), produce girdles with a large spread, indicating fold interference due to transport over both frontal and lateral ramps. The overall sinuous map pattern of bedding surface traces also reflects fold interference in regions with extensive lateral ramps.

3.5.3.2. Cross-Section Construction and Restorations

Cross-sections (C-C', D-D' and E-E' Figure 3.3) were constructed parallel to the inferred transport direction. The folds generated by transport along the Parsons Pond Thrust are defined by a broad shallow-dipping back limb and a narrow forelimb which has been rotated in a steep to overturned fault-propagation fold (Figures 3.7a, 3.8a and 3.9a). To construct our cross-sections for restoration we approximate fold shapes in the broad limb using kink geometries generated by fault bend folding (Suppe & Medwedeff, 1990) over anticlinal and synclinal bends in the Parsons Pond Thrust. The maximum elevation of the back limb is chosen as 800 m, the highest elevation recorded for basement rocks in the Long Range Mountains - the minimum elevation of the base of platform. Because strata are thinned by approximately 10 – 20 % in the forelimb, idealized models of fault-propagation folds, using kink geometries (i.e. Suppe & Medwedeff, 1990), do not adequately explain fold generation and simple line length balancing restorations cannot be used. For the steep forelimb we choose a sub-horizontal axial trace that does not bisect the interlimb angle, so as to achieve the approximate 14 % observed thinning.

We restore the sections using simple shear parallel to the axial traces in the steep limb so that area is maintained (Figures 3.7b, 3.8b, and 3.9b). In the gentle limbs we use a standard kink-construction that assumes simple shear parallel to bedding surfaces. We unfold the hanging wall to our datum elevation of 800 m. We passively rotate faults (including the Long Range Thrust) while unfolding, moving cut-offs parallel to axial traces. Faults and fault blocks are restored in Figures 3.7b, 3.8b and 3.9b to pre-thrusting positions. When restored, shallow-dipping faults have an apparent dip shallower than that of the Parsons Pond and Long Range thrusts (Figure 3.7b). The Parsons Pond and Long Range thrusts (which we refer to as the Parson Pond and Long Range precursor faults respectively in their restored Taconian configuration) have similar dips of approximately 38° in the restorations. However, it should be noted that these dips are dependant to some extent on the geometries assumed in the eroded portions of the hanging wall.

A more rounded fold geometry would lead to steeper restored dips, whereas more angular folds would restore to shallower geometries.

Gently east-dipping thrust and normal faults in the PPTS demonstrate an interesting geometry in present-day cross-section. Normal faults are contractional (e.g. Devil's Bight Fault, DBF in Figure 3.7a and reverse faults are extensional e.g. Neddy's Hole Fault, NHF in Figure 3.8a). Two possible structural scenarios would lead to this geometry. Either the beds were overturned and later cross-cut by gently-dipping faults or these faults were initially formed at steeper orientations and rotated to their current orientations. Seismic data (i.e. Figures 3.5 and 3.6) indicate that platform-cutting normal faults in the footwall of the PPT have steep dips, consistent with their development at shallow depths in a stress regime with a maximum compressive stress near vertical. It is therefore unlikely that the gently-dipping contractional normal faults formed in their current orientation (e.g. Devil's Bight Fault: Figure 3.7a). Furthermore, restoration of the section in Figure 3.7 shows that a gently-dipping normal fault initially had a much steeper orientation before shortening; its current orientation is due to rotation in the overturned limb of a fault-propagation fold. This strongly suggests that these gently dipping faults, together with the strata they offset, were rotated during development of the Parsons Pond Thrust.

Displacement along the Parsons Pond Thrust is significant, with minimum estimates of approximately 8-9 km implied from the cross-sections (Figures. 3.7, 3.8, and 3.9). Interpretations of the most northern seismic line (line A-A', Figure 3.3) indicate that transport increases northward, reaching upwards of 12 km near Portland Creek Pond (Figure 3.6). There is little (< 1 km) displacement along the Long Range Thrust. This interpretation differs significantly from that of Cawood and Williams (1988) who estimate approximately 2 km of motion along the Long Range Thrust and interpret the Parsons Pond Thrust as a more minor splay.

3.5.3.3. Southern Extent of the Parsons Pond Thrust System

Mapping demonstrates that the Parsons Pond Thrust runs offshore at Green Point (Figure 3.1); its southern extent past this region is not currently recognized. The Long Range Thrust also terminates in this region, curving to a north-striking orientation before running into the east arm of Bonne Bay. Interpretations from our cross-sections indicate that displacement generally decreases to the south, perhaps indicating that the southern portions of these faults are blind, not cutting the surface. In this interpretation, the platform and Long Range Mountains are folded into a large, basement-cored fault-propagation fold above a deeper basement fault (Parsons Pond Thrust) which has not breached the surface farther south.

The deep-seated nature of the Parson Pond Thrust and the presence of a footwall shortcut thrust (Figure 3.5), overturned fault-propagation folds, and fault-scarp deposits in the hanging wall of the thrust, lead us to infer that the Parsons Pond Thrust is structurally analogous to the Round Head Thrust (Waldron et al. 1993, Stockmal et al. 1998, 2004) on the Port au Port Peninsula approximately 150 km to the south. Although geographically disconnected, these faults may be genetically linked and related to the same network of basement thrust faults that are responsible for the distinct present day distribution of tectonostratigraphic zones in the Laurentian Realm of western Newfoundland, where platform rocks appear east of the Humber Arm Allochthon everywhere (Figure 3.1).

3.5.4. Fault History

Basement faults in the Parsons Pond region demonstrate a protracted history of motion during opening and subsequent closure of the Iapetus (Figure 3.14). Several lines of evidence indicate that many observed faults in the Parsons Pond region originated during late Neoproterozoic rifting (Figure 3.14a). For example, Taconian and Acadian basement faults observed in western Newfoundland (Figure 3.13b) are generally parallel to Neoproterozoic to Cambrian rift-related faults (Thomas 1977, Allen et al. 2010) and igneous intrusions (Miller & Barr 2004, Burton & Southworth 2010) outside the Parsons Pond region. In addition, outcrop and seismic evidence of rift-related Bradore Formation in the hanging walls of the Long Range and Parson Pond thrusts (Figure 3.3, inset 1, location 2 and Figure 3.6 respectively) suggest that these faults were active during rifting.

The earliest convergent orogenic episode, the Taconian Orogeny (Figure 3.14c), is traditionally viewed as a predominantly contractional deformation event forming mainly thin-skinned structures such as the Humber Arm Allochthon (Figure 3.14c). However, Middle Ordovician limestone conglomerates (Cape Cormorant Formation and Daniels Harbour Member) indicate that normal faults played a significant role in Middle Ordovician Taconian deformation (Figure 3.14c). Clasts within the Daniels Harbour conglomerate are derived from local uplifts of the Table Head Group (Stenzel et al. 1990) with minor contributions from the underlying St. George Group, indicating an instantaneous scarp-height of 60 – 375 m (the thickness range of the Table Head Group from Stenzel et al. 1990). Our reconstructions (Figures 3.7b, 3.8b and 3.9b) do not constrain the normal throw along the Parsons Pond precursor fault (Figures 3.7b, 3.8b, and 3.9b); however, we are able to provide minimum estimates for total throw along the system of normal faults which ranges from 700 m to greater than 2500 m. Lenses of Daniels Harbour conglomerate, occurring at variable stratigraphic positions within the Goose Tickle Group, probably record pulses of fault reactivation which contributed to this overall throw.

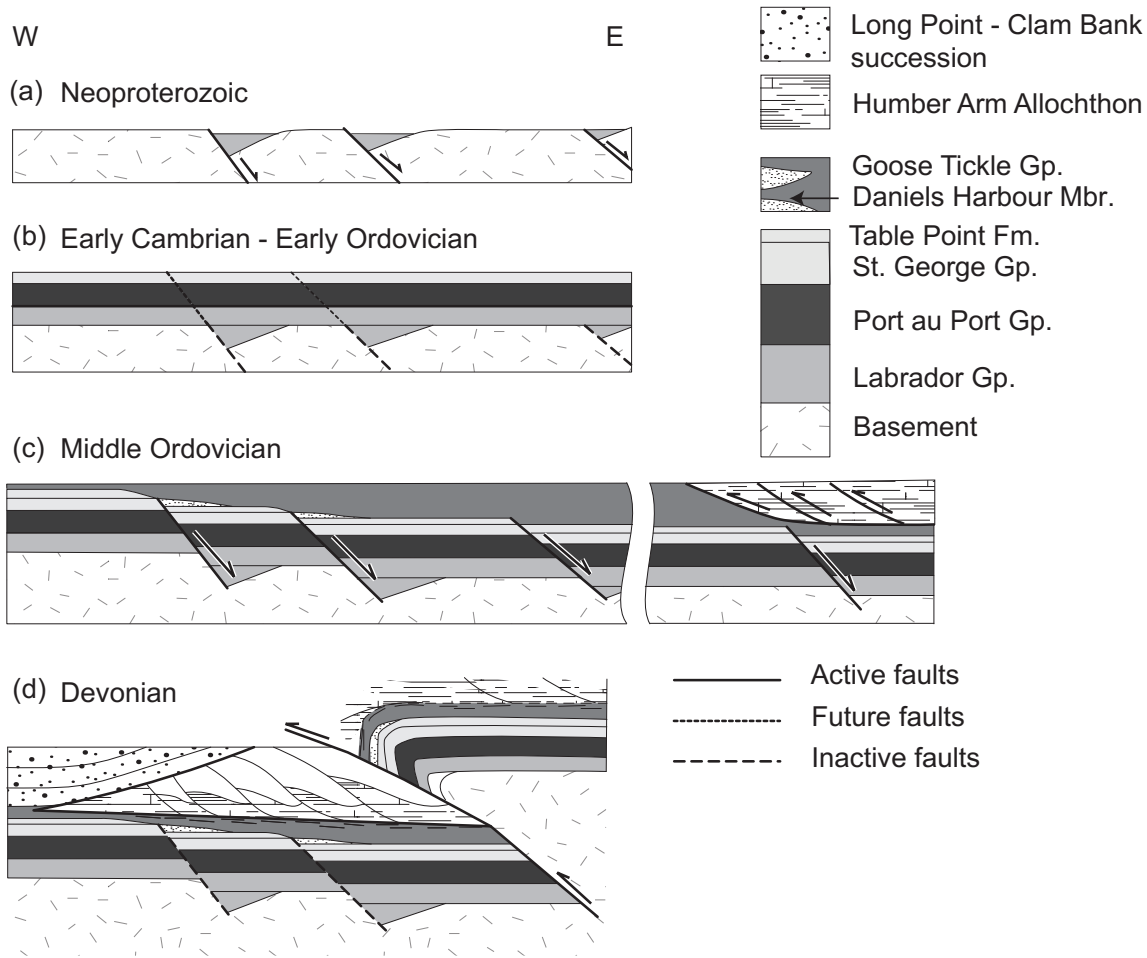


Figure 3.14: Summary of faulting history of Parsons Pond area. (a) Neoproterozoic rifting related to opening of the Iapetus Ocean. Rift-related sediments of the Bradore Formation (Labrador Group) are deposited at this time. (b) Cambrian through Early Ordovician passive margin development on the eastern margin of Laurentia. (c) Middle Ordovician extension during loading of the Laurentian margin by the Humber Arm Allochthon during the Taconian Orogeny. Earlier rift-related faults are reactivated and fault scarp limestone conglomerate units, including the Daniels Harbour Member, are deposited into graben. (d) Inversion of basement normal faults previously active in (a) and (c) during the Acadian Orogeny.

On the Port au Port Peninsula, the Cape Cormorant Formation of the Table Head Group is interpreted to have been generated in a similar tectonic setting; however, the age range of carbonate clasts indicates that they were derived from an escarpment which exposed at least 1000 m of platform (Stenzel et al. 1990). This suggests that faster slip rates in the Port au Port Peninsula region outpaced sediment accumulation. We interpret these basement faults to have been activated during Ordovician flexural extension as the platform was loaded by Taconian allochthons.

At present day, rift-related Bradore Formation and Taconian syntectonic limestone conglomerate units (Daniels Harbour Member and Cape Cormorant Formation) lie predominantly in the hanging walls of deep-seated major thrust faults, indicating that many Middle Ordovician (and possibly Neoproterozoic) normal faults were reactivated and inverted after the Taconian Orogeny, probably during the Devonian Period (Figure 3.14d). We interpret that both the Round Head and Parsons Pond thrusts are inverted normal faults, the Parsons Pond and Round Head precursor faults, prior to inversion (Figure 3.1). Both the Round Head and Parsons Pond thrusts demonstrate significant displacement (up to 9 and 12 km of transport respectively) during inversion and are responsible for the distinctive present day distribution of parautochthonous platform rocks in western Newfoundland. It is clear however, from younger-over-older relationships preserved in the Parsons Pond thrust sheet, that not all pre-existing normal faults were reactivated during Acadian Orogenesis. Some were instead transported passively in the Parsons Pond thrust sheet (Figure 3.3: Domain 1 and Figure 3.7a), where shallow normal faults represent originally steeper features that have been rotated in the overturned limb of a basement cored fault-propagation fold.

Although cross-cutting and stratigraphic relationships can only constrain basement thrusting in the Parsons Pond region as post-Taconian, structural similarities to the Early Devonian Round Head Thrust on the Port au Port Peninsula lead us to interpret that basement-involved thrusting in Parsons Pond is also Acadian. These two faults are likely genetically linked and define two large portions of an extensive Acadian structural front in western Newfoundland that inverted earlier Taconian features during closure of the Iapetus Ocean.

3.5.5. Regional Correlations

Farther south in Québec, Vermont and New York, similar deep-seated basement faults have also been interpreted to result from lower-plate extension during Taconian convergence. In southern Québec, the Upper Ordovician Lacolle Breccia (Figure 3.1b) (Globensky 1981) has the same significance as the Cape Cormorant Formation (Lavoie 1994), likely a fault-scarp deposit, in the hanging walls of basement normal faults. Like the Round Head and Parsons Pond Precursor faults, this fault had significant throw, at least 600 m, interpreted from clast

compositions corresponding to upper portions of the platform in Québec (Lavoie 1994). The Late Ordovician age of the conglomerate is consistent with the timing of Taconian Orogenesis in Québec. This fault however, if reactivated during Acadian orogenesis, was not completely inverted, and therefore does not show a reverse sense of offset at present day.

Farther south, in the Champlain Valley, Hayman & Kidd (2002) interpret that basement normal faults, which cut platform and foreland units, were also active during the Taconian Orogeny and were reactivated as inversion structures during later orogenesis. They interpret that the Taconic Frontal Thrust (a post-Taconian feature) developed along an extensive shelf-parallel normal fault, originally formed during Taconian craton loading (Hayman & Kidd, 2002). Like the Parsons Pond Thrust, the Taconic Frontal Thrust is an out-of-sequence thrust which places shelf rocks above units of the Taconian allochthon. The Taconic Frontal Thrust can be traced under Silurian cover in New York State, and cannot be Devonian in age (Hayman & Kidd 2002). However, crenulation cleavage associated with the Taconic Frontal Thrust is Devonian, so at least some of the shortening may be due to Acadian contraction (Zen 1972, Chan et al. 2001).

The structural framework observed in western Newfoundland also resembles the large-scale structure of Mesoproterozoic inliers in Vermont and Massachusetts. Here antiformal domes, including the Green Mountain and Berkshire inliers (Figure 3.1b), expose Grenvillian basement cores which are unconformably overlain by rift and shelf successions. These parautochthonous units have been structurally uplifted along the eastern margin of Taconian allochthons (Hibbard et al. 2006). Uplift and folding of these inliers must post-date the Taconian emplacement of adjacent allochthons to the west; however, timing of faulting in the Green Mountain and Berkshire inliers is not well constrained (Karabinos 1988). The structures are potential analogues for those seen in Newfoundland, although the Acadian metamorphic and structural overprint is stronger.

3.5.6. Analogues in Other Orogens

A number of studies demonstrate the reactivation and/or inversion of pre-existing basement faults during the evolution of various orogens around the world including: Taiwan (Lee et al. 2002, Lacombe & Mouthereau 2002), Zagros (Jackson 1980), the Alps (Lacombe & Mouthereau 2002, De Graciansky et al. 2011, Granado et al. 2016), the Carpathians (Granado et al. 2016), and the Pyrenees (Lacombe & Mouthereau 2002). In particular, Granado et al. (2016) interpret that normal deep-seated faults at the Alpine-Carpathian junction in Austria formed during rifting and were reactivated during development of the thin-skinned fold and thrust belt. Continued orogenesis resulted in small amounts of tectonic inversion and shortening along these pre-existing structures (Granado et al. 2016). These examples indicate that basement-involved faulting and inversion of rift-related structures is a common process in the development of an

orogen during the Wilson Cycle. The presence of basement-cored antiformal massifs and major out-of-sequence structures within fold and thrust belts around the world suggests that thick-skinned structures may be as important as thin-skinned structures in the development of fold and thrust belts.

3.5.7. A Laramide-Type Orogen

The Late-Cretaceous-early Tertiary Laramide Orogeny in the western US has also been interpreted to involve the reactivation and inversion of pre-existing basement normal faults, resulting in fault bounded, basement cored uplifts (Mitra & Mount 1998, Bump 2003). Evidence used to suggest reactivation and inversion of pre-existing structures is similar to that used in this study. In the Grand Canyon, Huntoon (1993) documents Precambrian syn-extensional strata in the hanging wall of Laramide reverse faults. Others have used large-scale map patterns of Laramide faulting, showing dominant fault orientations which parallel known Precambrian rifts in the southern Rocky Mountains (Marshak et al. 2000). Schmidt & Garihan (1983) demonstrate that Laramide faults parallel Precambrian dykes and shear zones and are therefore localized along these pre-existing weaknesses in the crust.

Laramide folds, associated with basement uplifts, are described as fault-propagation folds (Bump 2003) displaying broad antiformal to monoclinical geometries with long back limbs and relatively short, thinned forelimbs (Allmendinger 1998, Mitra & Mount 1998), similar to those produced by faulting along the Parsons Pond Thrust in western Newfoundland. Dips are dominantly 30° – 60° and dips steepen from 90° to 75° where strata are overturned towards the fault (Figure 3.3 in Bump 2003). Mitra & Mount 1998) present multiple cross-sections through these structures in the Bighorn, Uinta and Delaware basins and the similarities are striking. We interpret that the Acadian Orogeny in the northern Appalachians may be analogous in this respect to the Laramide Orogeny in western USA.

3.6. Conclusions

Deep-seated basement faults in western Newfoundland have a protracted history of movement during the opening and subsequent closure of the Iapetus Ocean. Many steep basement faults have orientations that parallel previously recognized rift-related structures (Thomas 1977, Miller & Barr 2004, Allen et al. 2010, Burton & Southworth 2010) and have rift-related sediments in their hanging walls, indicating activation during Neoproterozoic rifting associated with opening of the Iapetus Ocean. These basement faults were reactivated during the Taconian Orogeny as the down-going Laurentian plate underwent flexural extension during assembly and emplacement of the Humber Arm Allochthon. In the Parsons Pond region the

allochthon forms typical structures observed in thin-skinned fold and thrust belts such as stacked and folded duplexes.

Acadian deformation involved reactivation and inversion of these deep-seated basement-involved normal faults. The Parsons Pond Thrust, the major structural boundary in the Parsons Pond region, placed parautochthonous units on top of the eastern margin of the Humber Arm Allochthon. The Parsons Pond Thrust sheet was transported at least 8 km to the NW, and up to 12 km to the NW near Portland Creek Pond. Inversion of basement faults is responsible for the current high structural level of the Long Range Mountains. Basement-cored fault-propagation folds associated with these faults have characteristic broad, shallow-dipping back limbs and steep to overturned forelimbs, and are structurally analogous to basement inversion structures formed during the Laramide Orogeny in western USA.

The Parsons Pond Thrust is analogous to the Early Devonian Round Head Thrust to the south in Newfoundland. Farther south, in New York and Vermont, the Taconic Frontal Thrust is also structurally analogous to the Parsons Pond and Round Head thrusts, placing parautochthonous rocks above Taconian allochthons during inversion. Farther south the large-scale structure of Mesoproterozoic inliers in Vermont and Massachusetts also resembles the structural framework observed in western Newfoundland. These observations lead us to suggest that the structures are all genetically linked, forming an extensive, deep-seated Acadian thrust front along the length of the entire northern Appalachians, formed by inversion of earlier structures.

3.7. References

- ALLEN J. S., THOMAS W. A. & LAVOIE D. 2010. The Laurentian margin of northeastern North America. In: *From Rodinia to Pangea: The Lithotectonic Record of the Appalachian Region* (Ed. by R. P. Tollo, M. J. Bartholomew, J. P. Hibbard & P. M. Karabinos), pp. 71–90.
- ALLMENDINGER R. W. 1998. Inverse and forward modeling of trishear fault-propagation folds. *Tectonics* 17: 640–656.
- ANONYMOUS 1998. Interpretation report of seismic survey LABMIN 92-T9G: Parsons Pond (E.P. 92-101). In: p. 3. Labrador Mining and Exploration Co. Ltd.
- BIRD J. M. & DEWEY J. F. 1970. Lithosphere plate-continental margin tectonics and the evolution of the Appalachian orogen. *Geological Society of America Bulletin* 81: 1031–1060.
- BOTSFORD J. W. 1988. Geochemistry and petrology of Lower Paleozoic platform-equivalent shales, western Newfoundland. *Newfoundland and Labrador, Department of Mines, Mineral Development Division, Report 88-1*: 85–98.

- BRADLEY D. C. 1983. Tectonics of the Acadian orogeny in New England and adjacent Canada. *The Journal of Geology* 91: 381–400.
- BRADLEY D. C. & KIDD W. S. F. 1991. Flexural extension of the upper continental crust in collisional foredeeps. *Geological Society of America Bulletin* 103: 1416–1438.
- BUMP A. P. 2003. Reactivation, trishear modeling, and folded basement in Laramide. *GSA Today*: 4–10.
- BURDEN E. T. & WILLIAMS S. H. 1995. Biostratigraphy and thermal maturity of strata in Hunt-Pan Canadian Port au Port well # 1. Hunt oil, St. John's Newfoundland.
- BURTON W. C. & SOUTHWORTH S. 2010. A model for Iapetan rifting of Laurentia based on Neoproterozoic dikes and related rocks. *Geological Society of America Memoirs* 206: 455–476.
- BUTLER R. W. H. 1982. *Journal of Structural Geology* 4: 239–245.
- CAWOOD P. A., MCCAUSLAND P. J. & DUNNING G. R. 2001. Opening Iapetus: Constraints from the Laurentian margin in Newfoundland. *Geological Society of America Bulletin* 113: 443–453.
- CAWOOD P. A. & WILLIAMS H. 1988. Acadian basement thrusting, crustal delamination, and structural styles in and around the Humber Arm allochthon, western Newfoundland. *Geology* 16: 370.
- CHAN Y. C., CRESPI J. M. & HODGES K. V. 2001. Dating cleavage formation in slates and phyllites with the western New England Appalachians, U.S.A: *Terra Nova* 12: 264–271.
- CHOW N. & JAMES N. P. 1987. Cambrian Grand Cycles: A northern Appalachian perspective. *Geological Society of America Bulletin* 98: 418.
- COOK L. A. & KILFOIL G. J. 2009. Aeromagnetic Survey - Gros Morne - Port au Choix Area, Newfoundland: NTS map area 12H/12. Nalcor Energy; Energy Branch, Department of Natural Resources.
- DE GRACIANSKY P.-C., ROBERTS D. G. & TRICART P. 2011. Chapter Thirteen - Birth of the Western and Central Alps: Structural Inversion and the Onset of Orogenesis. In: *The Western Alps, from Rift to Passive Margin to Orogenic Belt* (Ed. by P.-C. De Graciansky, D. G. Roberts & P. Tricart), pp. 269–288. Elsevier.
- DEWEY J. F. & BIRD J. M. 1971. Origin and emplacement of the ophiolite suite: Appalachian ophiolite in Newfoundland. *American Geophysical Union* 76: 3179–3206.
- DEWEY J. F. & CASEY J. F. 2013. The sole of an ophiolite: the Ordovician Bay of Islands Complex, Newfoundland. *Journal of the Geological Society* 170: 715–722.
- DUNNING G. R. & KROGH T. E. 1985. Geochronology of ophiolites of the Newfoundland Appalachians. *Canadian Journal of Earth Sciences* 22: 1659–1670.

- DUNNING G. R., O'BRIEN S. J., COLMAN S. S. P., BLACKWOOD R. F., DICKSON W. L., O'NEILL P. P. & KROGH T. E. 1990. Silurian orogeny in the Newfoundland Appalachians. *Journal of Geology* 98: 895–913.
- ELLIOTT D. & JOHNSON M. R. . 1980. Structural evolution in the northern part of the Moine thrust belt, NW Scotland. *Transactions of the Royal Society of Edinburgh: Earth Sciences* 71: 69–96.
- GLOBENSKY Y. 1981. Régions de Lacolle Saint-Jean (s). In: p. 197. Rapport géologique, Ministère de l'Énergie et des Ressources du Québec.
- GODLEWSKI M. 1997. Geophysical interpretation report Portland/Bellburns program west Newfoundland. Talisman Energy Inc.
- GRANADO P., THONY W., CARRERA N., GRATZER O., STRAUSS P. & MUNOZ J. A. 2016. Basement-involved reactivation in foreland fold-and-thrust belts: the Alpine?Carpathian Junction (Austria). *Geological Magazine* 153: 1110–1135.
- HAYMAN N. W. & KIDD W. S. F. 2002. Reactivation of prethrusting, synconvergence normal faults as ramps within the Ordovician Champlain-Taconic thrust system. *Geological Society of America Bulletin* 114: 476–489.
- HIBBARD J. P., VAN STAAL C. R., RANKIN D. W. & WILLIAMS H. 2006. Lithotectonic Map of the Appalachian Orogen, Canada- United States of America. Geological Survey of Canada.
- HUNTOON P. W. 1993. Influence of inherited Precambrian basement structures on the localization and form of Laramide monoclines, Grande Canyon, Arizona. In: *Laramide basement deformation in the Rocky Mountain foreland of the western United States: Boulder Colorado* (Ed. by C. J. Schmidt), pp. 243–256. Geological Society of America Special Paper 280.
- JACKSON J. A. 1980. Reactivation of basement faults and crustal shortening in orogenic belts. *Nature* 283: 343–346.
- JACOBI R. D. 1981. Peripheral bulge-a causal mechanism for the Lower/Middle Ordovician unconformity along the western margin of the Northern Appalachians. *Earth and Planetary Science Letters* 51: 245–251.
- JAMES N. P. & STEVENS R. K. 1986. Stratigraphy and Correlation of the Cambro-Ordovician Cow Head Group, Western Newfoundland. *Geological Survey of Canada Bulletin* 366: 143.
- KARABINOS P. 1988. Tectonic significance of basement-cover relationships in the Green Mountain massif, Vermont. *The Journal of Geology* 96: 445–454.
- KNIGHT I. & JAMES N. P. 1987. The stratigraphy of the Lower Ordovician St. George Group, western Newfoundland: the interaction between eustasy and tectonics. *Canadian Journal of Earth Sciences* 24: 1927–1951.

- KNIGHT I., JAMES N. P. & LANE T. E. 1991. The Ordovician St. George Unconformity, northern Appalachians: the relationship of plate convergence at the St. Lawrence Promontory to the Sauk/Tippecanoe sequence boundary. *Geological Society of America Bulletin* 103: 1200–1225.
- KUMARAPELI P. S. 1985. Vestiges of Iapetan rifting in the craton west of the northern Appalachians. *Journal of the Geological Association of Canada* 12: 54–59.
- LACOMBE O. & MOUTHEREAU F. 2002. Basement-involved shortening and deep detachment tectonics in forelands of orogens: Insights from recent collision belts (Taiwan, Western Alps, Pyrenees). *Tectonics* 21: 12–1--12–22.
- LAVOIE D. 1994. Diachronous tectonic collapse of the Ordovician continental margin, eastern Canada: comparison between the Quebec Reentrant and St. Lawrence Promontory. *Canadian Journal of Earth Sciences* 31: 1309–1319.
- LEE C.-I., CHANG Y.-L. & COWARD M. P. 2002. Inversion tectonics of the fold-and-thrust belt, western Taiwan. In: *Geophysics of an Arc-Continent Collision, Taiwan* (Ed. by T. B. Byrne & C.-S. Liu), pp. 13–30. Geological Society of America, Boulder, Colorado.
- MARSHAK S., KARLSTROM K. & TIMMONS J. M. 2000. Inversion of Proterozoic extensional faults: An explanation for the pattern of Laramide and ancestral Rockies intracratonic deformation, United States. *Geology* 28: 735–738.
- MILLER B. V. & BARR S. M. 2004. Metamorphosed Gabbroic Dikes Related to Opening of Iapetus ocean at the St. Lawrence Promontory: Blair River Inlier, Nova Scotia, Canada. *The Journal of Geology* 112: 277–288.
- MITRA S. & MOUNT V. S. 1998. Foreland basement-involved structures. *AAPG bulletin* 82: 70–109.
- PALMER S. E., BURDEN E. & WALDRON J. W. F. 2001. Stratigraphy of the Curling Group (Cambrian), Humber Arm Allochthon, Bay of Islands. *GSC Current research 2001–1*: 105–112.
- PALMER S. E., WALDRON J. W. F. & SKILLITER D. M. 2002. Post-Taconian shortening, inversion and strike slip in the Stephenville area, western Newfoundland Appalachians. *Canadian Journal of Earth Sciences* 39: 1393–1410.
- QUINN L. A. 1992. Foreland and trench slope basin sandstones of the Goose Tickle group and Lower Head Formation, western Newfoundland. PhD Thesis, Memorial University of Newfoundland, St. John's Newfoundland.
- REEVES C. 2005. Aeromagnetic surveys: Principles, Practice and Interpretation. *Geosoft*.
- RIVERS T. 2008. Assembly and preservation of lower, mid, and upper orogenic crust in the Grenville Province—Implications for the evolution of large hot long-duration orogens. *Precambrian Research* 167: 237–259.

- ROBERTS M. 2011. Nalcor Energy - Oil and Gas Inc. Final Well Report for Nalcor Energy et al Finnegan # 1 at Permit 03-102, Western Newfoundland. In: p. 845. Nalcor Energy, Oil and Gas.
- SCHMIDT C. J. & GARIHAN J. M. 1983. Laramide tectonic development in the Rocky Mountain foreland of southwestern Montana. In: *Rocky Mountain foreland basins and uplifts* (Ed. by J. D. Lowell), pp. 271–294. Rocky Mountain Association of Geologists, Denver.
- ST. JULIEN P. & HUBERT C. 1975. Evolution of the Taconic orogen in the Quebec Appalachians. *American Journal of Science* 275–A: 337–362.
- VAN STAAL C. R., WHALEN J. B., VALVERDE-VAQUERO P., ZAGOREVSKI A. & ROGERS N. 2009. Pre-Carboniferous, episodic accretion-related, orogenesis along the Laurentian margin of the northern Appalachians. In: *Ancient Orogens and Modern Analogues* (Ed. by J. B. Murphy, J. D. Keppie & A. J. Hynes), pp. 271–316. Geological Society, London, Special Publications.
- STENZEL S. R., KNIGHT I. & JAMES N. P. 1990. Carbonate platform to foreland basin: revised stratigraphy of the Table Head Group (Middle Ordovician), western Newfoundland. *Canadian Journal of Earth Sciences* 27: 14–26.
- STEVENS R. K. 1970. Cambro-Ordovician flysch sedimentation and tectonics in west Newfoundland and their possible bearing on a proto-Atlantic Ocean. In: *Flysch Sedimentology in North America* (Ed. by P. Lajoie), pp. 165–177. Geological Association of Canada.
- STOCKMAL G. S., SLINGSBY A. & WALDRON J. W. 1998. Deformation styles at the Appalachian structural front, western Newfoundland: implications of new industry seismic reflection data. *Canadian Journal of Earth Sciences* 35: 1288–1306.
- STOCKMAL G. S., SLINGSBY A. & WALDRON J. W. F. 2004. Basement-involved inversion at the Appalachian structural front, western Newfoundland: an interpretation of seismic reflection data with implications for petroleum prospectivity. *Bulletin of Canadian Petroleum Geology* 52: 215–233.
- SUPPE J. & MEDWEDEFF D. A. 1990. Geometry and kinematics of fault-propagation folding. *Eclogae Geologicae Helveticae* 83: 409–454.
- THOMAS W. A. 1977. Evolution of Appalachian-Ouachita salients and recesses from reentrants and promontories in the continental margin. *American Journal of Science* 277: 1233–1278.
- TREMBLAY A., LONG B. & MASSÉ M. 2003. Supracrustal faults of the St. Lawrence rift system, Québec: kinematics and geometry as revealed by field mapping and marine seismic reflection data. *Tectonophysics* 369: 231–252.

- VAN STAAL C. R., ZAGOREVSKI A., MCNICOLL V. J. & ROGERS N. 2014. Time-Transgressive Salinic and Acadian Orogenesis, Magmatism and Old Red Sandstone Sedimentation in Newfoundland. *Geoscience Canada* 41: 138.
- VOLLMER F. W. 1986. *Orient 3.2. 0 Spherical Projection and Orientation Data Analysis Software User Manual*.
- VOLLMER F. W. 1990. An application of eigenvalue methods to structural domain analysis. *Geological Society of America Bulletin* 102: 786–791.
- VOLLMER F. W. 2015. Orient 3; a new integrated software program for orientation data analysis, kinematic analysis, spherical projections, and Schmidt plots. *Abstracts with Programs - Geological Society of America* 47: 49–49.
- WALDRON J. W. F., HENRY A. D., BRADLEY J. C. & PALMER S. E. 2003. Development of a folded thrust stack: Humber Arm Allochthon, Bay of Islands, Newfoundland Appalachians. *Canadian Journal of Earth Sciences* 40: 237–253.
- WALDRON J. W. F., SCHOFIELD D. I. & MURPHY J. B. 2017. Diachronous Palaeozoic accretion of peri-Gondwanan terranes at the Laurentian margin. In: *Fifty Years of the Wilson Cycle* (Ed. by R. W. Wilson, G. A. Houseman, K. J. W. McCaffrey, A. G. Dore & S. J. H. Buiter), p.
- WALDRON J. W. F., STOCKMAL G. S., CORNEY R. E. & STENZEL S. R. 1993. Basin development and inversion at the Appalachian structural front, Port au Port Peninsula, western Newfoundland Appalachians. *Canadian Journal of Earth Sciences* 30: 1759–1772.
- WALDRON J. W. & VAN STAAL C. R. 2001. Taconian orogeny and the accretion of the Dashwoods block: A peri-Laurentian microcontinent in the Iapetus Ocean. *Geology* 29: 811–814.
- WILLIAMS H. & CAWOOD P. A. 1989. Geology of Humber Arm Allochthon, Newfoundland. Geologic Survey of Canada, western Newfoundland.
- WILLIAMS H. & HISCOTT R. N. 1987. Definition of the Iapetus rift-drift transition in western Newfoundland. *Geology* 15: 1044–1047.
- WILLIAMS H., JAMES N. P. & STEVENS R. K. 1985a. Humber Arm Allochthon and nearby groups between Bonne Bay and Portland Creek, western Newfoundland. In: *Current Research* (Ed. by M. J. Kiel & D. Busby), pp. 399–406. Geologic Survey of Canada.
- WILLIAMS H., JAMES N. P. & STEVENS R. K. 1985b. *Humber Arm Allochthon and nearby groups between Bonne Bay and Portland Creek, western Newfoundland*. Geologic Survey of Canada.
- WILLIAMS H. & STEVENS R. K. 1974. Taconic Orogeny and the development of the ancient continental margin of eastern North American in Newfoundland. *Journal of the Geological Association of Canada* 1: 31–33.
- WILSON J. T. 1966. Did the Atlantic close and then re-open. *Nature* 211: 676–681.

ZEN E. 1972. Some revisions in the interpretation of the Taconic allochthon in west-central Vermont. *Geological Society of America Bulletin* 83: 2573–2588.

Chapter 4: Provenance of the Newfoundland Appalachian Foreland Basins

The provenance of foreland basin sedimentary rocks can provide important insights into the history of an adjacent orogen. U/Pb ages of detrital zircon within the foreland basin successions offshore of western Newfoundland have Mesoproterozoic, Paleoproterozoic and Archean ages, consistent with derivation from Laurentian sources. Previously published results from the oldest foreland succession, the Middle Ordovician Goose Tickle Group, demonstrates ages similar to units preserved with the Humber Arm Allochthon, including a predominant Paleoproterozoic peak at 1.85 Ga, confirming their derivation from the allochthon, emplaced during Middle Ordovician Taconian orogenesis. In this study we investigated U/Pb geochronology of detrital zircons from younger foreland successions including, the Long Point Group, Clam Bank Formation, and Red Island Road Formation. The largest proportion of analyses within all foreland successions fall between 0.95 and 1.3 Ga, with largest peaks occurring between 1.0 and 1.1 Ga, typical of zircons derived from the Grenville Orogen. Earlier Mesoproterozoic and Paleoproterozoic ages range from 1.3 – 2.0. The abundance of Mesoproterozoic grains and conspicuous lack of Paleoproterozoic zircons at 1.85 Ga in the overlying Upper Ordovician Long Point Group and latest Silurian to Early Devonian Clam Bank Formation indicates that these sediments were not derived from units within the Humber Arm Allochthon. Probability density plots of continental margin units in the Québec/New England segment of the orogen demonstrate a similar strong Mesoproterozoic and weak Paleoproterozoic signature, suggesting derivation of the Long Point Group from the Québec segment of the orogen. Within the mid-Paleozoic Clam Bank - Red Island Road succession, typical Gondwanan ages are absent and 1.0 Ga grains derived from the Grenville Orogen are abundant. This is consistent with underthrusting of the Gondwanan microcontinents Ganderia and Avalonia during Salinian and Acadian orogenesis. Only Mesoproterozoic zircons were found in the Early Devonian Red Island Road Formation, consistent with derivation from Mesoproterozoic Grenville massifs in western Newfoundland or Cape Breton Island which were uplifted during Devonian Acadian inversion.

4.1. Introduction

Foreland basins provide valuable records of events involved in the building of an orogen. Foreland basins are formed by orogenic loading through flexure of the lithosphere, while the developing orogen provides the source of detritus to fill the basin. Because of this intrinsic link

between orogen and basin the provenance of foreland basin fills provides evidence of uplift and erosion of source regions within the orogen.

The current understanding of Appalachian orogenesis is based largely on stratigraphic and isotopic dating of deformed, metamorphosed and magmatic units within the orogen. The earliest convergent episode, the Ordovician Taconian Orogeny, involved the collision of an island arc and peri-Laurentian microcontinents with Laurentia, and westward emplacement of allochthons (including the Humber Arm Allochthon in Newfoundland) on top of the Laurentian margin (Stevens 1970, Williams & Stevens 1974, Waldron & van Staal 2001, van Staal et al. 2009). Later orogenic episodes, including the Silurian Salinian Orogeny (Dunning et al. 1990) and Early Devonian Acadian Orogeny (van Staal et al. 2014) involved the accretion of exotic terranes to the composite margin. Although stratigraphic and isotopic evidence within the orogen (van Staal et al. 1998, 2009, Waldron et al. 2017) provides constraint on what accreted and when, important questions remain unanswered. These include: (1) what was the specific transport direction of accreted material, (2) which portions of the orogen were uplifted and (3) what were the positions and variability of loads along the orogen during orogenesis?

In this study we use detrital zircon geochronology to help resolve these complexities in the northern Appalachian Orogen. Because zircon is highly refractory at the surface of the Earth it occurs in virtually all siliciclastic deposits, and the presence of U, and therefore of radiogenic Pb, in zircon allows dating using U/Pb geochronology. These features have made detrital zircon geochronology one of the best methods for determining basin provenance.

In this study we analyse five samples from the foreland basin successions in western Newfoundland (Figure 4.1). The foreland sediments were largely derived from erosion of uplifted thrust sheets of allochthonous continental margin and local basement units (Bradley 1983, Cawood & Nemchin 2001, McLennan et al. 2001, Thomas & Becker 2007). We discuss our new data in comparison with previously published zircon ages from the Paleozoic continental margin and regional basement and aim to provide new interpretations of Appalachian orogenic history in context of the current tectonic understanding of the orogen.

4.2. Tectonic Setting and Source Regions

4.2.1. Laurentian Basement

The Paleozoic continental margin, on which the Appalachian Orogen developed, was founded on Mesoproterozoic and older rocks of eastern Laurentia (Figure 4.2) (Cawood & Nemchin 2001). The Superior and North Atlantic cratons, that represent the Archean cores of eastern Laurentia, were stitched together by 2.0-1.8 Ga Paleoproterozoic orogens (Hoffman 1988). In eastern Laurentia these include: the Trans-Hudson, New Québec, Torngat, and

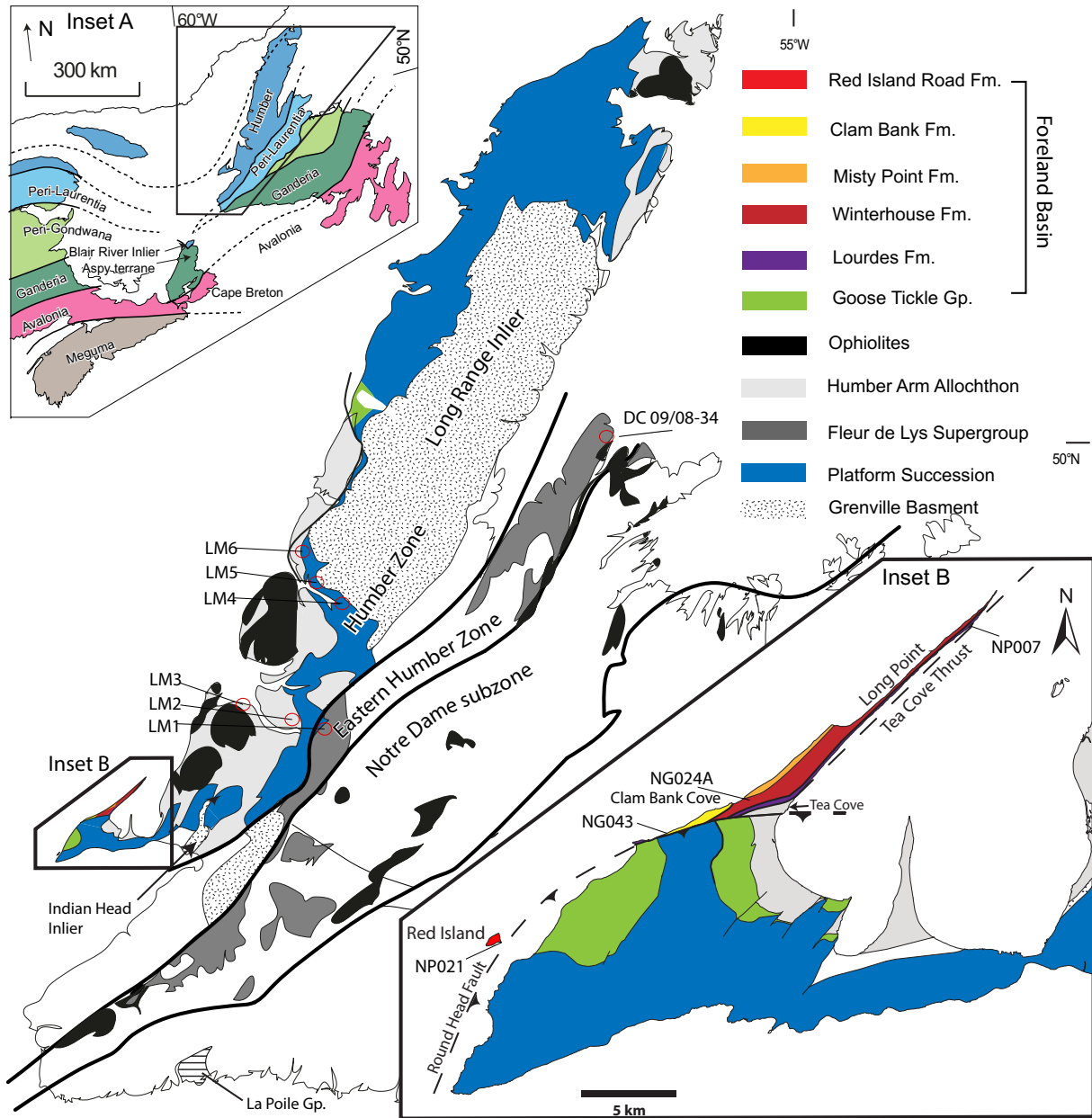


Figure 4.1: Geological map of western Newfoundland showing important place names, locations, structures, and sample sites from previously published works. Inset A is a tectonic zonation map of a portion of the northern Appalachians (Modified from Waldron & van Staal 2001). Inset B is a geological map of the Port au Port Peninsula showing sample sites from this study.

Makkovik orogens. Along the eastern margin of Laurentia lies the Grenville Province (Rivers 1997) dominated by the ~ 1.0 Ga Grenville Orogen, although older pre-Grenvillian crust (1.7-1.2 Ga) is preserved within the Grenville Province (Rivers 1997) (Figure 4.2). Populations of zircons sourced from Laurentia generate age spectra with characteristic peaks and gaps indicative of derivation from these provinces; a number of studies show excellent examples of such Laurentia-derived zircons (Figure 4.3, Inset 1) and the associated probability density distributions which characterize Laurentian sources (Cawood & Nemchin 2001, Cawood et al. 2007, Waldron et al. 2008, 2012). The probability density function shown in inset 1 of figure 4.3 is a typical Laurentian signature with major peaks at 1.1, 1.8 and 2.7 Ga coinciding with the ages of major Laurentian crustal components.

The western zone of the Appalachian Orogen, the Humber Zone (Figure 4.1), contains deformed Paleozoic rocks of Laurentian affinity and older Mesoproterozoic basement of the Grenville Province (Rivers, 1997; Heaman et al., 2002). To the east, the Dashwoods and Notre Dame subzones are interpreted as portions of a larger peri-Laurentian microcontinental block (Waldron & van Staal 2001: Figure 4.1), although its basement is nowhere exposed. Terranes farther east contain units of exotic affinity and zircon populations derived from these terranes have age spectra indicative of Gondwanan, not Laurentian, sources (Macdonald et al., 2014; Pothier et al., 2015; Murphy et al., 2004; Waldron et al., 2011). Zircons derived from terranes of Gondwanan affinity generate probability distributions which cannot be explained by derivation from Laurentia. The spectra typically lack the 1.0 Ga Grenville peak, which is typical of Laurentian detritus. They also contain prominent peaks between 550 and 650 Ma, typical of units derived from either the Brasiliano or Pan-African orogen of the Amazonian or West African craton respectively. Gondwanan units also typically contain grains with ages ranging from 2.0 to 2.2 Ga, derived from either the Eburnean Orogen of West Africa or Trans-Amazonia Orogen of Amazonia. These ages are typically absent in detritus derived from eastern Laurentia.

4.2.2. Rift and Passive Margin Units

The oldest stratified rocks in western Newfoundland were deposited above Mesoproterozoic basement during several episodes of Neoproterozoic to early Cambrian rifting (Cawood et al. 2001). These events led to the opening of an ocean basin (the Iapetus), the development of conjugate margins of Laurentia and Amazonia (Cawood & Williams 1988, Cawood et al. 2001), and the rifting of crustal ribbons from both Laurentian (e.g. Dashwoods block) and Amazonian margins (van Staal et al. 1998, Waldron & van Staal 2001, van Staal et al. 2013).

Rifting generated a series of NE-striking and lesser NW-striking deep-seated extensional faults within the basin, forming grabens into which thick successions of clastic and local mafic

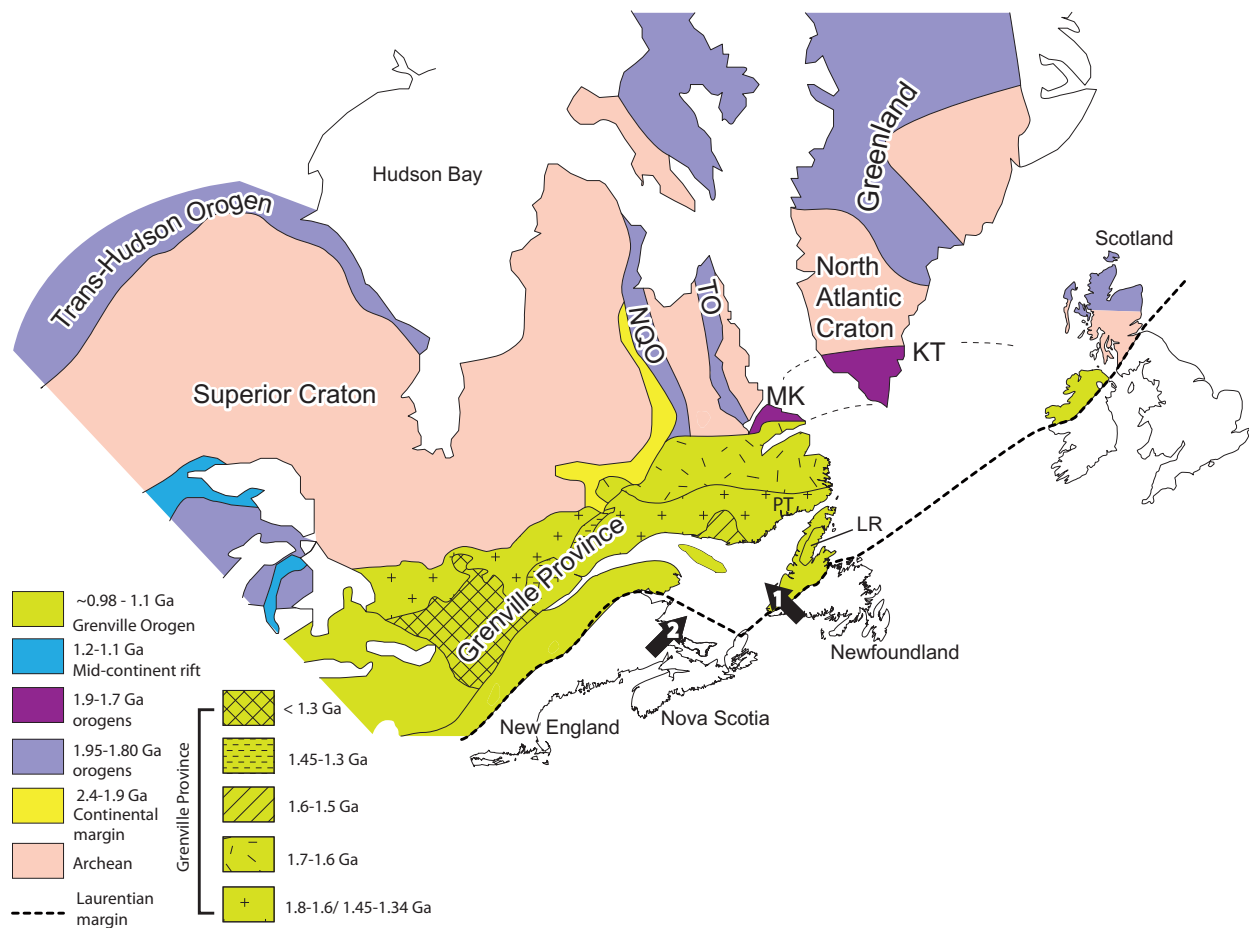
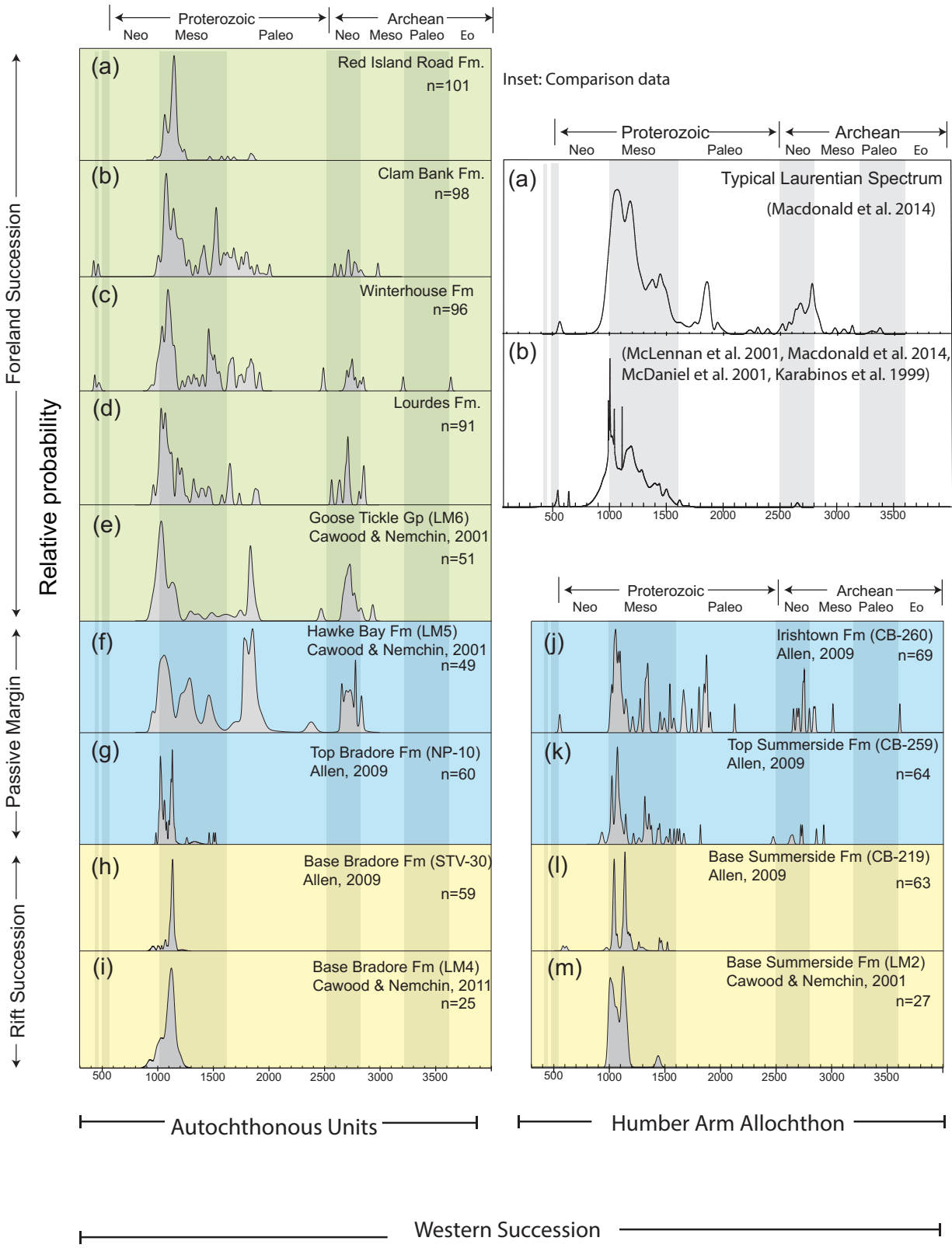
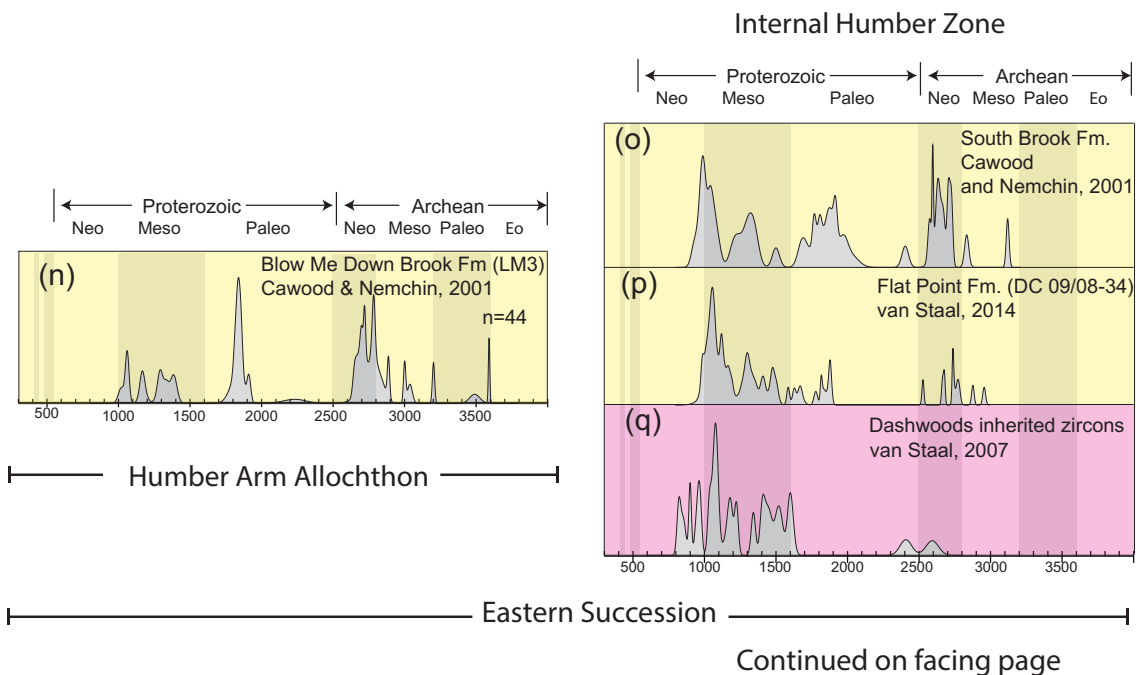


Figure 4.2: Map showing major structural provinces which make up eastern Laurentia. KT, Ketilidian Orogen; MK, Makkovik Orogen; NQO, New Québec Orogen; TO, Torngat Orogen. Arrow 1 is transport direction for Goose Tickle Group detritus. Arrow 2 is transport direction for Long Point Group detritus.



Continued on facing page

Figure 4.3: Detrital zircon probability density functions for data from this study and previously published data (references are on figure). Vertical scale is in arbitrary units of relative probability density. **(a)** NP007 (Lourdes Fm.) **(b)** NG024A (Winterhouse Fm.) **(c)** NG043 (Clam Bank Fm.) **(d)** NP021 (Red Island Road Fm.) **(e)** LM6 (American Tickle Fm.) **(f)** LM5 (Hawke Bay Fm.) **(g)** NP-10 (top Bradore Fm.) **(h)** STV-30 (base Bradore Fm.) **(i)** LM4 (base Bradore Fm.) **(j)** CB-260 (Irishtown Fm.) **(k)** CB-259 (top Summerside Fm.) **(l)** CB-219 (base Summerside Fm.) **(m)** LM2 (base Summerside Fm.) **(n)** LM3 (Blow Me Down Brook Fm.) **(o)** LM1 (South Brook Fm.) **(p)** DC 09/08-34 (Flat Brook Fm.) **(q)** inherited zircons in Notre Dame Arc. Inset 1: Probability density functions for comparison with our data. **(a)** Typical Laurentian age spectra (Rowe Formation: Macdonald et al. 2014). **(b)** Laurentian zircon analyses from passive margin units in Quebec and New England. The spectrum is a compilation of multiple sources including: Poughquag quartzite (McLennan et al. 2001), Cheshire Formation (Macdonald et al. 2014), Trap Falls Formation (McDaniel et al. 1997), and Cavendish Formation (Karabinos et al. 1999).



volcanic rocks were deposited (Williams & Hiscott 1987, Allen et al. 2010). Clastic units deposited into these basins include the autochthonous Cambrian Bradore Formation, and the Summerside and Blow Me Down Brook formations (Figure 4.4) exposed in thrust slices within the Humber Arm Allochthon (Palmer et al. 2001) (Figure 4.1). Within the metamorphosed eastern portion of the Humber Zone (Figure 4.1), the South Brook and Flat Point formations of the Fleur de Lys Supergroup represent equivalent synrift clastic units of the Laurentian margin. A dominantly carbonate middle Cambrian – Early Ordovician passive margin overlies the rift-related units. Occurring near the base of this succession are the autochthonous Hawke Bay and allochthonous Irishtown formations, the only coarse-grained siliciclastic units within the passive margin succession (Figure 4.4). Thinly bedded high-energy carbonates of the middle to upper Cambrian Port au Port Group (Chow & James 1987) overlie the Hawke Bay Formation, which in turn are overlain by massive, thick-bedded lower-energy limestone and dolostone of the Lower Ordovician St. George Group (Knight & James 1987). The Cow Head Group represents deep-water lateral equivalents of this carbonate platform now exposed in the Humber Arm Allochthon (Figure 4.4).

Previous U/Pb analyses of zircon in clastic portions of the rift and passive margin successions have been carried out by Cawood & Nemchin (2001), Allen (2009), van Staal et al. (2013). We have divided these into eastern and western units, based on their interpreted depositional position relative to the Laurentian margin (Figure 4.3). Samples collected from the most westerly rift units display remarkably similar narrow age spectra dominated by strong peaks between 1.0 and 1.2 Ga (Figure 4.3). The basal Bradore Formation contains only one peak at 1.0 Ga; this narrow age spectrum is consistent with derivation from the immediate basement of the Grenville Orogen. The basal Summerside Formation and upper Bradore Formation are characterised by two distinct peaks at ~1.0 and 1.1 Ga, which we suggest might possibly delineate the Rigolet and Ottawa phases (Rivers 2015) of the Grenville Orogeny respectively. These units also contain a small percentage (~15%) of older Mesoproterozoic grains, also consistent with derivation from the Grenville Province. In higher portions of the stratigraphic section, representing the passive margin succession, a broader range of ages is observed. The Hawke Bay and Irishtown formations both contain abundant Mesoproterozoic peaks between 1.2 and 1.6 Ga and very strong peaks at 1.85 Ga. These grains could be derived from either the Makkovik or associated Paleoproterozoic orogens (New Québec or Torngat) in the north or the Trans-Hudson region to the west. Both passive margin units have strong Archean signatures dominated by peaks at 2.7 – 2.8 Ga, typical of derivation from either the Superior or North Atlantic cratons.

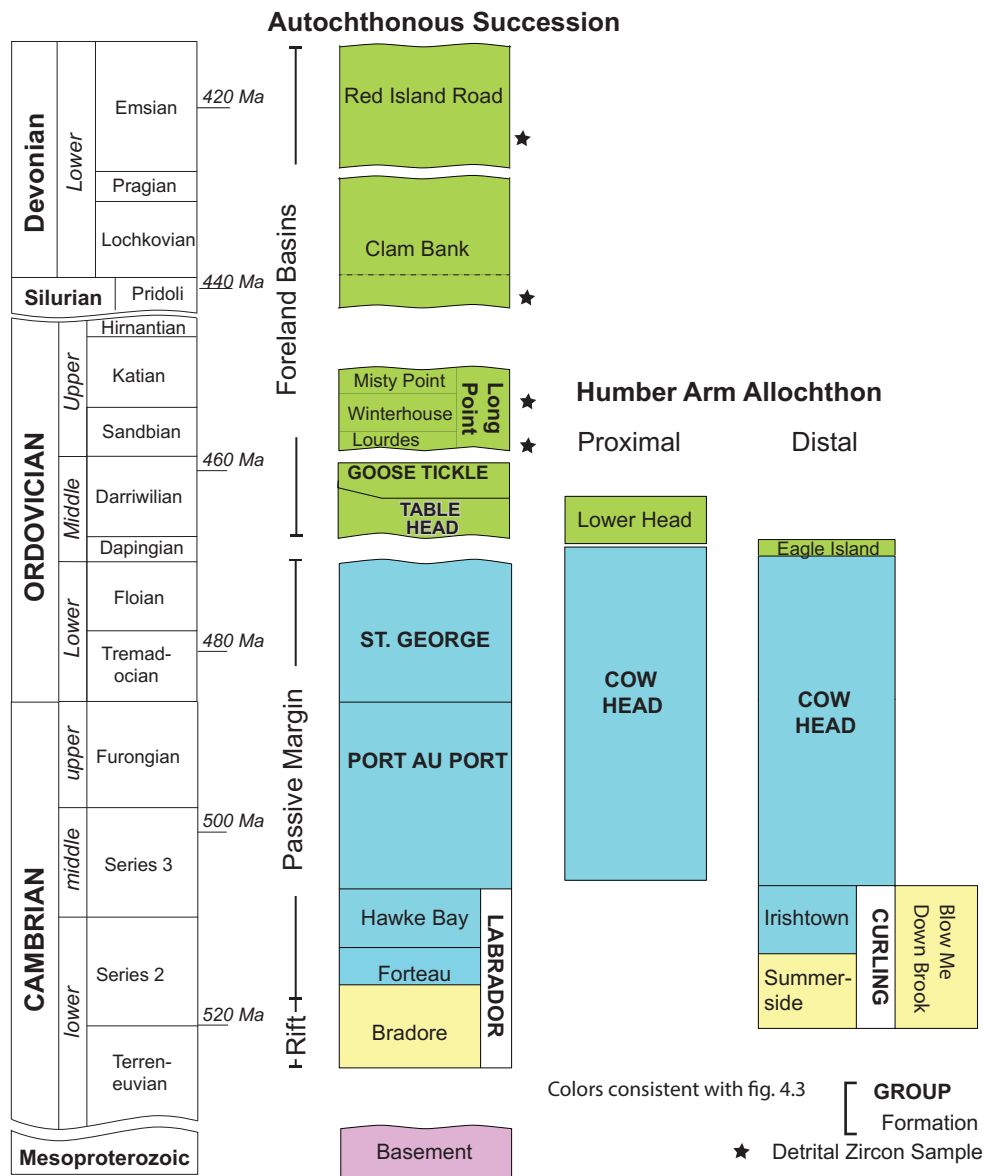


Figure 4.4: Stratigraphic column of western Newfoundland including autochthonous and allochthonous successions.

Metamorphosed clastic units in the eastern Humber Zone (South Brook Formation) and Notre Dame Subzone (Flat Point Formation) (Figure 4.1), together with the structurally highest synrift unit of the Humber Arm Allochthon (the Blow Me Down Brook Formation), contain a much larger spread of ages compared to rift-related units deposited to the west, closer to the Laurentian margin (Bradore and Summerside formations) (Figure 4.3). Although these units still contain a significant population of Grenville zircons, forming peaks at 1.0 – 1.1 Ga, these peaks are diluted by the large proportion of Paleoproterozoic zircons within the spectra. The largest peak within the Blow Me Down Brook Formation occurs at 1.85 Ga, while Paleoproterozoic ages in the Fleur de Lys Supergroup are dominated by 1.90 Ga peaks. These Paleoproterozoic peaks are consistent with derivation from Paleoproterozoic orogens either north (e.g. Makkovik and/or Ketilidian orogens) or west (e.g. Trans-Hudson Orogen) of the basin. Archean grains are dominated by Neoproterozoic detritus with strongest peaks ranging from 2.6 to 2.8 Ga. Smaller, but significant Mesoproterozoic peaks are observed while approximately 7% of grains in the Blow Me Down Brook Formation have Archean ages. Archean ages suggest derivation from either the Superior or North Atlantic craton.

4.2.3. Ordovician Taconian Orogeny and Foreland Basin

The Ordovician Taconian Orogeny involved the collision of peri-Laurentian microcontinents, such as the Dashwoods block (Waldron & van Staal 2001, van Staal et al. 2009), and westward emplacement of allochthons (Williams & Stevens 1974, St. Julien & Hubert 1975) on top of the Laurentian margin. Continental rift, slope and rise successions are exposed in a series of stacked thrust sheets within the allochthon (Waldron et al. 2003), the highest of which contains ~ 485 Ma (Dunning & Krogh 1985) suprasubduction zone ophiolites which represent arcs (Dewey & Bird 1971, Dewey & Casey 2013) formed within the Iapetus Ocean. Structurally below the allochthons, and within the developing pro-arc foreland basin, deep-seated normal faults were activated in response to flexure of the lower Laurentian plate during orogenic loading and slab pull (Chapter 2).

The St. George unconformity, at the top of the autochthonous passive margin, represents the transition to a tectonically active basin (Knight et al. 1991) (Figure 4.4). The unconformity is overlain by the dominantly carbonate Table Head Group (Stenzel et al. 1990) which is in turn stratigraphically overlain by sandstone and siltstone of the Goose Tickle Group. Overall basin geometry (Chapter 2) and ophiolitic detritus within turbiditic sandstone units (Stevens 1970, Hiscott 1984) indicate that the Goose Tickle Group filled a foreland basin, sediments being derived from the Newfoundland portion of the orogen.

Only one published work by Cawood and Nemchin (2001) records U/Pb analyses of zircon from the Goose Tickle Group (Figure 4.3). The age spectrum is dominated by a strong

peak at 1.05 Ga. This peak and older, smaller Mesoproterozoic peaks are consistent with ages of units in local Grenvillian basement. A strong peak at 1.85 Ga is consistent with unit ages within any of the eastern Laurentian Paleoproterozoic orogens (Trans-Hudson, Makkovik or New Québec Torngat). A strong Archean signature, dominated by 2.70 Ga grains, is also consistent with the age of units within the Superior and North Atlantic cratons. Although the spectrum can be explained by derivation from Laurentian basement units, the ages can also be explained by derivation from clastic units within the Humber Arm Allochthon. The presence of ophiolitic detritus within the Goose Tickle Group (Hiscott 1984, Quinn 1992) indicates that it is more likely that the grains within the Goose Tickle Group were derived from recycling of clastic units within the Humber Arm Allochthon.

4.2.4. Late Ordovician Long Point Group

The Long Point Group, comprising the Lourdes, Winterhouse and Misty Point formations, represents the Late Ordovician foreland basin succession in western Newfoundland. The Lourdes Formation, a 75 m thick unit of shallow-marine limestone, disconformably overlies the Goose Tickle Group and represents the base of the Long Point Group. The depositional age for the Lourdes Formation is constrained by Upper Ordovician (Sandbian) conodonts (*gerdae* zone) and graptolites (*multidens* biozone) (Bergström et al. 1974). Batten Hender and Dix (2008) describe the formation as a narrow, high-energy, mixed siliclastic-carbonate ramp succession. The Lourdes Formation is gradationally overlain by thin-to medium-bedded fine-grained sandstone and shale units of the Winterhouse Formation, interpreted to represent a storm-dominated shelf assemblage (Quinn et al. 1999). Graptolite species *Climacograptus spiniferus* and *Geniculograptus pygmaeus* indicate a Late Ordovician (Katian) depositional age (Quinn et al. 1999). These rocks are gradationally overlain by medium- to coarse-grained red sandstone units of the Misty Point Formation interpreted to have been deposited in a marginal marine to terrestrial setting (Quinn et al. 1999). The presence of Ordovician brachiopods *Sowerbyella sericea* and *Rafinesquina deltoidea*, associated with species of *Trigrammaria*, also indicate a Katian age of deposition (Quinn et al. 1999). No previous geochronologic work has been carried out on any units within the Long Point Group.

White (Chapter 2) demonstrates, using seismic horizon mapping, that the narrow Lourdes shelf is restricted to southern portions of the basin. White (Chapter 2) interprets this to indicate that the Lourdes Formation possibly filled residual topography remaining after the Taconian Orogeny. The remainder of the Long Point Group thickens dramatically southwards, indicating basin subsidence as a result of loading in the Québec Appalachians where Taconian arc-continent collision continued into the Late Ordovician (Chapter 2). During this interval, subduction polarity reversal had already occurred in Newfoundland (Zagorevski et al. 2009), leading to

westward subduction beneath the developing orogen, placing the Long Point Group in a retro-arc setting (Chapter 2), though it was fed along-margin from a region still in a pro-arc position.

4.2.5. Silurian to Early Devonian Clam Bank Formation

The Clam Bank Formation unconformably overlies the Long Point Group (Figure 4.4). This unconformity (the Clam Bank unconformity) is significant, removing the majority of the Silurian system in western Newfoundland; however, it is not exposed anywhere on land because the units above and below are juxtaposed by a fault at their only exposed contact. The lowest units in the Clam Bank Formation consist of red and green thin-bedded calcareous mudstone and siltstone interlayered with noncalcareous siltstone and sandstone. These rocks are interpreted to have been deposited in a shallow-marine to terrestrial environment (Burden et al. 2002). A conodont assemblage of *Ozarkodina remscheidensis eosteinhornensis* and *O. remscheidensis* ssp. (Burden et al. 2002) indicates a maximum depositional age of Pridoli to Lochkovian for this portion of the Clam Bank Formation. An unconformity above this mixed lower portion marks the transition to a dominantly siliciclastic succession of coarse-grained sandstone, interpreted to have been deposited in a terrestrial environment (Burden et al. 2002).

The Clam Bank unconformity correlates with the timing of the Salinian Orogeny (440-422 Ma; Dunning et al. 1990, Cawood et al. 1994, van Staal et al. 2009), resulting from collision of the Ganderian microcontinent with the composite Laurentian margin (van Staal et al. 1998, 2009, Waldron et al. 2017). The foreland basin, forming on top of the Laurentian plate, likely underwent significant uplift and erosion as the Ganderian microcontinent was underthrust beneath it. The Clam Bank Formation was deposited as a result of later erosion of the Salinian Orogen into a retro-arc foreland basin (Chapter 2).

4.2.6. Early Devonian Red Island Road Formation

The Red Island Road Formation, exposed only offshore on Red Island (Figure 4.1), is the youngest foreland basin succession in western Newfoundland. The unit is interpreted to overlie the Clam Bank Formation (Quinn et al. 2004), although the contact is nowhere exposed on land. The Red Island Road Formation mainly consists of cobble to boulder conglomerate with a matrix of coarse-grained sandstone. Clasts within the conglomerate include a mix of lithologies including sedimentary, metasedimentary and igneous; felsic volcanic rocks make up a large proportion of the clasts, for which no local source is known. The formation has been interpreted as a high-gradient gravel river bed deposit (Quinn et al. 2004). Quinn et al. (2004) discovered palynomorphs within the unit, placing the Red Island Road Formation in the Emsian *Emphanisporites annulatus* – *Camarozonotriletes sextantii* Assemblage Zone.

The Early Devonian Acadian Orogeny in Newfoundland, occurring from ~ 420-400 Ma (van Staal et al., 2009), overlaps with deposition of the Red Island Road Formation. The orogeny has been attributed to the accretion of Avalonia to Laurentia (Bird & Dewey 1970, Bradley 1983, van Staal et al. 2009) via west-dipping subduction (Murphy et al., 1999; Waldron et al., 1996; van Staal et al., 2014), implying that the Acadian foreland basin developed as a retro-arc basin (Chapter 2); the Red Island Road Formation filled this Early Devonian basin (Chapter 2). In western Newfoundland, the orogeny led to reactivation and inversion of earlier Taconian and Neoproterozoic basement faults and the uplift of basement massifs, including the Long Range and Indian Head Inliers (Chapter 3).

4.3. Sampled Units

We chose samples from four foreland basin units for detrital zircon geochronology: the Lourdes, Winterhouse, Clam Bank and Red Island Road formations (Figure 4.4). Geographic and stratigraphic sample locations are shown in figures 4.1 and 4.4 respectively. Samples were chosen based on fossil control, where available, in order to constrain depositional age. Coarse-grained sandstones were collected, where possible, to maximize the likelihood of obtaining zircon of suitable size for analysis. One sample of a typical rhyolite boulder from a conglomeratic bed within the Red Island Road Formation was collected for U-Pb age dating of zircon using Chemical Abrasion Thermal Ionization Mass Spectrometry (CA-TIMS).

4.3.1. Lourdes Formation

The sample of the Lourdes Formation (NP007) was collected on Long Point (Figure 4.1). Bedding in this location dips shallowly to moderately northwest and the rocks have not been penetratively deformed. Biostratigraphically significant fossils mainly occur in the middle unit (Black Duck Member) of the Lourdes Formation and include Upper Ordovician (Sandbian) conodonts (*gerdae* zone; Bergström et al. 1974) and graptolites (*multidens* biozone: Bergström et al. 1974). Specific diagnostic species of conodonts include *Appalachignathus delicatulus* (Bergström et al. 1974), *Belodina* sp., *Periodon* sp., and *Walliserodus ethingtoni* (Fåhraeus 1966). Our sample was taken from the overlying Beach Point Member because it contained a significant amount of clastic material. The age is constrained, by these underlying fossils and those found in the overlying Winterhouse Formation, as Sandbian or Late Ordovician.

The sample of the Lourdes Formation was collected from a thin laminated bed of very fine-grained calcareous sandstone and limestone, the coarsest material available. The outcrop was a medium to thick bedded succession of burrow mottled limestone, punctuated by a few thin layers of very fine-grained calcareous sandstone. The sample collected for analysis was a well

sorted, subrounded, very fine-grained arkosic arenite (Figure 4.5a). Grains are predominantly quartz, feldspar and lesser carbonate, held together with carbonate cement.

4.3.2. Winterhouse Formation

We collected the sample of the Winterhouse Formation (NG024A) from the stratigraphically highest portion of the Formation, near the contact with the stratigraphically overlying Misty Point Formation. This location is the waterfall reference section of Quinn et al. (1999) (Figure 4.1), which has a well constrained depositional age based on graptolite species *C. spiniferus* and *G. pygmaeus*, placing this locality in the lower part of the *pygmaeus* Zone, indicating a Late Ordovician, Katian age.

The sample was collected from an outcrop of parallel-laminated, thin-bedded sandstone. It is an arkosic arenite, predominantly composed of feldspar (50%) and quartz (35%) (Figure 4.5b). Feldspars, both plagioclase and microcline, are strongly altered to clay minerals. Biotite, making up approximately 5-10 % of grains, is partially altered to a fine-grained clay mineral. Minor grain components include actinolite, chlorite and opaque minerals.

4.3.3. Clam Bank Formation

The sample of Clam Bank Formation (NG043) was taken in the footwall of the Round Head thrust where bedding is steep to overturned (Figure 4.1). There are no fossils in this portion of the Clam Bank succession; however, fossils, including a conodont assemblage of *Ozarkodina remscheidensis eosteinhornensis* and *O. remscheidensis* ssp. from the marine portion of the Clam Bank Formation (Burden et al. 2002), a few meters above the sampled bed, indicate a maximum depositional age of Pridoli to Lochkovian.

We took the sample from a thick overturned bed of coarse-grained, well sorted, quartz-rich sandstone near the stratigraphic base of the exposed on-land section of Clam Bank Formation. The sample is a well sorted, moderately rounded quartz-rich arenite with a carbonate cement (Figure 4.5c). Grains are predominantly quartz and a minor proportion (10%) are feldspars (predominantly microcline) and lithic fragments.

4.3.4. Red Island Road Formation

The Red Island Road Formation (NP021) was sampled on Red Island, the only place the unit is exposed (Figure 4.1). The beds are subhorizontal, dipping very gently (~05°) north. The depositional age of the unit is constrained by biostratigraphically significant palynomorphs above the sampled location, which place the unit in the Emsian *Emphanisporites annulatus* – *Camarozonotriletes sextantii* Assemblage Zone (Quinn et al. 2004).

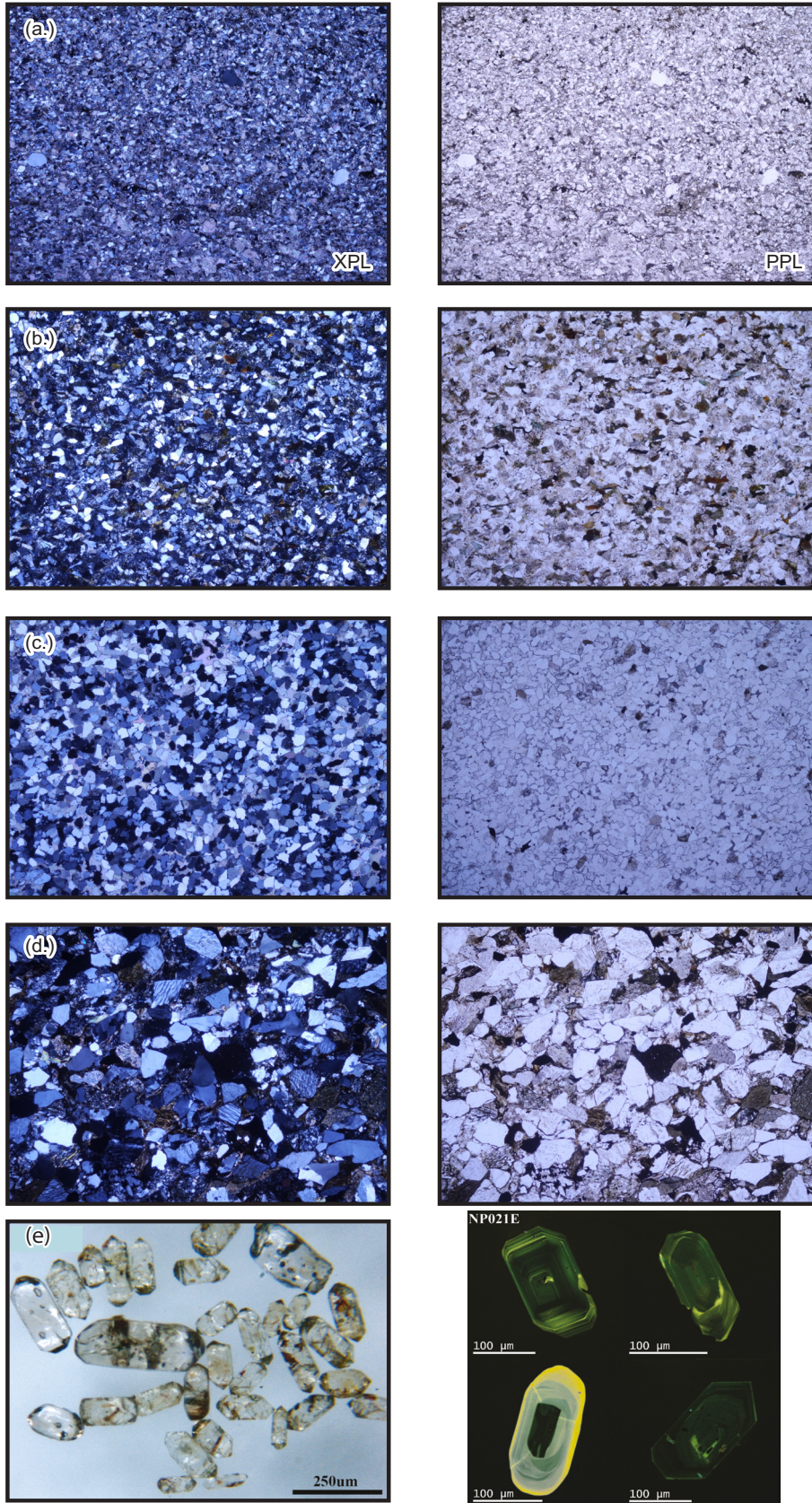


Figure 4.5: Photomicrographs of sampled foreland basin units including (a) NP007 (Lourdes Formation), (b) NG024A (Winterhouse Formation), (c) NG043 (Clam Bank Formation), (d) NP021 (Red Island Road Formation), (e) and NP021E (zircons from rhyolite boulder on the left and cathodeluminescence image of grains on the right).

We sampled a medium bed of coarse-grained sandstone interlayered between thick beds of cobble to boulder conglomerate, in which rhyolite clasts are common. The sandstone is a moderately sorted, angular, coarse-grained lithic arenite. Over 40% of grains are rock fragments (Figure 4.5d). About 50% of the unit consists of quartz and feldspar, the majority of feldspars showing perthitic exsolution texture. The same, relatively texturally immature, sandstone forms a matrix which contrasts with the well-rounded, mature clasts within the conglomerate.

A typical rhyolite boulder (~ 30 cm in diameter) from a conglomeratic bed within the Red Island Road Formation (NP 021E) (Location: Figure 4.1) was also collected. This boulder is representative of the most common lithology of cobbles and boulders within the conglomerate and all rhyolites within the unit appear the same. The sample collected is porphyritic rhyolite, with phenocrysts of quartz and potassium feldspar in an aphanitic matrix.

4.4. U/Pb Geochronology of Detritus

4.4.1. Sample Preparation

All samples were crushed and then sieved through a 250 μm sieve. Light minerals were then removed using a Wilfley table. The remaining heavy separates were then bathed in 10% acetic acid to remove carbonate material (except NP021A as it did not contain carbonate) and then all samples were bathed in 3% hydrogen peroxide to clean clays from the material. After washing, samples were placed in sodium polytungstate ($\rho = 2.8$) for further heavy mineral extraction before processing using the Frantz Isodynamic and Barrier separators (e.g. Rosenblum and Brownfield, 2000) to remove magnetic minerals. Finally, the remaining heavy separates were placed in diiodomethane (MI) to extract the final heavy mineral separate that contained the zircon which was analysed.

To ensure an unbiased sample, zircons were not individually picked. We placed all grains from the heavy separates in a tray and obvious material that was not zircon was removed. All remaining grains were then mounted on epoxy. In order to expose sections in the grains, the mounts were polished using 1200 μm paper and then by using 0.3 μm Al oxide powder on a Pellon polishing cloth. Grains were imaged using secondary electrons and cathodeluminescence imaging using the scanning electron microscope in the Canadian Center for Isotope Microanalysis (CCIM) facility at the University of Alberta.

4.4.2. Analysis

The analyses were carried out in the ICPMS facility at the University of Alberta, using the Nu Plasma U-Pb laser ablation multicollector inductively coupled plasma mass spectrometer

(LA-MC-ICP-MS). Procedures were modified from Simonetti et al. (2005). A beam diameter of 30 μm was used. Because of the small size of most grains only a single analysis was carried out per zircon. We used zircon images to avoid straddling any obvious core-rim boundaries during analyses. The zircons were analysed in groups of 10 to 15, separated by analysis of in-house standards: LH94-15 (1830 ± 1 Ma; Ashton et al., 1999; Simonetti et al., 2005) and GJ1-32 (608 Ma; Jackson et al., 2004; Elhlou et al., 2006). The total number of sample grains analyzed ranged from 111 to 137. In cases where counts at mass 204 were significantly elevated (> 450 counts per second), a common-Pb correction was applied using the two stage evolution model (Stacey & Kramers 1975) to estimate the common-Pb isotopic composition.

4.4.3. Data Reduction

All analytical results are reported in the Appendix. Data were reduced using an Excel-based spreadsheet in which isotopic ratios were corrected based on standard analyses. For grains with uncorrected $^{207}\text{Pb}/^{206}\text{Pb}$ ratios less than 0.0658 (corresponding to an age of 800 Ma) we normalize using in-house standard GJ1-32 (608 Ma; Jackson et al., 2004) and report the $^{206}\text{Pb}/^{238}\text{U}$ age which is typically more precise for younger grains. For grains with uncorrected $^{207}\text{Pb}/^{206}\text{Pb}$ greater than 0.0658 (800 Ma) we normalize to in-house standard LH94-15 (1.83 Ga; Ashton et al., 1999) and report $^{207}\text{Pb}/^{206}\text{Pb}$ age. All errors are expressed as 2σ and are a quadratic combination of the standard deviation of the standard means and standard error of the measured isotopic ratio. Only grains which were $> 90\%$ concordant were used in our calculations and interpretations.

4.4.4. Data Presentation

The software Isoplot (Ludwig 2012) was used to produce probability density functions (PDF) (Figure 4.3) for all samples analysed in this study. Concordia diagrams (Figure 4.6), weighted means, mean square of weighted deviates (MSWD) calculations, and other statistical analyses were prepared with the same software. Cumulative density functions (Figure 4.7) and Kolmogorov-Smirnov (K-S) critical values (Table 1) were calculated using analysis tools from the Arizona LaserChron Center (Gehrels et al. 2006).

The PDF, the most common tool used when comparing zircon age distributions, is the sum of the probability distributions derived from individual grains and their analytical errors, which compares the probability of finding zircons of different ages within the sample. The function displays this information in an intuitive fashion (Figure 4.3) so that we subjectively

identify similar age peaks, gaps in data, and differences in peak height as a method of comparing and contrasting the data sets.

Detrital zircon data collected by others and used in this study are re-plotted as PDFs in order draw comparisons with our results (Figure 4.3). We use our chosen cutoff age (800 Ma) when plotting the $^{206}\text{Pb}/^{207}\text{Pb}$ versus $^{206}\text{Pb}/^{238}\text{U}$ age for others' data. We also exclude analyses which are discordant by >10%. These adjustments account for minor differences between the re-plotted PDFs (Figure 4.3) and previously published plots.

In addition to PDFs, we also use the Kolmogorov-Smirnoff (K-S) test as a means of mathematically comparing distributions in order to determine if there is a statistically significant difference between the distributions. This method, based on the cumulative density functions (CDF), tests the null hypothesis that the two samples are derived from the same parent population. If the maximum difference in probability between two curves (D) is greater than a critical value (dependent on the number of analyses), the null hypothesis is rejected.

4.5. TIMS analysis

4.5.1. Sample Preparation and Analysis

A rhyolite boulder from a conglomeratic bed within the Red Island Road Formation (NP 021E) was collected for U-Pb dating of zircon using Chemical Abrasion Thermal Ionization Mass Spectrometry (CA-TIMS). Preparation and analyses were carried out at Memorial University of Newfoundland. The boulder was washed and scrubbed to remove any debris, then processed with standard techniques of crushing and concentration of a heavy mineral separate and then zircon separation. Zircon crystals were examined under the microscope and the clearest, sharpest euhedral prisms were selected for analysis (Figure 4.5e). The zircons are high quality small euhedral prisms and inclusions, of likely apatite and/or melt, are visible as well as clear hematite staining along fractures (Figure 4.5e)

All grains were chemically abraded using the Mattison (2005) chemical abrasion thermal ion mass spectrometry (CA-TIMS) technique. Selected grains were annealed 36 hours in an oven at 1000 °C, then etched in concentrated hydrofluoric acid in a Teflon capsule at 200 °C in an oven for 4 hours. This procedure is designed to remove any altered domains in the crystal that may have undergone Pb loss. Pb and U isotopic ratios were measured by thermal ionization mass spectrometry, and results calculated using ISOPLOT. Further details of the lab procedures are presented in Sparkes and Dunning, (2014).

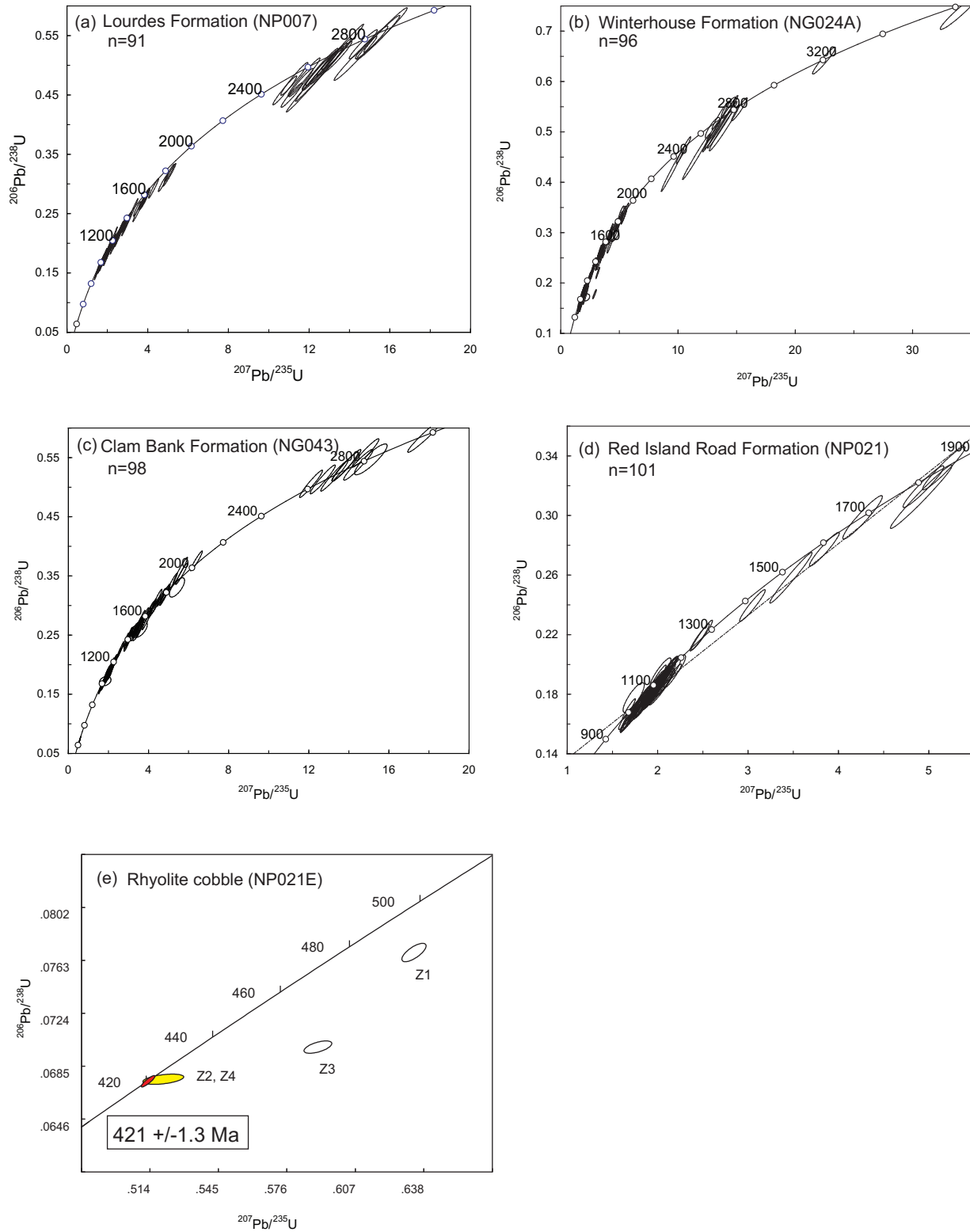
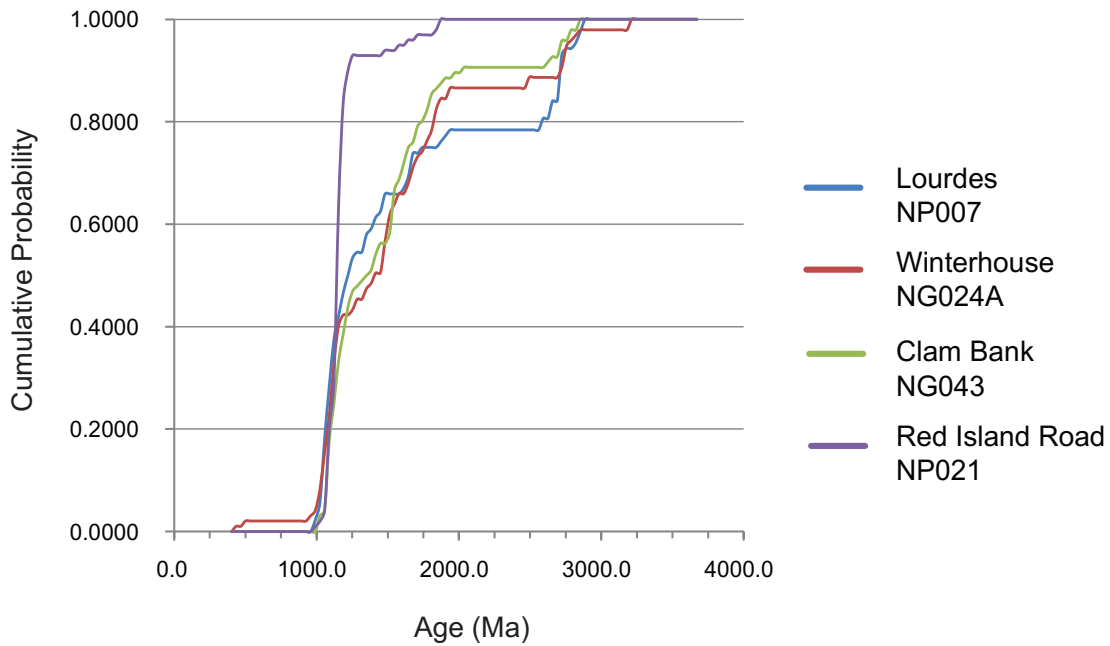


Figure 4.6: U-Pb concordia plots for detrital zircon data from this study including: (a) NP007 (Lourdes Formation), (b) NG024A (Winterhouse Formation), (c): NG043 (Clam Bank Formation), (d) NP021 (Red Island Road Formation), and (e) NP021E (zircons from rhyolite boulder). Ellipses represent 2σ uncertainties.



	Lourdes NP007	Winterhouse NG024A	Clam Bank NG043	Red Island Road NP021
Lourdes NP007		0.535	0.497	0.000
Winterhouse NG024A	0.535		0.833	0.000
Clam Bank NG043	0.497	0.833		0.000
Red Island Road NP021	0.000	0.000	0.000	

Figure 4.7: Detrital zircon cumulative density plots and results of the K-S test expressed as a value P for all pairs of samples analysed in this study.

4.6. Results

4.6.1. Lourdes Formation

Of the 130 grains analysed, 91 grains are less than 10 % discordant. Of the concordant grains almost 80 % are Mesoproterozoic (Figure 4.3). The largest proportion of analyses falls between 0.95 and 1.3 Ga, comprising over 50 % of the grains. The largest peak within this range occurs between 1.0 and 1.1 Ga, a typical age range for zircons derived from the Grenville Orogen. A significant number of zircons, 26 %, are spread throughout the earlier Mesoproterozoic to Paleoproterozoic, between approximately 1.3 and 2.0 Ga, with the largest peak within this range at ~ 1.65 Ga. A 1.85 Ga peak, generally typical of Laurentian zircons (Cawood & Nemchin 2001), is absent. About 21 % of grains give Archean ages from 2.5 – 2.9 Ga, with the largest peak at ~2.75 Ga, a common age for Laurentian zircons derived from either the Superior or North Atlantic craton (Calvert & Ludden 1999, Corfu & Lin 2000, Downey et al. 2009). A conspicuous gap between ~2.0 to 2.5 Ga is observed (Figure 4.3), which is also typical of zircon populations derived from eastern Laurentia (Cawood & Nemchin 2001, Waldron et al. 2008).

4.6.2. Winterhouse Formation

A total of 96 out of 125 analysed grains were less than 10% discordant within the Winterhouse Formation. Approximately 43 % of zircons range from 0.95-1.2 Ga, the largest peak within this range occurring at 1.1 Ga, typical of local Grenvillian units. A significant percentage of analyses, about 42 %, are of earlier Mesoproterozoic to Paleoproterozoic age, ranging from 1.3 to 2.0 Ga. In common with the Lourdes Formation, a conspicuous gap is observed between 2.0 and 2.5 Ga and a small proportion of analyses (11%) give Archean ages ranging from 2.5-2.9 Ga with the largest peak at 2.75 Ga. These age populations are similar to those observed in the Lourdes Formation (Figure 4.3). Two older Archean grains at 3.2 and 3.6 Ga are present in the Winterhouse Formation; comparable grains are not observed in any other foreland basin unit. Two grains have much younger Paleozoic ages. A grain with an age of 470 Ma is consistent with the timing of ophiolite obduction onto the Laurentian margin and may represent a metamorphic age associated with this Taconian event. The other grain, although having an anomalously young $^{206}\text{Pb}/^{238}\text{U}$ age of 435 Ma, younger than the depositional age, is 7% discordant and has a $^{207}\text{Pb}/^{206}\text{Pb}$ age of 465 Ma. The grain most likely suffered lead loss. The $^{207}\text{Pb}/^{206}\text{Pb}$ age is consistent with metamorphism during Taconian orogenesis.

4.6.3. Clam Bank Formation

The Clam Bank Formation displays a probability density function similar to those of both the Winterhouse and Lourdes formations (Figure 4.3). The distribution includes 98 analyses which were less than 10% discordant out of 137 total analyses. Approximately 45% of analyzed concordant grains are within the range of 1.0 – 1.2 Ga and the largest peak occurs at 1.1 Ga, similar to both the older formations. A major proportion of the grains (43 %) span the age range 1.2-2.0 Ga. There is a complete absence of grains between 2.0 and 2.6 Ga, also similar to the Winterhouse and Lourdes formations. A smaller, but still significant proportion of grains occur from 2.6 to 3.0 Ga, with the largest peak at 2.75 Ga. Only two grains yielded Paleozoic ages of 425 and 465 Ma. The 425 Ma age is very close to the depositional age of the unit while the 465 Ma zircon is consistent with derivation from a Taconian source.

4.6.4. Red Island Road Formation

The probability density function for analyses from the Red Island Road Formation notably differs from the distributions of the three younger units (Figure 4.3). Of the 101 concordant analyses, 93 had Mesoproterozoic ages between 950 Ma and 1.2 Ga. The largest peak is at 1.15 Ga. Only four analyses have ages between 1.5 to 1.7 Ga and three other zircons make a small peak at approximately 1.85 Ga. There were no Archean grains, in contrast to all other foreland basin units.

Two of the four analysis carried out on the rhyolite boulder from the Red Island Road Formation (Z2, Z4) are concordant (Figure 4.6e). The other two are significantly discordant, having much older $^{207}\text{Pb}/^{206}\text{Pb}$ ages than the $^{206}\text{Pb}/^{238}\text{U}$ ages. This is indicative of an inherited zircon component in at least one crystal of each fraction. Two of the concordant analyses have $^{206}\text{Pb}/^{238}\text{U}$ ages of 421 +/- 1.8 and 421 +/- 2.1 Ma, each at 2σ . The weighted average $^{206}\text{Pb}/^{238}\text{U}$ age is 421 +/-1.3 Ma (ISOPLOT, 95% confidence interval, MSWD = 0.44). This age is in the Pridoli Epoch (latest Silurian) using the timescale of Melchin et al. (2012).

4.6.5. K-S Test

Figure 4.7 displays the results of the K-S test, based on measuring the maximum difference (D) between each pair of cumulative distribution functions (CDF's) for each of the four sampled foreland basin units in this study (Figure 4.7). Results are expressed as a value P which is the probability that the observed D values could result from random sampling of a single population. High values of P indicate that the samples could have been drawn from the same source population. For the three oldest samples, the Lourdes, Winterhouse and Clam Bank formations, $D < D_{\text{crit}}$ for all pairs and we therefore accept the null hypothesis that these samples

could have been derived from the same source region. This agrees with our earlier qualitative observations from the PDFs, which are all similar to one another. However, the cumulative probability difference between the CDF's of these older units and that of the youngest Red Island Road Formation is greater than D_{crit} . We therefore reject the null hypothesis and interpret that this youngest unit was not derived from the same source region as the older foreland units. This also agrees with our earlier qualitative interpretations, that the Red Island Road Formation has a distinctly different detrital zircon age spectrum from all other units analysed in this study.

4.7. Discussion

In this discussion we aim to discuss new detrital zircon data from this study in context of previously published data and a current understanding of tectonic evolution of the northern Appalachians.

We suggest that previously published detrital zircon data from the Goose Tickle Group (Cawood and Nemchin, 2001) demonstrate age populations that can be explained by derivation from siliciclastic units preserved in the Humber Arm Allochthon (Figure 4.3). Although Mesoproterozoic peaks between 1.2 and 1.7 Ga are diminished, relative to continental margin units preserved in the allochthon, a large Paleoproterozoic peak is present at 1.85 Ga, similar to that observed in the most distal rift and passive margin units. Previous interpretations, based on paleocurrent analyses (Quinn 1992) and geochemical work on detritus (Hiscott 1978, Quinn 1992), also point towards derivation from the Humber Arm Allochthon immediately east of the basin. However, more recent work by White (Chapter 2) indicates that the succession is derived from more northern regions of the Newfoundland orogen.

The overlying Lourdes, Winterhouse and Clam Bank formations all display probability density plots which are very similar to one another and, using the results from the K-S test, we accept the null hypothesis that these three samples could have been derived from the same source region. We did not perform the K-S test using the Goose Tickle Group due to the great disparity in the number of analyses relative to our samples. Although zircon ages from these units are similar to those observed in the Goose Tickle Group and siliciclastic units of the Humber Arm Allochthon, the proportions of ages (i.e. relative peak heights) differ drastically. The most obvious difference is the conspicuously low abundance of Paleoproterozoic grains with ages of ~ 1.85 Ga, which are abundant in Goose Tickle Group. In the Lourdes Formation the peak is completely absent (Figure 4.3). This diminished/absent peak indicates a major shift in provenance during development of the Long Point Group basin.

This shift in provenance coincides with a major shift in Late Ordovician basin geometry, recognized by White (Chapter 2) who shows that prior to deposition of the Long Point Group, the foreland basin thickened northward and eastward, implying loading by the northern

Newfoundland segment of the orogen. A dramatic shift, to a southward-thickening basin, followed during Late Ordovician deposition of the Long Point Group (Chapter 2) where it is interpreted that loading along the southern margin of the basin by Taconian allochthons, now preserved on the Gaspé Peninsula in Québec, generated the basin into which the Long Point Group was deposited.

Compositionally, the Winterhouse and Misty Point formations are similar to the Goose Tickle Group. Batten Hender and Dix, (2008) show that ratio ranges of Y/Ni and Cr/V for all three units are similar, suggesting all three units are derived from ophiolitic sources (Hiscott 1984, Quinn 1992). We suggest that, combined with prominent unidirectional northeast-directed paleocurrent indicators, these compositional similarities indicate that, although all units are sourced from Taconian allochthons, the younger Long Point Group is derived from the allochthons in Québec, not Newfoundland (Figure 4.2, arrow 2).

Although no detrital zircon studies have been carried out on continental margin clastics within allochthons on the Gaspé Peninsula, data have been collected farther south, in New England (McLennan et al. 2001, Macdonald et al. 2014). The PDFs of Laurentian derived zircons from the Paleozoic metasedimentary rocks in New England all display a much diluted Paleoproterozoic (~1.85 Ga) peak, similar to the relatively small 1.85 Ga peak within the Long Point Group and Clam Bank Formation in Newfoundland. Other studies which look at zircons in the Cambrian passive margin units in New England demonstrate a complete absence of Paleoproterozoic ages (McLennan et al., 2001; McDaniel et al., 1997; Gaudette et al., 1981). We interpret that the decrease in 1.85 Ga ages within the Upper Ordovician to Early Devonian (Figure 4.3) foreland basin succession of western Newfoundland signals the transition from a basin filled by erosion of the Humber Arm Allochthon to a basin filled by southerly derived detritus from the Québec and New England Appalachians (Figure 4.2, arrows 1 and 2).

The youngest foreland basin succession, the Red Island Road Formation (Figure 4.4), has a distinctly different age distribution compared to those from older foreland units, with only one large peak in the population at 1.15 Ga, a handful of Mesoproterozoic and Paleoproterozoic grains, and a complete absence of all other populations (Figure 4.3). Combined with the results from the K-S test (Table 1), this indicates that the Red Island Road Formation is not derived from the same source region as the older foreland units. Provenance studies by Quinn et al. (2004) also suggest, from the mineralogy of matrix and clasts, which include high grade metamorphics and felsic volcanic rocks, that no other foreland basin or platform unit was cannibalized to provide detritus to the unit.

The most striking observation is the similarity of the Red Island Road Formation spectrum to those of autochthonous Bradore Formation (Figure 4.3). This unit also displays a very restricted spectrum of ages, the majority of which combine to form a strong 1.15 Ga peak,

consistent with derivation from local Grenvillian basement. These observations may be explained by orogen development during the Acadian Orogeny. White (Chapter 3) demonstrates that Middle Ordovician and Neoproterozoic basement-involved faults were reactivated and inverted during the Acadian Orogeny, uplifting basement massifs and transporting large, basement-cored fault-propagation folds up to 12 km towards the west. A strong influx of Grenvillian detritus was likely shed from Acadian basement uplifts into developing Acadian foreland basins suggesting that these massifs formed major topographic highs which are preserved today in the Long Range Mountains in Newfoundland.

Although the detrital zircons in the sandstone sample can all be derived from the Grenville Province, the larger rhyolite cobble within the conglomerate facies has an age of 421 ± 1.3 Ma (Figure 4.6e). No local sources for Silurian felsic volcanic units are known in this region, although Heaman et al. (2002) note the occurrence of Silurian (430.5 ± 2.5 Ma) mafic volcanic units in the Long Range Inlier. In southwestern Newfoundland, the Silurian La Poile Group (Figure 4.1) contains felsic volcanic rocks, dated at $420 \pm 8/-2$ Ma (Dunning et al. 1990), deposited on Precambrian basement (O'Brien & O'Brien 1989). Bashforth (1995) and Quinn et al. (2004) suggested, based on lithological matching, that these volcanic units sourced cobbles within the Red Island Road Formation. Quinn et al. (1999) also suggest that other regions within the Notre Dame subzone may have sourced the conglomerate. Although both the La Poile Group and Notre Dame Subzone can explain Silurian volcanic cobbles, the prevalence of Grenvillian zircons is not well explained by derivation from either of these terranes as neither of these regions has any exposure of Grenville basement.

We should also consider terranes presently outside Newfoundland as potential sources because the relative positions of source terranes have been modified by later tectonism. A restoration of Appalachian terranes prior to Carboniferous motion by Waldron et al. (2015) shows Cape Breton Island directly east of the present position of the Port au Port Peninsula. Two main possibilities for Silurian source terranes exist there. First, the Aspy terrane (Figure 4.1) contains abundant plutons which are age equivalent (Lin et al. 2007) and compositionally similar to rhyolitic cobbles within rocks of the Red Island Road Formation. However, the Peri-Gondwanan Aspy terrane displays a wide range of ages. Metasedimentary units have detrital zircons ranging in age from 573 to 1520 Ma and igneous units range in age from 428 to ~ 620 Ma (Lin et al. 2007). One might expect, if detritus were derived from here, a larger span of detrital zircon ages within the Red Island Road Formation. The second option is the Blair River Complex in northern Cape Breton Island (Figure 4.1), Nova Scotia, interpreted as an inlier of Grenvillian basement (Miller & Barr 2000). Paleozoic igneous activity within the inlier is demonstrated by the $435 \pm 7/-3$ Ma Sammys Barren granite (Miller et al. 1996) and other units interpreted to be Paleozoic in age, including the Fox Back Ridge granodiorite, smaller gabbroic plutons, and

mafic and felsic dykes (Miller 1997) which may be the feeders to volcanic rocks observed in the Acadian foreland basin. We interpret that the Blair River Inlier is the likely source terrane for the Red Island Road Formation as it explains both the prevalence of Grenvillian zircons and Silurian felsic volcanic cobbles.

All foreland basin successions in western Newfoundland demonstrate Laurentian affinity (Figure 4.3 inset 1) despite the fact that Gondwanan terranes were accreted to the composite Laurentian margin during both the Salinian and Acadian orogenies. A possible explanation for the lack of Gondwanan detritus within the basin is that all Gondwanan terranes were accreted to the Laurentian (Waldron et al. 2012) margin on the lower plate, and underthrust beneath Laurentia. It's likely that this material was topographically lower than the orogen to the west, and Gondwanan detritus was only incorporated into basins developed on top or to the east of the orogen.

4.8. Conclusions

New detrital zircon geochronology results from the foreland basin successions in western Newfoundland indicate that the post-Taconian successions are not derived from the same source region as the earlier Middle Ordovician Goose Tickle Group. Our interpretation of previously published U/Pb analyses of zircon indicates that the Goose Tickle Group was derived from clastic units within the Humber Arm Allochthon. We interpret a major shift in provenance during deposition of the Long Point Group, indicated by a drastic decrease in the relative abundance of 1.85 Ga zircons accompanied by a 180° reversal in dominant unidirectional paleoflow indicators from SW to NE. The dominant 1.1 Ga Grenville peaks within spectra of the Long Point Group and Clam Bank Formation are similar to age spectra presented in detrital zircon studies of rift and passive margin clastics in the Québec and New England Appalachians (Figure 4.3). We suggest that the Long Point Group was sourced from either the Québec or New England portion of the orogen. Another major shift in provenance occurs during deposition of the Early Devonian Red Island Road Formation. An overwhelming abundance of 1.1 Ga zircons and a minor proportion of older Mesoproterozoic zircons indicate derivation from a similar source region to that which provided detritus to the oldest rift-related sediments – basement units of the Grenville Orogen. In addition to an entirely Grenvillian derived sandstone units, there are abundant rhyolite cobbles which are dated at 421 Ma – a lithology with no known local source. The combination of U/Pb age data and lithologic observations lead us to suggest that the Grenville Blair River Inlier in Cape Breton, which has a palinspastically restored position east of the basin during the Devonian, is the source terrane. Basement massifs were uplifted along deep-seated basement faults during Acadian orogenesis and detritus from these massifs likely filled Acadian foreland basins.

4.9. References

- Allen, J.S. 2009. Paleogeographic Reconstruction of the St. Lawrence Promontory, Western Newfoundland. PhD Thesis. University of Kentucky, Lexington, Kentucky
- Ashton, K.E., Heaman, L.M., Lewry, J.F., Hartlaub, R.P. & Shi, R. 1999. Age and origin of the Jan Lake Complex: a glimpse at the buried Archean craton of the Trans-Hudson Orogen. *Canadian Journal of Earth Sciences*, **36**, 185–208.
- Bashforth, A.R. 1995. *Provenance of the Red Island Road Formation, Western Newfoundland*. B. Sc. Thesis, Brandon University, Manitoba
- Batten Hender, K.L. & Dix, G.R. 2008. Facies development of a Late Ordovician mixed carbonate-siliciclastic ramp proximal to the developing Taconic orogen: Lourdes Formation, Newfoundland, Canada. *Facies*, **54**, 121–149,
- Bergström, S.M., Riva, J. & Kay, M. 1974. Significance of conodonts, graptolites, and shelly faunas from the Ordovician of western and north-central Newfoundland. *Canadian Journal of Earth Sciences*, **11**, 1625–1660.
- Bird, J.M. & Dewey, J.F. 1970. Lithosphere plate-continental margin tectonics and the evolution of the Appalachian orogen. *Geological Society of America Bulletin*, **81**, 1031–1060.
- Bradley, D.C. 1983. Tectonics of the Acadian orogeny in New England and adjacent Canada. *The Journal of Geology*, **91**, 381–400.
- Burden, E.T., Quinn, L., Nowlan, G.S. & Bailey-Nill, L.A. 2002. Palynology and micropaleontology of the Clam Bank Formation (Lower Devonian) of western Newfoundland, Canada. *Palynology*, **26**, 185–215.
- Calvert, A.J. & Ludden, J.N. 1999. Archean continental assembly in the southeastern Superior Province of Canada. *Tectonics*, **18**, 412–429.
- Cawood, P.A. & Nemchin, A.A. 2001. Paleogeographic development of the east Laurentian margin: Constraints from U-Pb dating of detrital zircons in the Newfoundland Appalachians. *Geological Society of America Bulletin*, **113**, 1234–1246.
- Cawood, P.A. & Williams, H. 1988. Acadian basement thrusting, crustal delamination, and structural styles in and around the Humber Arm allochthon, western Newfoundland. *Geology*, **16**, 370.
- Cawood, P.A., Dunning, G.R., Lux, D. & van Gool, J.A.M. 1994. Timing of peak metamorphism and deformation along the Appalachian margin of Laurentia in Newfoundland: Silurian, not Ordovician. *Geology*, **22**, 399–402.
- Cawood, P.A., McCausland, P.J. & Dunning, G.R. 2001. Opening Iapetus: Constraints from the Laurentian margin in Newfoundland. *Geological Society of America Bulletin*, **113**, 443–453.

- Cawood, P.A., Nemchin, A.A. & Strachan, R. 2007. Provenance record of Laurentian passive-margin strata in the northern Caledonides: Implications for paleodrainage and paleogeography. *Geological Society of America Bulletin*, **119**, 993–1003.
- Chow, N. & James, N.P. 1987. Cambrian Grand Cycles: A northern Appalachian perspective. *Geological Society of America Bulletin*, **98**, 418.
- Corfu, F. & Lin, S. 2000. Geology and U-Pb geochronology of the Island Lake greenstone belt, northwestern Superior Province, Manitoba. *Canadian Journal of Earth Sciences*, **37**, 1275–1286.
- Dewey, J.F. & Bird, J.M. 1971. Origin and Emplacement of the Ophiolite Suite: Appalachian Ophiolites in Newfoundland. *Journal of Geophysical Research*, **76**, 3179–3206.
- Dewey, J.F. & Casey, J.F. 2013. The sole of an ophiolite: the Ordovician Bay of Islands Complex, Newfoundland. *Journal of the Geological Society*, **170**, 715–722.
- Downey, M.W., Lin, S., Böhm, C.O. & Rayner, N.M. 2009. Timing and kinematics of crustal movement in the Northern Superior superterrane: Insights from the Gull Rapids area of the Split Lake Block, Manitoba. *Precambrian Research*, **168**, 134–148.
- Dunning, G.R. & Krogh, T.E. 1985. Geochronology of ophiolites of the Newfoundland Appalachians. *Canadian Journal of Earth Sciences*, **22**, 1659–1670.
- Dunning, G.R., O'Brien, S.J., Colman-Sadd, S.P., Blackwood, R.F., Dickson, W.L., O'Neill, P.P. & Krogh, T.E. 1990. Silurian Orogeny in the Newfoundland Appalachians. *The Journal of Geology*, **98**, 895–913.
- Elhlou, S., Belousova, E., Griffin, W.L., Pearson, N.J. & O'Reilly, S.Y. 2006. Trace element and isotopic composition of GJ-red zircon standard by laser ablation. *Geochimica et Cosmochimica Acta*, **70**.
- Fåhraeus, L.E. 1966. Lower Viruan (Middle Ordovician) conodonts from the Gullhogen quarry, southern central Sweden. *Sveriges Geologiska Undersökning Ser C*, **610**, 1–40.
- Gehrels, G., Valencia, V. & Pullen, A. 2006. Detrital zircon geochronology by laser ablation multicollector ICPMS at the Arizona Laserchron Center. *In: Olszewski, T. D. (ed.) Geochronology: Emerging Opportunities*. Paleontological Society Papers, 67–76.
- Heaman, L.M., Erdmer, P. & Owen, J.V. 2002. U–Pb geochronologic constraints on the crustal evolution of the Long Range Inlier, Newfoundland. *Canadian Journal of Earth Sciences*, **39**, 845–865.
- Hiscott, R.N. 1978. Provenance of Ordovician deep-water sandstones, Tourelle Formation, Quebec, and implications for initiation of the Taconic orogeny. *Canadian Journal of Earth Sciences*, **15**, 1579–1597.
- Hiscott, R.N. 1984. Ophiolitic source rocks for Taconic-age flysch: Trace-element evidence. *Geological Society of America Bulletin*, **95**, 1261–1267.

- Hoffman, P.F. 1988. United Plates of America, The Birth of a Craton: Early Proterozoic Assembly and Growth of Laurentia. *Annual Review of Earth and Planetary Sciences*, **16**, 543–603.
- Jackson, S.E., Pearson, N.J., Griffin, W.L. & Belousova, E.A. 2004. The application of laser ablation-inductively coupled plasma-mass spectrometry to in situ U–Pb zircon geochronology. *Chemical Geology*, **211**, 47–69.
- Knight, I. & James, N.P. 1987. The stratigraphy of the Lower Ordovician St. George Group, western Newfoundland: the interaction between eustasy and tectonics. *Canadian Journal of Earth Sciences*, **24**, 1927–1951.
- Lin, S., Davis, D.W., Barr, S.M., Van Staal, C.R., Chen, Y. & Constantin, M. 2007. U-Pb geochronological constraints on the evolution of the Aspy terrane, Cape Breton Island: implications for relationships between Aspy and Bras d’Or terranes and Ganderia in the Canadian Appalachians. *American Journal of Science*, **307**, 371–398.
- Ludwig, K.R. 2012. User’s manual for Isoplot 3.75. *Berkeley Geochronology Center Special Publication*, **5**, 75.
- Macdonald, F.A., Ryan-Davis, J., Coish, R.A., Crowley, J.L. & Karabinos, P. 2014. A newly identified Gondwanan terrane in the northern Appalachian Mountains: Implications for the Taconic orogeny and closure of the Iapetus Ocean. *Geology*, **42**, 539–542.
- McDaniel, D.K., Hanson, G.N., McLennan, S.M. & Sevigny, J.H. 1997. Grenvillian provenance for the amphibolite-grade Trap Falls Formation: implications for early Paleozoic tectonic history of New England. *Canadian Journal of Earth Sciences*, **34**, 1286–1294.
- McLennan, S.M., Bock, B., Compston, W., Hemming, S.R. & McDaniel, D.K. 2001. Detrital zircon geochronology of Taconian and Acadian foreland sedimentary rocks in New England. *Journal of Sedimentary Research*, **71**, 305–317.
- Melchin, M.J., Sadler, P.M., Cramer, B.D., Cooper, R.A., Gradstein, F.M. & Hammer, O. 2012. The Geologic Time Scale 2012. In: Gradstein, F. M., Ogg, J. G., Schmidt, M. & Ogg, G. (eds) *The Silurian Period*. Elsevier, 525–558.
- Miller, B.V. 1997. *Geology, Geochronology, and Tectonic Significance of the Blair River Inlier, Northern Cape Breton Island, Nova Scotia*. PhD, Dalhousie University.
- Miller, B.V. & Barr, S.M. 2000. Petrology and Isotopic Composition of the Grenvillian Basement Fragment in the Northern Appalachian Orogen: Blair River Inlier, Nova Scotia, Canada. *Journal of Petrology*, **41**, 1777–1804.
- Miller, B.V., Dunning, G.R., Barr, S.M., Raeside, R.P., Jamieson, R.A. & Reynolds, P.H. 1996. Magmatism and metamorphism in a Grenvillian fragment: U-Pb and $^{40}\text{Ar}/^{39}\text{Ar}$ ages from the Blair River Complex, northern Cape Breton Island, Nova Scotia, Canada. *Geological Society of America Bulletin*, **108**, 127–140.

- Murphy, J.B., Fernández-Suárez, J., Keppie, J.D. & Jeffries, T.E. 2004. Contiguous rather than discrete Paleozoic histories for the Avalon and Meguma terranes based on detrital zircon data. *Geology*, **32**, 585–588.
- O'Brien, B. & O'Brien, S. 1989. *Geology of the Western Hermitage Flexure: Bay D'est Fault and South (Parts of 11 O/9, 11 O/16, 11 P/12 and 11 P/13), Southwest Newfoundland*. Newfoundland Department of Mines and Energy, Map 89-133.
- Pothier, H.D., Waldron, J.W.F., Schofield, D.I. & DuFrane, S.A. 2015. Peri-Gondwanan terrane interactions recorded in the Cambrian–Ordovician detrital zircon geochronology of North Wales. *Gondwana Research*, **28**, 987–1001,
- Quinn, L., Williams, S.H., Harper, D.A.T. & Clarkson, E.N.K. 1999. Late Ordovician foreland basin fill: Long Point Group of onshore western Newfoundland. *Bulletin of Canadian Petroleum Geology*, **47**, 63–80.
- Quinn, L., Bashforth, A.R., Burden, E.T., Gillespie, H., Springer, R.K. & Williams, S.H. 2004. The Red Island Road Formation: Early Devonian terrestrial fill in the Anticosti Foreland Basin, western Newfoundland. *Canadian Journal of Earth Sciences*, **41**, 587–602.
- Quinn, L.A. 1992. *Foreland and Trench Slope Basin Sandstones of the Goose Tickle Group and Lower Head Formation, Western Newfoundland*. PhD Thesis, Memorial University of Newfoundland.
- Rivers, T. 1997. Lithotectonic elements of the Grenville Province: review and tectonic implications. *Precambrian Research*, **86**, 117–154, \
- Rivers, T. 2015. Tectonic Setting and Evolution of the Grenville Orogen: An Assessment of Progress Over the Last 40 Years. *Geoscience Canada*, **42**, 77–124,
- Simonetti, A., Heaman, L.M., Hartlaub, R.P., Creaser, R.A., MacHattie, T.G. & Böhm, C. 2005. U–Pb zircon dating by laser ablation-MC-ICP-MS using a new multiple ion counting Faraday collector array. *Journal of Analytical Atomic Spectrometry*, **20**, 677.
- Sparkes, G.W. & Dunning, G.R. 2014. Late Neoproterozoic epithermal alteration and mineralization in the western Avalon Zone: a summary of mineralogical investigations and new U/Pb geochronological results. *Current Research, Newfoundland and Labrador Department of Natural Resources Geological Survey, Report*, 14–1, 99-128.
- St. Julien, P. & Hubert, C. 1975. Evolution of the Taconic orogen in the Quebec Appalachians. *American Journal of Science*, **275–A**, 337–362.
- Stacey, J. t & Kramers, IJD. 1975. Approximation of terrestrial lead isotope evolution by a two-stage model. *Earth and planetary science letters*, **26**, 207–221.
- Stevens, R.K. 1970. Cambro-Ordovician flysch sedimentation and tectonics in west Newfoundland and their possible bearing on a proto-Atlantic Ocean. *In: Lajoie, P. (ed.)*

- Flysch Sedimentology in North America*. Geological Association of Canada, Special Paper 7, 165–177.
- Thomas, W.A. & Becker, T.P. 2007. Crustal recycling in the Appalachian foreland. *In: Geological Society of America Memoirs*. Geological Society of America, 33–40., [https://doi.org/10.1130/2007.1200\(03\)](https://doi.org/10.1130/2007.1200(03)).
- van Staal, C.R., Dewey, J.F., Niocaill, C.M. & McKerrow, W.S. 1998. The Cambrian-Silurian tectonic evolution of the northern Appalachians and British Caledonides: history of a complex, west and southwest Pacific-type segment of Iapetus. *In: Blundell, D. J. & Scott, A. C. (eds) Lyell, the Past Is the Key to the Present*. Geological Society, London, Special Publications, 197–242.
- van Staal, C.R., Whalen, J.B., Valverde-Vaquero, P., Zagorevski, A. & Rogers, N. 2009. Pre-Carboniferous, episodic accretion-related, orogenesis along the Laurentian margin of the northern Appalachians. *In: Murphy, J. B., Keppie, J. D. & Hynes, A. J. (eds) Ancient Orogens and Modern Analogues*. Geological Society, London, Special Publications, 271–316.
- van Staal, C.R., Chew, D.M., et al. 2013. Evidence of Late Ediacaran Hyperextension of the Laurentian Iapetan Margin in the Birchy Complex, Baie Verte Peninsula, Northwest Newfoundland: Implications for the Opening of Iapetus, Formation of Peri-Laurentian Microcontinents and Taconic – Grampian Orogenesis. *Geoscience Canada*, **40**, 94.
- van Staal, C.R., Zagorevski, A., McNicoll, V.J. & Rogers, N. 2014. Time-Transgressive Salinic and Acadian Orogenesis, Magmatism and Old Red Sandstone Sedimentation in Newfoundland. *Geoscience Canada*, **41**, 138.
- Waldron, J.W.F. & van Staal, C.R. 2001. Taconian orogeny and the accretion of the Dashwoods block: A peri-Laurentian microcontinent in the Iapetus Ocean. *Geology*, **29**, 811–814.
- Waldron, J.W.F., Henry, A.D., Bradley, J.C. & Palmer, S.E. 2003. Development of a folded thrust stack: Humber Arm Allochthon, Bay of Islands, Newfoundland Appalachians. *Canadian Journal of Earth Sciences*, **40**, 237–253.
- Waldron, J.W.F., Floyd, J.D., Simonetti, A. & Heaman, L.M. 2008. Ancient Laurentian detrital zircon in the closing Iapetus ocean, Southern Uplands terrane, Scotland. *Geology*, **36**, 527–530.
- Waldron, J.W.F., Schofield, D.I., White, C.E. & Barr, S.M. 2011. Cambrian successions of the Meguma Terrane, Nova Scotia, and Harlech Dome, North Wales: dispersed fragments of a peri-Gondwanan basin? *Journal of the Geological Society*, **168**, 83–98.
- Waldron, J.W.F., McNicoll, V.J. & van Staal, C.R. 2012. Laurentia-derived detritus in the Badger Group of central Newfoundland: deposition during closing of the Iapetus. *Canadian Journal of Earth Sciences*, **49**, 207–221.

- Waldron, J.W.F., Barr, S.M., Park, A.F., White, C.E. & Hibbard, J. 2015. Late Paleozoic strike-slip faults in Maritime Canada and their role in the reconfiguration of the northern Appalachian orogen. *Tectonics*, **34**, 1661–1684.
- Waldron, J.W.F., Schofield, D.I. & Murphy, J.B. 2017. Diachronous Palaeozoic accretion of peri-Gondwanan terranes at the Laurentian margin. *In: Wilson, R. W., Houseman, G. A., McCaffrey, K. J. W., Dore, A. G. & Buitter, S. J. H. (eds) Fifty Years of the Wilson Cycle*. 470.
- Williams, H. & Hiscott, R.N. 1987. Definition of the lapetus rift-drift transition in western Newfoundland. *Geology*, **15**, 1044–1047.
- Williams, H. & Stevens, R.K. 1974. The ancient continental margin of eastern North America. *In: In Burk, C.A. and Drake, C.L., Eds., The Geology of Continental Margins*. New York, Springer-Verlag, 781–796.
- Zagorevski, A., Lissenberg, C.J. & van Staal, C.R. 2009. Dynamics of accretion of arc and backarc crust to continental margins: Inferences from the Annieopsquotch accretionary tract, Newfoundland Appalachians. *Tectonophysics*, **479**, 150–164.

Chapter 5: Along-Strike Variations in Foreland Provenance and Orogenesis in the Northern Appalachians: Inherited Geometry of Rifted Margins and Arcs

Neoproterozoic to Cambrian break-up of Rodinia resulted in opening of the Iapetus Ocean and formation of an irregular Laurentian margin, defined by NE-striking rift zones offset by NW-striking transfer faults. Contrasts in detrital zircon populations from Newfoundland indicate two distinct provenance domains in clastic rift-to-drift rocks. A proximal western succession is dominated by Mesoproterozoic detritus with strong peaks at 1.1 Ga, indicating derivation from local basement and from the Grenville Province to the west. A distal succession to the east displays similarities with the Laurentian margin in Greenland and Scotland, with prominent 1.85 Ga peaks and many Archean grains, mainly ~2.7 Ga. These contrasts are consistent with a major NW-striking transfer fault, blocking sediment transport, between the Newfoundland Promontory and Québec Embayment.

Microcontinents, severed from the Laurentian margin, were deformed during earliest stages of Taconian arc-continent collision. This deformation was strongly diachronous as was subsequent closure of the Taconic Seaway. In Newfoundland, closure began at ~ 470 Ma and resulted in obduction of the Humber Arm Allochthon above the Laurentian margin. In Québec the seaway began to close at ~ 461 Ma and allochthon emplacement continued until ~450 Ma. In New England the seaway closed ~ 455 Ma. Pro-arc foreland basins developed in the Middle Ordovician in Newfoundland, but in the Late Ordovician in the Québec Embayment.

Subduction polarity reversal occurred in Newfoundland at ~460 Ma. Subduction polarity reversal farther south was later (~450 Ma). Simultaneous westward and eastward subduction at different places along the Laurentian margin resulted in the unique setting of the Upper Ordovician Long Point Group in Newfoundland, analogous to the current Australian Plate near Papua New Guinea.

Continued westward subduction and accretion of Gondwanan fragments led to the 440-420 Ma Salinian and 420-400 Ma Acadian orogenies in Newfoundland. In Québec the Acadian Orogeny continued later, until ~ 380 Ma. In the foreland, the Salinian Orogeny is manifested by major unconformities (e.g. Clam Bank unconformity), while the Acadian orogeny resulted in deposition of thick clastic wedges. Acadian inversion at the structural front and uplift and erosion of basement massifs are interpreted as Emsian in Newfoundland but Frasian in New England.

All major episodes of deformation affecting the northern Laurentian margin were diachronous. This resulted from: the irregularity of the Laurentian margin; the distribution of off-margin microcontinents; and/or the geometry of colliding arcs and microcontinents.

5.1. Introduction

5.1.1. Objectives of this paper

The Appalachian Orogen (Figure 5.1) has been important in the history of research in plate tectonics and, in particular, to the understanding of mountain building processes (e.g. Wilson, 1966). Rocks preserved within the orogen provide a detailed record of lithospheric plate motion including rifting, ocean opening, subduction, accretion and orogenesis during opening and closing of the Iapetus Ocean (e.g. Harland and Gayer 1972, Williams 1975, van Staal et al. 2009). General features of the evolution of the Laurentian margin in the northern Appalachians are well understood (Williams et al. 1988, van Staal et al. 1998, 2009, Hibbard et al. 2007); however, these generalized interpretations do not explain along margin changes in foreland basin style, geometry, timing, and provenance which we have demonstrated in chapters 2, 3 and 4 of this thesis.

The aim of this paper is to generate an evolutionary model for eastern Laurentia that honours all the existing data and observations from previously published sources and new data from this thesis. We will reinterpret previously published data in light of new seismic interpretations, geologic mapping, geochronologic data, and the increasingly available detrital zircon data from published literature. By doing this we hope to make sense of observations from both the foreland basin and allochthonous margin which are inconsistent with current orogenic models based predominantly on geochronologic ages of magmatic arcs and metamorphosed units within the orogen.

5.1.2. Previous syntheses of the margin

The eastern Laurentian margin was generated as a result of the break-up of the supercontinent Rodinia into multiple large cratons, including: Laurentia, Amazonia, and Baltica (Cawood et al. 2007b). This break-up led to the opening of the Iapetus Ocean, the development of conjugate margins of eastern Laurentia and western Amazonia (Cawood & Williams 1988, Cawood et al. 2001), and the rifting of crustal ribbons from both Laurentian and Amazonian margins (van Staal et al. 1998, 2013, Waldron & van Staal 2001). Break-up is recorded by a Late Neoproterozoic to early Cambrian clastic and volcanic rift succession (Cawood et al. 2001, Allen et al. 2010), deposited on top of older (>1.0 Ga) Laurentian basement and structurally controlled by an extensive basement-involved rift system which is interpreted to parallel the present-day

geometry of promontories and embayments along the Appalachians (Thomas 1977, Allen et al. 2010).

The transition, from an active rift basin to a passive margin, is recorded by the deposition of an extensive mixed clastic and carbonate shelf formed along the margin of eastern Laurentia from the early Cambrian (Lavoie et al. 2003). The passive margin persisted until approximately the Middle Ordovician, at which time closure of the Iapetus Ocean was underway and the effects of deformation associated with Taconian arc-continent collision were felt. An extensive time-transgressive unconformity was formed at the top of the passive margin (Knight et al. 1991) along the length of the Appalachians which marked the westward passage of a peripheral bulge formed as a result of loading of the margin by Taconian allochthons (Jacobi 1981). These allochthons transported deeper-water equivalents of the passive margin and ophiolites westward, on top of the subducting Laurentian craton (Waldron et al. 2003), and material was shed from the advancing allochthons into the developing foreland basin (Stevens 1970). These events are attributed to the Taconian Orogeny (Williams 1975, Stanley & Ratcliffe 1985).

The Taconian Orogeny was followed by subduction polarity reversal (Karabinos et al. 1998, Zagorevski et al. 2009). Westward subduction and contraction led to underthrusting of exotic Gondwanan terranes beneath the composite Laurentian margin (van Staal et al. 1998, 2009, Waldron et al. 2017). This episodic accretion was accompanied by orogenic episodes (including the Silurian Salinian Orogeny, and the Devonian Acadian and NeoAcadian orogenies), ocean closure, and continued development of foreland basins on the Laurentian craton. The latest phase of deformation records a prolonged episode of Late Devonian to Pennsylvanian dextral transtension and transpression felt along the northern Appalachian margin (van Staal et al. 2009; Hibbard and Waldron 2009; Hibbard et al. 2010; Waldron et al. 2015). This dextral motion resulted in opening of the Maritimes Basin and reactivation of major fault systems along which large amounts (up to 250 km) of dextral strike slip took place (Waldron et al. 2015).

5.2. Cambrian to Early Ordovician Evolution of the Laurentian Margin in

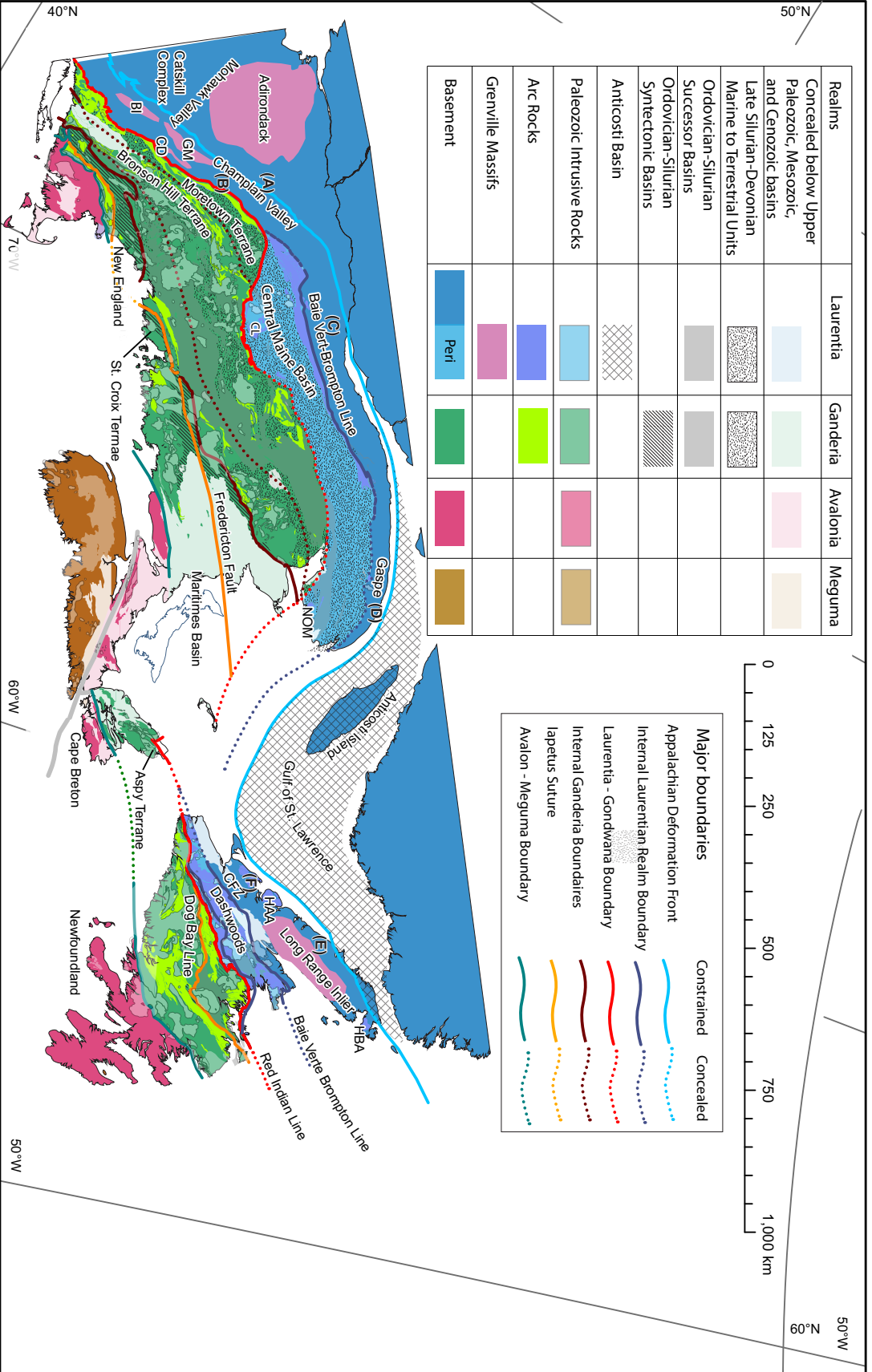


Figure 5.1: Map of present day tectonostratigraphic realms in the Northern Appalachians (modified from Waldron et al. 2017). Letters A, B, C, D, E and F correspond to approximate locations of stratigraphic sections in figure 5.3. CFZ, Cabot Fault Zone; CL, Chain Lakes; CD, Chester Dome; GM, Green Mountain massif; BI, Berkshire inlier; HAA, Humber Arm Allochthon; HB, Hare Bay Allochthon; MM, Maqueran-Mictaw inlier; NOM, Nadeau Ophiolite.

Newfoundland

5.2.1. Laurentian Basement

The eastern Laurentian margin was developed above basement rocks of Laurentia, a composite of crustal domains which evolved over a significant period in Earth history from ~ 3.6 to 1.0 Ga (Hoffman 1988). A brief description of the structural provinces and domains which make up the continent is important to the understanding of the provenance of detrital zircons found in Paleozoic basins deposited along Laurentia's eastern margin.

The Superior Craton underlies much of eastern Laurentia (Figure 5.2). A large proportion of the Superior Craton contains Neoproterozoic and Mesoproterozoic crust formed during various magmatic and metamorphic episodes (Corfu et al. 1998, Calvert & Ludden 1999, Corfu & Lin 2000). Neoproterozoic ages of ~ 2.7 Ga are interpreted to have been generated during large-scale magmatic arc activity and tectonism which occurred during the Kenoran Orogeny (Calvert & Ludden 1999, Corfu & Lin 2000, Downey et al. 2009). Older Paleoproterozoic and Eoproterozoic crustal ages are observed near the margins of the Superior Craton (Bickford et al. 2006; Boehm et al., 2000).

The Archean North Atlantic Craton is exposed to the north in Labrador and southern Greenland (Figure 5.2). Crustal ages range from 2.5-3.8 Ga. The majority of the craton is dominated by Neoproterozoic and Mesoproterozoic terranes, with smaller Paleoproterozoic gneissic complexes scattered throughout (Nutman et al. 2004).

Major contributors to Laurentian crust are Paleoproterozoic orogens which stitched together the Archean cratons during the assembly of Laurentia (Hoffman 1988). The Trans-Hudson Orogen (1.82 Ga) bounds the western margin of the Superior Craton, while the New Québec (1.82 Ga), Torngat (1.86 Ga), and Makkovik (~1.87 Ga) orogens are to the north (LaFlamme et al. 2013, Hoffman 2014) (Figure 5.2). At the southern tip of Greenland, the Ketilidian Orogen, involving major magmatic and metamorphic events dated at ~ 1.9 – 1.73 Ga (Garde et al. 2002), is interpreted to represent an eastern extension of the Makkovik orogen (Figure 5.2) in Canada.

The Grenville Province lies east of the Superior Craton (Figure 5.2) and extends along the eastern margin of Laurentia, from Labrador to Mexico (Rivers 1997). The majority of the province consists of metamorphic and magmatic rocks generated during the 980 – 1090 Ma Grenville Orogeny (Rivers 2008, 2015). The Grenville Orogeny is defined by two distinct orogenic pulses, the (~ 980 Ma – 1.0 Ga) Rigolet and (~ 1.0 – 1.1 Ga) Ottawa orogenic phases (Rivers 2015). Late Mesoproterozoic to Paleoproterozoic pre-Grenvillian crust (~ 1.2- 1.7 Ga) is preserved in the Grenville Province, including the Pinware terrane in Labrador (Figure 5.2).

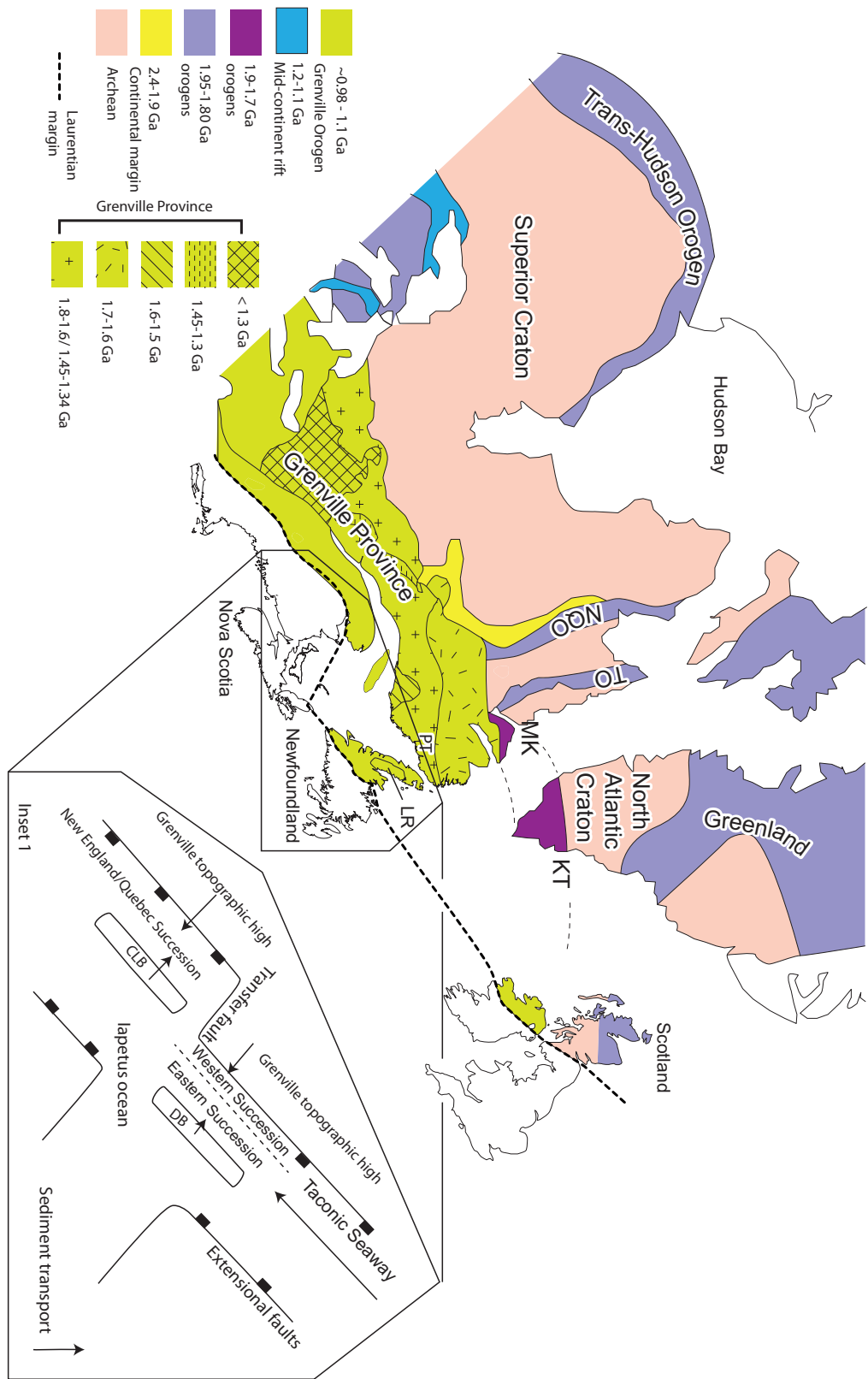


Figure 5.2: Map of eastern Laurentia after Neoproterozoic and Cambrian rifting episodes. KT, Ketildian Orogen; MK, Makkovik Orogen; NQO, New Québec Orogen; TO, Torngat Orogen; DB, Dashwoods block; CLB, Chain Lakes block.

These late Mesoproterozoic crustal ages are interpreted by Rivers (1997) as evidence that an active margin, forming arcs and accreting new crust, existed from ~ 1.2 – 1.7 Ga along the margin of southeastern Laurentia.

Basement rocks exposed in western Newfoundland (Figure 5.1) have long been recognized as part of the Grenville structural province (Owen & Erdmer 1989, Heaman et al. 2002); however, U-Pb dating of basement units exposed in the Long Range Inlier indicates that the majority of gneissic rocks have protolith ages of about 1530-1466 Ma (Heaman et al. 2002) correlating with the timing of Pinwarian magmatism in Labrador (1510-1450 Ma: Tucker and Gower, 1994). Heaman et al. (2002) suggested that the Long Range Inlier and the Pinware terrane in Labrador (Figure 5.2) form a single contiguous terrane, extending beneath the Gulf of St. Lawrence (Figure 5.1).

5.2.2. Rift-Related Rocks

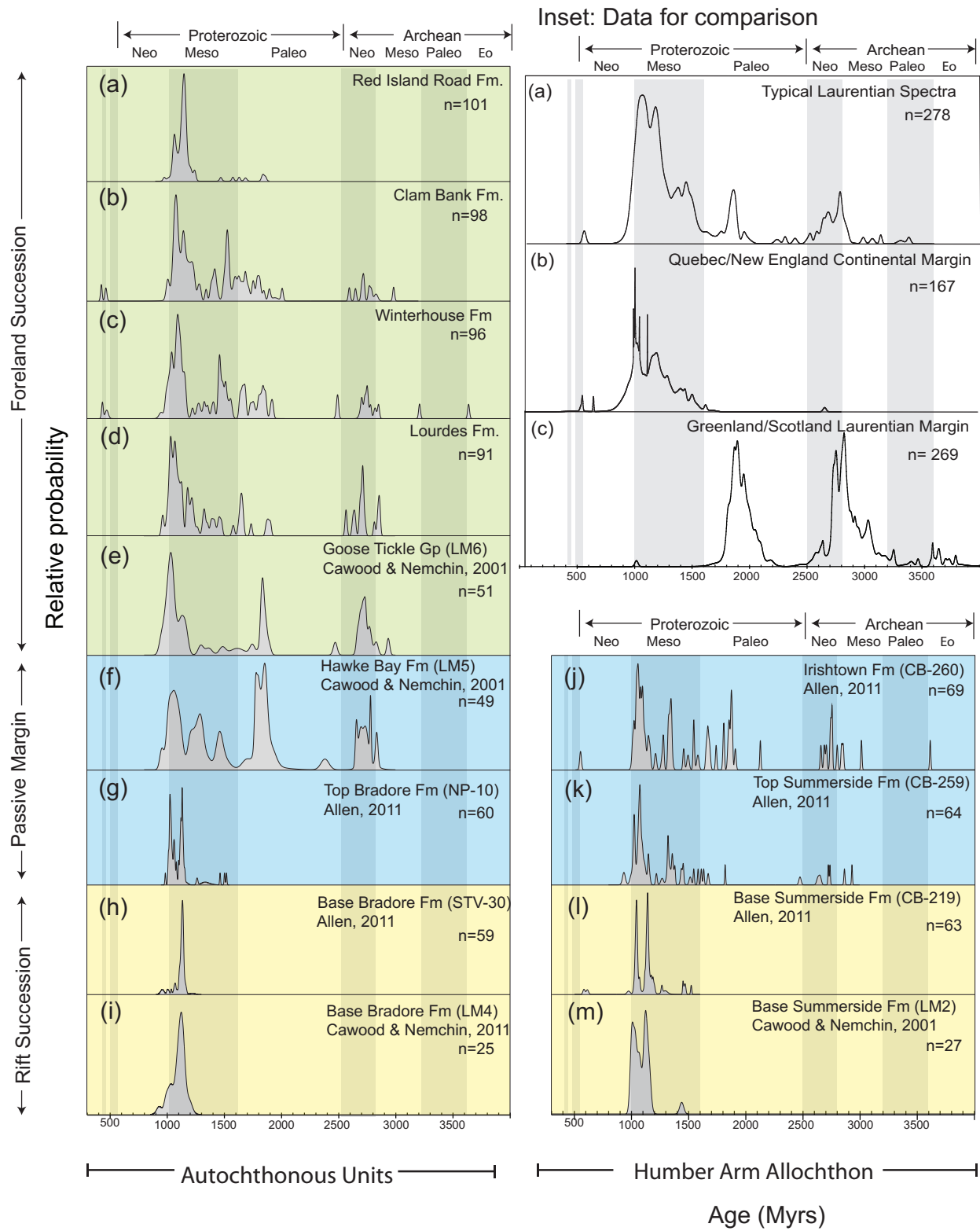
5.2.2.1. Western Newfoundland

5.2.2.1.1. Autochthonous Rift Succession

The oldest rift-related units deposited on Mesoproterozoic basement are coarse conglomerate units of the Precambrian Bateau Formation. These units, containing boulders of basement gneiss near the base and finer conglomerate and sandstone up-section, are only exposed along the most northern part of Newfoundland and in Labrador. Mafic volcanic units of the Lighthouse Cove Formation overlie the Bateau Formation (Williams & Hiscott 1987). Arkosic sandstone and conglomerate of the Bradore Formation overlies the Lighthouse Cove Formation or rests directly on top of autochthonous basement. These units are interpreted to have been deposited in a relatively shallow, nearshore marine environment (Williams & Hiscott 1987).

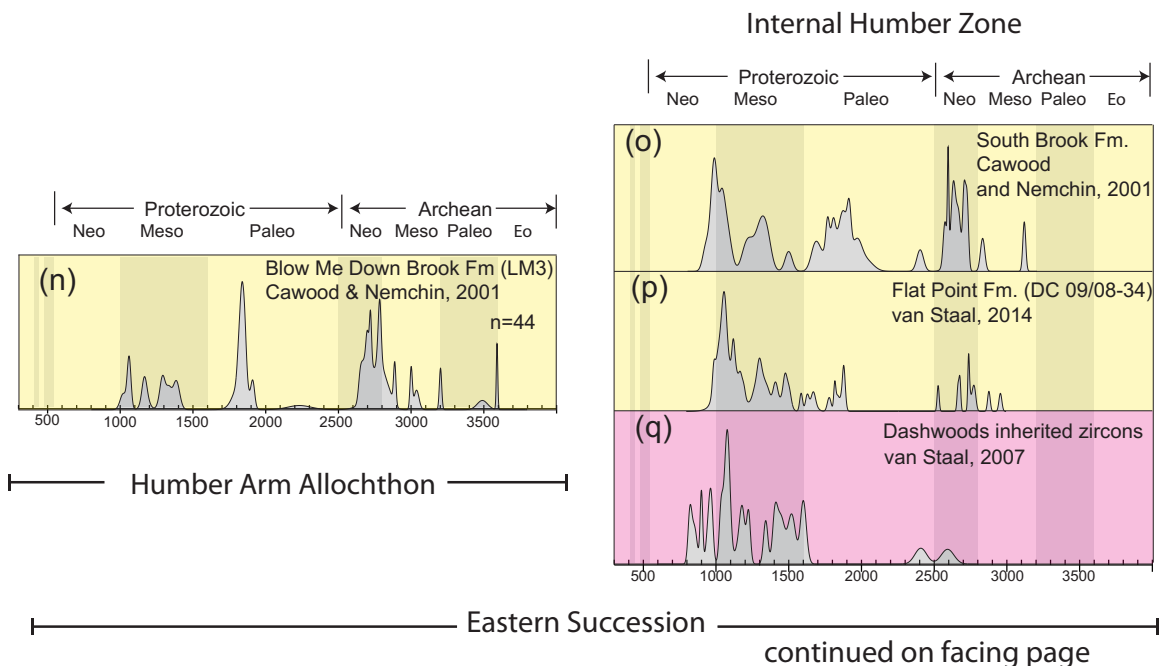
The Bradore Formation (Figure 5.3) is the only autochthonous rift-related unit which has been sampled for U/Pb analyses of detrital zircons (Cawood & Nemchin 2001, Allen 2009). Probability density functions for two samples near the base and one near the top of the unit are shown in figure 5.4. Two samples near the base of the unit are characterized by a conspicuously narrow age spectrum containing only one major statistical peak at 1.1 Ga. The 1.1 Ga age indicates derivation from the immediate basement of the Grenville Orogen. A sample near the top of the Bradore Formation has a spectrum which contains older Mesoproterozoic ages (Figure 5.4) consistent with derivation from local basement of the Grenville Province exposed in the Long Range Inlier (Figure 5.5). Also present is another well-defined peak at ~1.0 Ga. We interpret that the two distinct peaks at ~1.0 and 1.1 Ga may represent the Rigolet and Ottawa orogenic phases respectively.

Figure 5.3: Stratigraphic columns of western Newfoundland, Quebec and New England autochthonous and allochthonous passive margin and foreland successions. Biostratigraphic information for New England stratigraphy from Landing (2012), Bolton et al. (1991) and Rowley and Kidd (1982). Biostratigraphic information for Quebec stratigraphy from Dix et al. (2013), Hersi et al. (2003), Lavoie et al. (2003) and Bolton et al. (1991). Biostratigraphic info for Newfoundland from Lacombe (2016). A, B, C, D, E and F correspond to locations of the sections on figure 5.1.



continued on facing page

Figure 5.4: Detrital zircon probability density functions for data from this study and previously published data in Newfoundland (References on figure). Vertical scale is in arbitrary units of relative probability density. **(a)** NP007 (Lourdes Fm.) **(b)** NG024A (Winterhouse Fm.) **(c)** NG043 (Clam Bank Fm.) **(d)** NP021 (Red Island Road Fm.) **(e)** LM6 (American Tickle Fm.) **(f)** LM5 (Hawke Bay Fm.) **(g)** NP-10 (top Bradore Fm.) **(h)** STV-30 (base Bradore Fm.) **(i)** LM4 (base Bradore Fm.) **(j)** CB-260 (Irishtown Fm.) **(k)** CB-259 (top Summerside Fm.) **(l)** CB-219 (base Summerside Fm.) **(m)** LM2 (base Summerside Fm.) **(n)** LM3 (Blow Me Down Brook Fm.) **(o)** LM1 (South Brook Fm.) **(p)** DC 09/08-34 (Flat Brook Fm.) **(q)** inherited zircons in Notre Dame Arc. **Inset:** Probability density functions for comparison. **(a)** Typical Laurentian age spectra (Rowe Formation: Macdonald et al. 2014). **(b)** Composite probability density function of zircon analyses from Laurentian passive margin units in Quebec and New England. Data sources include: Poughquag quartzite (McLennan et al. 2001), Cheshire Formation (Macdonald et al. 2014), Trap Falls Formation (McDaniel et al. 1997), and Cavendish Formation (Karabinos et al. 1999a). **(c)** Composite probability density function of zircon analyses from Laurentian continental margin units in Greenland and Scotland. Data from the following units: Ardvrek Group (Scotland) and Trekant and Zebra series (Greenland) in (Cawood et al. 2007).



5.2.2.1.2. *Allochthonous Rift Succession*

Rift-related rocks preserved within the Ordovician Humber Arm Allochthon (Figure 5.5) are interpreted as distal time-equivalents of the Bradore Formation (Botsford 1987, Palmer et al. 2001) and include the Cambrian Summerside and Blow Me Down Brook formations of the Curling Group (Figure 5.3) (Botsford, 1988). The structurally higher Blow Me Down Brook Formation is considered the most distal unit (Palmer et al. 2001). It unconformably overlies pillow basalts, suggesting deposition in a rift environment. Both formations contain compositionally similar coarse-grained quartz-rich arkosic sandstone (Palmer et al. 2001). However, fine-grained clastics are much more abundant in the Summerside Formation. Both formations contain sedimentary structures indicative of rapid deposition and are interpreted to have been deposited by turbidity currents or other types of sediment-gravity flows (Palmer et al. 2001).

Two samples from the base of the Summerside Formation (Cawood & Nemchin 2001, Allen 2009), representing distal equivalents of the Bradore Formation (Figure 5.3), display remarkably similar age spectra with one another and the sample from near the top of the Bradore succession (Figure 5.4). Two strong peaks at ~1.05 and 1.15 Ga and a scattering of older Mesoproterozoic grains indicate that these sediments were also derived from the underlying basement units of the Grenville Province. In the younger sample, the age spectrum of the Summerside Formation broadens. More Mesoproterozoic grains are present, as are peaks in the Paleoproterozoic and a scattering of grains showing Neoproterozoic and Mesoarchean ages. This spectrum of Proterozoic and Archean grains is typical of sediments from the Laurentian interior (Cawood & Nemchin 2001).

The age spectrum of the Blow Me Down Brook Formation (Cawood & Nemchin 2001) contains a larger spread of ages than that of the Summerside Formation (Cawood & Nemchin 2001, Allen 2009) (Figure 5.4). Archean grains are dominated by Neoproterozoic detritus with strongest peaks ranging from 2.6 – 2.8 Ga. Similar but less prominent peaks are observed near the top of the more proximal Summerside Formation. Smaller, but significant Mesoarchean peaks are observed as are a few Paleoproterozoic peaks at 3.2, 3.5, and 3.6 Ga, not seen in the Summerside Formation. These Archean ages are characteristic of either the Superior Craton to the west or North Atlantic Craton to the north (Figure 5.2). The largest statistical peak occurs at 1.85 Ga, unlike all other more proximal units which demonstrate strong Grenville peaks between 1.0 and 1.2 Ga. This large 1.85 Ga peak implies contribution of detritus from Paleoproterozoic orogens which lie west (Trans-Hudson Orogen) or north (e.g. New Québec, Makkovik or Ketilidian orogens) of the basin. Only a relatively small proportion of zircons display Mesoproterozoic ages between 1.0 and 1.4 Ga.

5.2.2.1.3. *Metamorphosed Rift-Related Units*

The South Brook and Flat Point formations, exposed in the eastern Humber Zone, are rift-related metasedimentary units of the Fleur de Lys Supergroup (Figure 5.5). Quartz-rich metasediments of the South Brook Formation unconformably overlie Grenville basement and rift-related igneous units (Cawood et al. 1996). This unit has been interpreted as a metamorphosed equivalent of the Curling Group. Metasediments of the early Cambrian Flat Point Formation also overlie rift-related igneous units (Figure 5.5).

Samples from the South Brook and Flat Point formations (Cawood & Nemchin 2001, van Staal et al. 2013) have zircon populations similar to those in the Blow Me Down Brook Formation. The Archean grains are dominated by Neoproterozoic ages, with the highest peaks at 2.6 and 2.75 Ga. The 2.6 Ga peak in the South Brook Formation is the strongest peak in the spectrum. A significant proportion of Paleoproterozoic grains, from 1.7 to 2.0 Ga, are also present in both spectra. A conspicuous gap in the spectra occurs between 2.0 and 2.4 Ga. Mesoproterozoic ages, from 1.0 to 1.6 Ga, are dominated by peaks at 1.0 and 1.1 Ga.

5.2.2.2. *Québec and New England*

5.2.2.2.1. *Autochthonous Rift-Related Rocks*

In Québec and New England, sandstone and conglomerate of the Potsdam Group (Formation in New England) are the oldest clastic units deposited along the autochthonous Laurentian margin (Lavoie et al. 2003). These clastics, deposited in rift-related basins, unconformably overlie Mesoproterozoic basement of the Grenville Province (Macdonald et al. 2017). Although lowermost sandstone units of the Potsdam are unfossiliferous, higher portions contain middle Cambrian trilobites (*Crepicephalus* Zone) and the trace fossil *Oldhamia* indicating a Cambrian age (Landing 2012) (Figure 5.3). The transition from rift to drift has been interpreted to occur within the Potsdam Group (Salad Hersi et al. 2002, Lavoie et al. 2003).

In New England, detrital zircon studies have been carried out on the Potsdam Formation (Montario and Garver, 2009; Gaudette et al., 1981) and parautochthonous clastic units (Poughquag Quartzite, McLennan et al. 2001; Cheshire Formation, Macdonald et al. 2014) which unconformably overlie Mesoproterozoic basement and have been correlated with the Bradore Formation in Newfoundland (Landing 2012). These early clastic successions demonstrate a conspicuous abundance of Mesoproterozoic ages (Figure 5.4, inset). Montario and Garver (2009) report that ~ 90% of U-Pb ages fall between 950 and 1200 Ma, consistent with derivation from the local Grenville Orogen.

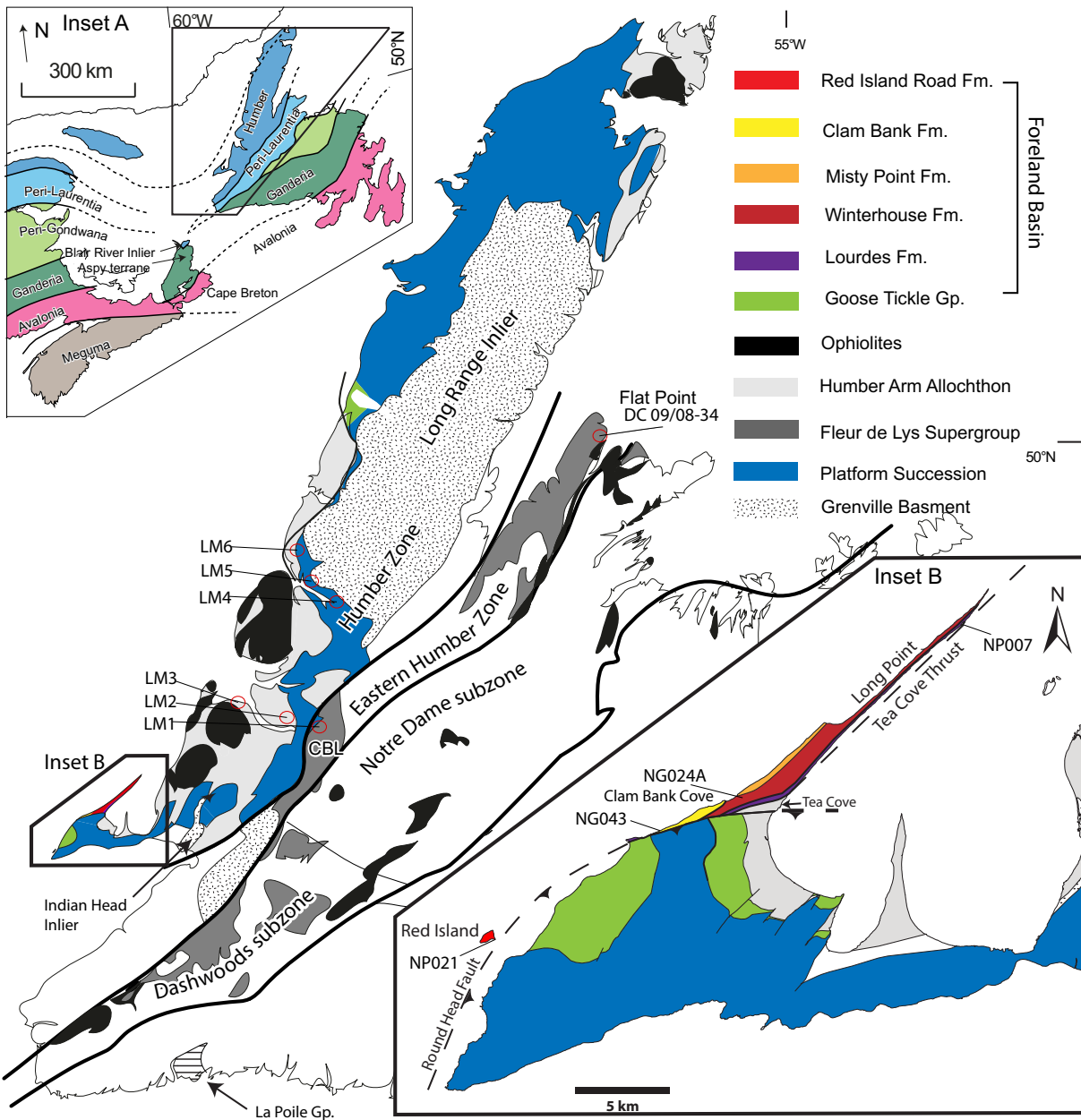


Figure 5.5: Geologic map of western Newfoundland including important place names, sample locations, and structures (Modified from Waldron & van Staal 2001).

5.2.2.2.2. *Allochthonous Rift-Related Rocks*

Within allochthonous nappes on the Gaspé Peninsula in Québec, shallow-marine clastic and carbonate units of the lower to middle Cambrian Oak Hill Group (and correlatives) overlie Late Proterozoic rift-related volcanic units such as the Tibbit Hill and Montagne de Saint-Anselme formations (Figure 5.3) (Lavoie et al. 2003). The Oak Hill Group has been interpreted to record the rift-drift transition (Lavoie et al. 2003). Farther south in New England, rift deposits are also present in thrust sheets of the Taconic allochthon (Zen 1967, Rowley & Kidd 1982, Macdonald et al. 2017). In the western portion of the allochthon, the Late Neoproterozoic to Cambrian Nassau Formation is the stratigraphically lowest preserved unit. Landing (2012) interpreted that immature sandstone and slate units of the Nassau Formation were deposited during rifting. The transition to overlying turbiditic mudstone of the Truthville Member (of the Nassau Formation) has been interpreted to represent the transition to a passive margin (Landing 2012). No detrital zircon data are available for these units.

5.2.2.2.3. *Metamorphosed Rift-Related Rocks (Peri-Laurentian Massifs)*

Massifs of intensely deformed metasedimentary rocks are exposed in the peri-Laurentian realm of the northern Appalachians (Figure 5.1). Polydeformed metaclastic units within these massifs have been shown to have stratigraphic ties to the Laurentian margin (Waldron & van Staal 2001, Gerbi et al. 2006, Allen et al. 2010). Although basement is not exposed in the majority of these massifs, interpretations of Precambrian Laurentian crust at depth have been made using various lines of geophysical, geochemical, and stratigraphic evidence (Cheatham et al. 1989, Spencer et al. 1989, Dunning & Cousineau 1990, Stewart et al. 1993, Waldron & van Staal 2001, van Staal et al. 2007). From north to south these massifs include: the Maquereau-Mictaw inlier on the Gaspé Peninsula, the Chain Lakes massif in Québec and Maine (Gerbi et al. 2006), and the Chester Dome in Vermont (Macdonald et al. 2014) (Figure 5.1). Within the Maquereau -Mictaw Inlier, the Maquereau Group consists of sandstone, conglomerate, and volcanic units that have been deformed and metamorphosed to greenschist facies (DeBroucker, 1987). Although unfossiliferous, they demonstrate lithologic similarities to Laurentian rift units and have been inferred as a late Neoproterozoic or Early Cambrian (DeBroucker, 1987) Laurentian synrift succession (Allen et al. 2010). In New England, within the Chester Dome, the oldest metasedimentary rocks, overlying Mesoproterozoic Grenvillie basement, are interpreted as Neoproterozoic to Cambrian (Karabinos et al. 1999).

5.2.3. Passive Margin

5.2.3.1. Western Newfoundland

In Newfoundland, shallow-marine limestone and deeper-marine shale units of the Forteau Formation stratigraphically overlie the Bradore Formation (Figure 5.3) and represent the transition to a passive margin (Williams & Hiscott 1987). These units have been interpreted to reflect upward-deepening in the basin during thermal subsidence following the active rifting phase (Williams & Hiscott 1987). Shallow-marine sandstone units of the Hawke Bay Formation conformably overlie the Forteau Formation and have been interpreted to mark a regression following basin deepening (Williams & Hiscott 1987). Thinly bedded high-energy carbonates of the middle to upper Cambrian Port au Port Group (Chow & James 1987) conformably overlie the Hawke Bay Formation. These units are overlain by massive, thick-bedded lower-energy limestone and dolostone of the Lower Ordovician St. George Group (Knight & James 1987).

Distal equivalents of the passive margin are exposed within the Humber Arm Allochthon (Figure 5.5). Black shale, quartzose sandstone, and local conglomerate units of the Irishtown Formation are lateral equivalents of the autochthonous Hawke Bay Formation (Palmer et al. 2001). Palmer et al. (2001) interpreted that the Irishtown Formation was deposited in a highly channelized, submarine fan environment, comparable to river-fed fans observed in modern passive margins. The Irishtown Formation is overlain by carbonate and deep-water slope and rise units of the Cow Head Group (James & Stevens 1986).

Only the lowest clastic units in the passive margin have been analyzed using detrital zircon geochronology (Cawood & Nemchin 2001, Allen 2009). In general, there is a broader range of ages observed in the passive margin than in older rift-related units (Figure 5.4). Both the Hawke Bay and Irishtown formations contain abundant Mesoproterozoic peaks between 1.2 and 1.6 Ga, ages characteristic of the Grenville Province. A strong statistical peak at 1.85 Ga, present in both units, is the strongest peak in the Hawke Bay spectrum. These grains could be derived from either the Makkovik or other Paleoproterozoic orogens (New Québec or Torngat) to the north of Newfoundland or the Trans-Hudson Orogen to the west (Figure 5.2). Both passive margin units have strong Archean signatures dominated by zircons ranging from 2.7 to 2.8 Ga.

5.2.3.2. Québec and New England

Platform carbonate units of the Beekmantown Group overlie the Potsdam Group/Formation in both Québec and New England (Lavoie et al. 2003, Landing 2012). In Québec, the Lower to Middle Ordovician Beekmantown Group unconformably overlies the Potsdam Group.

In New England, the Beekmantown Group includes older (upper Cambrian) rocks (Landing 2012) time equivalent to parts of the Potsdam Group in Québec (Figure 5.3).

Only the lowermost units of the autochthonous passive margin have been sampled for U/Pb dating of zircons. In New England, Montario and Garver (2009) sample the base of the Beekmantown Group (Galway Formation) on the New York Promontory. Strongest peaks occur at 1.1 and 1.2 Ga and smaller, older Mesoproterozoic peaks are present. Montario and Garver (2009) note that U-Pb ages of detrital zircon indicate derivation of these units almost entirely from the Grenville Province, although a few grains have older Archean ages from 2.65 – 2.75 Ga.

In the Québec Embayment, the slope succession, correlative with the more proximal Beekmantown Group, is exposed in a number of thrust slices within the Gaspé allochthons (Lavoie et al. 2003). This succession of mudstone, limestone, sandstone, and conglomerate gradationally overlies clastic and carbonate units of the Oak Hill Group (Figure 5.3). Graptolites within youngest units of the Cap des Rosiers Group (Maletz 2001) constrain the top of the slope succession at ~ 465 Ma (Figure 5.3). In New England the slope succession is also preserved in the Taconic allochthon. The succession consists predominantly of slate with intervals of limestone, thin beds of quartz arenite, and minor conglomerate. The uppermost slate units within the succession are the Indian River and Mount Merino formations (Landing, 2012). A volcanic ash horizon within the uppermost Indian River Formation was dated by Macdonald et al. (2017) at 464 Ma, while graptolites (*N. gracilis* Zone Landing 2012) within the black slates of the Mount Merino Formation constrain the youngest units deposited on the slope as ~ 454 Ma (Figure 5.3). Ordovician ages are according to the time scale of Cooper et al. (2012).

5.3. Ordovician Orogenic Record along Eastern Laurentian Margin

5.3.1. Foreland Basins Successions in Western Newfoundland

5.3.1.1. Middle Ordovician

5.3.1.1.1. St. George Unconformity

The top of the autochthonous shelf succession is marked by the St. George unconformity. The unconformity marks the passage of a peripheral bulge, generated by loading of the eastward subducting Laurentian margin by overriding Middle Ordovician allochthons during the Taconian Orogeny (Jacobi 1981). The unconformity generally youngs towards the west, reflecting the

cratonward migration of the bulge due to west-directed transport and emplacement of the allochthons (Knight et al. 1991).

5.3.1.1.2. Table Head Group

Middle Ordovician carbonate units of the Table Head Group are the first units deposited into the developing foreland basin, above the St. George unconformity, generated as a result of Taconian orogenesis (Stenzel et al. 1990, Waldron et al. 1998). These units vary in both thickness and facies, as a result of deposition on a karstic and faulted topography. The youngest unit of the Table Head Group, the Cape Cormorant Formation (Stenzel et al. 1990), is dominated by limestone conglomerate and is locally developed in the hanging walls of steep basement faults. Clasts were derived from the older shelf succession as a result of normal faulting during continued plate flexure and orogenic loading (Stenzel et al. 1990).

5.3.1.1.3. Goose Tickle Group

Siliciclastic units of the Middle Ordovician Goose Tickle Group lie stratigraphically above the Table Head Group. This unit, containing medium to fine-grained sandstone and laminated siltstone, displays graded beds, Bouma sequences, and flute casts and grooves on basal surfaces, indicating rapid and high energy deposition by turbidity currents (Quinn 1992). Intervals of limestone conglomerate, the Daniels Harbour Member (Stenzel et al. 1990), have lithologies consistent with derivation from the underlying Table Head Group; they occur only in the hanging walls of steep normal faults, which continued to be active during orogenic loading (Chapter 3).

Cawood and Nemchin (2001) report U/Pb analyses of zircon for a sample of the Goose Tickle Group (Figure 5.4). The strong 1.05 Ga peak and smaller Mesoproterozoic peaks are consistent with derivation from the basement of the Grenville Province. Another strong peak at 1.85 Ga is consistent with the age of Laurentian Paleoproterozoic Orogens (e.g. Trans-Hudson, Makkovik, New Québec, and Torngat). A strong Archean signature, dominated by 2.70 Ga grains, is consistent with the age of either the Superior or North Atlantic craton. We also note a conspicuous gap between 2.0 and 2.5 Ga, which is typical of zircon populations derived from eastern Laurentia (Cawood & Nemchin 2001, Waldron et al. 2008).

In Chapter 2, we used interpretations from 2D seismic reflection data to generate isochron thickness maps of major foreland basin successions offshore western Newfoundland (Figure 2.8). These maps demonstrate that the Goose Tickle Group, which fills the Middle Ordovician basin adjacent and parallel to the Newfoundland segment of the Appalachians, shows an overall thickening towards the east but also significant thickening northwards. In Chapter 2, thicker portions of Goose Tickle Group strata are imaged in the hanging walls of deep-seated basement

faults on 2D seismic profiles, indicating fault activity during basin development, consistent with our field observations (Chapter 2).

5.3.1.2. Late Ordovician

The Upper Ordovician (Sandbian to Katian) Long Point Group, comprising the Lourdes, Winterhouse and Misty Point formations, represents the Upper Ordovician foreland basin succession in western Newfoundland. The Lourdes Formation, a 75 m thick unit of shallow-marine limestone, disconformably overlies the Goose Tickle Group and represents the base of the Long Point Group. Although this contact is nowhere preserved on land, Burden and Williams (1995) recognized the contact in a well, and we have been able to interpret its position on 2D seismic reflection profiles (Chapter 2). Batten Hender and Dix (2008) have interpreted that the Lourdes Formation represents a narrow, high-energy, mixed siliclastic-carbonate ramp succession. The Lourdes Formation is gradationally overlain by thin-to medium-bedded fine-grained sandstone and shale units of the Winterhouse Formation. These units, interpreted to represent a storm-dominated shelf assemblage (Quinn et al. 1999), are in turn overlain by medium- to coarse-grained red sandstone units of the Misty Point Formation, which have been interpreted as a marginal marine to terrestrial deposit (Quinn et al. 1999).

In Chapter 4 we reported U/Pb analyses of zircon for samples of both the Lourdes and Winterhouse formations (Figure 5.4). Both units have similar age populations to one another and the ages are similar to those that we observe in the Goose Tickle Group (Figure 5.4). Like the Goose Tickle Group, the largest statistical peak is at 1.1 Ga and there are a significant number of older Mesoproterozoic grains ranging from 1.2 – 1.6 Ga. A small spread of Paleoproterozoic peaks is observed between 1.6 and 2.0 Ga. Also similar to the Goose Tickle Group is a conspicuous gap between ~2.0 to 2.5 Ga (Figure 5.4) and a small spread of Archean grains with the largest peak at 2.75 Ga.

Compositionally, the Winterhouse and Misty Point formations of the Long Point Group are similar to the Goose Tickle Group. Batten Hender and Dix, (2008) show that ratio ranges of Y/Ni and Cr/V are similar for the units and suggest that they are all derived from ophiolitic sources (Hiscott 1984, Quinn 1992).

5.3.2. Foreland Basin Successions in Québec and New England

5.3.2.1. Knox/Beekmantown Unconformity

The top of the autochthonous shelf succession is interpreted to be marked by the 463 Ma Beekmantown and Knox unconformity in Québec and New England respectively (Knight

et al. 1991, Salad Hersi et al. 2003, Macdonald et al. 2017). These unconformities have been interpreted to bear the same significance as the St. George unconformity in Newfoundland (Knight et al. 1991, Salad Hersi et al. 2003, Macdonald et al. 2017), resulting from regional uplift due to the passage of a peripheral bulge generated by loading of the eastward subducting Laurentian margin by overriding Middle Ordovician allochthons during the Taconian Orogeny (Jacobi 1981). However, Knight et al. (1991) and Salad Hersi et al. (2003) recognize that these unconformities are relatively minor and coincide with a major eustatic sea-level low, the Middle Ordovician Sauk-Tippecanoe boundary of Sloss (1963), which separates two major cratonic sequences in eastern North America.

5.3.2.2. *Autochthonous Platform*

A Darriwilian to lower Sandbian carbonate platform, referred to as the Chazyan platform (Dix et al. 2013), was formed atop the Beekmantown Group in Québec in New England (Figure 5.3). The platform grades and thins northward from seaward reefal carbonate units (Chazy Group) in the Champlain Valley (New England, Figure 5.1: Landing 2012, Dix et al. 2013) to platform interior carbonate and siliclastic units (Laval Formation) in Québec (Dix et al. 2013). Lower portions of the Chazy platform are coeval with the uppermost foreland platform in Newfoundland (Table Head Group); however, carbonate platform generation continued through the Darriwilian and into the Sandbian in Québec and New England while orogen-derived flysch of the Darriwilian Goose Tickle Group and Sandbian Long Point Group were being deposited in the Newfoundland foreland basin (Figure 5.3).

In Québec and New England, the Laval Formation and Chazy Group are unconformably overlain by platform carbonate units of the Black River Group (Figure 5.3) (Landing 2012). Although the hiatus is relatively minor in Québec and in the Champlain Valley, it is much more profound in the Mohawk Valley (Figure 5.1), removing much of Floian to Darriwilian succession (Landing 2012). The Black River Formation is unconformably overlain by calcareous shale and limestone of the Trenton Group. The Lacolle Breccia, containing clasts derived from the Beekmantown Group, lies stratigraphically on top of the Trenton carbonate platform in Québec (Lavoie 1994). These conglomerates lie in the immediate hanging wall of a steep basement fault and are interpreted to have been derived from uplifted fault blocks of the platform (Lavoie 1994), similar to conglomerate units of the Cape Cormorant Formation of the Table Head Group in Newfoundland but significantly younger. We interpret that the Trenton Group, like the Table Head Group in Newfoundland (Figure 5.3), represents that final phase of foreland carbonate platform development in Québec and New England prior to its burial under deep-marine shales and synorogenic flysch.

5.3.2.3. *Autochthonous Flysch: Utica, Lorraine, and Sainte-Rosalie groups*

In both Québec and New England the Trenton Group is gradationally overlain by Katian deep-water siliciclastic and hemipelagic mud of the Utica Shale, the early flysch fill within the Taconian foreland basin (Bradley & Kidd 1991). The Utica Shale is comparable in facies to the lowest black shale units of the Goose Tickle Group (Black Cove Formation) but is significantly younger (Figure 5.3). The Utica Shale is overlain by synorogenic flysch units known as the Lorraine and Sainte-Rosalie groups in Québec (Konstantinovskaya et al. 2009), equivalent to the Schenectady and Frankfort formations in New England (Ettensohn 2004). In Québec, thickness estimates of the Ordovician flysch succession range from 2000 m (Konstantinovskaya et al. 2009) to earlier estimates of over 3500 m (Globensky 1987). These units are in turn overlain by an uppermost Ordovician molasse, which includes redbeds of the Queenston Group. There is no preserved record of post-Ordovician sedimentation in the Québec foreland; however, Lavoie et al. (2008) interpret from thermal maturation data (Bertrand, 1991) that the platform here was buried roughly 4-5 km.

5.3.2.4. *Allochthonous Flysch*

Within the structurally lowest thrust slices along the northern Gaspé Peninsula (Figure 5.1), Darrivilian flysch units of the Tourelle Formation conformably overlie deep-water shales of the Tremadocian through Darrivilian Riviere Ouelle Formation (Figure 5.3). These turbiditic siliciclastic units, containing ophiolitic detritus and with northeast-southwest directed paleocurrent indicators, are the earliest coarse siliciclastic material interpreted to be derived from the advancing orogen to the east (Hiscott 1978). A thick succession (~1500 m) of younger orogen-derived turbidites of the lower Upper Ordovician Deslandes Formation structurally overlies the Tourelle Formation. Siliciclastic units of the Upper Ordovician Cloridorme Formation structurally overlie the Deslandes Formation; lower turbiditic portions of this unit have been interpreted as orogen-derived (Prave et al. 2000).

In western portions of the Taconian allochthon in the Champlain Valley (Figure 5.1), the Mount Merino Formation is conformably to disconformably overlain by deep-water flysch of upper Sandbian to Katian age (Austin Glen Formation: Figure 5.3) (Rowley & Kidd 1982). This sandstone-shale flysch succession is interpreted to have been shed from the orogen developing to the east (Bock et al. 1998).

McLennan et al. (2001) carried out U/Pb analyses of 41 zircons from a sample of the Austin Glen Formation. Their results show the majority of zircons have Mesoproterozoic

ages, with a peak at ~ 1.5 Ga (Figure 5.6). Two zircons at 720 and 730 Ma are interpreted to correspond to an early episode of rifting (Bock et al. 1998). A single analysis is Archean, having an age of 3.3 Ga. The provenance study by Bock et al. (1998) notes a lack of ophiolitic detritus, which is ubiquitous in flysch to the north (Hiscott 1984), indicating that input of Taconian mafic material into the early flysch basin was relatively minor.

5.4. Later Paleozoic Orogenic Record

5.4.1. Newfoundland

5.4.1.1. Late Silurian to Devonian

The Silurian record of deposition in the Newfoundland foreland basin is highly incomplete due to a major hiatus (Figure 5.3) above the Long Point Group. This boundary, termed the Clam Bank unconformity, is nowhere observed on land although it is faulted at Clam Bank Cove (Figure 5.5). The Katian – Pridoli hiatus amounts to a gap of ~ 25 Myr in the stratigraphic record and suggests either an extensive period of non-deposition or uplift and erosion at some point prior to deposition of the Clam Bank Formation (Chapter 2).

The latest Silurian to Early Devonian Clam Bank Formation (Burden et al. 2002) represents renewed sedimentation in the foreland basin. The lowest units exposed are thin beds of red and green calcareous mudstone and siltstone interlayered with non-calcareous siltstone and sandstone. Burden et al. (2002) interpreted these rocks to represent deposition in a shallow-marine to terrestrial environment. A transition to a dominantly terrestrial environment is marked by an unconformity of unknown duration (Burden et al. 2002) which is overlain by a thick siliciclastic succession of medium to coarse-grained sandstone. In Chapter 2, we interpret that 2D seismic profiles demonstrate that the Clam Bank Formation has a constant thickness of approximately 1200 m, filling a basin which lacks the asymmetry that the Middle and Upper Ordovician basins display.

We carried out detrital zircon geochronology on a sample of the Clam Bank Formation (Chapter 4). The probability density function shows a strong 1.1 Ga peak, a spread of ages ranging from 1.3 – 2.0 Ga, and a spread of Archean grains dominated by ages of 2.75 Ga. These results show strong similarities with the underlying Long Point Group leading us to suggest that both groups were derived from a similar source region (Chapter 4).

5.4.1.2. Early Devonian

The Emsian Red Island Road Formation is only exposed on a small island off the coast of western Newfoundland. The unit is interpreted to overlie the Clam Bank Formation, although this contact is nowhere exposed. Rocks of the Red Island Road Formation predominantly comprise cobble to boulder conglomerate interlayered with coarse-grained sandstone.

In Chapter 4 we demonstrate that the Red Island Road Formation has a distinctly different age distribution from all older foreland units. The results (Figure 5.4) show U/Pb ages for 101 zircons within the Red Island Road Formation, 93 of which range from 1.1 – 1.2 Ga, in contrast to older foreland successions with a range of Mesoproterozoic, Paleoproterozoic and Archean ages. We suggest these results to indicate that the Red Island Road Formation was not derived from the same source region as any of the older foreland successions (Chapter 4). This interpretation is consistent with those of Quinn et al. (2004) who also suggested that the abundance of felsic volcanic clasts and unique composition of the sandstone indicates that the Red Island Road Formation was supplied by sources that have not contributed to any older foreland basin deposit. We note strong similarities between spectra of the Red Island Road Formation and the oldest rift-related sediments in the western succession (Figure 5.4) and interpret that this indicates that the Red Island Road Formation had a similar, Grenvillian source.

In Chapter 2, we note that the geometry of the basin which was filled by the Red Island Road Formation could not be determined due to the fact that the upper surface of the Red Island Road Formation is eroded everywhere (Chapter 2). However, we were able to make a minimum thickness estimate of ~670 m for the Red Island Road Formation (Chapter 2), much greater than the previous minimum estimate of 100 m (Quinn et al. 2004).

5.4.1.3. Late Devonian to Permian Maritimes Basin

The Late Devonian to Permian Maritimes basin, extending from Nova Scotia to Newfoundland, overlaps terranes assembled during the earlier orogenies (Waldron et al. 2015) (Figure 5.1). Oldest units within the basin are volcanic and sedimentary rocks and petrological characteristics of these units indicate deposition in a within-plate, rift-related setting (Cormier et al., 1995). In the Late Devonian, major dextral strike-slip motion (up to 250 km) is interpreted to have occurred along major northeast-southwest striking faults in Nova Scotia and Newfoundland (Hibbard and Waldron, 2009). The Maritimes basin has been interpreted as a pull-apart basin, formed by transtension at an oblique releasing bend to these major faults (Waldron et al. 2015).

5.4.2. Québec and New England

5.4.2.1. Silurian to Early Devonian

The Silurian to Devonian foreland basin succession has been largely removed adjacent to the Québec segment of the orogen due to later uplift of the Canadian Shield and Adirondack Mountains. However, Bradley et al. (2000) interpreted the Ludlow through Pragian metasandstone, metapelite, and turbiditic metasediments within the Central Maine Basin (Figure 5.1) as orogen-derived, foreland basin deposits. These units were penetratively deformed and metamorphosed during the Acadian Orogeny. Therefore, few primary structures and fossils survived and the basin was greatly shortened and detached from its depositional basement (Bradley et al. 2000). Farther south, in New York, the Late Ordovician to Early Silurian Cherokee unconformity bounds the base of a thin Early Silurian clastic wedge, the Llandoverly Medina Group, which unconformably overlies siliclastics of the Queenston Formation. Only the most distal portions of the clastic wedge are preserved in the northern Appalachians, reaching a maximum thickness of only 25 m (Ettensohn 2004).

5.4.2.2. Devonian to Mississippian

The Catskill complex in New England (Figure 5.1) is a delta-complex clastic wedge containing conglomerate, sandstone, shale, and lesser carbonate units. The complex comprises multiple sequences of cratonward migrating limestone, shale and coarse siliciclastic flysch which were deposited from the Early Devonian (Pragian) through to the Early Mississippian (Tournaisian) (Ettensohn 2004). Although the Catskill succession does not extend into Canada, Bradley et al. (2000) interpreted that the presence of Devonian limestone, sandstone, and siltstone clasts within a Cretaceous breccia near Montreal indicate that the basin may have extended as far as Montreal, Québec. McLennan et al. (2001) carried out U/Pb analyses of detrital zircons from the Frasnian (Klapper & Kirchgasser 2016) Sonyea Formation of the Catskill succession. The age spectra show a strong peak at ~ 1.0 Ga and another tight grouping of magmatic zircons at 419 – 467 Ma (Figure 5.6).

5.5. Discussion: History of the Laurentian margin

5.5.1. Rifted Margin of Laurentia

Neoproterozoic to Cambrian rifting and break-up of Rodina led to the separation of Laurentia and Gondwana and the formation of the intervening Iapetus Ocean (Cawood et al.

2001). Using available paleomagnetic, stratigraphic, and geochronologic data, Cawood et al. (2001) interpreted that ocean opening involved multiple phases of rifting. Rifting at ~570 Ma led to the initial separation of Laurentia from Gondwana and consequential opening of the Iapetus Ocean.

Following ocean opening, another extensional episode at ~540 – 535 Ma led to the rifting of further blocks into an already open ocean (Cawood et al. 2001). As a consequence, a seaway was generated, the Taconic Seaway, into which the earliest rift-related sediments exposed in Newfoundland were deposited (Waldron & van Staal 2001, Allen et al. 2010). In Newfoundland, the Dashwoods block (Figure 5.1 and 5.5) has been interpreted by Waldron & van Staal (2001) to represent one of these off-margin blocks because its later Taconian deformation began well before the shelf succession was affected (see below). In the Dashwoods block, Precambrian xenocrystic zircons and high negative ϵ_{Nd} values within the 489 – 477 Ma Notre Dame arc (Figure 5.5) (Whalen et al. 1997), confirm the presence of Laurentian crust at depth (van Staal et al. 2007). In order to determine the age of Laurentian crust, we plot (in figure 5.4) U/Pb ages of magmatic cores from inherited zircons within the Notre Dame plutonic suite, analyzed by van Staal et al. (2007). The age spectrum demonstrates a predominant Mesoproterozoic population (Figure 5.4). We interpret that this might indicate that the basement underlying Dashwoods is an extension of the Grenville Province (Figure 5.2). This interpretation is consistent with observations by van Staal et al. (2007) who interpreted that the Cape Ray granodiorite of the Notre Dame arc has geochemical and isotopic characteristics which resemble Grenvillian orthogneisses, likely resulting from high-percentage crustal partial melts of Grenvillian basement.

Whether other Laurentian massifs, exposed elsewhere in the peri-Laurentian realm (Figure 5.1), were ever severed from the Laurentian margin remains a controversial question. For example, the Chain Lakes massif in Québec and Maine (Figure 5.1 and 2.9) has held a somewhat enigmatic position in tectonic reconstructions of the margin, with some authors placing the massif as an autochthonous piece of Laurentia (Trzcinski et al. 1992) and others placing it off margin, representing a portion of a larger microcontinent (Boone & Boudette 1989) or sedimentary succession deposited close to an off margin block (Gerbi et al. 2006). Although basement is nowhere exposed in the massif, earlier seismic studies by Stewart et al. (1993) and Spencer et al. (1989) both infer that Grenville basement underlies the Chain Lakes massif. We argue in a later section that, like the Dashwoods block, this massif was affected by Taconian deformation well before the adjacent continental margin and therefore also represents an off-margin Grenvillian block. We also infer that the Chain Lakes block extended significantly beyond present exposure, as ophiolites farther north in Québec show evidence, from intrusions,

of emplacement above Laurentian crust (Pinet & Tremblay 1995, De Souza et al. 2012) well before Taconian deformation of the adjacent margin.

Farther south, in Vermont, Macdonald et al. (2014) also presented a case for the presence of a peri-Laurentian microcontinent outboard of the Laurentian margin in New England. They interpreted that the Rowe belt and allochthonous Grenville basement together formed a peri-Laurentian microcontinent, analogous to the Dashwoods block in Newfoundland (Macdonald et al. 2014). We interpret that the Chester Dome exposes this allochthonous basement and may represent the southern extension of the Chain Lakes block. Grenvillian units of the Mount Holly Complex (Karabinos et al. 1999) are exposed in the Chester Dome, the only massif where basement is exposed. Using the available stratigraphic, geochronologic, geochemical, and seismic evidence presented above, we suggest that the peri-Laurentian realm of the northern Appalachians (Figure 5.1) is an eastward extension of the Grenville Province (Figure 5.2).

5.5.2. Provenance of Eastern Laurentian Continental Margin in Newfoundland

Contrasts in the detrital zircon populations (Figure 5.4) recovered from the autochthonous rift and shelf, the Humber Arm Allochthon, and metamorphic rocks of the Fleur de Lys Supergroup, suggest that two distinct provenance domains are present in the clastic rift-to-drift rocks of western Newfoundland. A “western succession” comprises the Labrador Group and its off-margin equivalents in lower thrust sheets of the Humber Arm Allochthon (Bradore and Summerside formations). An “eastern succession” occurs in higher thrust sheets of the Humber Arm Allochthon (Blow Me Down Brook Formation) and in the Fleur de Lys Supergroup.

5.5.2.1. Western Succession: A Local Laurentian Source

In the western succession, the Bradore and Summerside formations are the oldest units. Samples collected by Cawood and Nemchin (2001) and Allen (2009) near the base of the Bradore Formation (Figure 5.4) display a conspicuously narrow age spectrum with a single peak at 1.1 Ga suggesting derivation from a localized source (Cawood & Nemchin 2001) in the immediate basement of the Grenville Orogen. Samples from the base of the Summerside Formation (Figure 5.3), representing distal equivalents of the Bradore Formation (Palmer et al. 2001), display remarkably similar age spectra (Figure 5.4). This restricted range of ages can be explained by their tectonic environment. During the earliest phases of rifting, the basement would have been segmented into smaller, restricted basins and detritus was likely sourced locally from the shoulders of uplifted basement blocks into adjacent grabens. Basins would be compartmentalized and axial flow would have been restricted by cross-over zones, isolating smaller basins within the rift system (Gawthorpe & Leeder 2000).

The top of the Bradore Formation, sampled by Allen (2009), also displays a relatively restricted spectrum, but contains older Mesoproterozoic ages (Figure 5.4), consistent with derivation from a somewhat wider area such as the Long Range Inlier in NW Newfoundland (Figure 5.5). Up-section within the Summerside Formation, however, the age spectrum broadens significantly (Figure 5.4). Mesoproterozoic peaks are stronger and Paleoproterozoic and Archean peaks occur that have no equivalents in spectra from stratigraphically lower units. The spectrum of Proterozoic and Archean grains is typical of sediments derived from the Laurentian interior and the overall upward increase in the diversity of provenance likely reflects the transition to an open-system rift-basin (Gawthorpe & Leeder 2000) where smaller compartments became connected.

The age spectra for the Hawke Bay and Irishtown formations (Figure 5.3) in the overlying passive margin demonstrate an even broader range of ages relative to those of underlying synrift-sediments (Figure 5.4). A huge influx of Paleoproterozoic grains at 1.85 Ga in both units cannot be explained by derivation from any older unit within the western succession, and must therefore have been derived from the Laurentian interior. These observations are consistent with the evolution of the basin from rift to passive margin; the basin was now open to detrital debris sourced from a wide area of Laurentia by large river systems and distributed by coastal and shelf sediment-transport processes.

Within early rift and passive margin units in Québec and New England, the predominance of Mesoproterozoic zircons and the scarcity of Paleoproterozoic grains require that these units, farther south, were disconnected from the Newfoundland segment of the margin which contains a much broader range of ages. This likely resulted from large offset of the rift system along a major northwest striking transfer fault (in inset of Figure 5.2) predicted in models of the early rifted margin (Thomas 1977, Allen et al. 2010). The predominance of Grenville zircons in the Québec segment also requires that the drainage systems supplying the rift did not extend into the Archean and Proterozoic units farther west in the Laurentian interior. This suggests that the Grenville Province formed a major topographic high, a result of thermal uplift of the rift margin.

5.5.2.2. Eastern Succession: Greenland Sources?

The Blow Me Down Brook, South Brook and Flat Point formations of the eastern succession were deposited farthest from the Laurentian margin. Unlike the rift units in the western succession, which predominantly contain Grenvillian zircons, the eastern succession (Figure 5.4) is dominated by Paleoproterozoic and Neoproterozoic detritus with prominent peaks at 1.85, 1.90 and 2.6 – 2.8 Ga resembling those of the younger passive margin in the western succession. The Laurentian interior west of the basin is an unlikely source, because Archean and Paleoproterozoic grains would have had to bypass the western rift succession on route to the

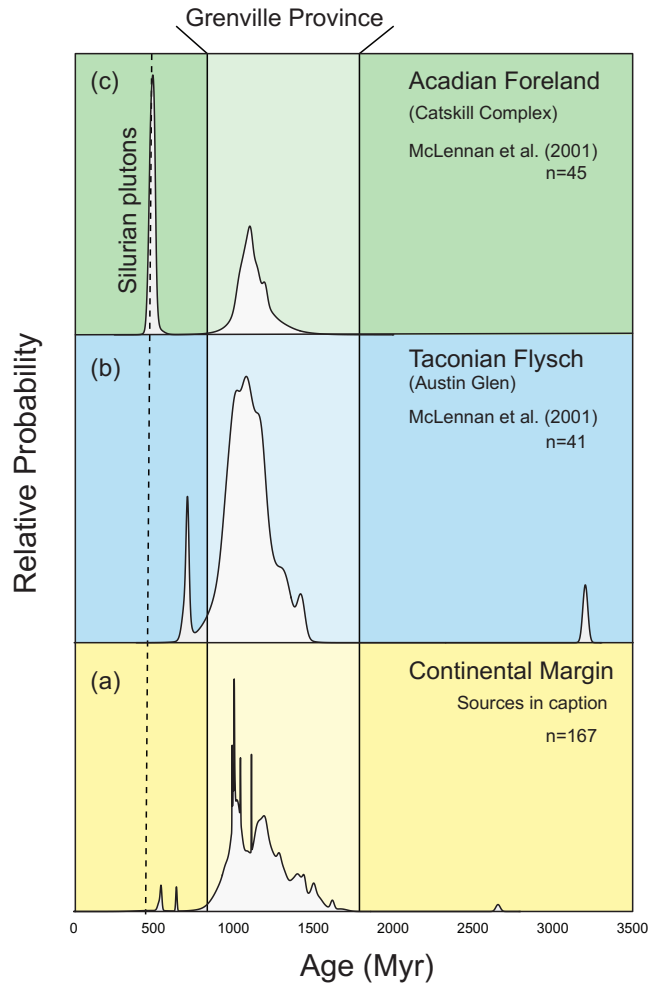


Figure 5.6: Detrital zircon probability density functions for units along the eastern Laurentian margin in Quebec and New England. (a) Rift and passive margin units (McDaniel et al. 1997, Karabinos et al. 1999b, McLennan et al. 2001, Macdonald et al. 2014) (b) Austin Glen Formation (McLennan et al. 2001) (c) Sonyea Formation of Catskills Complex (McLennan et al. 2001).

eastern part of the basin. This observation supports the theory of a Grenville topographic high, blocking eastward transport of Paleoproterozoic and Archean detritus. Other potential sources include: (a) the conjugate margin (Dashwoods block) to the east, (b) the reworked rift-succession to the south, or (c) the North Atlantic Craton and Ketilidian Orogen to the north (Figure 5.2).

- a) Dashwoods block: Models of the Neoproterozoic to Cambrian rift system (Thomas & Astini 1999, Allen et al. 2010) imply that the Dashwoods block is the upper, topographically elevated plate in an asymmetric rift system, which could easily have been eroded by drainage systems into the eastern basin (Figure 5.2, inset 1). Although basement is nowhere exposed in the Dashwoods block, inherited zircons within igneous units of the Notre Dame intrusive suite (van Staal et al. 2007) are predominantly Mesoproterozoic, with a minor proportion of Archean grains. The complete lack of Paleoproterozoic grains implies that, although the Dashwoods block may have contributed to the basin, it cannot have been the only source.
- b) Detrital zircon geochronology results from the earliest rift and passive margin units in New England lack Paleoproterozoic material and demonstrate predominantly Mesoproterozoic signatures (Figure 5.4, inset) indicating derivation almost entirely from the Grenville Province (McDaniel et al. 1997, McLennan et al. 2001, Montario & Garver 2009). It is therefore unlikely detritus was sourced from the south (Figure 5.2, inset 1).
- c) Derivation from the north could account for a wider range of ages in the spectra. The ~ 1.8-1.9 Ga Makkovik and/or Ketilidian orogens of Labrador and Greenland (LaFlamme et al. 2013) could have provided Paleoproterozoic detritus. Archean detritus, dominated by 2.7 and 2.8 Ga ages, could have been derived from the North Atlantic Craton. Although Grenville-age intrusions are also found to the north, a large portion of the northern Grenville Province is dominated by 1.4 and 1.6 Ga units of the Pinwarian and Labradorian orogens respectively (Heaman et al. 2002) and could have sourced the eastern units. The probability density functions of the eastern successions in Newfoundland strikingly resemble those of the Laurentian rift and passive margin sequences preserved in eastern Greenland and Scotland (Figure 5.4, inset). Cawood et al. (2007a) carried out detrital zircon analyses on the Ardvreck Group in northwest Scotland and the Zebra Series in northeast Greenland and the spectra are dominated by Paleoproterozoic ages, between 1.85 and 1.95 Ga (Figure 5.4, inset).

In conclusion, the eastern succession was most likely sourced from parts of Laurentia that lay well to the north of its current position in Newfoundland (Figure 5.2). Two possibilities can be envisaged for their southward transport: (i) sediments were transported southwards during Neoproterozoic and early Cambrian rifting along the axis of the rift (Figure 5.2, inset 1); or (ii) the eastern succession was tectonically transported southward during Taconian or later tectonic interactions. Notably, Waldron et al. (2015) envisage major dextral strike-slip along the margin during the late Paleozoic which would have transported eastern parts of the orogen southward relative to Laurentia. The roles of south-directed axial flow versus later tectonic transport cannot be resolved with the data in this study.

Newfoundland thus appears to lie at a critical juncture on the eastern Laurentian margin. South of Newfoundland, early Paleozoic units of the Laurentian margin are dominated by Mesoproterozoic detritus with strong peaks at ~1.1 Ga; Paleoproterozoic peaks at 1.85 Ga are weak or absent. However, north of Newfoundland, in Greenland and Scotland, the margin displays prominent 1.85 Ga peaks indicating sources in the Ketilidian or related Paleoproterozoic orogens. In Newfoundland, the western succession shows strong similarities with the Québec and New England Laurentian margin; whereas the eastern succession displays strong similarities with the Laurentian margin in Greenland and Scotland. These observations are a direct consequence of the inherited rifted margin (Figure 5.2, inset 1).

5.5.3. Taconian Arc-Continent Collision along the Margin

5.5.3.1. Collision with off-margin peri-Laurentian blocks

5.5.3.1.1. Newfoundland

The first evidence for tectonism along the Laurentian margin in Newfoundland is recorded by metamorphic and igneous rocks in the Dashwoods and Notre Dame subzones (Waldron & van Staal 2001) (Figure 5.5). In these regions, the Laurentian margin (Fleur des Lys Supergroup) was deformed, metamorphosed, and overthrust by the Lush's Bight ophiolite in the Cambrian Period prior to 488 Ma, the age of cross-cutting igneous units of the Notre Dame arc (Figure 5.5) (Waldron & van Staal 2001). Because of the persistence of the passive margin to the west until the end of the Early Ordovician (Figure 5.3), this Cambrian deformation must have involved an offshore microcontinent, the Dashwoods block, separate from the main Laurentian margin (Waldron & van Staal 2001). Waldron and van Staal (2001) interpreted that these earliest interactions took place at an east-dipping subduction zone, at which the Dashwoods block was partially subducted, resulting in westward transport and obduction of ophiolites.

5.5.3.1.2. *Québec and Maine*

In the Québec reentrant, initial collision, involving the obduction of ophiolites (e.g. Thetford Mines and Lac Brompton ophiolites) onto Laurentian crust, occurred between 479 and 472 Ma (Pinet & Tremblay 1995). The timing is constrained by U/Pb zircon ages of cross-cutting peridotite-hosted granites which are interpreted to have formed by anatectic melting of Laurentian crust beneath the ophiolites (Tremblay et al. 2011, De Souza et al. 2012). An $^{40}\text{Ar}/^{39}\text{Ar}$ muscovite cooling age of 475 Ma from similar granitoids cross-cutting the Nadeau Ophiolite, farther north on the Gaspé Peninsula, also indicates obduction onto Laurentian crust prior to 475 Ma (De Souza et al. 2012). The oldest deep-water flysch sediments in this part of the margin, the Darriwilian Tourelle Formation (Figure 5.3), were deposited conformably on deep-water shales of the Cap des Rosiers Group (Hiscott 1978) in the middle Darriwilian, indicating that a seaway between the obducting ophiolites and Laurentian margin existed until at least 465 Ma. A stable passive margin persisted to the west until at least ~ 463 Ma (the age of the youngest Beekmantown Group, figure 5.3; Salad Hersi et al. 2003) and possibly until ~456 Ma (top of the Chazy Formation, figure 5.3). We suggest that these observations indicate that early deformation, associated with ophiolite obduction in southern Québec and Gaspé, occurred on an off-margin block, separated from the Laurentian craton by a seaway.

East of the Baie Vert-Brompton line, at the border between Québec and Maine, the 484 – 477 Ma arc-related Boil Mountain ophiolite (Moench & Aleinikoff 2003) shows strong similarities in age and geochemistry with the southern Québec ophiolites (Tremblay & Pinet 2016). Tremblay & Pinet (2016) note that these similarities, and lack of evidence of a suture between both complexes, suggest that the ophiolites are part of the same oceanic domain. We agree with the interpretations of Tremblay & Pinet (2016) that this domain was rooted east of the Laurentian Chain Lakes massif and was obducted as a large oceanic slab; however, we suggest it obducted on an extensive off- margin microcontinent, the Chain Lakes block. In this interpretation, we suggest that the Chain Lakes block, like the Dashwoods, was partially subducted in this east-dipping subduction zone while ophiolites were transported westward across the Laurentian microcontinent. In southern Québec, obduction and transport has been interpreted to last ~ 20 Myrs, from ~ 480 – 460 Ma (Tremblay & Pinet 2016).

5.5.3.1.3. *New England*

In New England, the earliest Taconian orogenic episode has been interpreted to involve the collision of the Shelburne Falls arc with the Laurentian margin at ~475 Ma (Karabinos et al. 1998). This early arc has also been interpreted to have formed above an east-dipping subduction zone, similar to the earliest arc-related rocks and suprasubduction ophiolites preserved in

Québec and Newfoundland. More recently, Macdonald et al. (2014) have demonstrated, using detrital zircon geochronology, that the Shelburne Falls arc was formed on a rifted fragment of Gondwanan crust. Collision of Laurentia with this Gondwanan terrane, termed the Moretown terrane, is constrained at ~ 475 Ma by the arrival of Laurentian detritus across the Laurentian-Gondwanan suture (Macdonald et al. 2014). The authors interpreted that this collision involved the partial eastward subduction of a peri-Laurentian fragment under the Gondwanan Moretown terrane. We agree with these interpretations and suggest this microcontinent (part of the Chain Lakes block) is now exposed in the Chester Dome (Figure 3.1b). We also infer that the Taconic Seaway remained opened, separating the amalgamated Chain Lakes block and Moretown terranes from the Laurentian margin for at least another 15 Myr. Evidence of a persistent seaway is provided in the Taconic allochthon of New York, where a record of deep-water continental slope sedimentation continues into the Sandbian *Nemagraptus gracilis* zone (Rowley & Kidd 1982), between ~ 456 and 459 Ma using the timescale of Cooper et al. (2012).

5.5.3.1.4. Summary

Thus the earliest indications of Taconian deformation from Newfoundland to Vermont involve off-margin Laurentian crustal fragments. We assign these tentatively to two blocks - the Dashwoods and Chain Lakes blocks - but recognize that they may represent a single ribbon continent. In both the Newfoundland and the Québec – New England segments of the orogen, these blocks were deformed in the earliest stages of the Taconian Orogeny. However, this deformation was strongly diachronous, starting much earlier (>488 Ma) in the Newfoundland segment than further south, where the earliest evidence of arc-continent collision is at ~475 Ma. The nature of the emplaced allochthons also presents an along-strike contrast. In Newfoundland and Québec the over-riding thrust sheets were supra-subduction ophiolites, whereas in southern New England the colliding block appears to have been a Gondwanan microcontinent, the Moretown Terrane (Macdonald et al 2014).

5.5.3.2. Closure of the Humber Seaway

5.5.3.2.1. Newfoundland

After initial arc-continent collision, convergence continued, leading to the progressive destruction of the Taconic Seaway at an east-dipping subduction zone (van Staal et al. 2007). The negatively buoyant oceanic crust underlying the Taconic Seaway was probably most easily subducted at the interface with the buoyant, continental lithosphere (Nikolaeva et al. 2010) of the Dashwoods block to the east, which was already weakened by earlier deformation. This subduction zone led to the generation of Tremadocian juvenile ophiolites and intrusion of

arc granitoids of the (489-477 Ma) Notre Dame Arc into the Dashwoods microcontinent (van Staal et al. 2007). Continued contraction was signalled by the deposition of turbiditic flysch containing ophiolite-derived chromite (Stevens 1970) above cherty shales of the continental slope succession in the earliest Dapingian (~470-469 Ma), and uplift of the adjacent shelf at a peripheral bulge unconformity (Jacobi 1981, Knight et al. 1991) in late Dapingian or earliest Darriwilian time (~467 Ma). Loading of the Laurentian margin activated deep-seated extensional faults observed within the foreland (Chapter 2). This was accompanied by subsidence of the former shelf and accumulation of foreland basin sediments with Darriwilian 1-3 graptolites (~467 - 463 Ma: Goose Tickle Group, figure 5.3). Deformation resulted in assembly of the Humber Arm Allochthon, which carried deep-water slope and rise units, flysch, and ophiolites in a series of thin-skinned thrust slices on top of the Laurentian margin to the west.

5.5.3.2.2. Québec and New England

In Québec, we interpret that closure of the Taconic Seaway did not begin to affect the distal Laurentian margin until the mid-Darriwilian (~465 Ma), the age of both the youngest part of the outer slope succession (Cap des Rosiers Group) and the oldest deep-water flysch unit (Tourelle Formation). The ages of these two units are identical within the resolution of the graptolite biostratigraphy (the overlapping *Holmograptus lentus* and *Didymograptus artus* biozones respectively) (Prave 2000; Maletz 2001) (Figure 5.3). In New England, interpretations regarding closure of the Taconic Seaway are controversial. Macdonald et al. (2017) and Karabinos et al. (2017) interpreted that the seaway closed by ~ 464 Ma. The authors suggested that a 464 Ma volcanic ash within slates of the Indian River Formation (Figure 5.3) was emplaced as a result of explosive eruption following collision and consequential slab break-off of the Laurentian plate. We argue that this interpretation contradicts stratigraphic evidence of a persistent, open seaway. The stratigraphy preserved in the Taconic allochthon indicates that deep-marine, pelagic sedimentation continued until at least 458 Ma, the age of the youngest marine slate, the Mount Merino Formation. Orogen-derived flysch of the Austin Glen Member transitionally overlies upper portions of the Mount Merino slate (Rowley & Kidd 1982); both contain graptolites in the *Nemagraptus gracilis* biozone (Bock et al., 1998) constraining the first appearance of syntectonic sediment to the interval 458-456 Ma (timescale of Cooper et al. (2012)). Conformable stratigraphic relationships indicate that there was no major tectonic disturbance of the seaway prior to flysch sedimentation, which continues into the overlying *Didymograptus multidentis* zone (Rowley & Kidd 1982). We therefore suggest that closure of the seaway, as a result of eastward subduction, began to deform the distal continental margin at ~ 455 Ma.

5.5.3.3. *Allochthon emplacement above the former Laurentian shelf*

5.5.3.3.1. *Newfoundland Pro-arc Basin*

The obduction of material onto the Laurentian margin implies that the Middle Ordovician foreland basin initially formed on the subducting lower plate in front of the arc, as a pro-arc basin. This is consistent with interpretations of White (Chapter 2), who shows that subsidence rates (0.17 – 0.50 km/Myr) match those typical of pro-arc basins (Sinclair & Naylor, 2012). White (Chapter 2) also suggests that the overall eastward thickening trend is consistent with loading by the Taconian orogen in Newfoundland, which was developing east of the basin. The presence of major fault-scarp units within the Middle Ordovician basin indicates that subsidence was controlled by large faults, in addition to distributed flexure resulting from orogenic loading and slab pull (Chapter 2).

The sedimentary fill of the Middle Ordovician basin is generally regarded as orogen-derived, due to the presence of ophiolitic detritus (Stevens 1970). This interpretation is supported by predominant southwest-directed paleocurrents (Quinn 1992) and the spectrum of zircon ages in the Goose Tickle Group (Figure 5.4), attributable to derivation from clastic units within the Humber Arm Allochthon which lay to the east of the Middle Ordovician basin (Chapter 4).

5.5.3.3.2. *Québec and New England Pro-arc basin*

In Québec and New England authors have differed between pro-arc and retro-arc interpretations of the foreland basin developed above the Cambrian to Early Ordovician carbonate platform. Earlier interpretations (i.e. Rowley and Kidd, 1982), largely based on stratigraphic evidence, inferred that the Upper Ordovician basin developed (as a pro-arc basin) on the down-going Laurentian plate as it became involved in east-dipping subduction and arc-continent collision. However, more recent interpretations have largely implied that the Upper Ordovician basin in Québec and New England formed in a retro-arc setting, having formed on the upper plate above a west-dipping subduction zone (e.g. Coakley and Gurnis, 1995; Karabinos et al., 2017, 1998; Macdonald et al., 2017; Bock et al., 1998; Dix et al., 2013).

An initial exposure of the margin is recorded in the foreland by the ~463 Ma Beekmantown unconformity, interpreted as the product of peripheral bulge migration by Jacobi (1981), similar to the interpretation of the St. George unconformity in Newfoundland (Knight et al. 1991). However, Knight et al. (1991) point out that the Dapingian to early Darriwilian timing of this unconformity coincides with a eustatic sea-level low, the Sauk-Tippecanoe boundary of Sloss (1963). In Québec, the top-most Beekmantown contains conodonts indicative of the *E. suecicus* Biozone (Salad Hersi et al. 2003), while the overlying Chazy Group has conodonts

indicative of the *P. serra* Biozone (Bolton 1981). These observations suggest a relatively minor hiatus. Field observations of transitional contacts and boundary-crossing burrows (Salad Hersi et al. 2003) also point towards a relatively minor hiatus consistent with eustatic control. The sub-Black River Group unconformity of Landing (2012), at the base of the overlying Black River – Trenton succession, (Figure 5.3) is much more variable. In the Champlain Valley it removes only a few million years of the record within the Sandbian; however, in the Mohawk Valley it is much more profound, removing much of the Floian to Darriwilian succession (Macdonald et al. 2017). We suggest that this younger unconformity represents the peripheral bulge resulting from arc-continent collision in Québec and New England. An overlying deep-water shale and flysch basin is recorded by the Utica, Lorraine, and Sainte-Rosalie succession in Québec and the Utica, Schenectady, and Frankfort succession in New England (Figure 5.3). Thickness estimates of the early shale and flysch fill in Québec range from 2000 m up to 3500 m. Using the more modest thickness estimates of 2000 m and total depositional time of ~ 8 My (Figure 5.3), we interpret sedimentation rates of at least ~ 0.25 km/Myr. Because these units were deposited below sea level above shallow marine carbonates, subsidence rates must have been at least this fast. This rate of subsidence is well above rates predicted for retro-arc basins elsewhere (i.e. > 0.05 km/Myr; Sinclair & Naylor, 2012). Macdonald et al. (2017) plotted subsidence curves for the successions in the Champlain Valley; their curves demonstrated significant increases in subsidence in the Late Ordovician (at ~ 455 Ma). Although Macdonald et al. (2017) interpreted a retro-arc setting in the Late Ordovician, the subsidence rates of the late Ordovician foreland basins are more consistent with a pro-arc setting. We therefore interpret that the history of arc-continent collision in Québec and New England post-dated that in Newfoundland by approximately 10 Myr, and that the Late Ordovician Utica shale and overlying flysch units represent the foreland basin deposited in a pro-arc setting developed in advance of this collision.

In addition to these timing differences, there are notable along-strike changes in the provenance of foreland basin deposits. Predominantly Mesoproterozoic ages of detrital zircons within earliest allochthonous flysch units in the Taconian Allochthon of New England (Austin Glen Formation) indicate derivation from the local Grenville Province (Bock et al. 1998, McLennan et al. 2001). Provenance work by Bock et al. (1998) demonstrates a conspicuous absence of ophiolitic detritus, which farther north in Québec and Newfoundland is abundant and used as evidence to interpret derivation from ophiolitic allochthons east of the basin. We correlate these differences to along-strike changes in the nature of the colliding block. To the north, in Newfoundland and Québec, earliest interaction involved the obduction and transport of ophiolites westward across a partially subducted Laurentian block. In southern New England,

the earliest collision was between the Gondwanan Moretown terrane and the Chain Lakes block, explaining the absence of ophiolitic detritus from the Taconic flysch.

5.5.4. Subduction Polarity Reversal

5.5.4.1. Newfoundland

During the collision of the Dashwoods block and closure of the Taconic Seaway, a west-dipping subduction zone formed outboard of the Dashwoods block, as recorded by the (471-459 Ma) Annieopsquotch Accretionary Tract to the southeast (van Staal et al. 2009, Zagorevski et al. 2009), as a result of slowing convergence within the seaway. Slab break-off of the east-dipping Laurentian plate led to the consequential reversal in subduction polarity at the Newfoundland Laurentian margin by ~ 460 Ma (van Staal et al. 2009). This newly developed west-dipping subduction zone led to underthrusting of the peri-Gondwanan Victoria arc beneath the Laurentian margin and formation of the Red Indian Line, identified by Williams et al. (1988) as the boundary between peri- Laurentian and peri-Gondwanan terranes in the Newfoundland Appalachians.

The Late Ordovician Windsor Point Group which unconformably overlies the Notre Dame arc, represents the earliest sediments that were deposited in a fore-arc basin following subduction polarity reversal in Newfoundland (Waldron et al. 2017). The age of this volcanic and sedimentary succession is constrained by the 453 +5/-5 Ma age of a Windsor Point Group rhyolite (Dubé et al. 1996).

5.5.4.2. Québec and New England

In the Québec Embayment, the Ordovician to Devonian Matapédia basin, which unconformably overlies the Taconian thrust belt, began to develop in a fore-arc position following subduction polarity reversal in the Late Ordovician. The oldest strata in this basin (Garin Formation) contain graptolites of the *Climacograptus spiniferus* Biozone (Waldron et al. 2017), the same zone as those in the youngest thrust sheets in the Taconian allochthons below (Cloridorme Formation), effectively constraining subduction polarity reversal between 451 and 450 Ma in the timescale of Cooper et al. (2012). Van Staal et al (2008) reached similar conclusions based on relationships in the peri-Gondwanan Miramichi Terrane to the south. Ongoing subduction led to the eventual accretion of this terrane which includes Laurentia-derived flysch (Tomogonops Formation, < 453 Ma; Wilson et al. 2015). Units of the Miramichi Terrane were partially subducted at the Laurentian margin and metamorphosed at blueschist facies close to the Ordovician-Silurian boundary ~442 Ma (van Staal et al. 2008)

Karabinos et al. (1998) and Moench and Aleinikoff (2003) interpreted that subduction polarity reversal in New England occurred by 454 Ma and 458 Ma respectively, constrained by the age of units within the Bronson Hill Arc, which are interpreted to have formed above a west-dipping subduction zone east of the Shelburne Falls Arc (Karabinos et al. 1998, Moench & Aleinikoff 2003). A more recent study by Dorais et al. (2011) demonstrates that the 450 Ma Oliverian Plutonic Suite, which cross-cuts the 470-460 Ma Ammonoosuc Volcanics (Moench & Aleinikoff 2003) of the Bronson Hill Arc, has Laurentian isotopic signatures, indicating that the arc-related Ammonoosuc volcanics were obducted on top of the Laurentian margin by at least 450 Ma. We suggest that slab break-off of the east-dipping subduction zone and subduction polarity reversal occurred after these units were obducted. The timing of obduction is constrained as sometime between the end of arc magmatism (~460 Ma) and intrusion of the ~450 Ma Oliverian plutonic units. Therefore, in Québec and New England, subduction polarity reversal occurred ~ 10 Myr later than it did in Newfoundland.

5.5.4.3. Retroarc Foreland Basins

5.5.4.3.1. Newfoundland

Subduction polarity reversal by ~460 Ma in Newfoundland led to the deposition of the Upper Ordovician Long Point Group in a retro-arc basin with respect to the newly developed west-dipping subduction system east of the basin. However, White's (Chapter 2) estimate of subsidence rate (~ 0.17 km/Myr) is actually consistent with rates that Sinclair and Naylor (2012) predicted for pro-arc basins. Not only is the estimated subsidence rate inconsistent with development in a retro-arc setting, but the geometry of the Long Point Group is inconsistent with a basin developed by loading along its eastern margin, by the Newfoundland segment of the orogen. Unlike the Goose Tickle Group, which thickens to the east, the Long Point Group demonstrates a dramatic thickening to the south (Chapter 2). White (Chapter 2) interprets that this geometry indicates loading along the southern margin of the basin, in Québec. The interpreted delayed subduction polarity reversal of ~ 10 Myr, by ~450 Ma in the Québec Embayment, is consistent with these observations. We agree that subduction polarity reversal placed the Long Point Group in a retro-arc setting with respect to Newfoundland; however, we suggest that continued loading of the Laurentian plate and eastward subduction in the Québec Embayment until ~ 450 Ma led to a hybrid retro- and pro-arc setting.

Although detrital zircon data indicate that there are similarities between the Long Point Group and older Goose Tickle Group, peak heights notably contrast (Chapter 4). White (Chapter 4) interprets the striking decline in the abundance of 1.85 Ga zircon to reflect a shift in provenance between the Goose Tickle and Long Point groups. Combined with compositional

similarities and unidirectional northeast-directed paleocurrents, these observations suggest that the Long Point Group was derived from the allochthons in Québec, not Newfoundland (Chapter 4).

5.5.5. Salinian Accretion of Ganderia

Polarity reversal in Newfoundland was followed by the arrival and accretion of the first peri-Gondwanan fragment to the Laurentian margin (Zagorevski et al. 2007). Zagorevski et al. (2008) and van Staal et al. (2009) interpreted that the Gondwanan Victoria Arc was underthrust (at the Red Indian Line), beneath the Laurentian margin at ~ 450 Ma. Farther south, in the Québec Embayment, the Popelogan Inlier is interpreted as the first Gondwanan arc to be accreted to the Laurentian margin (van Staal et al. 2016), prior to ~ 448 – 445 Ma, the age of the earliest post-accretion sediments (Wilson et al., 2004). Although timing of accretion is constrained in the Québec Embayment, whether accretion involved obduction on or underthrusting beneath the margin is ambiguous due to significant cover of younger Ordovician through Silurian sediments (Figure 5.1). In New England the first Gondwanan - Laurentian interactions involved the earlier off-margin collision of the Gondwanan Moretown terrane with a Laurentian block (which we term the Chain Lakes block) at ~ 475 Ma (Macdonald et al. 2014).

Following the accretion of the Gondwanan Victoria Arc to Laurentia in Newfoundland, west-dipping subduction of Iapetan oceanic crust continued beneath the margin (van Staal et al. 2009). Waldron et al. (2017) demonstrated that subduction and ocean closure involved the accretion of multiple Ganderian fragments to the composite Laurentian margin during the Katian – Wenlock interval. The last of these collisions in Newfoundland brought the Gander terrane (Figure 5.1) in contact with the margin, closing a remaining tract of the Iapetus Ocean by the Wenlock (Pollock et al. 2007, van Staal et al. 2009). In Newfoundland, the resulting suture has been termed the Dog Bay Line. In New Brunswick, accretion of the last Ganderian fragment occurred with the collision of the St. Croix terrane with the Laurentian margin along the equivalent boundary in New Brunswick; Dokken et al. (in review 2017) argued that the Fredericton Fault, which has a later history of strike slip motion, marks the position of this boundary in Maritime Canada. In New England, the boundary is obscured by Acadian high-grade metamorphism and faulting, though Waldron et al. (2017) suggested that the Clinton-Newbury Fault (Figure 5.1), may represent the position of the equivalent boundary. Following accretion of the final Ganderian fragment to the Laurentian margin, break-off of the west-dipping subducting slab occurred, likely resulting from a decreased subduction rate as buoyant continental crust entered the subduction zone. Whalen et al. (2006) used temporal and compositional variations in magmatism to constrain break-off at ~ 433 – 425 Ma.

5.5.5.1. Salinian Retro-arc Basin

The foreland basin continued to develop in a retro-arc setting intermittently in the Newfoundland sector due to west-dipping subduction along the length of the northern Appalachian margin (Chapter 2). However, an extensive hiatus from the Late Ordovician to latest Silurian (Clam Bank unconformity) indicates that a retro-arc succession associated with Salinian Orogenesis is not preserved in Newfoundland. We interpret that the Clam Bank unconformity (~423 Ma) likely represents a period of uplift and erosion following break-off of the westward subducting Iapetan crust.

The foreland basin succession has also been largely removed adjacent to the Québec segment of the orogen due to later uplift of the Canadian Shield and Adirondack Mountains. Only a thin succession (Medina Group) of Llandovery foreland basin rocks is preserved south of the Adirondacks, and provides little evidence of the retro-arc foreland basin. Meanwhile, a substantial forearc basin (Central Maine Trough) developed above Ganderian fragments accreted by west-dipping subduction from Late Ordovician to Wenlock time (Waldron et al. (2017) in press and references therein.)

5.5.6. Acadian Collision of Avalonia

Accretion of Ganderia and slab break-off was followed by a stepping back of the west-dipping subduction zone and arrival of Avalonia at the composite Laurentian margin (Bird & Dewey 1970, Bradley 1983, van Staal et al. 2009). These events led to the Acadian Orogeny which, in Newfoundland, began at ~ 420 Ma and continued until ~ 400 Ma (van Staal et al. 2009); in Québec however, Bradley et al. (2000) interpreted that deformation and magmatism associated with Acadian orogenesis continued until at least the Late Devonian, until ~ 380 Ma, progressively younging towards the west.

5.5.6.1. The Acadian Structural Front

In western Newfoundland, White (Chapter 3) demonstrates that the Acadian thrust front marks a deep-seated basement-involved feature, inverted along its length in the Early Devonian, but reactivating earlier structures formed during earlier Middle Ordovician Taconian extension and even Neoproterozoic rifting. White (Chapter 3) demonstrates that inversion along these faults generated basement-cored fault-propagation folds, defined by steep to overturned forelimbs and broad shallow-dipping to subhorizontal backlimbs. Major basement massifs in western Newfoundland, including the Long Range Inlier, represent the present day exposures of these anitformal cores above which the passive margin succession has been eroded. These structures, although geographically disconnected in western Newfoundland, form a genetically

linked network of basement thrust faults that are responsible for the distinct present-day distribution of rock units in the Humber Zone of western Newfoundland, where platform rocks appear east of the Humber Arm Allochthon everywhere.

Structurally analogous features in Québec and New England may be genetically linked to those in Newfoundland, and represent the southern extension of the Acadian thrust front (Chapter 3). For example, the Taconic Frontal Thrust in the Champlain Valley is an out-of-sequence thrust that places shelf rocks above and along the eastern margin of the Taconian allochthon (Hayman & Kidd 2002). The large-scale structure of Mesoproterozoic inliers in Vermont and Massachusetts also have strong similarities with the structural framework observed in Newfoundland (Chapter 3). Here antiformal domes, including the Green Mountain and Berkshire inliers (Figure 5.1), expose Grenvillian basement cores which are unconformably overlain by rift and shelf successions and have been structurally uplifted along the eastern margin of Taconian allochthons (Hibbard et al. 2006). These observations led White (Chapter 3) to interpret that these structures are genetically linked and form an extensive, deep-seated Acadian thrust front at the boundary between basement massifs and antiformal domes (Green Mountain and Sutton Mountain anticlines) of parautochthonous platform and Taconian allochthons, that inverts earlier structures along the length of the entire northern Appalachians (Figure 3.1b).

Bradley et al. (2000) have interpreted the position and relative timing of the Acadian deformation front in Maine and Québec, demonstrating a northwestward migration of deformation during Acadian orogenesis. The authors demonstrated latest deformation associated with Acadian Orogenesis was during Frasian time and suggested that the final northwest limit of Acadian shortening may have reached as far as the Paleozoic thrust front of the orogen (Bradley et al. 2000). We therefore interpret that activation (and possibly inversion) of the deep-seated Acadian Thrust Front in Québec and New England occurred during or shortly after the Frasian.

5.5.6.2. *Acadian Retro-arc Basin*

The (~ 423 – 430 Ma) Clam Bank Formation was deposited during the waning stages of (440 – 420 Ma) Salinian Orogenesis (Dunning et al. 1990, van Staal et al. 2014), and during the early part of the (420 – 400 Ma) Acadian Orogeny (van Staal et al. 2014). This timing indicates that the succession likely represents the early Acadian retro-arc basin fill in Newfoundland (Chapter 2). The Emsian Red Island Road Formation, overlying the Clam Bank Formation, overlaps in time with Acadian orogenesis, and represents the younger (dominantly terrestrial) portion of the Acadian retro-arc foreland succession. The absence of Gondwanan zircons within the Clam Bank – Red Island Road succession is likely due to the fact that, during both Salinian and Acadian orogenesis, Ganderia and Avalonia were both underthrust beneath the Laurentian margin (Chapter 4).

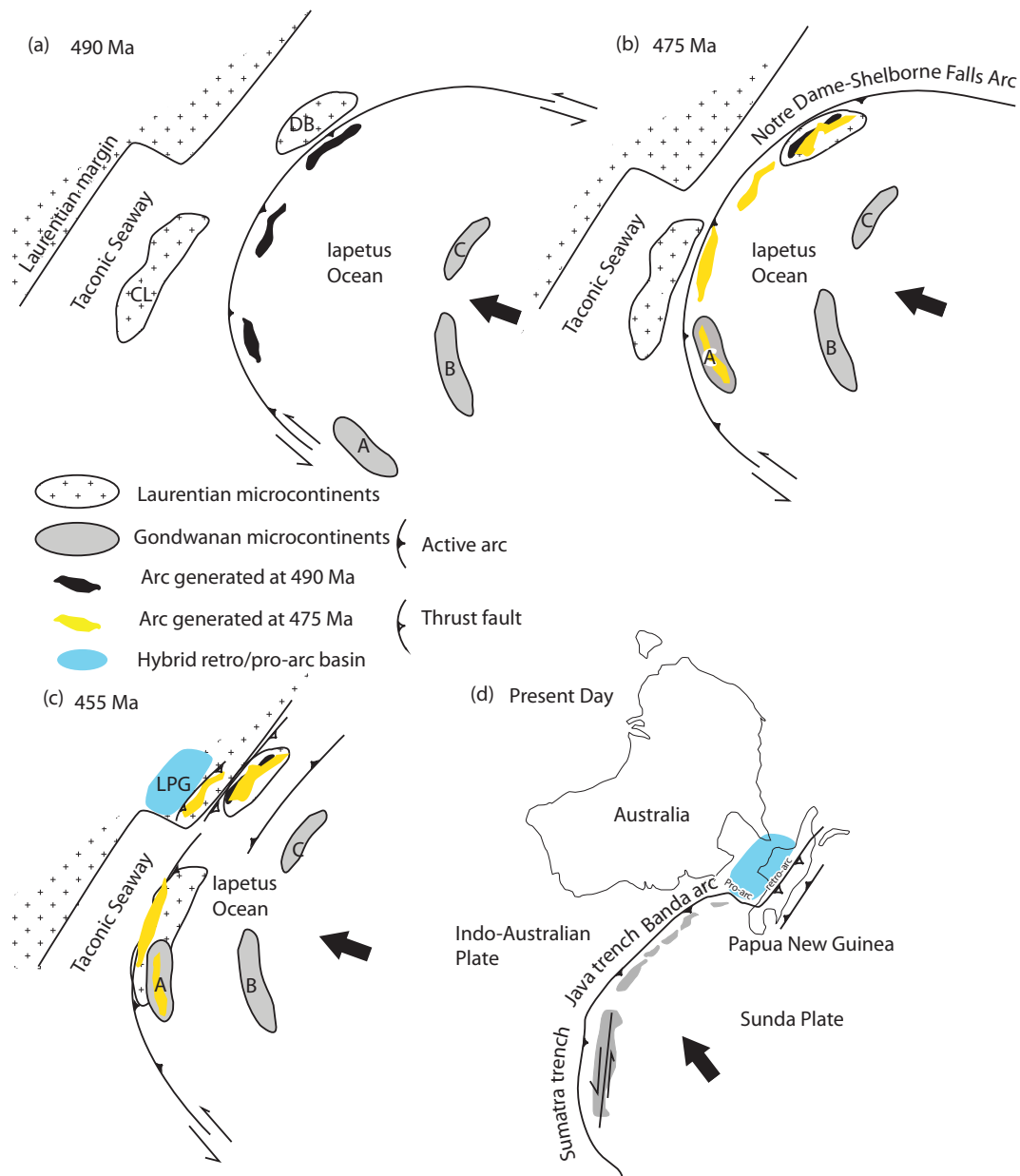


Figure 5.7: Schematic diagram demonstrating how inherited shape of rifted margin and arc cause diachronous collision along a cratons margin at various times. A, B and C are Gondwanan microcontinents. (a) (490 Ma) Earliest arc-continent collision occurs on an off-margin block DB (Dashwoods Block) at the promontory. (b) (475 Ma) Later arc-continent collision occurred at off-margin block CL (Chain Lakes Block) at the embayment while the Dashwoods Block (DB) is already colliding with the promontory. (c) (455 Ma) Subduction polarity reversal at the promontory (beneath the craton) and continued craton subduction at the embayment. The Long Point Group (LPG) is in a hybrid retro/pro-arc setting. (d) Reflected and rotated image of northern margin of Australia showing present day tectonic configuration which is similar to (c), the Late Ordovician eastern Laurentian configuration. The basin forming on the Australian plate is also in a hybrid retro/pro-arc setting.

The Clam Bank – Red Island Road retro-arc succession transitions from shallow-marine to dominantly terrestrial, indicating the basin was in an overfilled stage, where sediment supply outpaced accommodation. Slow subsidence and/or rapid supply could account for the observed facies. The constant thickness (i.e., lack of asymmetry) observed indicates that the Clam Bank Formation was deposited as an extensive siliciclastic blanket. Together, the geometry and facies imply the basin was broad and shallow. We explain these observations by recognizing that, by the time the Clam Bank – Red Island Road retro-arc basin formed, the lithosphere below the basin was likely cooler and stronger than it was in the Ordovician, the orogenic load was spread out over a great area, and the locus of tectonism was far removed from the developing basin (Chapter 2).

In Québec and Maine, where Acadian orogenesis continued until ~ 380 Ma, Bradley et al. (2000) demonstrated that an early Ludlow to early Givetian foreland succession, preserved within the Central Maine Basin, represents the Acadian retro-arc succession. In New York, the Pragian to Tournaisian Catskill clastic wedge (Figure 5.1) is considered the Acadian foreland retro-arc succession (Ettensohn 2004). Bradley et al. (2000) demonstrated that the Acadian foreland basin, like the deformation front, has a much more protracted history than observed in Newfoundland and migrated northward during deposition from the early Ludlow to at least the early Givetian. Farther south, in New York, Ettensohn (2004) noted a similar protracted history of deposition and cratonward migration of the Catskill clastic wedge; deposition of these clastics began in the Pragian and continued until the Tournaisian. These ages clearly demonstrate an along-orogen younging trend of deposition and deformation towards the south, a feature recognized by Ettensohn (2004).

5.5.6.3. Record of Acadian Inversion in the Foreland Basins

In Newfoundland, White (Chapter 3) interprets the predominance of Mesoproterozoic zircons within the Acadian Red Island Road succession to indicate derivation from Grenvillian basement uplifted during Early Devonian (Emsian) inversion, or reactivation by thrusting along earlier formed normal faults, along the deep-seated Acadian structural front.

McLennan et al. (2001) demonstrated the age spectra of detrital zircons from the Frasnian (Klapper & Kirchgasser 2016) Sonyea Formation of the Catskill succession and suggested that the strong Mesoproterozoic signature indicates derivation from a proximal Grenville source to the southeast (Figure 5.6). This observation agrees with previous work which demonstrates that these sediments coarsen and thicken to the east and that paleoflow was directed westward (Allen and Friend, 1969; Rickard 1975). We suggest that the Berkshire inlier, a Grenville massif intruded by Paleozoic granite sills dated at ~ 430 to 435 Ma (Karabinos et al. 2008), is the likely source of the detritus in this upper Devonian succession. The age of deposition (Frasian) of this

portion of the Catskill succession is coeval with our interpreted time of uplift and inversion of basement massifs along the Acadian structural front in New England.

5.5.7. Diachronism in Collisions

Much of the previous work in Appalachian orogenesis has been related to grouping deformation events into distinct orogenic episodes. Deformation in the Appalachians has typically been illustrated with two dimensional models, or cross-sections, showing the history of collisions in time. Such models, though valuable, encourage the perception that orogenesis occurred in discrete episodes of deformation that punctuated steady-state margin evolution. In contrast, the history outlined above is one of almost continuous deformation somewhere on the Laurentian margin from late Cambrian to Late Devonian. All the major episodes of deformation affecting the northern Laurentian margin – Taconian, Salinian and Acadian – have been shown to be diachronous. Three possible sources of this diachronism can be envisaged: the irregularity of the main Laurentian margin; the distribution of off-margin microcontinents; and the geometry of arcs and microcontinents on the colliding plate.

5.5.7.1. Inherited Rifted Margin: North Australian Margin as an Analog

Diachroneity in collisions along the Laurentian margin has long been recognized to result from the irregular margin shape, inherited from Neoproterozoic to Cambrian rifting (Thomas 1977, Allen et al. 2010). Many authors recognize earlier collisions on the St. Lawrence Promontory in Newfoundland, followed by the southward progression of deformation in the Québec Embayment during various episodes of Appalachian orogenesis (Bradley 1983, Malo et al. 1995, Bradley et al. 2000, Tremblay et al. 2000, Pincivy et al. 2003, Ettensohn 2004).

The combined retro and pro-arc setting of the Long Point Group (Figure 5.7c) is interpreted as a consequence of the irregular margin shape (Figure 5.7c) and is analogous to the present day plate boundary configuration along the northern Australian Plate near Papua New Guinea (Figure 5.7d). Figure 5.7d demonstrates that the northwestern margin of the Australian plate resembles a mirror image of the Laurentian margin (Figure 5.7c) and that the present tectonic configuration along this portion of the margin is much like that proposed for the Late Ordovician in Newfoundland (Figure 5.7c and 2.9c). The following points compare the more recent geologic history of the northern Australian margin to the Ordovician history of the eastern Laurentian margin.

Upper Cretaceous ophiolites (Papuan ultramafic belt) preserved along the central portion of Papua New Guinea (Figure 5.7d) were obducted onto the Australian margin shortly after their generation, during the Late Paleocene to earliest Eocene (Lus et al. 2004). These ophiolites are analogous to the Early Ordovician Bay of Islands ophiolites in Newfoundland which were

obducted onto the Laurentian margin during Middle Ordovician Taconian orogenesis. Ophiolite obduction occurred first at the promontory along both the Laurentian and Australian margins (Figure 5.7a). This led to the development of the foreland basin in a pro-arc setting, on top of the subducting Laurentian and Australian plates (Figure 5.7b).

Following ophiolite obduction onto the Australian margin, subduction polarity reversed along the New Guinea Trench. This reversal, occurring first at the promontory, led to south-dipping subduction beneath the Australian plate which continues today (Figure 5.7d). Analogously, Late Ordovician subduction polarity reversal in Newfoundland occurred following ophiolite obduction onto the Laurentian promontory and led to subduction beneath the Laurentian Craton (Figure 5.7d). Polarity reversal and subduction beneath the cratons led to the transition of the foreland from a pro-arc to retro-arc basin on both the Australian and Laurentian plates.

Along the north Australian embayment (Figure 5.7d) however, active arc-continent collision is occurring as the Banda arc is being thrust above the Australian continent via north-dipping subduction. This configuration, of subduction beneath the craton at the promontory and subduction of the craton at the embayment, is exactly the model we propose in Newfoundland during the Late Ordovician. This delay in subduction polarity reversal at the embayment allows for the unique hybrid basin setting interpreted for the Upper Ordovician Long Point Group and the current foreland basin in Australia (Figure 5.7c, d).

5.5.7.2. Other Variables

The more recent recognition of off-margin microcontinents (Waldron & van Staal 2001, Macdonald et al. 2014) complicates this picture. The off-margin position of the Dashwoods microcontinent accounts for the earliest arc-continent collision in the Canadian Appalachians (Figure 5.7a). Figure 5.7a shows the earliest collision of the Dashwoods with an arc at the promontory. Similar, off-margin microcontinents in Québec and New England account for arc-continent collisions during continued passive margin development farther west within a protected seaway. Figure 5.7b demonstrates later (than at the promontory) arc-continent collision at the Chain Lakes block in the embayment while the seaway persisted between the Chain Lakes block and the craton.

Another reason for diachroneity in collisions along the Laurentian margin may have been the shape of the colliding arc (e.g. Figure 5.7d). If the earliest Notre Dame-Shelborne Falls arc (Figure 5.7b) were straight, the irregular margin shape would only explain the observed north to south progression of deformation but would not explain the earliest (475 Ma) arc-continent

collision in New England involving a peri-Gondwanan arc. Figure 5.7a shows a possible configuration of 3 microcontinents (A, B and C) which have been severed from Gondwana and are travelling across the Iapetus Ocean towards an active arc. Near the center of the arc, where curvature reaches a maximum, motion of the overriding plate is approximately normal to the arc. However, along the north and south segments of the arc, motion is oblique. Gondwanan fragment A is transported in an overall sinistral sense across the ocean while B and C move normal towards the arc. Gondwana A (Moretown Terrane) arrives and collides with Laurentia (Chain Lakes block) well in advance of Gondwanan fragments B and C (Ganderia) (Figure 5.7c), closing a small tract of the otherwise still open Iapetus Ocean. The plate motion described is much like the present-day plate motion of the Sunda Plate relative to the Java and Sumatra portions of the arc (Figure 5.7d). The Sunda plate moves normal to the Java trench (Diament et al. 1992), while oblique convergence between the Indo-Australian and Sunda plates near Sumatra leads to subduction along the trench and upper plate strike-slip faulting on the Sumatran fault zone (Bradley et al. 2017).

5.6. Conclusions

Neoproterozoic rifting and break-up of Rodinia resulted in opening of the Iapetus Ocean (Cawood et al. 2001) and the severing of the Dashwoods and Chain Lakes blocks into an already open Iapetus Ocean. We propose that portions of the Chain Lakes block are exposed in the Maquereau-Mictaw inlier, the Chain Lakes massif (Gerbi et al. 2006), and the Chester Dome (Macdonald et al. 2014), within the peri-Laurentian realm of the northern Appalachians (Figure 5.1). The early Laurentian rift-drift succession was formed within the Taconic Seaway which separated these microcontinents from the Laurentian margin (Cawood et al. 2001, Allen et al. 2010).

Contrasts in the detrital zircon populations recovered from the rift and shelf successions exposed in western Newfoundland suggest that two distinct provenance domains are present in the clastic rift-to-drift rocks. A proximal western succession was derived from local basement and from the Grenville Province to the west, while a distal eastern succession was derived from the north, possibly from Greenland. The provenance of the Québec and New England rift and shelf rocks indicates a disconnect from the Newfoundland basin, explained by offset of the rift by a major NW-striking transfer fault (Figure 5.2). The lack of Archean and Paleoproterozoic detritus in the western rift succession in Newfoundland and in the rift-to-drift succession in Québec and New England can be explained by a Grenville topographic high, formed by thermal uplift at the margin of the rift (Figure 5.2 inset 1).

Earliest arc-continent collisions in the northern Appalachians occurred in Newfoundland on the off-margin Dashwoods block. These earliest interactions are interpreted to have taken place in the Cambrian along an east-dipping subduction zone, at which the Dashwoods block was partially subducted, resulting in westward transport and obduction of ophiolites (Waldron & van Staal 2001). In Québec and New England earliest arc-continent collision occurred later, in the Middle Ordovician (Pinet & Tremblay 1995, De Souza et al. 2012). In Québec, ophiolites were obducted and transported westward onto the partially subducted Chain Lakes block. In New England, the Moretown terrane was thrust on top of the Chain Lakes block.

Arc-continent collision was followed by diachronous closure of the Taconic Seaway. In Newfoundland, closure began at ~ 470 Ma and resulted in obduction of the Humber Arm Allochthon on top of the Laurentian margin (van Staal et al. 2007). In Québec we suggest that the seaway did not begin to close until at least ~ 461 Ma and allochthon emplacement onto the margin continued until ~450 Ma. In New England the seaway did not begin to close until at least 455 Ma.

Closure of the Taconic Seaway and loading of the down-going Laurentian plate led to development of a foreland basin on top of the Laurentian craton. East-dipping subduction implied deposition of foreland sediments into a pro-arc basin, and subsidence rates are consistent with pro-arc basin development. Earliest units within the foreland basin are platform carbonate units followed by deep-marine shale and orogen derived flysch. In Newfoundland this basin developed in the Middle Ordovician; however, in the Québec Embayment the pro-arc basin developed in the Late Ordovician.

Subduction polarity reversal occurred first along the St. Lawrence Promontory in Newfoundland at 460 Ma (Zagorevski et al. 2009) and led to the development of an Upper Ordovician retro-arc basin in Newfoundland. Delayed subduction polarity reversal farther south in the embayment (~450 Ma) implies that the Québec segment of the orogen was still in a pro-arc setting at this time. Simultaneous westward and eastward subduction along the Laurentian margin resulted in the unique retro and pro-arc setting of the Upper Ordovician Long Point Group in Newfoundland. The tectonic setting of the Long Point Group is analogous to the current tectonic setting of the northern portion of the Australian Plate near Papua New Guinea and was a direct consequence of the irregular margin shape.

Continued westward subduction and accretion of Gondwanan fragments led to the 440-420 Ma Salinian and 420-400 Ma Acadian orogenies in Newfoundland (van Staal et al. 2014). In Québec the Acadian Orogeny continued later, until ~ 380 Ma (Bradley et al. 2000). The Salinian Orogeny is largely manifested by major unconformities in the foreland (e.g. Clam Bank unconformity), while the Acadian orogeny resulted in deposition of thick clastic wedges in Newfoundland, Québec, and New England. The Acadian Orogeny resulted in inversion of

the basement-involved structural front and uplift and erosion of Grenvillian massifs into the developing foreland. Inversion in Newfoundland is interpreted as Emsian, while inversion in New England is interpreted to have occurred later, in the Frasian.

All major episodes of deformation affecting the northern Laurentian margin - Taconian, Salinian and Acadian - were diachronous. We interpret that diachronism resulted from a combination of the irregularity of the Laurentian margin, the distribution of off-margin microcontinents, and the geometry of arcs and microcontinents on the colliding plate.

5.7. References

- Allen, J.S. 2009. Paleogeographic Reconstruction of the St. Lawrence Promontory, Western Newfoundland. PhD Thesis. University of Kentucky, Lexington, Kentucky
- Allen, J.S., Thomas, W.A. & Lavoie, D. 2010. The Laurentian margin of northeastern North America. In: Tollo, R. P., Bartholomew, M. J., Hibbard, J. P. & Karabinos, P. M. (eds) From Rodinia to Pangea: The Lithotectonic Record of the Appalachian Region. 71–90.
- Batten Hender, K.L. & Dix, G.R. 2008. Facies development of a Late Ordovician mixed carbonate-siliciclastic ramp proximal to the developing Taconic orogen: Lourdes Formation, Newfoundland, Canada. *Facies*, **54**, 121–149.
- Bickford, M.E., Wooden, J.L. & Bauer, R.L. 2006. SHRIMP study of zircons from Early Archean rocks in the Minnesota River Valley: Implications for the tectonic history of the Superior Province. *Geological Society of America Bulletin*, **118**, 94–108.
- Bird, J.M. & Dewey, J.F. 1970. Lithosphere plate-continental margin tectonics and the evolution of the Appalachian orogen. *Geological Society of America Bulletin*, **81**, 1031–1060.
- Bock, B., McLennan, S.M. & Hanson, G.N. 1998. Geochemistry and provenance of the middle Ordovician Austin Glen member (Normanskill formation) and the Taconic orogeny in New England. *Sedimentology*, **45**, 635–655.
- Boone, G.M. & Boudette, E.L. 1989. Accretion of the Boundary Mountains terrane within the northern Appalachian orotectonic zone. *Geological Society of America Special Papers*, **228**, 17–42.
- Botsford, J.W. 1987. Depositional History of Middle Cambrian to Lower Ordovician Deep Water Sediments, Bay of Islands, Western Newfoundland. PhD Thesis, Memorial University of Newfoundland.
- Bradley, D.C. 1983. Tectonics of the Acadian orogeny in New England and adjacent Canada. *The Journal of Geology*, **91**, 381–400.
- Bradley, D.C. & Kidd, W.S.F. 1991. Flexural extension of the upper continental crust in collisional foredeeps. *Geological Society of America Bulletin*, **103**, 1416–1438.

- Bradley, D.C., Tucker, R.D., Lux, D.R., Harris, A.G. & McGregor, D.C. 2000. Migration of the Acadian orogen and foreland basin across the northern Appalachians of Maine and adjacent areas. U.S. Geological Survey, **Professional paper 1624**, 49.
- Bradley, K.E., Feng, L., Hill, E.M., Natawidjaja, D.H. & Sieh, K. 2017. Implications of the diffuse deformation of the Indian Ocean lithosphere for slip partitioning of oblique plate convergence in Sumatra: Sumatran Slip Partitioning. *Journal of Geophysical Research: Solid Earth*, **122**, 572–591.
- Burden, E.T. & Williams, S.H. 1995. Biostratigraphy and Thermal Maturity of Strata in Hunt-Pan Canadian Port Au Port Well # 1. St. John's Newfoundland, Hunt oil, **Final Contract Report**.
- Burden, E.T., Quinn, L., Nowlan, G.S. & Bailey-Nill, L.A. 2002. Palynology and micropaleontology of the Clam Bank Formation (Lower Devonian) of western Newfoundland, Canada. *Palynology*, **26**, 185–215.
- Calvert, A.J. & Ludden, J.N. 1999. Archean continental assembly in the southeastern Superior Province of Canada. *Tectonics*, **18**, 412–429.
- Cawood, P.A. & Nemchin, A.A. 2001. Paleogeographic development of the east Laurentian margin: Constraints from U-Pb dating of detrital zircons in the Newfoundland Appalachians. *Geological Society of America Bulletin*, **113**, 1234–1246.
- Cawood, P.A. & Williams, H. 1988. Acadian basement thrusting, crustal delamination, and structural styles in and around the Humber Arm allochthon, western Newfoundland. *Geology*, **16**, 370.
- Cawood, P.A., van Gool, J.A. & Dunning, G.R. 1996. Geological development of eastern Humber and western Dunnage zones: Corner Brook–Glover Island region, Newfoundland. *Canadian Journal of Earth Sciences*, **33**, 182–198.
- Cawood, P.A., McCausland, P.J. & Dunning, G.R. 2001. Opening Iapetus: Constraints from the Laurentian margin in Newfoundland. *Geological Society of America Bulletin*, **113**, 443–453.
- Cawood, P.A., Nemchin, A.A. & Strachan, R. 2007a. Provenance record of Laurentian passive-margin strata in the northern Caledonides: Implications for paleodrainage and paleogeography. *Geological Society of America Bulletin*, **119**, 993–1003.
- Cawood, P.A., Nemchin, A.A., Strachan, R., Prave, T. & Krabbendam, M. 2007b. Sedimentary basin and detrital zircon record along East Laurentia and Baltica during assembly and breakup of Rodinia. *Journal of the Geological Society*, **164**, 257–275.
- Cheatham, M.L., Olszewski, W.J. & Gaudette, H.E. 1989. Interpretation of the regional significance of the Chain Lakes massif, Maine based on preliminary isotopic studies.

- In: Tucker, R. D. & Marvinney, R. G. (eds) *Studies in Maine Geology*. Augusta, Maine, Maine Geological Survey, 125–137.
- Chow, N. & James, N.P. 1987. Cambrian Grand Cycles: A northern Appalachian perspective. *Geological Society of America Bulletin*, **98**, 418.
- Cooper, R.A., Sadler, P.M., Hammer, O. & Gradstein, F.M. 2012. The Ordovician Period. In: Gradstein, F. M., Ogg, J. G., Schmitz, M. & Ogg, G. (eds) *The Geologic Time Scale*. Elsevier, 489–523.
- Corfu, F. & Lin, S. 2000. Geology and U-Pb geochronology of the Island Lake greenstone belt, northwestern Superior Province, Manitoba. *Canadian Journal of Earth Sciences*, **37**, 1275–1286.
- Corfu, F., Davis, D.W., Stone, D. & Moore, M.L. 1998. Chronostratigraphic constraints on the genesis of Archean greenstone belts, northwestern Superior Province, Ontario, Canada. *Precambrian Research*, **92**, 277–295.
- Cormier, C.F.M., Barr, S.M., & Dunning, G.R. 1995. Geological setting and petrochemistry of early Middle Devonian volcanic and gabbroic rocks in the Guysborough area, Nova Scotia. *Atlantic Geology*, **31** (3), 153-166.
- De Souza, S., Tremblay, A., Ruffet, G. & Pinet, N. 2012. Ophiolite obduction in the Quebec Appalachians, Canada. *Canadian Journal of Earth Sciences*, **49**, 91–110.
- Diamant, M., Harjono, H., et al. 1992. Mentawai fault zone off Sumatra: A new key to the geodynamics of western Indonesia. *Geology*, **20**, 259.
- Dix, G.R., Nehza, O. & Okon, I. 2013. Tectonostratigraphy of the Chazyan (Late Middle-Early Late Ordovician) Mixed Siliciclastic-Carbonate Platform, Quebec Embayment. *Journal of Sedimentary Research*, **83**, 451–474, <https://doi.org/10.2110/jsr.2013.39>.
- Dorais, M.J., Atkinson, M., Kim, J., West, D.P., Kirby, G.A. & Murphy, B. 2011. Where is the Iapetus suture in northern New England? A study of the Ammonoosuc Volcanics, Bronson Hill terrane, New Hampshire. *Canadian Journal of Earth Sciences*, **49**, 189–205.
- Downey, M.W., Lin, S., Böhm, C.O. & Rayner, N.M. 2009. Timing and kinematics of crustal movement in the Northern Superior superterrane: Insights from the Gull Rapids area of the Split Lake Block, Manitoba. *Precambrian Research*, **168**, 134–148.
- Dubé, B., Dunning, G.R., Lauziere, K. & Roddick, J.C. 1996. New insights into the Appalachian Orogen from geology and geochronology along the Cape Ray fault zone, southwest Newfoundland. *Geological Society of America Bulletin*, **108**, 101–116.
- Dunning, G.R. & Cousineau, P.A. 1990. U/Pb ages of single zircons from Chain Lakes massif and a correlative unit in ophiolitic melange in Quebec. *Geological Society of America Abstracts with Programs*, **22**, 13.

- Dunning, G.R., O'Brien, S.J., Colman-Sadd, S.P., Blackwood, R.F., Dickson, W.L., O'Neill, P.P. & Krogh, T.E. 1990. Silurian Orogeny in the Newfoundland Appalachians. *The Journal of Geology*, **98**, 895–913.
- Ettensohn, F.R. 2004. Modeling the nature and development of major paleozoic clastic wedges in the Appalachian Basin, USA. *Journal of Geodynamics*, **37**, 657–681.
- Garde, A.A., Hamilton, M.A., Chadwick, B., Grocott, J. & McCaffrey, K.J. 2002. The Ketilidian orogen of South Greenland: geochronology, tectonics, magmatism, and fore-arc accretion during Palaeoproterozoic oblique convergence. *Canadian Journal of Earth Sciences*, **39**.
- Gawthorpe, R.L. & Leeder, M.R. 2000. Tectono-sedimentary evolution of active extensional basins. *Basin Research*, **12**, 195–218.
- Gerbi, C.C., Johnson, S.E. & Aleinikoff, J.N. 2006. Origin and orogenic role of the Chain Lakes massif, Maine and Quebec. *Canadian Journal of Earth Sciences*, **43**, 339–366.
- Globensky, Y. 1987. *Geologie des Basses-Terres du Sainte-Laurent, Quebec*. Ministère des Richesses Naturelles de Quebec, **MM 85-02**, 63.
- Hayman, N.W. & Kidd, W.S.F. 2002. Reactivation of prethrusting, synconvergence normal faults as ramps within the Ordovician Champlain-Taconic thrust system. *Geological Society of America Bulletin*, **114**, 476–489.
- Heaman, L.M., Erdmer, P. & Owen, J.V. 2002. U–Pb geochronologic constraints on the crustal evolution of the Long Range Inlier, Newfoundland. *Canadian Journal of Earth Sciences*, **39**, 845–865.
- Hibbard, J.P., van Staal, C.R., Rankin, D.W. & Williams, H. 2006. Lithotectonic Map of the Appalachian Orogen, Canada- United States of America. Geological Survey of Canada, Map 2096A.
- Hibbard, J.P., Van Staal, C.R. & Rankin, D.W. 2007. A comparative analysis of pre-Silurian crustal building blocks of the northern and the southern Appalachian orogen. *American Journal of Science*, **307**, 23–45.
- Hibbard, J.P., van Staal, C.R. & Rankin, D.W. 2010. Comparative analysis of the geological evolution of the northern and southern Appalachian orogen: Late Ordovician-Permian. In: Tollo, R. P., Bartholomew, M. J., Hibbard, J. P. & Karabinos, P. M. (eds) *From Rodinia to Pangea: The Lithotectonic Record of the Appalachian Region*. Geological Society of America, 51–69.
- Hiscott, R.N. 1978. Provenance of Ordovician deep-water sandstones, Tourelle Formation, Quebec, and implications for initiation of the Taconic orogeny. *Canadian Journal of Earth Sciences*, **15**, 1579–1597.
- Hiscott, R.N. 1984. Ophiolitic source rocks for Taconic-age flysch: Trace-element evidence. *Geological Society of America Bulletin*, **95**, 1261–1267.

- Hoffman, P.F. 1988. United Plates of America, The Birth of a Craton: Early Proterozoic Assembly and Growth of Laurentia. *Annual Review of Earth and Planetary Sciences*, **16**, 543–603.
- Hoffman, P.F. 2014. The Origin of Laurentia: Rae Craton as the Backstop for Proto-Laurentian Amalgamation by Slab Suction. *Geoscience Canada*, **41**, 313.
- Jacobi, R.D. 1981. Peripheral bulge—a causal mechanism for the Lower/Middle Ordovician unconformity along the western margin of the Northern Appalachians. *Earth and Planetary Science Letters*, **51**, 245–251.
- James, N.P. & Stevens, R.K. 1986. Stratigraphy and Correlation of the Cambro-Ordovician Cow Head Group, Western Newfoundland. *Geological Survey of Canada Bulletin*, **366**, 143.
- Karabinos, P., Samson, S.D., Hepburn, J.C. & Stoll, H.M. 1998. Taconian orogeny in the New England Appalachians: Collision between Laurentia and the Shelburne Falls arc. *Geology*, **26**, 215–218.
- Karabinos, P., Aleinikoff, J.N. & Fanning, C.M. 1999. Distinguishing Grenvillian basement from pre-Taconian cover rocks in the northern Appalachians. *American Journal of Science*, **299**, 502–515.
- Karabinos, P., Morris, D., Hamilton, M. & Rayner, N. 2008. Age, origin, and tectonic significance of Mesoproterozoic and Silurian felsic sills in the Berkshire massif, Massachusetts. *American Journal of Science*, **308**, 787–812.
- Karabinos, P., Macdonald, F.A. & Crowley, J.L. 2017. Bridging the gap between the foreland and hinterland I: Geochronology and plate tectonic geometry of Ordovician magmatism and terrane accretion on the Laurentian margin of New England. *American Journal of Science*, **317**, 515–554.
- Klapper, G. & Kirchgasser, W.T. 2016. Frasnian Late Devonian conodont biostratigraphy in New York: graphic correlation and taxonomy. *Journal of Paleontology*, **90**, 525–554.
- Knight, I. & James, N.P. 1987. The stratigraphy of the Lower Ordovician St. George Group, western Newfoundland: the interaction between eustasy and tectonics. *Canadian Journal of Earth Sciences*, **24**, 1927–1951.
- Knight, I., James, N.P. & Lane, T.E. 1991. The Ordovician St. George Unconformity, northern Appalachians: The relationship of plate convergence at the St. Lawrence Promontory to the Sauk/Tippecanoe sequence boundary. *Geological Society of America Bulletin*, **103**, 1200–1225.
- Konstantinovskaya, E.A., Rodriguez, D., Kirkwood, D., Harris, L.B. & Theriault, R. 2009. Effects of basement structure, sedimentation and erosion on thrust wedge geometry: an example from the Quebec Appalachians and analogue models. *Bulletin of Canadian Petroleum Geology*, **57**, 34–62.

- LaFlamme, C., Sylvester, P.J., Hinchey, A.M. & Davis, W.J. 2013. U–Pb age and Hf-isotope geochemistry of zircon from felsic volcanic rocks of the Paleoproterozoic Aillik Group, Makkovik Province, Labrador. *Precambrian Research*, **224**, 129–142.
- Landing, E. 2012. The Great American Carbonate Bank in eastern Laurentia: its births, deaths, and linkage to paleoceanic oxygenation (Early Cambrian–Late Ordovician). In: Derby, J. R., Fritz, R. D., Longacre, W. A. & Morgan, C. A. (eds) *The Great American Carbonate Bank: The Geology and Economic Resources of the Cambrian-Ordovician Sauk Megasequence of Laurentia*. 451–492.
- Lavoie, D. 1994. Diachronous tectonic collapse of the Ordovician continental margin, eastern Canada: comparison between the Quebec Reentrant and St. Lawrence Promontory. *Canadian Journal of Earth Sciences*, **31**, 1309–1319.
- Lavoie, D., Burden, E. & Lebel, D. 2003. Stratigraphic framework for the Cambrian Ordovician rift and passive margin successions from southern Quebec to western Newfoundland. *Canadian Journal of Earth Sciences*, **40**, 177–205.
- Lavoie, D., Hamblin, A.P., ThÚriault, R., Beaulieu, J. & Kirkwood, D. 2008. Geological Survey of Canada, Open File 5900. Natural Resources Canada.
- Lus, W.Y., McDougall, I. & Davies, H.L. 2004. Age of the metamorphic sole of the Papuan Ultramafic Belt ophiolite, Papua New Guinea. *Tectonophysics*, **392**, 85–101.
- Macdonald, F.A., Ryan-Davis, J., Coish, R.A., Crowley, J.L. & Karabinos, P. 2014. A newly identified Gondwanan terrane in the northern Appalachian Mountains: Implications for the Taconic orogeny and closure of the Iapetus Ocean. *Geology*, **42**, 539–542.
- Macdonald, F.A., Karabinos, P.M., Crowley, J.L., Hodgin, E.B., Crockford, P.W. & Delano, J.W. 2017. Bridging the gap between the foreland and hinterland II: Geochronology and tectonic setting of Ordovician magmatism and basin formation on the Laurentian margin from New England to Newfoundland. *American Journal of Science*, **317**, 555–596.
- Maletz, J. 2001. A condensed Lower to Middle Ordovician graptolite succession at Matane, Quebec, Canada. *Canadian Journal of Earth Sciences*, **38**, 1531–1539.
- Malo, M., Tremblay, A. & Kirkwood, D. 1995. Along-strike Acadian structural variations in the Quebec Appalachians: Consequence of a collision along an irregular margin. *Tectonics*, **14**, 1327–1338.
- McDaniel, D.K., Hanson, G.N., McLennan, S.M. & Sevigny, J.H. 1997. Grenvillian provenance for the amphibolite-grade Trap Falls Formation: implications for early Paleozoic tectonic history of New England. *Canadian Journal of Earth Sciences*, **34**, 1286–1294.
- McLennan, S.M., Bock, B., Compston, W., Hemming, S.R. & McDaniel, D.K. 2001. Detrital zircon geochronology of Taconian and Acadian foreland sedimentary rocks in New England. *Journal of Sedimentary Research*, **71**, 305–317.

- Moench, R.H. & Aleinikoff, J.N. 2003. Erratum to “Stratigraphy, geochronology, and accretionary terrane settings of two Bronson Hill arc sequences, northern New England”. *Physics and Chemistry of the Earth*, **28**, 113–160.
- Montario, M.J. & Garver, J.I. 2009. The Thermal Evolution of the Grenville Terrane Revealed through U-Pb and Fission-Track Analysis of Detrital Zircon from Cambro-Ordovician Quartz Arenites of the Potsdam and Galway Formations. *The Journal of Geology*, **117**, 595–614, <https://doi.org/10.1086/605778>.
- Nikolaeva, K., Gerya, T.V. & Marques, F.O. 2010. Subduction initiation at passive margins: Numerical modeling. *Journal of Geophysical Research*, **115**.
- Nutman, A. & Friend, C. 2007. Adjacent terranes with ca. 2715 and 2650Ma high-pressure metamorphic assemblages in the Nuuk region of the North Atlantic Craton, southern West Greenland: Complexities of Neoproterozoic collisional orogeny. *Precambrian Research*, **155**, 159–203.
- Nutman, A.P., Friend, C.R.L., Barker, S.L.L. & McGregor, V.R. 2004. Inventory and assessment of Palaeoproterozoic gneiss terrains and detrital zircons in southern West Greenland. *Precambrian Research*, **135**, 281–314.
- Owen, J.V. & Erdmer, P. 1989. Metamorphic geology and regional geothermobarometry of a Grenvillian massif: the Long Range Inlier, Newfoundland. *Precambrian Research*, **43**, 79–100.
- Palmer, S.E., Burden, E. & Waldron, J.W.F. 2001. Stratigraphy of the Curling Group (Cambrian), Humber Arm Allochthon, Bay of Islands. *GSC Current research 2001–1*, 105–112.
- Pincivy, A., Malo, M., Ruffet, G., Tremblay, A. & Sacks, P.E. 2003. Regional metamorphism of the Appalachian Humber zone of Gaspé Peninsula: $^{40}\text{Ar}/^{39}\text{Ar}$ evidence for crustal thickening during the Taconian orogeny. *Canadian Journal of Earth Sciences*, **40**, 301–315.
- Pinet, N. & Tremblay, A. 1995. Tectonic evolution of the Quebec-Maine Appalachians: from oceanic spreading to obduction and collision in the northern Appalachians. *American Journal of Science*, **295**, 173–200.
- Pollock, J.C., Wilton, D.H.C., Van Staal, C.R. & Morrissey, K.D. 2007. U-Pb detrital zircon geochronological constraints on the Early Silurian collision of Ganderia and Laurentia along the Dog Bay Line: The terminal Iapetan suture in the Newfoundland Appalachians. *American Journal of Science*, **307**, 399–433.
- Prave, A.R., Kessler II, L.G., Malo, M., Bloechl, W.V. & Riva, J. 2000. Ordovician arc collision and foredeep evolution in the Gaspé Peninsula, Québec: the Taconic Orogeny in Canada and its bearing on the Grampian Orogeny in Scotland. *Journal of the Geological Society, London*, **157**, 393–400.

- Quinn, L., Williams, S.H., Harper, D.A.T. & Clarkson, E.N.K. 1999. Late Ordovician foreland basin fill: Long Point Group of onshore western Newfoundland. *Bulletin of Canadian Petroleum Geology*, **47**, 63–80.
- Quinn, L., Bashforth, A.R., Burden, E.T., Gillespie, H., Springer, R.K. & Williams, S.H. 2004. The Red Island Road Formation: Early Devonian terrestrial fill in the Anticosti Foreland Basin, western Newfoundland. *Canadian Journal of Earth Sciences*, **41**, 587–602.
- Quinn, L.A. 1992. Foreland and Trench Slope Basin Sandstones of the Goose Tickle Group and Lower Head Formation, Western Newfoundland. PhD Thesis, Memorial University of Newfoundland.
- Rivers, T. 1997. Lithotectonic elements of the Grenville Province: review and tectonic implications. *Precambrian Research*, **86**, 117–154.
- Rivers, T. 2008. Assembly and preservation of lower, mid, and upper orogenic crust in the Grenville Province—Implications for the evolution of large hot long-duration orogens. *Precambrian Research*, **167**, 237–259, <https://doi.org/10.1016/j.precamres.2008.08.005>.
- Rivers, T. 2015. Tectonic Setting and Evolution of the Grenville Orogen: An Assessment of Progress Over the Last 40 Years. *Geoscience Canada*, **42**, 77–124.
- Rowley, D.B. & Kidd, W.S.F. 1982. Stratigraphic relationships and detrital composition of the medial flysch of western New England: implications for the tectonic evolution of the Taconic Orogeny. *Journal of Geology*, **90**, 219–226.
- Salad Hersi, O., Lavoie, D., Mohamed, A.H. & Nowlan, G.S. 2002. Subaerial unconformity at the Potsdam-Beekmantown contact in the Quebec reentrant: regional significance for the Laurentian continental margin history. *Bulletin of Canadian Petroleum Geology*, **50**, 419–440.
- Salad Hersi, O., Lavoie, D. & Nowlan, G.S. 2003. Reappraisal of the Beekmantown Group sedimentology and stratigraphy, Montréal area, southwestern Quebec: implications for understanding the depositional evolution of the Lower-Middle Ordovician Laurentian passive margin of eastern Canada. *Canadian Journal of Earth Sciences*, **40**, 149–176.
- Sinclair, H.D. & Naylor, M. 2012. Foreland basin subsidence driven by topographic growth versus plate subduction. *Geological Society of America Bulletin*, **124**, 368–379.
- Sloss, L.L. 1963. Sequences in the cratonic interior of North America. *Geological Society of America Bulletin*, **74**, 93–114.
- Spencer, C., Green, A., Milkereit, B., Luetgert, J., Stewart, D., Unger, J. & Phillips, J. 1989. The extension of Grenville Basement beneath the northern Appalachians: Results from the Quebec-Maine seismic reflection and refraction surveys. *Tectonics*, **8**, 677–696.
- Stanley, R.S. & Ratcliffe, N.M. 1985. Tectonic synthesis of the Taconian orogeny in western New England. *Geological Society of America Bulletin*, **96**, 1227–1250.

- Stenzel, S.R., Knight, I. & James, N.P. 1990. Carbonate platform to foreland basin: revised stratigraphy of the Table Head Group (Middle Ordovician), western Newfoundland. *Canadian Journal of Earth Sciences*, **27**, 14–26.
- Stewart, D.B., Wright, B.E., Phillips, J.D. & Hutchinson, D.R. 1993. Global Geoscience Transect 8: Quebec-Maine-Gulf of Maine Transect, Southeastern Canada, Northeastern United States of America. U.S. Geological Survey.
- Thomas, W.A. 1977. Evolution of Appalachian-Ouachita salients and recesses from reentrants and promontories in the continental margin. *American Journal of Science*, **277**, 1233–1278.
- Thomas, W.A. & Astini, R.A. 1999. Simple-shear conjugate rift margins of the Argentine Precordillera and the Ouachita embayment of Laurentia. *Geological Society of America Bulletin*, **111**, 1069–1079.
- Tremblay, A. & Pinet, N. 2016. Late Neoproterozoic to Permian tectonic evolution of the Quebec Appalachians, Canada. *Earth-Science Reviews*, **160**, 131–170.
- Tremblay, A., Ruffet, G. & Castonguay, S. 2000. Acadian metamorphism in the Dunnage zone of southern Québec, northern Appalachians: $^{40}\text{Ar}/^{39}\text{Ar}$ evidence for collision diachronism. *Geological Society of America Bulletin*, **112**, 136–146.
- Tremblay, A., Ruffet, G. & Bédard, J.H. 2011. Obduction of Tethyan-type ophiolites—A case-study from the Thetford-Mines ophiolitic Complex, Quebec Appalachians, Canada. *Lithos*, **125**, 10–26.
- Trzcinski, W.E., Rodgers, J. & Guidotti, C.V. 1992. Alternative hypotheses for the Chain Lakes ‘Massif,’ Maine and Quebec. *American Journal of Science*, **292**, 508–532.
- Tucker, R.D. & Gower, C.F. 1994. A U-Pb geochronological framework for the Pinware terrane, Grenville Province, southeast Labrador. *The Journal of Geology*, **102**, 67–78.
- van Staal, C.R., Dewey, J.F., Niocaill, C.M. & McKerrow, W.S. 1998. The Cambrian-Silurian tectonic evolution of the northern Appalachians and British Caledonides: history of a complex, west and southwest Pacific-type segment of Iapetus. In: Blundell, D. J. & Scott, A. C. (eds) *Lyell, the Past Is the Key to the Present*. Geological Society, London, Special Publications, 197–242.
- van Staal, C.R., Whalen, J.B., et al. 2007. The Notre Dame arc and the Taconic orogeny in Newfoundland. In: Hatcher, R. D., Carlson, M. P., McBride, J. H. & Martinez Catalan, J. R. (eds) *4-D Framework of Continental Crust*. 511–552.
- van Staal, C.R., Whalen, J.B., Valverde-Vaquero, P., Zagorevski, A. & Rogers, N. 2009. Pre-Carboniferous, episodic accretion-related, orogenesis along the Laurentian margin of the northern Appalachians. In: Murphy, J. B., Keppie, J. D. & Hynes, A. J. (eds) *Ancient*

- Orogens and Modern Analogues. Geological Society, London, Special Publications, 271–316.
- van Staal, C.R., Chew, D.M., et al. 2013. Evidence of Late Ediacaran Hyperextension of the Laurentian Iapetan Margin in the Birchy Complex, Baie Verte Peninsula, Northwest Newfoundland: Implications for the Opening of Iapetus, Formation of Peri-Laurentian Microcontinents and Taconic – Grampian Orogenesis. *Geoscience Canada*, **40**, 94.
- van Staal, C.R., Zagorevski, A., McNicoll, V.J. & Rogers, N. 2014. Time-Transgressive Salinic and Acadian Orogenesis, Magmatism and Old Red Sandstone Sedimentation in Newfoundland. *Geoscience Canada*, **41**, 138.
- van Staal, C.R., Wilson, R.A., Kamo, S.L., McClelland, W.C. & McNicoll, V. 2016. Evolution of the Early to Middle Ordovician Popelogan arc in New Brunswick, Canada, and adjacent Maine, USA: Record of arc-trench migration and multiple phases of rifting. *Geological Society of America Bulletin*, **128**, 122–146.
- Waldron, J.W., Anderson, S.D., et al. 1998. Evolution of the Appalachian Laurentian margin: Lithoprobe results in western Newfoundland. *Canadian Journal of Earth Sciences*, **35**, 1271–1287.
- Waldron, J.W., Floyd, J.D., Simonetti, A. & Heaman, L.M. 2008. Ancient Laurentian detrital zircon in the closing Iapetus ocean, Southern Uplands terrane, Scotland. *Geology*, **36**, 527–530.
- Waldron, J.W.F. & van Staal, C.R. 2001. Taconian orogeny and the accretion of the Dashwoods block: A peri-Laurentian microcontinent in the Iapetus Ocean. *Geology*, **29**, 811–814.
- Waldron, J.W.F., Barr, S.M., Park, A.F., White, C.E. & Hibbard, J. 2015. Late Paleozoic strike-slip faults in Maritime Canada and their role in the reconfiguration of the northern Appalachian orogen. *Tectonics*, **34**, 1661–1684.
- Waldron, J.W.F., Schofield, D.I. & Murphy, J.B. 2017. Diachronous Palaeozoic accretion of peri-Gondwanan terranes at the Laurentian margin. In: Wilson, R. W., Houseman, G. A., McCaffrey, K. J. W., Dore, A. G. & Buiters, S. J. H. (eds) *Fifty Years of the Wilson Cycle*. 470.
- Walliser, O.H. n.d. Conodonten des Silurs. *Abhandlungen des Hessischen Landesamtes für Bodenforschung*, **41**, 106.
- Whalen, J.B., Jenner, G.A., Longstaffe, F.J., Gariépy, C. & Fryer, B.J. 1997. Implications of granitoid geochemical and isotopic (Nd, O, Pb) data from the Cambrian-Ordoovician Notre Dame arc for the evolution of the Central Mobile belt, Newfoundland Appalachians. In: Sinha, A. K., Whalen, J. B. & Hogan, J. P. (eds) *The Nature of Magmatism in the Appalachian Orogen*. Geological Society of America, 367–395.

- Whalen, J.B., McNicoll, V.J., van Staal, C.R., Lissenberg, C.J., Longstaffe, F.J., Jenner, G.A. & van Breeman, O. 2006. Spatial, temporal and geochemical characteristics of Silurian collision-zone magmatism, Newfoundland Appalachians: An example of a rapidly evolving magmatic system related to slab break-off. *Lithos*, **89**, 377–404.
- Williams, H. 1975. Structural succession, nomenclature, and interpretation of transported rocks in western Newfoundland. *Canadian Journal of Earth Sciences*, **12**, 1874–1894.
- Williams, H. & Hiscott, R.N. 1987. Definition of the lapetus rift-drift transition in western Newfoundland. *Geology*, **15**, 1044–1047.
- Williams, H., Colman-Sadd, S.P. & Swinden, H.S. 1988. Tectonic-stratigraphic subdivisions of central Newfoundland. *Geological Survey of Canada*, 91–98.
- Wilson, J.T. 1966. Did the Atlantic close and then re-open. *Nature*, **211**, 676–681.
- Wilson, R.A., Burden, E.T., Bertrand, R., Asselin, E. & McCracken, A.D. 2004. Stratigraphy and tectono-sedimentary evolution of the Late Ordovician to Middle Devonian Gaspé Belt in northern New Brunswick: evidence from the Restigouche area. *Canadian Journal of Earth Sciences*, **41**, 527–551.
- Zagorevski, A., van Staal, C.R., McNicoll, V., Rogers, N. & Valverde-Vaquero, P. 2007. Tectonic architecture of an arc-arc collision zone, Newfoundland Appalachians. In: Draut, A., Clift, P. D. & Scholl, D. W. (eds) *Formation and Applications of the Sedimentary Record in Arc Collision Zones*. The Geological Society of America, 309–333.
- Zagorevski, A., Lissenberg, C.J. & van Staal, C.R. 2009. Dynamics of accretion of arc and backarc crust to continental margins: Inferences from the Annieopsquotch accretionary tract, Newfoundland Appalachians. *Tectonophysics*, **479**, 150–164.
- Zen, E.A. 1967. Time and space relationships of the Taconic allochthon and autochthon. *Geological Society of America Special Papers*, **97**, 1–82.

Chapter 6: Conclusions

The studies in this thesis have used a multidisciplinary approach to the investigation of the West Newfoundland Appalachians and their relationship to other parts of the Northern Appalachians. Multiple data sources including geologic mapping results, geophysical data, and detrital geochronology, have been used to make significant advances in our understanding of the evolution of the orogen.

6.1. Chapter 2

In Chapter 2, we examined a variety of geophysical data to image and interpret foreland basin successions in Western Newfoundland and the adjacent Gulf of St. Lawrence. The Middle Ordovician Goose Tickle Group shows deep marine facies, and was deposited in an orogen-parallel basin which thins generally and onlaps underlying strata to the west. These observations indicate that it represents a foredeep, loaded by the developing orogen, and filled by sediments that were derived from the Newfoundland portion of the orogen. This geometry and fast subsidence rate (>0.05 km/Myr) indicate that the Goose Tickle Group developed in a pro-arc basin above an east-dipping subduction zone during Taconian continent-arc collision.

Tectonic models of Appalachian evolution in Newfoundland (Zagorevski et al. 2009) suggest subduction polarity reversal by the Late Ordovician. This implies that the Upper Ordovician Long Point Group was deposited on the upper plate in a retro-arc setting. However, fast subsidence rates of ~ 0.17 km/Myr are consistent with development in a pro-arc setting. These subsidence rates, along with major southward thickening, indicate the Late Ordovician basin resulted from loading by the Québec Appalachians. The basin in which the Long Point Group was deposited therefore has combined aspects of both retro and pro-arc settings, similar to the present day tectonic configuration of parts of the northeastern Australian continental margin.

A major unconformity removes the vast majority of the Silurian record of from the foreland basin. It likely resulted from break-off of the west-dipping Salinian subducting slab.

The Early Devonian Acadian Orogeny overlapped in time with deposition of both the Clam Bank and Red Island Road formations in the foreland basin. It is therefore interpreted that this succession represents the Acadian retro-arc foreland basin in Newfoundland.

6.2. Chapter 3

Chapter 3 examines deep-seated basement faults which had had a protracted history of movement during the opening and subsequent closure of the Iapetus Ocean. We observe that many steep basement faults have orientations that parallel rift-related dykes (Miller & Barr 2004; Burton & Southworth 2010) and have rift-related sediments in their hanging walls,

indicating activity during Neoproterozoic rifting and opening of the Iapetus Ocean. Ordovician conglomerates indicate that these basement faults were reactivated during the Taconian Orogeny as the down-going Laurentian plate underwent extension during emplacement of the Humber Arm Allochthon.

Acadian deformation reactivated and inverted these deep-seated basement-involved faults. One of these faults, the Parsons Pond Thrust, is a significant geologic boundary. During Acadian inversion it transported parautochthonous units above the Humber Arm Allochthon. Westward displacement was significant, at least 8 km near Parsons Pond, increasing upwards of 12 km near Portland Creek Pond. The Parsons Pond thrust is structurally analogous to the Round Head thrust farther south.

Basement-cored fault-propagation folds associated with Parsons Pond Thrust have characteristic broad, shallow-dipping back limbs and steep to overturned forelimbs. These are analogous to basement inversion structures formed during the Laramide Orogeny in western USA.

Farther south in the Appalachians, in New England, major faults placed parautochthonous rocks above Taconian allochthons during inversion. We suggest these structures are genetically linked, forming a deep-seated Acadian thrust front along the length of the entire northern Appalachians, formed by inversion of earlier structures.

6.3. Chapter 4

In Chapter 4 we describe and interpret new detrital zircon geochronology results from the Upper Ordovician through Devonian foreland basin successions in western Newfoundland, and relate them to previously published data from older units.

Previously published U-Pb ages of detrital zircon from the underlying Goose Tickle Group are consistent with derivation from clastic units within the Humber Arm Allochthon.

We interpret a major shift in provenance during deposition of the overlying Long Point Group, indicated by a drastic decrease in the relative abundance of 1.85 Ga zircons. This change accompanies a 180° reversal in dominant unidirectional paleoflow indicators from SW to NE, documented by Quinn (1992) and Batten Hender and Dix (2008). Spectra of the Long Point Group and Clam Bank Formation are similar to those from rift and passive margin clastics in the Québec and New England Appalachians (McLennan et al. 2001; Macdonald et al. 2014). We suggest that the Long Point Group was sourced from either the Québec or New England portion of the orogen.

Another major shift in provenance occurred during deposition of the Early Devonian Red Island Road Formation. The vast majority of grains have ages close to 1.1 Ga, strikingly similar to spectra from proximal rift-related units (Cawood & Nemchin 2001). This indicates derivation

from a similar source, Grenvillian basement units. Rhyolite cobbles, one of which was dated in this study at 421 Ma (Chapter 4), are common within the Red Island Road Formation. The combination of U/Pb age data and lithologic observations lead us to suggest that the Grenville Blair River Inlier in Cape Breton, which Waldron et al. (2015) has demonstrated to have a palinspastically restored position east of the basin during the Devonian, was the most likely source.

6.4. Chapter 5

In Chapter 5 we review implications of the above results for the evolution of the northern Appalachians as a whole.

Neoproterozoic rifting and break-up of Rodinia resulted in opening of the Iapetus Ocean and the severing of Laurentian microcontinents into an already open Iapetus Ocean (Waldron & van Staal 2001). South of Newfoundland, we suggest that the Maqueriau-Mictaw inlier in Quebec and the Chain Lakes massif and Chester Dome in New England might represent portions of a similar microcontinent, here termed the Chain Lakes block. The Cambrian through Ordovician rift-drift succession was formed within the Taconic Seaway which separated these microcontinents from the Laurentian margin (Waldron & van Staal 2001, Macdonald et al. 2014). We interpret that the previously published detrital zircon data which we compiled from this succession in western Newfoundland indicates two distinct provenance domains. A proximal western succession, derived from local basement of the Grenville Province, and a distal eastern succession which was derived from the north, possibly from Greenland.

Earliest arc-continent collisions involved the off-margin microcontinents. These collisions occurred in the Cambrian in Newfoundland (Waldron & van Staal 2001) and later in the Ordovician in Québec and New England (De Souza et al. 2012, Macdonald et al. 2014, Tremblay & Pinet 2016) probably at an east-dipping subduction zone. Arc-continent collision was followed by diachronous closure of the Taconic Seaway. In Newfoundland, closure began at ~ 470 Ma (Waldron & van Staal 2001). In Québec we interpret that the seaway did not begin to close until at least ~ 461 Ma.

Arc-continent collision was followed by subduction polarity reversal (Zagorevski et al. 2009), which we interpret as diachronous along the margin. Westward subduction and accretion of Gondwanan fragments probably led to the Salinian and Acadian orogenies (van Staal et al. 2014). The Salinian Orogeny is largely manifested by major unconformities in the foreland (e.g. Clam Bank unconformity), while the Acadian orogeny resulted in deposition of thick clastic wedges in Newfoundland, Québec, and New England (e.g. Ettensohn 2005, Bradley & O'Sullivan 2016).

We conclude that all major episodes of deformation affecting the northern Laurentian margin - Taconian, Salinian and Acadian - were diachronous. We interpret that diachronism resulted from a combination of the irregularity of the Laurentian margin, the distribution of off-margin microcontinents, and the geometry of arcs and microcontinents on the colliding plate.

6.5. Future Work

A study of this magnitude inevitably leaves questions unanswered. The results presented in Chapters 2 through 5 have highlighted gaps in knowledge, particularly in the Quebec and New England Appalachians. The following are suggested as topics for potential future projects.

1. In Québec and New England, there are few detrital zircon data from clastic units preserved within the Taconian allochthons. A study of detrital zircon populations within the rift-related units will help constrain margin geometry.
2. Detrital zircon geochronology studies of the foreland basin units, both allochthonous and autochthonous, in Québec and New England will provide information on the kinematics of Taconian deformation and the role of along margin sediment transport.
3. Field studies in the Laurentian realm of the Québec and New England Appalachians should focus on the role of basement faulting during contractional events. We have shown that identifying sedimentary units related to fault scarps is important for the recognition of inversion structures. These techniques should be applied farther south in the Appalachians.
4. The carbonate-dominated northern margin of Australia is currently undergoing diachronous arc-continent collision, and presents close analogies with the Ordovician collision in the northern Appalachians. Further comparative study of the two areas may shed light on distinctive but poorly understood features of Appalachian deformation, including normal faults developed within foreland basins, hybrid basins with retro-arc and pro-arc characteristics, and the inversion of rift-related structures in collisional settings.

6.6. References

- BATTEN HENDER K. L. & DIX G. R. 2008. Facies development of a Late Ordovician mixed carbonate-siliciclastic ramp proximal to the developing Taconic orogen: Lourdes Formation, Newfoundland, Canada. *Facies* 54: 121–149.
- BRADLEY D. C. & O’SULLIVAN P. 2016. Detrital zircon geochronology of pre-and syn-collisional strata, Acadian orogen, Maine Appalachians. *Basin Research*: n/a-n/a.

- BURTON W. C. & SOUTHWORTH S. 2010. A model for Iapetan rifting of Laurentia based on Neoproterozoic dikes and related rocks. *Geological Society of America Memoirs* 206: 455–476.
- CAWOOD P. A. & NEMCHIN A. A. 2001. Paleogeographic development of the east Laurentian margin: Constraints from U-Pb dating of detrital zircons in the Newfoundland Appalachians. *Geological Society of America Bulletin* 113: 1234–1246.
- DE SOUZA S., TREMBLAY A., RUFFET G. & PINET N. 2012. Ophiolite obduction in the Quebec Appalachians, Canada—. *Canadian Journal of Earth Sciences* 49: 91–110.
- ETTENSohn F. R. 2005. 5. The sedimentary record of foreland-basin, tectophase cycles: Examples from the Appalachian Basin, USA. In: *Developments in Sedimentology* pp. 139–172. Elsevier.
- MACDONALD F. A., RYAN-DAVIS J., COISH R. A., CROWLEY J. L. & KARABINOS P. 2014. A newly identified Gondwanan terrane in the northern Appalachian Mountains: Implications for the Taconic orogeny and closure of the Iapetus Ocean. *Geology* 42: 539–542.
- MCLENNAN S. M., BOCK B., COMPSTON W., HEMMING S. R. & MCDANIEL D. K. 2001. Detrital zircon geochronology of Taconian and Acadian foreland sedimentary rocks in New England. *Journal of Sedimentary Research* 71: 305–317.
- MILLER B. V. & BARR S. M. 2004. Metamorphosed Gabbroic Dikes Related to Opening of Iapetus Ocean at the St. Lawrence Promontory: Blair River Inlier, Nova Scotia, Canada. *The Journal of Geology* 112: 277–288.
- QUINN L. 1992. Diagenesis of the Goose Tickle Group, western Newfoundland. In: p. 26. Report for Mobil Oil.
- TREMBLAY A. & PINET N. 2016. Late Neoproterozoic to Permian tectonic evolution of the Quebec Appalachians, Canada. *Earth-Science Reviews* 160: 131–170.
- VAN STAAL C. R., ZAGOREVSKI A., MCNICOLL V. J. & ROGERS N. 2014. Time-Transgressive Salinic and Acadian Orogenesis, Magmatism and Old Red Sandstone Sedimentation in Newfoundland. *Geoscience Canada* 41: 138.
- WALDRON J. W. F., BARR S. M., PARK A. F., WHITE C. E. & HIBBARD J. 2015. Late Paleozoic strike-slip faults in Maritime Canada and their role in the reconfiguration of the northern Appalachian orogen. *Tectonics* 34: 1661–1684.
- WALDRON J. W. & VAN STAAL C. R. 2001. Taconian orogeny and the accretion of the Dashwoods block: A peri-Laurentian microcontinent in the Iapetus Ocean. *Geology* 29: 811–814.
- ZAGOREVSKI A., LISSEBERG C. J. & VAN STAAL C. R. 2009. Dynamics of accretion of arc and backarc crust to continental margins: Inferences from the Annieopsquotch accretionary tract, Newfoundland Appalachians. *Tectonophysics* 479: 150–164.

Bibliography

- ALLEN J. S. 2009. Paleogeographic reconstruction of the St. Lawrence promontory, western Newfoundland. PhD, University of Kentucky.
- ALLEN J. S., THOMAS W. A. & LAVOIE D. 2010. The Laurentian margin of northeastern North America. In: *From Rodinia to Pangea: The Lithotectonic Record of the Appalachian Region* (Ed. by R. P. Tollo, M. J. Bartholomew, J. P. Hibbard & P. M. Karabinos), pp. 71–90.
- ALLMENDINGER R. W. 1998. Inverse and forward modeling of trishear fault-propagation folds. *Tectonics* 17: 640–656.
- ANONYMOUS 1998. Interpretation report of seismic survey LABMIN 92-T9G: Parsons Pond (E.P. 92-101). In: p. 3. Labrador Mining and Exploration Co. Ltd.
- ASHTON K. E., HEAMAN L. M., LEWRY J. F., HARTLAUB R. P. & SHI R. 1999. Age and origin of the Jan Lake Complex: a glimpse at the buried Archean craton of the Trans-Hudson Orogen. *Canadian Journal of Earth Sciences* 36: 185–208.
- BASHFORTH A. R. 1995. Provenance of the Red Island Road Formation, western Newfoundland. B. Sc. Thesis, Brandon University, Brandon Man.
- BATTEN HENDER K. L. 2007. Mixed siliciclastic-carbonate ramp sediments and coral bioherms of the Late Ordovician Lourdes Formation, western Newfoundland: Sedimentology, stratigraphy, and tectonic significance. PhD Thesis, Carleton University, Ottawa.
- BATTEN HENDER K. L. & DIX G. R. 2006. Facies, geometry and geological significance of Late Ordovician (early Caradocian) coral bioherms: Lourdes Formation, western Newfoundland. *Sedimentology* 53: 1361–1379.
- BATTEN HENDER K. L. & DIX G. R. 2008. Facies development of a Late Ordovician mixed carbonate-siliciclastic ramp proximal to the developing Taconic orogen: Lourdes Formation, Newfoundland, Canada. *Facies* 54: 121–149.
- BEAUMONT C. 1981. Foreland basins. *Geophysical Journal International* 65: 291–329.
- BERGSTRÖM S. M., RIVA J. & KAY M. 1974. Significance of conodonts, graptolites, and shelly faunas from the Ordovician of western and north-central Newfoundland. *Canadian Journal of Earth Sciences* 11: 1625–1660.
- BICKFORD M. E., WOODEN J. L. & BAUER R. L. 2006. SHRIMP study of zircons from Early Archean rocks in the Minnesota River Valley: Implications for the tectonic history of the Superior Province. *Geological Society of America Bulletin* 118: 94–108.
- BIRD J. M. & DEWEY J. F. 1970. Lithosphere plate-continental margin tectonics and the evolution of the Appalachian orogen. *Geological Society of America Bulletin* 81: 1031–1060.

- BOCK B., McLENNAN S. M. & HANSON G. N. 1998. Geochemistry and provenance of the middle Ordovician Austin Glen member (Normanskill formation) and the Taconian orogeny in New England. *Sedimentology* 45: 635–655.
- BOONE G. M. & BOUDETTE E. L. 1989. Accretion of the Boundary Mountains terrane within the northern Appalachian orthotectonic zone. *Geological Society of America Special Papers* 228: 17–42.
- BOSWORTH W. 1989. Mélange fabrics in the unmetamorphosed external terranes of the northern Appalachians. In: *Melanges and Olistostromes of the U.S. Appalachians* (Ed. by J. W. Horton & N. Rast), pp. 65–92. Geological Society of America.
- BOTSFORD J. W. 1987. Depositional history of Middle Cambrian to Lower Ordovician deep water sediments, Bay of Islands, western Newfoundland. PhD Thesis, Memorial University of Newfoundland.
- BOTSFORD J. W. 1988. Geochemistry and petrology of Lower Paleozoic platform-equivalent shales, western Newfoundland. *Newfoundland and Labrador, Department of Mines, Mineral Development Division, Report 88-1*: 85–98.
- BRADLEY D. C. 1983. Tectonics of the Acadian orogeny in New England and adjacent Canada. *The Journal of Geology* 91: 381–400.
- BRADLEY D. C. & KIDD W. S. F. 1991. Flexural extension of the upper continental crust in collisional foredeeps. *Geological Society of America Bulletin* 103: 1416–1438.
- BRADLEY D. C., TUCKER R. D., LUX D. R., HARRIS A. G. & MCGREGOR D. C. 2000. Migration of the Acadian orogen and foreland basin across the northern Appalachians of Maine and adjacent areas. *U.S. Geological Survey Professional paper* 1624: 49.
- BRADLEY K. E., FENG L., HILL E. M., NATAWIDJAJA D. H. & SIEH K. 2017. Implications of the diffuse deformation of the Indian Ocean lithosphere for slip partitioning of oblique plate convergence in Sumatra: Sumatran Slip Partitioning. *Journal of Geophysical Research: Solid Earth* 122: 572–591.
- BUMP A. P. 2003. Reactivation, trishear modeling, and folded basement in Laramide. *GSA Today*: 4–10.
- BURDEN E. T., QUINN L., NOWLAN G. S. & BAILEY-NILL L. A. 2002. Palynology and micropaleontology of the Clam Bank Formation (Lower Devonian) of western Newfoundland, Canada. *Palynology* 26: 185–215.
- BURDEN E. T. & WILLIAMS S. H. 1995. Biostratigraphy and thermal maturity of strata in Hunt-Pan Canadian Port au Port well # 1. Hunt oil, St. John's Newfoundland.
- BURTON W. C. & SOUTHWORTH S. 2010. A model for Iapetan rifting of Laurentia based on Neoproterozoic dikes and related rocks. *Geological Society of America Memoirs* 206: 455–476.

- BUTLER R. W. H. 1982. . *Journal of Structural Geology* 4: 239–245.
- CALVERT A. J. & LUDDEN J. N. 1999. Archean continental assembly in the southeastern Superior Province of Canada. *Tectonics* 18: 412–429.
- CASTONGUAY S., RUFFET G., TREMBLAY A. & FÉRAUD G. 2001. Tectonometamorphic evolution of the southern Quebec Appalachians: 40Ar/39Ar evidence for Middle Ordovician crustal thickening and Silurian–Early Devonian exhumation of the internal Humber zone. *Geological Society of America Bulletin* 113: 144–160.
- CASTONGUAY S., VAN STAAL C. R., JOYCE N., SKULSKI T. & HIBBARD J. P. 2014. Taconic Metamorphism Preserved in the Baie Verte Peninsula, Newfoundland Appalachians: Geochronological Evidence for Ophiolite Obduction and Subduction and Exhumation of the Leading Edge of the Laurentian (Humber) Margin During Closure of the Taconic Seaway. *Geoscience Canada* 41: 459.
- CATUNEANU O. 2004. Retroarc foreland systems-evolution through time. *Journal of African Earth Science* 38: 225–242.
- CAWOOD P. A. 1993. Acadian orogeny in west Newfoundland: Definition, character, and significance. *Geological Society of America Special Papers* 275: 135–152.
- CAWOOD P. A., DUNNING G. R., LUX D. & VAN GOOL J. A. M. 1994. Timing of peak metamorphism and deformation along the Appalachian margin of Laurentia in Newfoundland: Silurian, not Ordovician. *Geology* 22: 399–402.
- CAWOOD P. A., VAN GOOL J. A. & DUNNING G. R. 1996. Geological development of eastern Humber and western Dunnage zones: Corner Brook–Glover Island region, Newfoundland. *Canadian Journal of Earth Sciences* 33: 182–198.
- CAWOOD P. A., MCCAUSLAND P. J. & DUNNING G. R. 2001. Opening Iapetus: Constraints from the Laurentian margin in Newfoundland. *Geological Society of America Bulletin* 113: 443–453.
- CAWOOD P. A. & NEMCHIN A. A. 2001. Paleogeographic development of the east Laurentian margin: Constraints from U-Pb dating of detrital zircons in the Newfoundland Appalachians. *Geological Society of America Bulletin* 113: 1234–1246.
- CAWOOD P. A., NEMCHIN A. A. & STRACHAN R. 2007. Provenance record of Laurentian passive-margin strata in the northern Caledonides: Implications for paleodrainage and paleogeography. *Geological Society of America Bulletin* 119: 993–1003.
- CAWOOD P. A., NEMCHIN A. A., STRACHAN R., PRAVE T. & KRABBENDAM M. 2007c. Sedimentary basin and detrital zircon record along East Laurentia and Baltica during assembly and breakup of Rodinia. *Journal of the Geological Society* 164: 257–275.
- CAWOOD P. A. & WILLIAMS H. 1987. Geology of Portland Creek Area (121/4) Western Newfoundland. Geologic Survey of Canada.

- CAWOOD P. A. & WILLIAMS H. 1988. Acadian basement thrusting, crustal delamination, and structural styles in and around the Humber Arm allochthon, western Newfoundland. *Geology* 16: 370.
- CHAN Y. C., CRESPI J. M. & HODGES K. V. 2001. Dating cleavage formation in slates and phyllites with the western New England Appalachians, U.S.A: *Terra Nova* 12: 264–271.
- CHEATHAM M. L., OLSZEWSKI W. J. & GAUDETTE H. E. 1989. Interpretation of the regional significance of the Chain Lakes massif, Maine based on preliminary isotopic studies. In: *Studies in Maine geology* (Ed. by R. D. Tucker & R. G. Marvinney), pp. 125–137. Maine Geological Survey, Augusta, Maine.
- CHOW N. & JAMES N. P. 1987. Cambrian Grand Cycles: A northern Appalachian perspective. *Geological Society of America Bulletin* 98: 418.
- COAKLEY B. & GURNIS M. 1995. Far-field tilting of Laurentia during the Ordovician and constraints on the evolution of a slab under an ancient continent. *Far-field tilting of Laurentia during the Ordovician and constraints on the evolution of a slab under an ancient continent* 100: 6313–6327.
- COOK L. A. & KILFOIL G. J. 2009. Aeromagnetic Survey - Gros Morne - Port au Choix Area, Newfoundland: NTS map area 12H/12. Nalcor Energy; Energy Branch, Department of Natural Resources.
- COOPER M., WEISSENBERGER J., KNIGHT I., HOSTAD D., GILLESPIE D., WILLIAMS H., BURDEN E., PORTER-CHAUDHRY J., RAE D. & CLARK E. 2001. Basin evolution in western Newfoundland: new insights from hydrocarbon exploration. *AAPG bulletin* 85: 393–418.
- COOPER R. A., SADLER P. M., HAMMER O. & GRADSTEIN F. M. 2012. The Ordovician Period. In: *The Geologic Time Scale* (Ed. by F. M. Gradstein, J. G. Ogg, M. Schmitz & G. Ogg), pp. 489–523. Elsevier.
- CORFU F., DAVIS D. W., STONE D. & MOORE M. L. 1998. Chronostratigraphic constraints on the genesis of Archean greenstone belts, northwestern Superior Province, Ontario, Canada. *Precambrian Research* 92: 277–295.
- CORFU F. & LIN S. 2000. Geology and U-Pb geochronology of the Island Lake greenstone belt, northwestern Superior Province, Manitoba. *Canadian Journal of Earth Sciences* 37: 1275–1286.
- COURTNEY R. C. 2013. Canada GEESE 2: Visualization of Integrated Marine Geoscience Data for Canadian and Proximal Waters. *Geoscience Canada* 40: 141.
- DE GRACIANSKY P.-C., ROBERTS D. G. & TRICART P. 2011. Chapter Thirteen - Birth of the Western and Central Alps: Structural Inversion and the Onset of Orogenesis. In: *The Western Alps, from Rift to Passive Margin to Orogenic Belt* (Ed. by P.-C. De Graciansky, D. G. Roberts & P. Tricart), pp. 269–288. Elsevier.

- DE SOUZA S., TREMBLAY A., RUFFET G. & PINET N. 2012. Ophiolite obduction in the Quebec Appalachians, Canada. *Canadian Journal of Earth Sciences* 49: 91–110.
- DECELLES P. G. & GILES K. A. 1996. Foreland basin systems. *Basin research* 8: 105–123.
- DEWEY J. F. & BIRD J. M. 1971. Origin and emplacement of the ophiolite suite: Appalachian ophiolite in Newfoundland. *American Geophysical Union* 76: 3179–3206.
- DEWEY J. F. & CASEY J. F. 2013. The sole of an ophiolite: the Ordovician Bay of Islands Complex, Newfoundland. *Journal of the Geological Society* 170: 715–722.
- DIAMENT M., HARJONO H., KARTA K., DEPLUS C., DAHRIN D., ZEN, JR. M. T., GÉRARD M., LASSAL O., MARTIN A. & MALOD J. 1992. Mentawai fault zone off Sumatra: A new key to the geodynamics of western Indonesia. *Geology* 20: 259.
- DIETRICH J., LAVOIE D., HANNIGAN P., PINET N., CASTONGUAY S., GILES P. & HAMBLIN A. 2011. Geological setting and resource potential of conventional petroleum plays in Paleozoic basins in eastern Canada 59: 54–84.
- DIX G. R., NEHZA O. & OKON I. 2013. Tectonostratigraphy of the Chazyan (Late Middle-Early Late Ordovician) Mixed Siliciclastic-Carbonate Platform, Quebec Embayment. *Journal of Sedimentary Research* 83: 451–474.
- DIX G. R., ROBINSON G. W. & MCGREGOR D. C. 1998. Paleokarst in the Lower Ordovician Beekmantown Group, Ottawa Embayment: structural control inboard of the Appalachian orogen. *Geological Society of America Bulletin* 110: 1046–1059.
- DORAIS M. J., ATKINSON M., KIM J., WEST D. P., KIRBY G. A. & MURPHY B. 2011. Where is the Iapetus suture in northern New England? A study of the Ammonoosuc Volcanics, Bronson Hill terrane, New Hampshire. *Canadian Journal of Earth Sciences* 49: 189–205.
- DOWNEY M. W., LIN S., BÖHM C. O. & RAYNER N. M. 2009. Timing and kinematics of crustal movement in the Northern Superior superterrane: Insights from the Gull Rapids area of the Split Lake Block, Manitoba. *Precambrian Research* 168: 134–148.
- DUBÉ B., DUNNING G. R., LAUZIÈRE K. & RODDICK J. C. 1996. New insights into the Appalachian Orogen from geology and geochronology along the Cape Ray fault zone, southwest Newfoundland. *Geological Society of America Bulletin* 108: 101–116.
- DUMONT R. & JONES A. 2013. Aeromagnetic survey of offshore western Newfoundland, NTS 11, Newfoundland and Labrador / Levé aéromagnétique extracôtier de l'ouest de Terre-Neuve, SNRC 11, Terre-Neuve-et-Labrador. Newfoundland and Labrador Department of Natural Resources.
- DUNNING G. R. & COUSINEAU P. A. 1990. U/Pb ages of single zircons from Chain Lakes massif and a correlative unit in ophiolitic melange in Quebec. *Geological Society of America Abstracts with Programs* 22: 13.

- DUNNING G. R. & KROGH T. E. 1985. Geochronology of ophiolites of the Newfoundland Appalachians. *Canadian Journal of Earth Sciences* 22: 1659–1670.
- DUNNING G. R., O'BRIEN S. J., COLMAN-SADD S. P., BLACKWOOD R. F., DICKSON W. L., O'NEILL P. P. & KROGH T. E. 1990. Silurian Orogeny in the Newfoundland Appalachians. *The Journal of Geology* 98: 895–913.
- ELHLOU S., BELOUSOVA E., GRIFFIN W. L., PEARSON N. J. & O'REILLY S. Y. 2006. Trace element and isotopic composition of GJ-red zircon standard by laser ablation. *Geochimica et Cosmochimica Acta* 70: A158.
- ELLIOTT D. & JOHNSON M. R. . 1980. Structural evolution in the northern part of the Moine thrust belt, NW Scotland. *Transactions of the Royal Society of Edinburgh: Earth Sciences* 71: 69–96.
- ETTENSohn F. R. 2004. Modeling the nature and development of major paleozoic clastic wedges in the Appalachian Basin, USA. *Journal of Geodynamics* 37: 657–681.
- ETTENSohn F. R. 2005. 5. The sedimentary record of foreland-basin, tectophase cycles: Examples from the Appalachian Basin, USA. In: *Developments in Sedimentology* pp. 139–172. Elsevier.
- ETTENSohn F. R. & BRETT C. E. 2002. Stratigraphic evidence from the Appalachian basin for the continuation of the taconian orogeny into the Early Silurian time. *Physics and Chemistry of the Earth* 27: 279–288.
- FÄHRAEUS L. E. 1966. Lower Viruan (Middle Ordovician) conodonts from the Gullhogen quarry, southern central Sweden. *Sveriges Geologiska Undersökning Ser C* 610: 1–40.
- GARDE A. A., HAMILTON M. A., CHADWICK B., GROCOTT J. & MCCAFFREY K. J. 2002. The Ketilidian orogen of South Greenland: geochronology, tectonics, magmatism, and fore-arc accretion during Palaeoproterozoic oblique convergence. *Canadian Journal of Earth Sciences* 39: 765–793.
- GAWTHORPE R. L. & LEEDER M. R. 2000. Tectono-sedimentary evolution of active extensional basins. *Basin Research* 12: 195–218.
- GEHRELS G., VALENCIA V. & PULLEN A. 2006. Detrital zircon geochronology by laser ablation multicollector ICPMS at the Arizona Laserchron Center. In: *Geochronology: Emerging opportunities* (Ed. by T. D. Olszewski), pp. 67–76. Paleontological Society Papers.
- GERBI C. C., JOHNSON S. E. & ALEINIKOFF J. N. 2006. Origin and orogenic role of the Chain Lakes massif, Maine and Quebec. *Canadian Journal of Earth Sciences* 43: 339–366.
- GLOBENSKY Y. 1981. Régions de Lacolle Saint-Jean (s). In: p. 197. Rapport géologique, Ministère de l'Énergie et des Ressources du Québec.
- GLOBENSKY Y. 1987. Géologie des Basses-Terres du Sainte-Laurent, Quebec.. *Ministere des Richesses Naturelles de Quebec* MM 85-02: 63.

- GODLEWSKI M. 1997. Geophysical interpretation report Portland/Bellburns program west Newfoundland. Talisman Energy Inc.
- GRANADO P., THONY W., CARRERA N., GRATZER O., STRAUSS P. & MUNOZ J. A. 2016. Basement-involved reactivation in foreland fold-and-thrust belts: the Alpine-Carpathian Junction (Austria). *Geological Magazine* 153: 1110–1135.
- HADDAD D. & WATTS A. B. 1999. Subsidence history, gravity anomalies, and flexure of the northeast Australian margin in Papua New Guinea. *Tectonics* 18: 827–842.
- HAYMAN N. W. & KIDD W. S. F. 2002. Reactivation of prethrusting, synconvergence normal faults as ramps within the Ordovician Champlain-Taconic thrust system. *Geological Society of America Bulletin* 114: 476–489.
- HEAMAN L. M., ERDMER P. & OWEN J. V. 2002. U–Pb geochronologic constraints on the crustal evolution of the Long Range Inlier, Newfoundland. *Canadian Journal of Earth Sciences* 39: 845–865.
- HIBBARD J. P., VAN STAAL C. R. & RANKIN D. W. 2010. Comparative analysis of the geological evolution of the northern and southern Appalachian orogen: Late Ordovician-Permian. In: *From Rodinia to Pangea: The Lithotectonic Record of the Appalachian Region* (Ed. by R. P. Tollo, M. J. Bartholomew, J. P. Hibbard & P. M. Karabinos), pp. 51–69. Geological Society of America.
- HIBBARD J. P., VAN STAAL C. R., RANKIN D. W. & WILLIAMS H. 2006. Lithotectonic Map of the Appalachian Orogen, Canada- United States of America. Geological Survey of Canada.
- HIBBARD J. P., VAN STAAL C. R. & RANKIN D. W. 2007. A comparative analysis of pre-Silurian crustal building blocks of the northern and the southern Appalachian orogen. *American Journal of Science* 307: 23–45.
- HISCOTT R. N. 1978. Provenance of Ordovician deep-water sandstones, Tourelle Formation, Quebec, and implications for initiation of the Taconic orogeny. *Canadian Journal of Earth Sciences* 15: 1579–1597.
- HISCOTT R. N. 1984. Ophiolitic source rocks for Taconic-age flysch: Trace-element evidence. *Geological Society of America Bulletin* 95: 1261–1267.
- HOFFMAN P. F. 1988. United Plates of America, The Birth of a Craton: Early Proterozoic Assembly and Growth of Laurentia. *Annual Review of Earth and Planetary Sciences* 16: 543–603.
- HOFFMAN P. F. 2014. The Origin of Laurentia: Rae Craton as the Backstop for Proto-Laurentian Amalgamation by Slab Suction. *Geoscience Canada* 41: 313.
- HUNTOON P. W. 1993. Influence of inherited Precambrian basement structures on the localization and form of Laramide monoclines, Grande Canyon, Arizona. In: *Laramide basement deformation in the Rocky Mountain foreland of the western United States: Boulder*

- Colorado* (Ed. by C. J. Schmidt), pp. 243–256. Geological Society of America Special Paper 280.
- JACKSON J. A. 1980. Reactivation of basement faults and crustal shortening in orogenic belts. *Nature* 283: 343–346.
- JACKSON S. E., PEARSON N. J., GRIFFIN W. L. & BELOUSOVA E. A. 2004. The application of laser ablation-inductively coupled plasma-mass spectrometry to in situ U–Pb zircon geochronology. *Chemical Geology* 211: 47–69.
- JACOBI R. D. 1981. Peripheral bulge—a causal mechanism for the Lower/Middle Ordovician unconformity along the western margin of the Northern Appalachians. *Earth and Planetary Science Letters* 51: 245–251.
- JAMES N. P. & STEVENS R. K. 1986. Stratigraphy and Correlation of the Cambro-Ordovician Cow Head Group, Western Newfoundland. *Geological Survey of Canada Bulletin* 366: 143.
- JAMIESON R. A., BREEMEN O. VAN, SULLIVAN R. W. & CURRIE K. L. 1986. The age of igneous and metamorphic events in the western Cape Breton Highlands, Nova Scotia. *Canadian Journal of Earth Sciences* 23: 1891–1901.
- JORDAN T. E. 1981. Thrust loads and foreland basin evolution, Cretaceous, western United States. *AAPG bulletin* 65: 2506–2520.
- KARABINOS P. 1988. Tectonic significance of basement-cover relationships in the Green Mountain massif, Vermont. *The Journal of Geology* 96: 445–454.
- KARABINOS P., ALEINIKOFF J. N. & FANNING C. M. 1999. Distinguishing Grenvillian basement from pre-Taconian cover rocks in the northern Appalachians. *American Journal of Science* 299: 502–515.
- KARABINOS P., MACDONALD F. A. & CROWLEY J. L. 2017. Bridging the gap between the foreland and hinterland I: Geochronology and plate tectonic geometry of Ordovician magmatism and terrane accretion on the Laurentian margin of New England. *American Journal of Science* 317: 515–554.
- KARABINOS P., MORRIS D., HAMILTON M. & RAYNER N. 2008. Age, origin, and tectonic significance of Mesoproterozoic and Silurian felsic sills in the Berkshire massif, Massachusetts. *American Journal of Science* 308: 787–812.
- KARABINOS P., SAMSON S. D., HEPBURN J. C. & STOLL H. M. 1998. Taconian orogeny in the New England Appalachians: Collision between Laurentia and the Shelburne Falls arc. *Geology* 26: 215–218.
- KLAPPER G. & KIRCHGASSER W. T. 2016. Frasnian Late Devonian conodont biostratigraphy in New York: graphic correlation and taxonomy. *Journal of Paleontology* 90: 525–554.

- KNIGHT I. & JAMES N. P. 1987. The stratigraphy of the Lower Ordovician St. George Group, western Newfoundland: the interaction between eustasy and tectonics. *Canadian Journal of Earth Sciences* 24: 1927–1951.
- KNIGHT I., JAMES N. P. & LANE T. E. 1991a. The Ordovician St. George Unconformity, northern Appalachians: The relationship of plate convergence at the St. Lawrence Promontory to the Sauk/Tippecanoe sequence boundary. *Geological Society of America Bulletin* 103: 1200–1225.
- KNIGHT I., JAMES N. P. & LANE T. E. 1991. The Ordovician St. George Unconformity, northern Appalachians: The relationship of plate convergence at the St. Lawrence Promontory to the Sauk/Tippecanoe sequence boundary. *Geological Society of America Bulletin* 103: 1200–1225.
- KONSTANTINOVSKAYA E. A., RODRIGUEZ D., KIRKWOOD D., HARRIS L. B. & THERIAULT R. 2009. Effects of basement structure, sedimentation and erosion on thrust wedge geometry: an example from the Quebec Appalachians and analogue models. *Bulletin of Canadian Petroleum Geology* 57: 34–62.
- KUMARAPELI P. S. 1985. Vestiges of Iapetan rifting in the craton west of the northern Appalachians. *Journal of the Geological Association of Canada* 12: 54–59.
- LACOMBE O. & MOUTHEREAU F. 2002. Basement-involved shortening and deep detachment tectonics in forelands of orogens: Insights from recent collision belts (Taiwan, Western Alps, Pyrenees). *Tectonics* 21: 12–1--12–22.
- LACOMBE R. 2017. Stratigraphic and structural relationships in the foreland basin and Humber Arm Allochthon on Port au Port Peninsula, western Newfoundland. Masters Thesis, University of Alberta, Edmonton.
- LAFHAMME C., SYLVESTER P. J., HINCHEY A. M. & DAVIS W. J. 2013. U–Pb age and Hf-isotope geochemistry of zircon from felsic volcanic rocks of the Paleoproterozoic Aillik Group, Makkovik Province, Labrador. *Precambrian Research* 224: 129–142.
- LAMB A. T. 1976. Geophysical report on a seismic survey off western Newfoundland: Covering work done by Shell Canada Resources Limited with super long airgun (SLAG) and super long detector cable (SLDC) system during during October 1973.
- LANDING E. 2012. The Great American Carbonate Bank in eastern Laurentia: its births, deaths, and linkage to paleoceanic oxygenation (Early Cambrian–Late Ordovician). In: *The great American carbonate bank: The geology and economic resources of the Cambrian-Ordovician Sauk megasequence of Laurentia* (Ed. by J. R. Derby, R. D. Fritz, W. A. Longacre & C. A. Morgan), pp. 451–492.

- LAVOIE D. 1994. Diachronous tectonic collapse of the Ordovician continental margin, eastern Canada: comparison between the Quebec Reentrant and St. Lawrence Promontory. *Canadian Journal of Earth Sciences* 31: 1309–1319.
- LAVOIE D., BURDEN E. & LEBEL D. 2003. Stratigraphic framework for the Cambrian Ordovician rift and passive margin successions from southern Quebec to western Newfoundland. *Canadian Journal of Earth Sciences* 40: 177–205.
- LAVOIE D., HAMBLIN A. P., THÚRIAULT R., BEAULIEU J. & KIRKWOOD D. 2008. *Geological Survey of Canada, Open File 5900*. Natural Resources Canada.
- LEE C.-I., CHANG Y.-L. & COWARD M. P. 2002. Inversion tectonics of the fold-and-thrust belt, western Taiwan. In: *Geophysics of an Arc-Continent Collision, Taiwan* (Ed. by T. B. Byrne & C.-S. Liu), pp. 13–30. Geological Society of America, Boulder, Colorado.
- LIN S., DAVIS D. W., BARR S. M., VAN STAAL C. R., CHEN Y. & CONSTANTIN M. 2007. U-Pb geochronological constraints on the evolution of the Aspy terrane, Cape Breton Island: implications for relationships between Aspy and Bras d'Or terranes and Ganderia in the Canadian Appalachians. *American Journal of Science* 307: 371–398.
- LUDWIG K. R. 2012. User's manual for Isoplot 3.75. *Berkeley Geochronology Center Special Publication* 5: 75.
- LUS W. Y., MCDUGALL I. & DAVIES H. L. 2004. Age of the metamorphic sole of the Papuan Ultramafic Belt ophiolite, Papua New Guinea. *Tectonophysics* 392: 85–101.
- MACDONALD F. A., KARABINOS P. M., CROWLEY J. L., HODGIN E. B., CROCKFORD P. W. & DELANO J. W. 2017. Bridging the gap between the foreland and hinterland II: Geochronology and tectonic setting of Ordovician magmatism and basin formation on the Laurentian margin from New England to Newfoundland. *American Journal of Science* 317: 555–596.
- MACDONALD F. A., RYAN-DAVIS J., COISH R. A., CROWLEY J. L. & KARABINOS P. 2014. A newly identified Gondwanan terrane in the northern Appalachian Mountains: Implications for the Taconic orogeny and closure of the Iapetus Ocean. *Geology* 42: 539–542.
- MALETZ J. 2001. A condensed Lower to Middle Ordovician graptolite succession at Matane, Quebec, Canada. *Canadian Journal of Earth Sciences* 38: 1531–1539.
- MALO M., TREMBLAY A. & KIRKWOOD D. 1995. Along-strike Acadian structural variations in the Quebec Appalachians: Consequence of a collision along an irregular margin. *Tectonics* 14: 1327–1338.
- MARSHAK S., KARLSTROM K. & TIMMONS J. M. 2000. Inversion of Proterozoic extensional faults: An explanation for the pattern of Laramide and ancestral Rockies intracratonic deformation, United States. *Geology* 28: 735–738.

- MCDANIEL D. K., HANSON G. N., MCLENNAN S. M. & SEVIGNY J. H. 1997. Grenvillian provenance for the amphibolite-grade Trap Falls Formation: implications for early Paleozoic tectonic history of New England. *Canadian Journal of Earth Sciences* 34: 1286–1294.
- MCLENNAN S. M., BOCK B., COMPSTON W., HEMMING S. R. & MCDANIEL D. K. 2001. Detrital zircon geochronology of Taconian and Acadian foreland sedimentary rocks in New England. *Journal of Sedimentary Research* 71: 305–317.
- MELCHIN M. J., SADLER P. M., CRAMER B. D., COOPER R. A., GRADSTEIN F. M. & HAMMER O. 2012. The Geologic Time Scale 2012. In: *The Silurian Period* (Ed. by F. M. Gradstein, J. G. Ogg, M. Schmitz & G. Ogg), pp. 525–558. Elsevier.
- MILLER B. V. 1997. Geology, geochronology, and tectonic significance of the Blair River Inlier, northern Cape Breton Island, Nova Scotia. PhD, Dalhousie University, Halifax, Nova Scotia.
- MILLER B. V. & BARR S. M. 2000. Petrology and Isotopic Composition of the Grenvillian Basement Fragment in the Northern Appalachian Orogen: Blair River Inlier, Nova Scotia, Canada. *Journal of Petrology* 41: 1777–1804.
- MILLER B. V., DUNNING G. R., BARR S. M., RAESIDE R. P., JAMIESON R. A. & REYNOLDS P. H. 1996. Magmatism and metamorphism in a Grenvillian fragment: U-Pb and $^{40}\text{Ar}/^{39}\text{Ar}$ ages from the Blair River Complex, northern Cape Breton Island, Nova Scotia, Canada. *Geological Society of America Bulletin* 108: 127–140.
- MITRA S. & MOUNT V. S. 1998. Foreland basement-involved structures. *AAPG bulletin* 82: 70–109.
- MOENCH R. H. & ALEINIKOFF J. N. 2003. Erratum to “Stratigraphy, geochronology, and accretionary terrane settings of two Bronson Hill arc sequences, northern New England”. *Physics and Chemistry of the Earth* 28: 113–160.
- MONTARIO M. J. & GARVER J. I. 2009. The Thermal Evolution of the Grenville Terrane Revealed through U-Pb and Fission-Track Analysis of Detrital Zircon from Cambro-Ordovician Quartz Arenites of the Potsdam and Galway Formations. *The Journal of Geology* 117: 595–614.
- MURPHY J. B., FERNÁNDEZ-SUÁREZ J., KEPPIE J. D. & JEFFRIES T. E. 2004. Contiguous rather than discrete Paleozoic histories for the Avalon and Meguma terranes based on detrital zircon data. *Geology* 32: 585–588.
- MURPHY J. B., VAN STAAL C. R. & KEPPIE J. D. 1999. Middle to late Paleozoic Acadian orogeny in the northern Appalachians: A Laramide-style plume-modified orogeny?. *Geology* 27: 653–656.

- NIKOLAIEVA K., GERYA T. V. & MARQUES F. O. 2010. Subduction initiation at passive margins: Numerical modeling. *Journal of Geophysical Research* 115.
- NUTMAN A. P., FRIEND C. R. L., BARKER S. L. L. & MCGREGOR V. R. 2004. Inventory and assessment of Palaeoarchaeic gneiss terrains and detrital zircons in southern West Greenland. *Precambrian Research* 135: 281–314.
- O'BRIAN B. 2003. Geology of the central Notre Dame Bay region (parts of NTS areas 2E/3,6,11), northeastern Newfoundland. In: p. 147. Government of Newfoundland and Labrador, Department of Mines and Energy, Geological Survey, St. John's Newfoundland.
- O'BRIEN B. & O'BRIEN S. 1989. Geology of the Western Hermitage Flexure: Bay D'est fault and south (Parts of 11 O/9, 11 O/16, 11 P/12 and 11 P/13), southwest Newfoundland. Newfoundland Department of Mines and Energy.
- OWEN J. V. & ERDMER P. 1989. Metamorphic geology and regional geothermobarometry of a Grenvillian massif: the Long Range Inlier, Newfoundland. *Precambrian Research* 43: 79–100.
- PALMER S. E., BURDEN E. & WALDRON J. W. F. 2001. Stratigraphy of the Curling Group (Cambrian), Humber Arm Allochthon, Bay of Islands. *GSC Current research 2001-1*: 105–112.
- PALMER S. E., WALDRON J. W. F. & SKILLITER D. M. 2002. Post-Taconian shortening, inversion and strike slip in the Stephenville area, western Newfoundland Appalachians. *Canadian Journal of Earth Sciences* 39: 1393–1410.
- PENG S., BABCOCK L. E. & COOPER R. A. 2012. The Cambrian Period. In: *The Geologic Time Scale* (Ed. by F. M. Gradstein, J. G. Ogg, M. Schmitz & G. Ogg), pp. 437–488. Elsevier.
- PINCIVY A., MALO M., RUFFET G., TREMBLAY A. & SACKS P. E. 2003. Regional metamorphism of the Appalachian Humber zone of Gaspé Peninsula: $^{40}\text{Ar}/^{39}\text{Ar}$ evidence for crustal thickening during the Taconian orogeny. *Canadian Journal of Earth Sciences* 40: 301–315.
- PINET N., KEATING P., LAVOIE D., DIETRICH J., DUCHESNE M. J. & BRAKE V. 2012. Revisiting the Appalachian structural front and offshore Anticosti Basin (northern Gulf of St. Lawrence, Canada) by integrating old and new geophysical datasets. *Marine and Petroleum Geology* 32: 50–62.
- PINET N. & TREMBLAY A. 1995. Tectonic evolution of the Quebec-Maine Appalachians: from oceanic spreading to obduction and collision in the northern Appalachians. *American Journal of Science* 295: 173–200.
- POLLOCK J. C., WILTON D. H. C., VAN STAAL C. R. & MORRISSEY K. D. 2007. U-Pb detrital zircon geochronological constraints on the Early Silurian collision of Ganderia and

- Laurentia along the Dog Bay Line: The terminal Iapetan suture in the Newfoundland Appalachians. *American Journal of Science* 307: 399–433.
- POTHIER H. D., WALDRON J. W. F., SCHOFIELD D. I. & DUFRANE S. A. 2015. Peri-Gondwanan terrane interactions recorded in the Cambrian–Ordovician detrital zircon geochronology of North Wales. *Gondwana Research* 28: 987–1001.
- PRAVE A. R., KESSLER II L. G., MALO M., BLOECHL W. V. & RIVA J. 2000. Ordovician arc collision and foredeep evolution in the Gaspé Peninsula, Québec: the Taconic Orogeny in Canada and its bearing on the Grampian Orogeny in Scotland. *Journal of the Geological Society, London* 157: 393–400.
- QUINN L. 1992a. Diagenesis of the Goose Tickle Group, western Newfoundland. In: p. 26. Mobil Oil.
- QUINN L. A. 1992b. Foreland and trench slope basin sandstones of the Goose Tickle group and Lower Head Formation, western Newfoundland. PhD Thesis, Memorial University of Newfoundland, St. John's Newfoundland.
- QUINN L., BASHFORTH A. R., BURDEN E. T., GILLESPIE H., SPRINGER R. K. & WILLIAMS S. H. 2004. The Red Island Road Formation: Early Devonian terrestrial fill in the Anticosti Foreland Basin, western Newfoundland. *Canadian Journal of Earth Sciences* 41: 587–602.
- QUINN L., WILLIAMS S. H., HARPER D. A. T. & CLARKSON E. N. K. 1999. Late Ordovician foreland basin fill: Long Point Group of onshore western Newfoundland. *Bulletin of Canadian Petroleum Geology* 47: 63–80.
- REEVES C. 2005. Aeromagnetic surveys: Principles, Practice and Interpretation. *Geosoft*.
- REUSCH D. N. & VAN STAAL C. R. 2012. The Dog Bay–Liberty Line and its significance for Silurian tectonics of the northern Appalachian orogen. *Canadian Journal of Earth Sciences* 49: 239–258.
- RIVERS T. 1997. Lithotectonic elements of the Grenville Province: review and tectonic implications. *Precambrian Research* 86: 117–154.
- RIVERS T. 2008. Assembly and preservation of lower, mid, and upper orogenic crust in the Grenville Province—Implications for the evolution of large hot long-duration orogens. *Precambrian Research* 167: 237–259.
- RIVERS T. 2015. Tectonic Setting and Evolution of the Grenville Orogen: An Assessment of Progress Over the Last 40 Years. *Geoscience Canada* 42: 77–124.
- ROBERTS M. 2011. Nalcor Energy - Oil and Gas Inc. Final Well Report for Nalcor Energy et al Finnegan # 1 at Permit 03-102, Western Newfoundland. In: p. 845. Nalcor Energy, Oil and Gas.

- ROBINSON P., TUCKER R. D., BRADLEY D., BERRY IV H. N. & OSBERG P. H. 1998. Paleozoic orogens in New England, USA. *GFF* 120: 119–148.
- RODGERS J. 1965. Long Point and Clam Bank formations, western Newfoundland. *Geological Association of Canada Proceedings* 16: 83–94.
- RODGERS N. & VAN STAAL C. R. 2002. Toward a Victoria Lake Supergroup: a provisional stratigraphic revision of the Red Indian to Victoria lakes area, central Newfoundland. In: pp. 185–195. Newfoundland Department of Mines and Energy.
- ROWLEY D. B. & KIDD W. S. F. 1982. Stratigraphic relationships and detrital composition of the medial flysch of western New England: implications for the tectonic evolution of the Taconic Orogeny. *Journal of Geology* 90: 219–226.
- RUFFMAN A. & WOODSIDE J. 1970. The Odd-twins magnetic anomaly and its possible relationship to the Humber Arm Klippe of Western Newfoundland, Canada. *Canadian Journal of Earth Sciences* 7: 326–337.
- SALAD HERSI O., LAVOIE D. & NOWLAN G. S. 2003. Reappraisal of the Beekmantown Group sedimentology and stratigraphy, Montréal area, southwestern Quebec: implications for understanding the depositional evolution of the Lower-Middle Ordovician Laurentian passive margin of eastern Canada. *Canadian Journal of Earth Sciences* 40: 149–176.
- SANDFORD B. V. & GRANT A. C. 1990. Bedrock geological mapping and basin studies in the Gulf of St. Lawrence. In: p. 33.42. Geological Survey of Canada.
- SCHMIDT C. J. & GARIHAN J. M. 1983. Laramide tectonic development in the Rocky Mountain foreland of southwestern Montana. In: *Rocky Mountain foreland basins and uplifts* (Ed. by J. D. Lowell), pp. 271–294. Rocky Mountain Association of Geologists, Denver.
- SHAW J., COURTNEY R. C., CHRISTIAN H. & DEHLER S. 1997. Ground-truthing of multibeam bathymetry data in western Newfoundland: Bonne Bay, Bay of Islands, Port au Port region, and St. George's Bay. In: p. 25. Geologic Survey of Canada.
- SHEARER J. M. 1973. Bedrock and surficial geology of the northern Gulf of St. Lawrence as interpreted from continuous seismic reflection profiles. In: *Earth Science Symposium of Offshore Eastern Canada* (Ed. by J. D. Hood), pp. 285–303. Geologic Survey of Canada, Ottawa, ON, Canada.
- SIMONETTI A., HEAMAN L. M., HARTLAUB R. P., CREASER R. A., MACHATTIE T. G. & BÖHM C. 2005. U–Pb zircon dating by laser ablation-MC-ICP-MS using a new multiple ion counting Faraday collector array. *Journal of Analytical Atomic Spectrometry* 20: 677.
- SINCLAIR H. D. & NAYLOR M. 2012. Foreland basin subsidence driven by topographic growth versus plate subduction. *Geological Society of America Bulletin* 124: 368–379.

- SINCLAIR I. K. 1990. A Review of the Upper Precambrian and Lower Paleozoic geology of western Newfoundland and the hydrocarbon potential of the adjacent offshore area of the Gulf of St. Lawrence. Canada-Newfoundland Offshore Petroleum Board.
- SLOSS L. L. 1963. Sequences in the cratonic interior of North America. *Geological Society of America Bulletin* 74: 93–114.
- SPARKES G. W. & DUNNING G. R. 2014. Late Neoproterozoic epithermal alteration and mineralization in the western Avalon Zone: a summary of mineralogical investigations and new U/Pb geochronological results. *Current Research, Newfoundland and Labrador Department of Natural Resources Geological Survey, Report*: 14–1.
- SPENCER C., GREEN A., MILKEREIT B., LUETGERT J., STEWART D., UNGER J. & PHILLIPS J. 1989. The extension of Grenville Basement beneath the northern Appalachians: Results from the Quebec-Maine seismic reflection and refraction surveys. *Tectonics* 8: 677–696.
- ST. JULIEN P. & HUBERT C. 1975. Evolution of the Taconic orogen in the Quebec Appalachians. *American Journal of Science* 275–A: 337–362.
- VAN STAAL C. R. 2007. Pre-Carboniferous Tectonic Evolution and Metallogeny of the Canadian Appalachians. In: *Mineral Deposits of Canada: A Synthesis of Major Deposit-Types, District Metallogeny, the Evolution of Geological Provinces, and Exploration Methods* (Ed. by W. D. Goodfellow), pp. 793–818. Geological Association of Canada, Mineral Deposits Division.
- VAN STAAL C. R., CHEW D. M., ZAGOREVSKI A., MCNICOLL V., HIBBARD J., SKULSKI T., ESCAYOLA M. P., CASTONGUAY S. & SYLVESTER P. J. 2013. Evidence of Late Ediacaran Hyperextension of the Laurentian Iapetan Margin in the Birchy Complex, Baie Verte Peninsula, Northwest Newfoundland: Implications for the Opening of Iapetus, Formation of Peri-Laurentian Microcontinents and Taconic – Grampian Orogenesis. *Geoscience Canada* 40: 94.
- VAN STAAL C. R. & DE ROO J. A. 1995. Mid-Paeozoic tectonic evolution of the Appalachian Central Mobile Belt in northern New Brunswick. In: *Current Perspectives in the Appalachian-Caledonian Orogen* (Ed. by J. Hibbard, C. R. Van Staal & P. A. Cawood), pp. 367–389. Geological Association of Canada.
- VAN STAAL C. R., DEWEY J. F., NIOCAILL C. M. & MCKERROW W. S. 1998. The Cambrian-Silurian tectonic evolution of the northern Appalachians and British Caledonides: history of a complex, west and southwest Pacific-type segment of Iapetus. In: *Lyell, the Past is the Key to the Present* (Ed. by D. J. Blundell & A. C. Scott), pp. 197–242. Geological Society, London, Special Publications.
- VAN STAAL C. R., WHALEN J. B., MCNICOLL V. J., PEHRSSON S., LISSEBERG C. J., ZAGOREVSKI A., VAN BREEMEN O. & JENNER G. A. 2007. The Notre Dame arc and the Taconic orogeny

- in Newfoundland. In: *4-D Framework of Continental Crust* (Ed. by R. D. Hatcher, M. P. Carlson, J. H. McBride & J. R. Martinez Catalan), pp. 511–552.
- VAN STAAL C. R., WHALEN J. B., VALVERDE-VAQUERO P., ZAGOREVSKI A. & ROGERS N. 2009. Pre-Carboniferous, episodic accretion-related, orogenesis along the Laurentian margin of the northern Appalachians. In: *Ancient Orogens and Modern Analogues* (Ed. by J. B. Murphy, J. D. Keppie & A. J. Hynes), pp. 271–316. Geological Society, London, Special Publications.
- VAN STAAL C. R., WILSON R. A., KAMO S. L., MCCLELLAND W. C. & MCNICOLL V. 2016. Evolution of the Early to Middle Ordovician Popelogan arc in New Brunswick, Canada, and adjacent Maine, USA: Record of arc-trench migration and multiple phases of rifting. *Geological Society of America Bulletin* 128: 122–146.
- VAN STAAL C. R., WINCHESTER J. A. & BEDARD J. H. 1991. Geochemical variations in Middle Ordovician volcanic rocks of the northern Miramichi Highlands and their tectonic significance. *Canadian Journal of Earth Sciences* 28: 1031–1049.
- VAN STAAL C. R., ZAGOREVSKI A., MCNICOLL V. J. & ROGERS N. 2014. Time-Transgressive Salinic and Acadian Orogenesis, Magmatism and Old Red Sandstone Sedimentation in Newfoundland. *Geoscience Canada* 41: 138.
- STACEY J. T. & KRAMERS I. J. D. 1975. Approximation of terrestrial lead isotope evolution by a two-stage model. *Earth and planetary science letters* 26: 207–221.
- STAIT B. A. & BARNES C. R. 1991. Stratigraphy of the Middle Ordovician Long Point Group, western Newfoundland. In: *Advances in Ordovician Geology* (Ed. by C. R. Barnes & S. H. Williams), pp. 235–244. Geological Survey of Canada.
- STANLEY R. S. & RATCLIFFE N. M. 1985. Tectonic synthesis of the Taconian orogeny in western New England. *Geological Society of America Bulletin* 96: 1227–1250.
- STENZEL S. R., KNIGHT I. & JAMES N. P. 1990. Carbonate platform to foreland basin: revised stratigraphy of the Table Head Group (Middle Ordovician), western Newfoundland. *Canadian Journal of Earth Sciences* 27: 14–26.
- STEVENS R. K. 1970. Cambro-Ordovician flysch sedimentation and tectonics in west Newfoundland and their possible bearing on a proto-Atlantic Ocean. In: *Flysch Sedimentology in North America* (Ed. by P. Lajoie), pp. 165–177. Geological Association of Canada.
- STEWART D. B., WRIGHT B. E., PHILLIPS J. D. & HUTCHINSON D. R. 1993. Global Geoscience Transect 8: Quebec-Maine-Gulf of Maine Transect, Southeastern Canada, Northeastern United States of America. *U.S. Geological Survey*.

- STOCKMAL G. S., SLINGSBY A. & WALDRON J. W. 1998. Deformation styles at the Appalachian structural front, western Newfoundland: implications of new industry seismic reflection data. *Canadian Journal of Earth Sciences* 35: 1288–1306.
- STOCKMAL G. S., SLINGSBY A. & WALDRON J. W. F. 2004. Basement-involved inversion at the Appalachian structural front, western Newfoundland: an interpretation of seismic reflection data with implications for petroleum prospectivity. *Bulletin of Canadian Petroleum Geology* 52: 215–233.
- STOCKMAL G. S. & WALDRON J. W. F. 1990. Structure of the Appalachian deformation front in western Newfoundland: implications of multichannel seismic reflection data. *Geology* 18: 765–768.
- STOCKMAL G. S., WALDRON J. W. F. & QUINLAN G. M. 1995. Flexural modeling of Paleozoic foreland basin subsidence, offshore western Newfoundland: Evidence for substantial post-Taconian thrust transport. *The Journal of Geology* 103: 653–671.
- SUPPE J. & MEDWEDEFF D. A. 1990. Geometry and kinematics of fault-propagation folding. *Eclogae Geologicae Helveticae* 83: 409–454.
- TATE G. W., MCQUARRIE N., VAN HINSBERGEN D. J. J., BAKKER R. R., HARRIS R. & JIANG H. 2015. Australia going down under: Quantifying continental subduction during arc-continent accretion in Timor-Leste. *Geosphere* 11: 1860–1883.
- THOMAS W. A. 1977. Evolution of Appalachian-Ouachita salients and recesses from reentrants and promontories in the continental margin. *American Journal of Science* 277: 1233–1278.
- THOMAS W. A. & ASTINI R. A. 1999. Simple-shear conjugate rift margins of the Argentine Precordillera and the Ouachita embayment of Laurentia. *Geological Society of America Bulletin* 111: 1069–1079.
- TREMBLAY A. & CASTONGUAY S. 2002. Structural evolution of the Laurentian margin revisited (southern Quebec Appalachians): Implications for the Salinian orogeny and successor basins. *Geology* 30: 79–82.
- TREMBLAY A., LONG B. & MASSÉ M. 2003. Supracrustal faults of the St. Lawrence rift system, Québec: kinematics and geometry as revealed by field mapping and marine seismic reflection data. *Tectonophysics* 369: 231–252.
- TREMBLAY A. & PINET N. 2016. Late Neoproterozoic to Permian tectonic evolution of the Quebec Appalachians, Canada. *Earth-Science Reviews* 160: 131–170.
- TREMBLAY A., RUFFET G. & BÉDARD J. H. 2011. Obduction of Tethyan-type ophiolites—A case-study from the Thetford-Mines ophiolitic Complex, Quebec Appalachians, Canada. *Lithos* 125: 10–26.

- TREMBLAY A., RUFFET G. & CASTONGUAY S. 2000. Acadian metamorphism in the Dunnage zone of southern Québec, northern Appalachians: $^{40}\text{Ar}/^{39}\text{Ar}$ evidence for collision diachronism. *Geological Society of America Bulletin* 112: 136–146.
- TRZCIENSKI W. E., RODGERS J. & GUIDOTTI C. V. 1992. Alternative hypotheses for the Chain Lakes ‘Massif,’ Maine and Quebec. *American Journal of Science* 292: 508–532.
- TUCKER R. D. & GOWER C. F. 1994. A U-Pb geochronological framework for the Pinware terrane, Grenville Province, southeast Labrador. *The Journal of Geology* 102: 67–78.
- VAN DER VELDEN A. J., VAN STAAL C. R. & COOK F. A. 2004. Crustal structure, fossil subduction, and the tectonic evolution of the Newfoundland Appalachians: Evidence from a reprocessed seismic reflection survey. *Geological Society of America Bulletin* 116: 1485–1498.
- VOLLMER F. W. 1986. *Orient 3.2. 0 Spherical Projection and Orientation Data Analysis Software User Manual*.
- VOLLMER F. W. 1990. An application of eigenvalue methods to structural domain analysis. *Geological Society of America Bulletin* 102: 786–791.
- VOLLMER F. W. 2015. Orient 3; a new integrated software program for orientation data analysis, kinematic analysis, spherical projections, and Schmidt plots. *Abstracts with Programs - Geological Society of America* 47: 49–49.
- WALDRON J. W. F. 1985. Structural history of continental margin sediments beneath the Bay of Islands Ophiolite, Newfoundland. *Canadian Journal of Earth Sciences* 22: 1618–1632.
- WALDRON J. W. F., BARR S. M., PARK A. F., WHITE C. E. & HIBBARD J. 2015. Late Paleozoic strike-slip faults in Maritime Canada and their role in the reconfiguration of the northern Appalachian orogen: STRIKE SLIP, NORTHERN APPALACHIANS. *Tectonics*.
- WALDRON J. W. F., DEWOLFE J., COURTNEY R. & FOX D. 2002. Origin of the Odd-twins anomaly: magnetic effect of a unique stratigraphic marker in the Appalachian foreland basin, Gulf of St. Lawrence. *Canadian Journal of Earth Sciences* 39: 1675–1687.
- WALDRON J. W. F., FLOYD J. D., SIMONETTI A. & HEAMAN L. M. 2008a. Ancient Laurentian detrital zircon in the closing Iapetus ocean, Southern Uplands terrane, Scotland. *Geology* 36: 527–530.
- WALDRON J. W. F., HENRY A. D., BRADLEY J. C. & PALMER S. E. 2003. Development of a folded thrust stack: Humber Arm Allochthon, Bay of Islands, Newfoundland Appalachians. *Canadian Journal of Earth Sciences* 40: 237–253.
- WALDRON J. W. F., MCNICOLL V. J. & VAN STAAL C. R. 2012. Laurentia-derived detritus in the Badger Group of central Newfoundland: deposition during closing of the Iapetus Ocean. *Canadian Journal of Earth Sciences* 49: 207–221.

- WALDRON J. W. F., MURPHY J. B., MELCHIN M. J. & DAVIS G. 1996. Silurian tectonics of western Avalonia: strain-corrected subsidence history of the Arisaig Group, Nova Scotia. *The Journal of Geology*: 677–694.
- WALDRON J. W. F., SCHOFIELD D. I. & MURPHY J. B. 2017. Diachronous Palaeozoic accretion of peri-Gondwanan terranes at the Laurentian margin. In: *Fifty Years of the Wilson Cycle* (Ed. by R. W. Wilson, G. A. Houseman, K. J. W. McCaffrey, A. G. Dore & S. J. H. Buiter), p.
- WALDRON J. W. F., SCHOFIELD D. I., MURPHY J. B. & THOMAS C. W. 2014. How was the Iapetus Ocean infected with subduction?. *Geology* 42: 1095–1098.
- WALDRON J. W. F., SCHOFIELD D. I., WHITE C. E. & BARR S. M. 2011. Cambrian successions of the Meguma Terrane, Nova Scotia, and Harlech Dome, North Wales: dispersed fragments of a peri-Gondwanan basin?. *Journal of the Geological Society* 168: 83–98.
- WALDRON J. W. F. & STOCKMAL G. S. 1991. Mid-Paleozoic thrusting at the Appalachian deformation front: Port au Port Peninsula, western Newfoundland. *Canadian Journal of Earth Sciences* 28: 1992–2002.
- WALDRON J. W. F., STOCKMAL G. S., CORNEY R. E. & STENZEL S. R. 1993. Basin development and inversion at the Appalachian structural front, Port au Port Peninsula, western Newfoundland Appalachians. *Canadian Journal of Earth Sciences* 30: 1759–1772.
- WALDRON J. W., FLOYD J. D., SIMONETTI A. & HEAMAN L. M. 2008b. Ancient Laurentian detrital zircon in the closing Iapetus ocean, Southern Uplands terrane, Scotland. *Geology* 36: 527–530.
- WALDRON J. W. & VAN STAAL C. R. 2001. Taconian orogeny and the accretion of the Dashwoods block: A peri-Laurentian microcontinent in the Iapetus Ocean. *Geology* 29: 811–814.
- WEST D. P., LUDMAN A. & LUX D. R. 1992. Silurian age for the Pocomoonshine gabbro-diorite, southeastern Maine and its regional tectonic implications. *American Journal of Science* 292: 253–273.
- WHALEN J. B., JENNER G. A., LONGSTAFFE F. J., GARIEPY C. & FRYER B. J. 1997. Implications of granitoid geochemical and isotopic (Nd, O, Pb) data from the Cambrian-Ordovician Notre Dame arc for the evolution of the Central Mobile belt, Newfoundland Appalachians. In: *The Nature of Magmatism in the Appalachian Orogen* (Ed. by A. K. Sinha, J. B. Whalen & J. P. Hogan), pp. 367–395. Geological Society of America.
- WHALEN J. B., MCNICOLL V. J., VAN STAAL C. R., LISSEBERG C. J., LONGSTAFFE F. J., JENNER G. A. & VAN BREEMAN O. 2006. Spatial, temporal and geochemical characteristics of Silurian collision-zone magmatism, Newfoundland Appalachians: An example of a rapidly evolving magmatic system related to slab break-off. *Lithos* 89: 377–404.

- WILLIAMS H. 1975. Structural succession, nomenclature, and interpretation of transported rocks in western Newfoundland. *Canadian Journal of Earth Sciences* 12: 1874–1894.
- WILLIAMS H. 1993. Acadian orogeny in Newfoundland. *Geological Society of America Special Papers* 275: 123–134.
- WILLIAMS H., BURDEN E. T., QUINN L., VON BITTER P. & BASHFORTH A. 1996. Geology and Paleontology of the Port au Port Peninsula, Western Newfoundland. In: p. 74. Geological Association of Canada.
- WILLIAMS H. & CAWOOD P. A. 1989. Geology of Humber Arm Allochthon, Newfoundland. Geologic Survey of Canada, western Newfoundland.
- WILLIAMS H., COLMAN-SADD S. P. & SWINDEN H. S. 1988. Tectonic-stratigraphic subdivisions of central Newfoundland. *Geological Survey of Canada*: 91–98.
- WILLIAMS H., CURRIE K. L. & PIASECKI M. A. J. 1993. The Dog Bay Line: a major Silurian tectonic boundary in northeast Newfoundland. *Canadian Journal of Earth Sciences* 30: 2481–2494.
- WILLIAMS H. & HATCHER R. D. 1983. Appalachian suspect terranes. In: *Geological Society of America Memoirs* pp. 33–53. Geological Society of America.
- WILLIAMS H. & HISCOTT R. N. 1987. Definition of the lapetus rift-drift transition in western Newfoundland. *Geology* 15: 1044–1047.
- WILLIAMS H., JAMES N. P. & STEVENS R. K. 1985a. Humber Arm Allochthon and nearby groups between Bonne Bay and Portland Creek, western Newfoundland. In: *Current Research* (Ed. by M. J. Kiel & D. Busby), pp. 399–406. Geologic Survey of Canada.
- WILLIAMS H. & STEVENS R. K. 1974. Taconic Orogeny and the development of the ancient continental margin of eastern North American in Newfoundland. *Journal of the Geological Association of Canada* 1: 31–33.
- WILLIAMS H. & STEVENS R. K. 1974b. The ancient continental margin of eastern North America. In: *in Burk, C.A. and Drake, C.L., eds., The geology of Continental Margins* pp. 781–796. Springer-Verlag, New York.
- WILLIAMS S. H. 1991. Stratigraphy and graptolites of the Upper Ordovician Point Leamington Formation, central Newfoundland. *Canadian Journal of Earth Sciences* 28: 581–600.
- WILSON J. T. 1966. Did the Atlantic close and then re-open. *Nature* 211: 676–681.
- WILSON R. A., BURDEN E. T., BERTRAND R., ASSELIN E. & MCCracken A. D. 2004. Stratigraphy and tectono-sedimentary evolution of the Late Ordovician to Middle Devonian Gaspé Belt in northern New Brunswick: evidence from the Restigouche area. *Canadian Journal of Earth Sciences* 41: 527–551.

- ZAGOREVSKI A., LISSEBERG C. J. & VAN STAAL C. R. 2009. Dynamics of accretion of arc and backarc crust to continental margins: Inferences from the Annieopsquotch accretionary tract, Newfoundland Appalachians. *Tectonophysics* 479: 150–164.
- ZAGOREVSKI A., VAN STAAL C. R., MCNICOLL V., ROGERS N. & VALVERDE-VAQUERO P. 2007. Tectonic architecture of an arc-arc collision zone, Newfoundland Appalachians. In: *Formation and Applications of the Sedimentary Record in Arc Collision Zones* (Ed. by A. Draut, P. D. Clift & D. W. Scholl), pp. 309–333. The Geological Society of America.
- ZEN E. 1972. Some revisions in the interpretation of the Taconic allochthon in west-central Vermont. *Geological Society of America Bulletin* 83: 2573–2588.
- ZEN E. A. 1967. Time and space relationships of the Taconic allochthon and autochthon. *Geological Society of America Special Papers* 97: 1–82.

Appendix A

NP007 Lourdes Formation																	
Isotopic ratios																	
sample name	²⁰⁶ Pb (cps)	²⁰⁴ Pb (cps)	²¹⁰ Pb/ ²⁰⁶ Pb	2 s	²⁰⁷ Pb/ ²³⁵ U	2 s	²⁰⁶ Pb/ ²³⁸ U	2 s	f	Corr. Pb	Apparent age summary	discordance %					
										age (Ma)	error (Ma)	age (Ma)	error (Ma)	age (Ma)	error (Ma)	discordance %	
										207Pb/206Pb	2 s	207Pb/235U	2 s	206Pb/238U	2 s	206Pb/238U	2 s
Discordance > 10% or < -10%																	
NP007-100	75601	206	0.07128	0.00083	1.50576	0.11675	0.15322	0.01175	0.989	no	965	24	933	46	919	65	5.1
NP007-093	266284	210	0.07128	0.00075	1.54015	0.11533	0.15670	0.01162	0.990	no	966	21	947	45	938	64	3.0
NP007-086	1083036	201	0.07253	0.00079	1.65213	0.06878	0.16520	0.00664	0.965	no	1001	22	990	26	986	37	1.6
NP007-130	38613	175	0.07281	0.00086	1.60352	0.08603	0.15972	0.00856	0.976	no	1009	23	992	33	985	46	5.7
NP007-021	219977	244	0.07324	0.00084	1.67431	0.07151	0.16881	0.00682	0.963	no	1021	24	999	27	989	38	3.3
NP007-013	182951	174	0.07346	0.00080	1.70463	0.06767	0.16829	0.00642	0.961	no	1027	25	1010	25	1003	35	2.5
NP007-090	71413	220	0.07349	0.00090	1.69384	0.07294	0.16717	0.00690	0.959	no	1027	25	1006	27	996	38	3.3
NP007-073	126755	0	0.07359	0.00080	1.62240	0.07305	0.15989	0.00699	0.970	no	1030	22	979	28	956	39	7.7
NP007-088	124677	279	0.07369	0.00081	1.70886	0.08008	0.16820	0.00766	0.972	no	1033	22	1012	30	1002	42	3.2
NP007-102	246952	197	0.07373	0.00078	1.66759	0.08179	0.16404	0.00786	0.977	no	1034	21	996	31	979	43	5.7
NP007-025	137052	321	0.07379	0.00080	1.66832	0.06764	0.16397	0.00641	0.964	no	1036	22	997	25	979	35	5.9
NP007-110	138966	259	0.07387	0.00081	1.62306	0.06069	0.15935	0.00570	0.956	no	1038	22	979	23	953	32	8.8
NP007-049	111694	225	0.07399	0.00084	1.73969	0.09531	0.17054	0.00914	0.978	no	1041	23	1023	35	1015	50	2.7
NP007-036	64642	410	0.07409	0.00086	1.61426	0.06890	0.15802	0.00649	0.962	no	1044	23	976	26	946	36	10.1
NP007-055	102499	8	0.07421	0.00087	1.69092	0.06735	0.16526	0.00629	0.956	no	1047	23	1005	25	986	35	6.3
NP007-076	108989	0	0.07452	0.00087	1.66434	0.07108	0.16198	0.00665	0.961	no	1056	23	995	27	968	37	9.0
NP007-071	156752	0	0.07458	0.00087	1.66981	0.06806	0.16239	0.00634	0.958	no	1057	23	997	26	970	35	8.9
NP007-007	59093	13	0.07484	0.00094	1.70123	0.09761	0.16487	0.00923	0.976	no	1064	25	1009	36	984	51	8.1
NP007-085	680207	242	0.07487	0.00078	1.78663	0.09148	0.17306	0.00867	0.979	no	1065	21	1041	33	1029	47	3.7
NP007-124	90914	303	0.07507	0.00094	1.79782	0.10365	0.17370	0.00978	0.976	no	1070	25	1045	27	1032	33	3.8
NP007-024	949402	428	0.07509	0.00076	1.85468	0.08557	0.17915	0.00806	0.975	no	1071	20	1065	30	1062	44	0.9
NP007-064	151443	62	0.07511	0.00083	1.79241	0.06993	0.17307	0.00648	0.959	no	1072	22	1043	25	1029	36	4.3
NP007-030	91917	86	0.07527	0.00082	1.81064	0.07183	0.17447	0.00665	0.961	no	1076	22	1049	26	1037	36	3.9
NP007-030	151340	345	0.07536	0.00083	1.78164	0.06893	0.17146	0.00636	0.958	no	1078	22	1039	25	1032	35	5.8
NP007-048	203115	164	0.07539	0.00079	1.85139	0.11663	0.17811	0.01106	0.986	no	1079	22	1064	41	1057	60	2.2
NP007-062	905445	19	0.07580	0.00084	1.83234	0.08206	0.17532	0.00761	0.969	no	1090	21	1057	29	1041	42	4.8
NP007-051	85868	189	0.07587	0.00091	1.80932	0.10394	0.17296	0.00972	0.978	no	1092	24	1049	37	1028	53	6.3
NP007-005	159355	118	0.07589	0.00111	1.75969	0.13117	0.16818	0.01229	0.980	no	1092	29	1031	47	1044	67	8.9
NP007-029	59792	284	0.07627	0.00101	1.84853	0.07784	0.17578	0.00703	0.950	no	1102	26	1063	27	1044	38	5.7
NP007-048	98024	320	0.07635	0.00093	1.83491	0.07411	0.17430	0.00671	0.954	no	1104	24	1038	26	1036	37	6.7
NP007-065	99105	73	0.07651	0.00089	1.80982	0.07180	0.17156	0.00651	0.956	no	1108	23	1049	24	1021	36	8.6
NP007-058	76897	207	0.07672	0.00096	1.81463	0.06870	0.17154	0.00613	0.944	no	1114	25	1051	26	1021	34	9.1
NP007-070	72297	0	0.07696	0.00096	1.84778	0.07463	0.17414	0.00669	0.951	no	1120	25	1063	26	1035	37	8.2
NP007-114	237180	262	0.07738	0.00084	1.97373	0.21007	0.18499	0.01959	0.995	no	1131	21	1107	69	1094	106	3.5
NP007-068	113352	2	0.07742	0.00087	1.88845	0.08371	0.17691	0.00759	0.967	no	1132	22	1077	29	1050	41	7.9
NP007-016	111562	277	0.07748	0.00086	1.94329	0.07943	0.18191	0.00715	0.962	no	1134	22	1096	27	1077	39	5.4
NP007-094	198031	468	0.07767	0.00082	1.96982	0.14719	0.18395	0.01361	0.990	no	1138	21	1105	49	1088	74	4.8
NP007-018	94531	76	0.07925	0.00093	2.04131	0.09415	0.18226	0.00808	0.971	no	1178	22	1129	31	1104	45	6.9
NP007-035	251474	388	0.07931	0.00087	1.99295	0.09098	0.18226	0.00808	0.971	no	1180	22	1113	30	1079	44	9.3
NP007-014	783420	171	0.07935	0.00084	1.98865	0.07895	0.18176	0.00695	0.964	no	1181	21	1112	26	1077	38	9.6
NP007-117	266432	162	0.07953	0.00085	2.19153	0.24696	0.22442	0.0966	0.985	no	1185	21	1178	76	1175	119	1.0
NP007-057	57078	132	0.07993	0.00101	2.11445	0.09177	0.19386	0.00796	0.956	no	1195	25	1159	29	1140	43	5.1
NP007-019	241422	138	0.08040	0.00099	2.09425	0.08016	0.18892	0.00685	0.947	no	1207	24	1147	26	1116	37	8.2
NP007-045	314137	78	0.08077	0.00086	2.21216	0.12799	0.19865	0.01129	0.983	no	1216	23	1185	40	1168	60	4.3
NP007-113	73175	229	0.08107	0.00094	2.09599	0.22897	0.18751	0.02037	0.994	no	1223	23	1147	72	1108	110	10.2
NP007-097	115992	401	0.08118	0.00088	2.13718	0.15720	0.19094	0.01389	0.989	no	1226	21	1161	50	1126	75	8.8
NP007-020	170976	65	0.08173	0.00089	2.31442	0.08908	0.20538	0.00758	0.959	no	1239	21	1217	27	1204	47	3.1
NP007-039	45016	175	0.08293	0.00113	2.26569	0.10405	0.19815	0.00869	0.955	no	1268	26	1202	32	1165	40	8.8
NP007-061	272427	124	0.08517	0.00110	2.44381	0.09069	0.20810	0.00724	0.938	no	1319	26	1256	26	1219	39	8.4
NP007-112	29436	221	0.08562	0.00116	2.47036	0.26562	0.20926	0.02232	0.992	no	1330	25	1263	75	1225	118	8.6
NP007-127	233119	116	0.08569	0.00092	2.62087	0.14405	0.22183	0.01196	0.981	no	1331	21	1307	40	1292	63	3.3

Sample name	Isotopic ratios										Apparent age summary									
	^{206}Pb (cps)	^{204}Pb (cps)	$^{207}\text{Pb}/^{206}\text{Pb}$	2σ	$^{207}\text{Pb}/^{235}\text{U}$	2σ	$^{206}\text{Pb}/^{238}\text{U}$	2σ	f	Corrected?	Com Pb	age (Ma)	error (Ma)	discordance %						
NP007-120	135011	204	0.08688	0.00093	2.62781	2.8	0.27859	0.21938	0.02314	0.995	no	1358	20	1308	75	1279	121	64	6.4	
NP007-099	384569	319	0.08825	0.00092	2.60316	2.8	0.19397	0.21394	0.01579	0.990	no	1388	20	1302	53	1250	83	10.9	10.9	
NP007-128	206527	148	0.08899	0.00099	2.85287	2.8	0.15371	0.22522	0.01226	0.979	no	1404	21	1370	40	1348	64	4.4	4.4	
NP007-082	117808	469	0.08976	0.00096	2.88092	2.8	0.13187	0.23278	0.01036	0.972	no	1420	20	1377	34	1349	54	5.6	5.6	
NP007-060	41361	48	0.09128	0.00131	2.95602	2.8	0.12344	0.23486	0.00921	0.939	no	1453	27	1396	31	1360	48	7.1	7.1	
NP007-009	117003	0	0.09169	0.00106	2.98300	2.8	0.18100	0.23595	0.01405	0.982	no	1461	22	1403	45	1366	73	7.2	7.2	
NP007-119	484633	399	0.09264	0.00095	3.11533	2.8	0.32747	0.24390	0.02551	0.995	no	1481	18	1436	78	1407	131	5.5	5.5	
NP007-015	93842	305	0.09779	0.00117	3.47663	2.8	0.13942	0.25785	0.00987	0.955	no	1582	22	1522	31	1479	50	7.3	7.3	
NP007-095	84165	338	0.10034	0.00117	3.63804	2.8	0.30173	0.26295	0.02159	0.990	no	1630	19	1615	30	1505	64	8.6	8.6	
NP007-038	284102	277	0.10112	0.00105	3.90849	2.8	0.14842	0.28034	0.01024	0.962	no	1645	21	1615	30	1593	31	3.5	3.5	
NP007-032	85021	337	0.10150	0.00111	3.81809	2.8	0.18358	0.27283	0.01277	0.974	no	1652	20	1597	38	1555	64	6.6	6.6	
NP007-091A	223812	297	0.10159	0.00118	3.78926	2.8	0.16021	0.27052	0.01100	0.961	no	1653	20	1590	33	1543	56	7.5	7.5	
NP007-075	215385	26	0.10224	0.00112	3.89035	2.8	0.17237	0.27598	0.01185	0.969	no	1665	21	1612	35	1612	60	6.4	6.4	
NP007-012	93850	258	0.10225	0.00118	3.83435	2.8	0.15298	0.27197	0.01039	0.957	no	1665	21	1600	32	1551	52	7.7	7.7	
NP007-083	169283	665	0.10641	0.00112	4.29362	2.8	0.19975	0.29264	0.01326	0.974	no	1739	19	1692	38	1655	66	5.3	5.3	
NP007-108	69369	203	0.11456	0.00129	4.76395	2.8	0.19175	0.30161	0.01166	0.960	no	1873	20	1779	33	1699	57	10.5	10.5	
NP007-089	817955	333	0.11682	0.00123	5.08287	2.8	0.19819	0.31845	0.01196	0.962	no	1890	19	1832	33	1832	33	6.5	6.5	
NP007-037	216725	291	0.117109	0.00174	10.79527	2.8	0.48275	0.45761	0.01993	0.974	no	1908	18	1833	42	1768	75	8.4	8.4	
NP007-079	114510	1	0.11562	0.00191	11.26701	2.8	0.54672	0.47707	0.02253	0.973	no	2570	19	2545	44	2514	98	2.6	2.6	
NP007-081	43847	1	0.17129	0.00191	11.26701	2.8	0.64880	0.48049	0.02603	0.981	no	2628	18	2585	50	2529	112	4.5	4.5	
NP007-053	201402	78	0.17733	0.00191	11.74797	2.8	0.49202	0.45761	0.01993	0.974	no	2640	17	2506	41	2429	88	6.5	6.5	
NP007-105	395541	205	0.17839	0.00188	11.59477	2.8	0.42875	0.47086	0.01936	0.969	no	2650	19	2572	39	2487	84	7.0	7.0	
NP007-056	515812	75	0.17965	0.00187	11.13819	2.8	0.48282	0.44966	0.01666	0.963	no	2650	17	2535	35	2594	74	11.5	11.5	
NP007-006	655480	30	0.18421	0.00205	12.54935	2.8	0.72803	0.49409	0.02813	0.981	no	2691	18	2646	53	2588	53	4.6	4.6	
NP007-078	100839	1	0.18446	0.00192	12.45122	2.8	0.50730	0.48957	0.01928	0.967	no	2693	17	2639	38	2639	38	5.6	5.6	
NP007-001	325006	0	0.18517	0.00210	12.55261	2.8	0.72971	0.49165	0.02803	0.981	no	2700	17	2647	53	2578	120	5.5	5.5	
NP007-040	301756	166	0.18654	0.00190	13.16839	2.8	0.43311	0.51200	0.01601	0.951	no	2712	17	2692	31	2665	68	2.1	2.1	
NP007-028	722669	264	0.18679	0.00195	13.01344	2.8	0.51206	0.50529	0.01917	0.964	no	2714	17	2681	36	2636	82	3.5	3.5	
NP007-044	169575	126	0.18706	0.00191	12.97349	2.8	0.73909	0.50301	0.02819	0.984	no	2716	17	2678	52	2709	120	4.0	4.0	
NP007-121	848384	215	0.18717	0.00193	13.01260	2.8	1.37956	0.50423	0.05320	0.995	no	2717	17	2681	95	2632	224	3.8	3.8	
NP007-022	169575	270	0.18738	0.00191	12.48669	2.8	0.48330	0.51169	0.02150	0.970	no	2719	17	2642	95	2542	217	7.9	7.9	
NP007-023	691631	232	0.19890	0.00203	14.68409	2.8	0.56808	0.53543	0.01998	0.965	no	2817	17	2795	40	2709	2.7	2.7	2.7	
NP007-046	458600	118	0.20265	0.00221	14.29719	2.8	0.86443	0.51169	0.03043	0.984	no	2848	18	2770	36	2764	83	2.3	2.3	
NP007-054	135523	26	0.20336	0.00236	15.09937	2.8	0.65568	0.53851	0.02254	0.964	no	2853	17	2822	41	2777	94	3.3	3.3	
NP007-043	548024	182	0.20457	0.00211	15.42873	2.8	0.87388	0.54699	0.03046	0.983	no	2863	17	2842	53	2813	126	2.2	2.2	
NP007-042	97691	149	0.20461	0.00210	15.78749	2.8	0.87861	0.53960	0.03061	0.983	no	2863	17	2864	52	2865	125	-0.1	-0.1	
NP007-092	39036	214	0.07450	0.00102	1.62609	2.8	0.11280	0.15831	0.01176	0.984	no	1073	29	980	46	996	65	11.0	11.0	
NP007-087	31275	188	0.07518	0.00111	1.66723	2.8	0.06802	0.16084	0.00612	0.932	no	1073	29	996	26	961	34	3.4	3.4	
NP007-098	747358	430	0.11107	0.00114	4.38737	2.8	0.33258	0.28648	0.02152	0.991	no	1817	19	1710	61	1624	107	12.0	12.0	
NP007-103	534594	299	0.11317	0.00115	4.53717	2.8	0.18645	0.29077	0.01155	0.967	no	1851	19	1738	34	1645	57	12.6	12.6	
NP007-115	1399661	290	0.08557	0.00115	2.36995	2.8	0.26539	0.20087	0.02233	0.993	no	1829	26	1234	77	1180	119	12.2	12.2	
NP007-067	42643	3	0.07672	0.00101	1.75495	2.8	0.06748	0.16590	0.00599	0.940	no	1114	26	1029	25	989	33	12.1	12.1	
NP007-080	903121	43	0.11030	0.00115	4.27165	2.8	0.16621	0.28088	0.01053	0.963	no	1804	32	1688	32	1596	53	13.0	13.0	
NP007-002	53053	255	0.07753	0.00102	1.79199	2.8	0.11268	0.16764	0.01031	0.978	no	1135	26	1043	40	999	40	12.9	12.9	
NP007-017	73323	183	0.05774	0.00087	0.58189	2.8	0.03659	0.07309	0.00446	0.971	no	520	33	466	23	455	27	13.0	13.0	
NP007-107	36157	229	0.07710	0.00141	1.74493	2.8	0.08250	0.14670	0.00864	0.975	no	1124	36	1025	26	980	34	13.8	13.8	
NP007-003	80244	116	0.07300	0.00099	1.47652	2.8	0.08920	0.14670	0.00864	0.975	no	1014	27	921	36	882	48	13.9	13.9	
NP007-118	124658	150	0.05764	0.00069	0.57324	2.8	0.02532	0.07212	0.00307	0.963	no	516	26	460	16	449	18	13.5	13.5	
NP007-066	45905	12	0.08132	0.00142	2.02104	2.8	0.08155	0.18025	0.00656	0.902	no	1229	27	1123	27	1068	36	16.2	16.2	
NP007-126	475453	214	0.18678	0.00200	11.29400	2.8	0.43855	0.43855	0.02573	0.984	no	2714	18	2548	54	2344	114	14.2	14.2	
NP007-026	493482	358	0.10497	0.00112	3.72440	2.8	0.23740	0.25732	0.01617	0.986	no	1714	20	1577	50	1476	82	15.5	15.5	
NP007-101	321587	291	0.08233	0.00090	2.06843	2.8	0.15159	0.18220	0.01321	0.989	no	1253	21	1138	49	1079	72	15.1	15.1	

Isotopic ratios														Apparent age summary									
sample name	^{206}Pb (cps)	^{204}Pb (cps)	$^{207}\text{Pb}/^{206}\text{Pb}$	2 s	$^{207}\text{Pb}/^{235}\text{U}$	2 s	$^{206}\text{Pb}/^{238}\text{U}$	2 s	f	Com Pb corrected?	age (Ma)	error (Ma)	age (Ma)	error (Ma)	age (Ma)	error (Ma)	discordance %						
NP007-050	79314	186	0.09051	0.00105	2.61225	0.20114	0.20931	0.01593	0.988	no	1436	22	1304	55	1225	84	16.1						
NP007-010	29593	0	0.07934	0.00128	1.84727	0.11744	0.16887	0.01039	0.967	no	1181	31	1062	41	1006	57	16.0						
NP007-008	49608	13	0.07777	0.00132	1.73732	0.11047	0.16202	0.00993	0.964	no	1141	33	1022	40	968	55	16.3						
NP007-123	128435	491	0.08270	0.00166	2.05532	0.11279	0.18025	0.00921	0.931	no	1262	39	1134	37	1068	50	16.7						
NP007-125	37552	203	0.07725	0.00135	1.68589	0.09852	0.15829	0.00883	0.954	no	1128	34	1003	37	947	49	17.2						
NP007-004	630166	226	0.07799	0.00090	1.69228	0.10655	0.15738	0.00974	0.983	no	1147	23	1006	39	942	54	19.2						
NP007-033	20852	453	0.08102	0.00175	1.85790	0.08286	0.16632	0.00650	0.876	no	1222	42	1066	29	992	36	20.3						
NP007-047	36154	204	0.07942	0.00227	1.75115	0.11039	0.16028	0.00680	0.891	no	1183	55	1029	40	958	50	20.4						
NP007-027	342666	337	0.10802	0.00115	3.62783	0.13207	0.24358	0.00848	0.957	no	1766	19	1556	29	1405	44	22.7						
NP007-084	296239	484	0.07894	0.00109	1.68172	0.07653	0.15451	0.00670	0.953	no	1171	27	1002	29	926	37	22.4						
NP007-122	20294	303	0.18989	0.00206	10.30158	0.54765	0.39547	0.02048	0.979	no	2741	18	2462	48	2139	94	25.8						
NP007-106	758497	206	0.08302	0.00172	1.88864	0.08128	0.16500	0.00622	0.876	no	1270	40	1077	28	984	34	24.2						
NP007-122	20294	206	0.08302	0.00172	1.88864	0.08128	0.16500	0.00622	0.876	no	1270	40	1077	28	984	34	24.2						
NP007-077	10285	0	0.08526	0.00186	1.98595	0.09382	0.16894	0.00708	0.888	no	1321	42	1111	31	1006	39	25.7						
NP007-129	1388295	219	0.10033	0.00109	2.77019	0.14273	0.20025	0.01009	0.977	no	1630	20	1348	38	1177	54	30.4						
NP007-109	231313	459	0.09942	0.00102	2.70393	0.11649	0.19725	0.00975	0.979	no	1613	19	1330	37	1161	52	30.6						
NP007-069	367719	102	0.07971	0.00093	1.55858	0.10042	0.14181	0.00899	0.983	no	1190	23	954	39	855	51	30.0						
NP007-096	205712	204	0.11781	0.00177	3.67733	0.31983	0.22639	0.01939	0.985	no	1923	27	1566	67	1316	101	34.9						
NP007-034	7904	247	0.08919	0.00198	1.94748	0.10347	0.15837	0.00765	0.909	no	1408	42	1098	35	948	42	42						
NP007-072	491312	205	0.20820	0.00219	9.50435	0.53342	0.33109	0.01825	0.982	no	2892	17	2388	50	1844	88	41.5						
NP007-052	932757	558	0.16463	0.00186	6.03043	0.30309	0.26567	0.01301	0.974	no	2504	19	1980	43	1519	66	44.0						
NP007-104	607575	455	0.16264	0.00234	5.75194	0.37455	0.25650	0.01629	0.975	no	2483	24	1939	55	1472	83	45.4						
NP007-031	47188	299	0.06869	0.00312	0.68435	0.03967	0.07226	0.00261	0.622	no	889	91	529	24	450	16	51.2						
NP007-111	512834	279	0.18372	0.00224	4.54790	0.26550	0.17953	0.01025	0.978	no	2687	20	1740	47	1064	56	65.3						

NG024A Whitehouse Formation																				
Isotopic ratios																				
sample name	$^{206}\text{Pb}(\text{cps})$	$^{204}\text{Pb}(\text{cps})$	$^{207}\text{Pb}/^{206}\text{Pb}$	2 S	$^{207}\text{Pb}/^{235}\text{U}$	2 S	$^{206}\text{Pb}/^{238}\text{U}$	2 S	f corrected ^a	Apparent age summary										
										Com Pb corrected ^a	age (Ma)	error (Ma)	discordance %							
Better than $\pm 10\%$ discordant																				
Discordance >10% or <10%																				
NG024-100	171861		0.33439	0.00362	33.94395	1.29007	0.73622	0.02682	0.959	no	3637	16	3608	37	3557	99	2.9			
NG024-24	226799	54	0.25375	0.00261	22.44843	0.79631	0.64163	0.02178	0.957	no	3208	16	3203	34	3195	85	0.5			
NG024-109	251008	43	0.20285	0.00210	15.23789	0.54229	0.54882	0.01855	0.957	no	2849	17	2830	33	2804	77	2.0			
NG024-081	95204	248	0.19914	0.00273	13.95444	1.04857	0.50822	0.03755	0.983	no	2819	22	2747	69	2649	159	7.4			
NG024-083	358735	179	0.19436	0.00207	13.77726	1.02286	0.51411	0.03777	0.990	no	2779	17	2735	68	2674	159	4.6			
NG024-057	84284	270	0.19135	0.00202	13.69437	1.15530	0.51905	0.04344	0.992	no	2754	17	2729	77	2695	182	2.6			
NG024-055	226990	258	0.19078	0.00195	13.43827	1.09870	0.51088	0.04144	0.992	no	2749	17	2711	74	2660	174	3.9			
NG024-002	173510	0	0.18951	0.00349	14.32000	0.51854	0.54803	0.01708	0.861	no	2738	30	2771	34	2817	71	-3.6			
NG024-106	637337	59	0.18856	0.00192	13.03664	0.48527	0.50144	0.01796	0.962	no	2730	17	2682	35	2620	77	4.9			
NG024-049	166891	247	0.18555	0.00192	13.63566	0.59759	0.53299	0.02270	0.972	no	2703	17	2725	35	2754	95	-2.3			
NG024-007	84572	0	0.18477	0.00358	12.94360	0.49784	0.50807	0.01688	0.864	no	2696	32	2676	36	2648	72	2.2			
NG024-031	569121	14	0.16369	0.00166	10.46746	0.49760	0.46380	0.02154	0.977	no	2494	17	2477	43	2456	94	1.8			
NG024-064	641741	173	0.16293	0.00187	9.53130	0.78787	0.42428	0.03473	0.990	no	2486	19	2391	73	2280	155	9.8			
NG024A-118	473759	95	0.11784	0.00120	5.37071	0.18475	0.33056	0.01086	0.955	no	1924	18	1880	29	1841	52	4.9			
NG024A-040	279118	56	0.11688	0.00126	5.46660	0.26402	0.33921	0.01597	0.975	no	1909	19	1895	41	1883	76	1.6			
NG024A-012	407139	132	0.11394	0.00118	5.31982	0.18833	0.33860	0.01147	0.957	no	1863	19	1872	30	1880	55	-1.0			
NG024A-087	401069	271	0.11332	0.00124	4.84766	0.36304	0.30970	0.02294	0.986	no	1857	20	1793	61	1739	112	7.2			
NG024A-034	305630	73	0.11249	0.00117	4.96651	0.23763	0.31984	0.01495	0.976	no	1840	19	1813	40	1813	73	3.2			
NG024-103	106936	30	0.11236	0.00118	4.91221	0.17302	0.31707	0.01066	0.954	no	1838	19	1804	29	1775	52	3.9			
NG024A-010	212753	962	0.11163	0.00668	4.55619	0.31832	0.29602	0.01067	0.516	yes	1826	105	1741	31	1778	55	1.5			
NG024A-011	428062	148	0.11131	0.00114	5.05710	0.16529	0.32952	0.01019	0.946	no	1821	19	1829	27	1836	49	-1.0			
NG024A-001	580471	0	0.11050	0.00204	5.16746	0.19457	0.33918	0.01113	0.872	no	1808	33	1847	32	1835	53	-4.8			
NG024A-017	321547	163	0.11011	0.00118	4.82105	0.17826	0.31755	0.01124	0.957	no	1801	19	1789	31	1778	55	1.5			
NG024A-008	1360386	78	0.10766	0.00201	4.61698	0.19147	0.31102	0.01151	0.893	no	1760	34	1752	34	1746	56	0.9			
NG024-107	51385	41	0.10712	0.00145	4.55837	0.23866	0.30862	0.01561	0.966	no	1751	25	1742	43	1734	76	1.1			
NG024-099	150712	92	0.10575	0.00114	4.20867	0.14523	0.28863	0.00946	0.950	no	1727	20	1676	28	1635	47	6.1			
NG024A-019	202614	135	0.10330	0.00111	4.18410	0.14591	0.29376	0.00975	0.951	no	1684	20	1671	28	1660	48	1.6			
NG024A-068	76986	142	0.10321	0.00118	3.95548	0.32866	0.27795	0.02288	0.991	no	1683	21	1625	65	1581	114	6.8			
NG024A-033	292373	17	0.10272	0.00108	4.14467	0.20486	0.29265	0.01413	0.977	no	1674	19	1663	40	1655	70	1.3			
NG024A-050	414475	251	0.10201	0.00103	4.16760	0.18715	0.29632	0.01296	0.974	no	1661	19	1668	36	1673	64	-0.8			
NG024A-25	2434822	33	0.10177	0.00104	4.28343	0.14475	0.30525	0.00984	0.953	no	1657	19	1690	29	1717	48	-4.2			
NG024A-111	310498	33	0.10095	0.00106	4.04487	0.14783	0.29060	0.01017	0.958	no	1642	19	1643	29	1645	51	-0.2			
NG024A-088	310289	205	0.10063	0.00106	3.65026	0.26660	0.26308	0.01901	0.990	no	1636	19	1561	57	1506	96	8.9			
NG024A-30	524101	159	0.09670	0.00129	3.56141	0.17239	0.26711	0.01243	0.961	no	1561	25	1541	38	1526	63	2.5			
NG024A-070	335300	104	0.09524	0.00099	3.28506	0.26945	0.25016	0.02035	0.992	no	1533	20	1478	62	1439	104	6.8			
NG024A-072	110622	207	0.09624	0.00111	3.40670	0.28761	0.25673	0.02147	0.991	no	1552	21	1506	64	1473	109	5.7			
NG024A-093	180974	273	0.09436	0.00102	3.26941	0.24100	0.25129	0.01832	0.989	no	1515	20	1474	62	1445	94	5.2			
NG024A-041	514918	124	0.09419	0.00098	3.45354	0.16637	0.26592	0.01251	0.976	no	1512	19	1517	37	1520	63	-0.6			
NG024A-036	445648	53	0.09399	0.00098	3.40981	0.16355	0.26312	0.01232	0.976	no	1508	20	1507	37	1506	63	0.2			
NG024A-117	220322	32	0.09311	0.00099	3.19974	0.12112	0.24925	0.00906	0.960	no	1490	20	1457	29	1435	47	4.2			
NG024A-045	308605	221	0.09286	0.00101	3.31791	0.14722	0.25914	0.01115	0.970	no	1485	20	1485	34	1485	57	0.0			
NG024A-051	99335	298	0.09269	0.00109	3.26478	0.14780	0.25545	0.01117	0.966	no	1482	22	1473	35	1467	57	1.1			
NG024A-22	123995	64	0.09172	0.00115	3.18682	0.11109	0.25198	0.00819	0.933	no	1462	24	1454	27	1449	42	1.0			

NG024A Winterhouse Formation																							
Isotopic ratios																							
sample name	²⁰⁶ Pb (cps)	²⁰⁴ Pb (cps)	²⁰⁷ Pb/ ²⁰⁶ Pb	2 s	²⁰⁷ Pb/ ²³⁵ U	2 s	²⁰⁶ Pb/ ²³⁸ U	2 s	f	corrected?	Com Pb age (Ma)	error (Ma)											
Apparent age summary																							
											²⁰⁷ Pb/ ²⁰⁶ Pb	2 s	age (Ma)	error (Ma)	²⁰⁷ Pb/ ²³⁵ U	2 s	age (Ma)	error (Ma)	²⁰⁶ Pb/ ²³⁸ U	2 s	age (Ma)	error (Ma)	discordance %
NG024A-21	96586	74	0.09172	0.00103	3.14405	0.11005	0.24861	0.00824	0.947	no	1462	21	1444	27	1431	42	1431	42	2.3				
NG024A-21	96586	74	0.09172	0.00103	3.14405	0.11005	0.24861	0.00824	0.947	no	1462	21	1444	27	1431	42	1431	42	2.3				
NG024A-047	308224	207	0.09149	0.00095	3.29557	0.14881	0.26125	0.01148	0.973	no	1457	20	1480	35	1496	58	1480	35	-3.0				
NG024A-055	442091	32	0.09142	0.00095	3.16536	0.14803	0.25111	0.01145	0.975	no	1455	20	1449	35	1444	59	1449	35	0.9				
NG024A-013	68885	92	0.09118	0.00108	3.06128	0.11013	0.24350	0.00827	0.944	no	1450	22	1423	27	1405	43	1405	43	3.5				
NG024A-086	256049	270	0.08926	0.00095	2.81730	0.20894	0.22891	0.01680	0.990	no	1410	20	1360	54	1329	88	1360	54	6.4				
NG024A-123	67172	70	0.08851	0.00106	2.82262	0.11020	0.23128	0.00859	0.951	no	1394	23	1362	29	1341	45	1362	29	4.2				
NG024A-115	297200	21	0.08672	0.00096	2.84160	0.12172	0.23765	0.00983	0.966	no	1354	21	1367	32	1374	34	1367	32	-1.6				
NG024A-073	111526	215	0.08540	0.00090	2.51897	0.21448	0.21392	0.01807	0.992	no	1325	20	1278	60	1250	95	1278	60	6.2				
NG024A-038	42553	56	0.08529	0.00204	2.40847	0.16265	0.20479	0.01293	0.935	no	1322	46	1245	47	1201	69	1245	47	10.0				
NG024A-29	58014	38	0.08352	0.00111	2.44653	0.08934	0.21244	0.00723	0.932	no	1281	26	1256	26	1242	38	1256	26	3.4				
NG024A-044	27385	158	0.08282	0.00115	2.22784	0.10705	0.19509	0.00697	0.957	no	1265	27	1190	33	1149	48	1190	33	10.0				
NG024A-097A	121129	86	0.08101	0.00093	2.10197	0.07574	0.18818	0.00642	0.947	no	1222	22	1149	24	1112	35	1149	24	9.8				
NG024A-052	43490	305	0.07847	0.00121	2.03299	0.09515	0.18790	0.00830	0.944	no	1159	30	1127	31	1110	45	1127	31	4.6				
NG024A-037	283029	62	0.07839	0.00085	2.07800	0.09863	0.19226	0.00888	0.973	no	1142	21	1142	32	1134	48	1142	32	2.2				
NG024A-014	123942	114	0.07825	0.00110	1.93565	0.07485	0.17942	0.00647	0.932	no	1157	28	1157	26	1110	35	1157	26	8.4				
NG024A-080	289981	208	0.07813	0.00096	1.92778	0.14994	0.17848	0.01374	0.988	no	1150	24	1089	51	1064	75	1089	51	8.6				
NG024A-089	350800	219	0.07776	0.00080	1.95838	0.18267	0.18267	0.01455	0.992	no	1141	20	1101	53	1082	79	1141	20	5.6				
NG024A-004	31698	0	0.07714	0.00199	1.92537	0.07817	0.18102	0.00567	0.772	no	1125	51	1090	27	1073	31	1090	27	5.1				
NG024A-032	68755	20	0.07706	0.00095	1.96187	0.10137	0.18465	0.00926	0.971	no	1123	24	1103	34	1092	50	1103	34	2.9				
NG024A-020	55422	111	0.07704	0.00086	1.88520	0.06951	0.17747	0.00624	0.953	no	1122	25	1076	24	1053	34	1076	24	6.7				
NG024A-23	51454	34	0.07703	0.00099	1.89496	0.06888	0.17841	0.00606	0.935	no	1122	25	1079	24	1058	33	1079	24	6.2				
NG024A-116	178984	34	0.07678	0.00082	1.93896	0.07317	0.18315	0.00663	0.959	no	1116	21	1095	25	1084	36	1095	25	3.1				
NG024A-091	44543	280	0.07670	0.00090	1.83298	0.13498	0.17532	0.01260	0.987	no	1113	23	1057	47	1030	69	1057	47	8.1				
NG024A-114	83476	29	0.07657	0.00095	1.94230	0.07696	0.18400	0.00693	0.950	no	1110	24	1096	26	1089	38	1096	26	2.1				
NG024A-054	99996	289	0.07618	0.00091	1.88519	0.08674	0.17905	0.00796	0.966	no	1105	24	1076	30	1062	43	1076	30	4.2				
NG024A-28	82112	51	0.07618	0.00084	1.83809	0.06527	0.17499	0.00570	0.947	no	1100	22	1059	22	1040	31	1059	22	5.9				
NG024A-079	43407	33	0.07598	0.00112	1.77803	0.07561	0.16972	0.00677	0.938	no	1095	29	1037	27	1011	37	1037	27	8.3				
NG024A-27	264720	51	0.07593	0.00081	1.91822	0.06766	0.18323	0.00616	0.953	no	1093	21	1087	23	1085	33	1087	23	0.8				
NG024A-048	68905	235	0.07587	0.00106	1.80763	0.08244	0.17279	0.00750	0.952	no	1092	28	1048	29	1027	41	1048	29	6.4				
NG024A-048	73963	179	0.07586	0.00088	1.79271	0.13489	0.17139	0.01274	0.988	no	1091	23	1043	48	1020	70	1043	48	7.1				
NG024A-124	298833	185	0.07570	0.00083	1.83984	0.06800	0.17627	0.00622	0.955	no	1087	24	1060	24	1047	34	1060	24	4.0				
NG024A-042	90240	126	0.07551	0.00090	1.76994	0.08117	0.16999	0.00753	0.966	no	1082	22	1034	29	1012	41	1034	29	7.0				
NG024A-110	123109	42	0.07543	0.00085	1.93427	0.08893	0.18598	0.00829	0.970	no	1080	22	1093	30	1100	45	1093	30	-2.0				
NG024A-065	92739	126	0.07543	0.00089	1.84132	0.15124	0.17706	0.01439	0.990	no	1080	28	1060	53	1051	78	1060	53	2.9				
NG024A-122	162128	77	0.07505	0.00104	1.76874	0.06558	0.17093	0.00588	0.928	no	1070	25	1034	24	1017	32	1034	24	5.3				
NG024A-058	54010	258	0.07501	0.00095	1.71833	0.14349	0.16614	0.01371	0.988	no	1069	28	1015	52	991	75	1015	52	7.9				
NG024A-119	125401	41	0.07484	0.00082	1.79447	0.06752	0.17390	0.00626	0.957	no	1064	22	1043	24	1034	34	1064	24	3.1				
NG024A-059	153882	175	0.07416	0.00080	1.65148	0.13357	0.16151	0.01314	0.991	no	1046	22	990	51	965	73	990	51	8.3				
NG024A-067	119262	126	0.07410	0.00087	1.67060	0.13828	0.16351	0.01340	0.990	no	1044	24	1044	24	997	74	1044	24	7.0				
NG024A-113	217270	34	0.07402	0.00078	1.76326	0.06874	0.17278	0.00649	0.963	no	1042	21	1032	25	1027	36	1032	25	1.5				
NG024A-006	51386	0	0.07401	0.00147	1.82192	0.08006	0.17854	0.00700	0.892	no	1042	40	1053	28	1059	38	1053	28	-1.8				
NG024A-075	337488	253	0.07392	0.00078	1.78922	0.13261	0.17555	0.01288	0.990	no	1039	21	1042	47	1043	70	1042	47	-0.4				
NG024A-094	122518	249	0.07362	0.00079	1.71236	0.06110	0.16869	0.00574	0.954	no	1031	21	1013	23	1005	32	1013	23	2.7				

NG024 Winterhouse Formation

Isotopic ratios

sample name	²⁰⁶ Pb (cps)	²⁰⁴ Pb (cps)	²⁰⁷ Pb/ ²⁰⁶ Pb	2σ	²⁰⁷ Pb/ ²³⁵ U	2σ	²⁰⁶ Pb/ ²³⁸ U	2σ	f	corrected?	Apparent age summary						
											Com Pb	age (Ma)	error (Ma)	2σ	age (Ma)	error (Ma)	2σ
NG024A-066	36782	113	0.07351	0.00102	1.56997	0.13363	0.15451	0.01301	0.987	no	1028	28	957	52	926	72	10.6
NG024A-074	131163	215	0.07305	0.00079	1.68477	0.13932	0.16726	0.01371	0.992	no	1015	22	1003	51	997	75	2.0
NG024A-099	139202	0	0.07302	0.00136	1.75937	0.06905	0.17475	0.00604	0.880	no	1014	37	1031	25	1038	33	-2.5
NG024-104	103893	23	0.07288	0.00080	1.62386	0.06412	0.16161	0.00613	0.961	no	1010	22	979	25	966	34	4.8
NG024-098	290183	88	0.07232	0.00075	1.58362	0.05610	0.15872	0.00538	0.956	no	995	21	963	22	950	30	4.9
NG024A-26	112575	33	0.07205	0.00079	1.55194	0.05629	0.15621	0.00540	0.953	no	987	22	951	22	956	30	5.6
NG024A-005	146030	0	0.07068	0.00133	1.52555	0.06144	0.15655	0.00557	0.884	no	948	38	941	24	958	31	1.2
NG024A-043	139248	175	0.05700	0.00063	0.59591	0.03729	0.07382	0.00467	0.984	no	492	24	475	23	471	31	4.3
NG024A-120	51289	40	0.05633	0.00075	0.54031	0.02011	0.06957	0.00242	0.934	no	465	29	439	13	434	15	7.0
NG024A-112	64947	60	0.08123	0.00120	2.09240	0.07792	0.18682	0.00638	0.918	no	1227	29	1146	25	1104	35	10.9
NG024A-085	37099	206	0.08079	0.00103	2.05734	0.15155	0.18469	0.01340	0.985	no	1216	25	1135	49	1093	72	11.1
NG024A-053	40448	307	0.07495	0.00107	1.65671	0.07878	0.16031	0.00727	0.954	no	1067	28	992	30	958	40	11.0
NG024-096	98161	151	0.07472	0.00096	1.63943	0.06415	0.15913	0.00588	0.945	no	1061	26	985	24	952	33	11.1
NG024A-095	61728	249	0.07815	0.00099	1.85386	0.13758	0.17205	0.01258	0.985	no	1151	25	1065	48	1023	69	12.0
NG024A-062	659095	227	0.07429	0.00216	11.57016	0.96398	0.45094	0.03720	0.990	no	2708	19	2570	75	2399	163	13.6
NG024A-076	36720	164	0.07429	0.00096	1.58692	0.12036	0.15492	0.01158	0.985	no	1049	26	965	46	928	64	12.4
NG024A-078	30830	153	0.07746	0.00113	1.79140	0.13519	0.16772	0.01242	0.981	no	1133	29	1042	48	1000	68	12.7
NG024A-039	61370	46	0.07620	0.00120	1.69932	0.08383	0.16174	0.00756	0.948	no	1100	31	1008	31	966	42	13.1
NG024A-56	211954	331	0.08020	0.00136	1.96471	0.16376	0.17768	0.01450	0.979	no	1202	33	1103	55	1054	79	13.3
NG024A-060	81934	187	0.05702	0.00073	0.53398	0.03683	0.06817	0.00460	0.983	no	492	28	436	24	425	28	14.1
NG024-105	163904	162	0.11054	0.00157	4.16369	0.17952	0.27318	0.01112	0.944	no	1808	26	1667	53	1557	73	15.6
NG024A-069	20799	124	0.07636	0.00125	1.64153	0.14066	0.15591	0.01311	0.981	no	1105	32	986	53	934	56	16.6
NG024A-061	125625	191	0.05813	0.00069	0.57978	0.03928	0.07234	0.00482	0.984	no	534	26	464	25	450	29	16.3
NG024A-082	53216	209	0.08434	0.00208	2.12594	0.16608	0.18283	0.01335	0.949	no	1300	47	1157	53	1082	73	18.2
NG024-102	377553	183	0.08039	0.00164	1.76196	0.08022	0.15896	0.00647	0.894	no	1207	40	1032	29	951	36	22.8
NG024A-063	80437	161	0.05935	0.00070	0.59013	0.04058	0.07211	0.00488	0.985	no	580	26	471	26	449	29	23.4
NG024A-092	49702	319	0.08135	0.00143	1.77269	0.14087	0.15803	0.01225	0.975	no	1230	34	1056	50	946	68	24.8
NG024A-071	11757	160	0.08782	0.00170	2.13150	0.18707	0.17603	0.01507	0.975	no	1379	37	1159	59	1045	82	26.2
NG024A-015	446167	160	0.10403	0.00106	3.15486	0.13065	0.21995	0.00883	0.969	no	1697	19	1446	31	1282	46	27.0
NG024-101	78163	65	0.06138	0.00076	0.64601	0.02773	0.07633	0.00313	0.955	no	653	27	506	17	474	19	28.4
NG024A-121	103537	75	0.06082	0.00070	0.58895	0.02224	0.07023	0.00250	0.944	no	633	27	470	14	438	15	31.9
NG024A-003	320941	2528	0.09259	0.00907	2.18829	0.22592	0.17141	0.00559	0.316	yes	1480	175	1177	70	1020	31	33.6
NG024A-125	51861	227	0.11750	0.00168	2.88041	0.12232	0.17779	0.00711	0.941	no	1919	25	1377	32	1055	39	48.7
NG024A-077	43588	191	0.06462	0.00133	0.57779	0.04390	0.06485	0.00474	0.963	no	762	43	463	28	405	29	48.3
NG024A-016	30556	93	0.06628	0.00198	0.62689	0.02779	0.06860	0.00225	0.740	no	815	61	494	17	428	14	49.1
NG024A-046	219984	428	0.07165	0.00119	0.74385	0.03490	0.07529	0.00330	0.936	no	976	33	565	20	468	20	53.9

NG043 Clam Bank Formation																	
Isotopic ratios																	
sample name	²⁰⁶ Pb (cps)	²⁰⁴ Pb (cps)	²⁰⁷ Pb/ ²⁰⁶ Pb	2 s	²⁰⁷ Pb/ ²³⁵ U	2 s	²⁰⁶ Pb/ ²³⁸ U	2 s	f corrected?	Com Pb		discordance %					
										age (Ma)	error (Ma)		age (Ma)	error (Ma)			
Better than ± 10% discordant																	
NG043-074	234163	7	0.05631	0.00061	0.52847	0.01874	0.06807	0.00230	0.953	no	465	24	431	12	425	14	8.9
NG043-013	211962	0	0.05694	0.00068	0.58655	0.02399	0.07471	0.00292	0.956	no	489	26	469	15	464	18	5.2
NG043-015	98885	0	0.07254	0.00109	1.61569	0.06877	0.16154	0.00643	0.956	no	1001	30	976	26	965	36	3.9
NG043-133	433644	19	0.07270	0.00084	1.59139	0.06720	0.15877	0.00645	0.962	no	1005	23	967	26	950	36	5.9
NG043-031	2659920	2567	0.07330	0.00125	1.68872	0.07222	0.16708	0.00655	0.917	yes	1022	34	1004	27	996	36	2.8
NG043-107	544858	1	0.07413	0.00077	1.83233	0.07678	0.17926	0.00727	0.968	no	1045	21	1057	27	1063	40	-1.8
NG043-111	79028	0	0.07459	0.00130	1.69968	0.08115	0.16527	0.00735	0.931	no	1057	35	1008	30	986	41	7.3
NG043-060	373982	0	0.07465	0.00079	1.83093	0.07876	0.17789	0.00742	0.969	no	1059	21	1057	28	1055	40	0.4
NG043-120	1081866	3	0.07472	0.00078	1.91003	0.07766	0.18541	0.00729	0.967	no	1061	21	1085	27	1096	40	-3.6
NG043-127	263033	63	0.07478	0.00080	1.83114	0.07320	0.17760	0.00684	0.964	no	1063	21	1057	26	1054	37	0.9
NG043-124	458832	33	0.07494	0.00108	1.81675	0.10234	0.17583	0.00957	0.966	no	1067	29	1052	36	1044	52	2.3
NG043-052	142612	11	0.07495	0.00081	1.89273	0.07310	0.18315	0.00679	0.960	no	1067	22	1079	25	1084	37	-1.7
NG043-068	191411	0	0.07514	0.00086	1.84773	0.08004	0.17835	0.00745	0.964	no	1072	21	1063	28	1058	41	1.4
NG043-102	309343	2	0.07520	0.00080	1.89746	0.07884	0.18301	0.00735	0.967	no	1074	21	1080	27	1083	40	-1.0
NG043-079	205563	7	0.07530	0.00104	1.75902	0.07178	0.16943	0.00650	0.941	no	1077	28	1030	26	1009	36	6.8
NG043-003	281333	0	0.07555	0.00079	1.94627	0.09445	0.18685	0.00885	0.976	no	1083	21	1097	32	1104	48	-2.1
NG043-007	211793	47	0.07556	0.00082	1.92762	0.10000	0.18501	0.00939	0.978	no	1084	22	1091	34	1094	51	-1.1
NG043-131	425494	1	0.07559	0.00080	1.85283	0.08404	0.17777	0.00784	0.973	no	1084	21	1064	29	1055	43	3.0
NG043-123	151125	0	0.07575	0.00096	1.84374	0.07830	0.17652	0.00715	0.954	no	1089	25	1061	28	1048	39	4.0
NG043-104	63594	7	0.07580	0.00135	1.73066	0.07334	0.16558	0.00637	0.908	no	1090	35	1020	27	988	35	10.1
NG043-033	161313	103	0.07583	0.00099	1.80895	0.07493	0.17302	0.00663	0.947	no	1091	26	1049	26	1029	37	6.1
NG043-055	68955	4	0.07598	0.00097	1.84492	0.07342	0.17611	0.00663	0.947	no	1095	25	1062	26	1046	36	4.8
NG043-117	152208	0	0.07616	0.00111	1.79388	0.07157	0.17084	0.00635	0.931	no	1099	29	1043	26	1017	35	8.1
NG043-113	357892	0	0.07653	0.00079	2.00780	0.09016	0.19027	0.00831	0.973	no	1109	21	1118	30	1123	45	-1.4
NG043-029	71450	3	0.07673	0.00263	1.88733	0.09431	0.17839	0.00648	0.727	no	1114	67	1077	33	1058	35	5.5
NG043-010	164944	24	0.07688	0.00101	1.90171	0.09544	0.17939	0.00869	0.965	no	1118	26	1082	33	1064	47	5.3
NG043-037	180366	1336	0.07733	0.00960	1.83565	0.23810	0.17217	0.00645	0.289	yes	1130	229	1058	82	1024	35	10.1
NG043-134	141676	0	0.07749	0.00104	1.95891	0.08653	0.18335	0.00772	0.953	no	1134	27	1102	29	1085	42	4.7
NG043-072	188794	15	0.07756	0.00147	1.87656	0.07673	0.17546	0.00636	0.886	no	1136	37	1136	37	1042	35	8.9
NG043-039	252031	111	0.07764	0.00101	1.85212	0.07447	0.17301	0.00659	0.947	no	1138	26	1064	26	1029	36	10.4
NG043-022	250780	6	0.07766	0.00099	1.98374	0.08793	0.18526	0.00786	0.958	no	1138	25	1110	29	1096	43	4.1
NG043-005	47855	0	0.07772	0.00113	1.90417	0.09258	0.17770	0.00824	0.954	no	1140	29	1083	32	1054	45	8.1
NG043-040	218467	195	0.07792	0.00087	1.96671	0.08284	0.18305	0.00744	0.965	no	1145	22	1104	28	1084	40	5.8
NG043-038	56926	162	0.07803	0.00121	1.92030	0.08499	0.17848	0.00740	0.937	no	1148	30	1088	29	1059	40	8.4
NG043-047	965030	119	0.07846	0.00087	2.19206	0.08183	0.20263	0.00722	0.955	no	1159	22	1179	26	1189	39	-2.9
NG043-126	84285	7	0.07873	0.00122	1.98106	0.07541	0.18250	0.00634	0.913	no	1165	30	1109	25	1081	34	7.9
NG043-090	66343	2	0.07908	0.00163	1.95551	0.10104	0.17935	0.00850	0.917	no	1174	40	1100	34	1113	46	10.2
NG043-121	209915	25	0.07935	0.00117	2.06255	0.08462	0.18852	0.00922	0.933	no	1181	29	1136	28	1113	39	6.2
NG043-018	22117	36	0.07941	0.00346	2.02550	0.13516	0.18550	0.00935	0.757	no	1182	84	1124	44	1094	51	8.1
NG043-014	458927	46	0.07984	0.00203	2.06858	0.09388	0.18791	0.00706	0.828	no	1193	49	1138	31	1110	38	7.6
NG043-034	351605	258	0.07985	0.00148	2.02586	0.08093	0.18401	0.00651	0.885	no	1193	36	1124	27	1089	35	9.5
NG043-044	101833	151	0.08011	0.00197	2.03715	0.09224	0.18443	0.00700	0.839	no	1200	48	1128	30	1091	38	9.8

Apparent age summary

NG043 Clam Bank Formation																	
Isotopic ratios																	
sample name	^{206}Pb (cps)	^{204}Pb (cps)	$^{207}\text{Pb}/^{206}\text{Pb}$	2 s	$^{207}\text{Pu}/^{235}\text{U}$	2 s	$^{206}\text{Pu}/^{238}\text{U}$	2 s	f	Com Pb corrected?	age (Ma) $^{207}\text{Pb}/^{206}\text{Pb}$	error (Ma) 2 s	age (Ma) $^{207}\text{Pu}/^{235}\text{U}$	error (Ma) 2 s	age (Ma) $^{206}\text{Pb}/^{238}\text{U}$	error (Ma) 2 s	discordance %
NG043-008	207446	0	0.08019	0.00121	2.16717	0.10588	0.19600	0.00910	0.951	no	1202	30	1171	33	1154	49	4.4
NG043-110	205186	43	0.08075	0.00098	2.29157	0.10045	0.20583	0.00867	0.961	no	1215	24	1210	31	1207	46	0.8
NG043-051	83227	17	0.08139	0.00104	2.26020	0.09362	0.20141	0.00793	0.951	no	1231	25	1200	29	1183	29	4.3
NG043-058	70711	0	0.08157	0.00125	2.17410	0.09684	0.19331	0.00808	0.938	no	1235	30	1173	31	1139	44	8.5
NG043-046	54253	171	0.08158	0.00149	2.30393	0.12075	0.20483	0.01006	0.937	no	1235	35	1213	36	1201	54	3.0
NG043-069	1020449	6	0.08319	0.00086	2.50504	0.09747	0.21840	0.00819	0.964	no	1274	20	1273	28	1273	43	0.0
NG043-089	457500	1	0.08390	0.00088	2.61178	0.12267	0.22578	0.01034	0.975	no	1290	20	1304	34	1312	54	-1.9
NG043-023	578151	0	0.08612	0.00089	2.87522	0.11477	0.24213	0.00934	0.966	no	1341	20	1375	30	1398	48	-4.7
NG043-050	383282	74	0.08798	0.00093	3.06044	0.11171	0.25230	0.00881	0.957	no	1382	20	1423	28	1450	45	-5.5
NG043-057	407030	3	0.08867	0.00099	3.01843	0.11518	0.24690	0.00901	0.956	no	1397	21	1412	29	1422	46	-2.0
NG043-080	241251	51	0.08931	0.00138	2.93290	0.12772	0.23816	0.00970	0.935	no	1411	29	1390	32	1377	50	2.7
NG043-030	778055	1	0.08949	0.00097	3.11868	0.12145	0.25274	0.00945	0.960	no	1415	21	1437	30	1433	48	-3.0
NG043-109	291971	1	0.08983	0.00101	3.02299	0.12735	0.24407	0.00991	0.964	no	1422	21	1413	32	1408	51	1.1
NG043-033	346421	164	0.09056	0.00126	2.92392	0.12428	0.23418	0.00940	0.945	no	1437	26	1388	32	1356	49	6.2
NG043-053	391905	20	0.09227	0.00122	3.33200	0.13279	0.25910	0.00976	0.945	no	1493	24	1489	31	1485	50	0.6
NG043-026	643992	3	0.09371	0.00097	3.34425	0.12185	0.25882	0.00904	0.959	no	1502	19	1491	28	1484	46	1.4
NG043-088	353272	4	0.09452	0.00097	3.48118	0.13441	0.26713	0.00994	0.964	no	1519	20	1518	30	1526	50	-0.6
NG043-082	319778	7	0.09455	0.00098	3.46184	0.15191	0.26556	0.01132	0.971	no	1519	19	1519	34	1518	57	0.1
NG043-002	309386	3	0.09484	0.00097	3.48349	0.16780	0.26640	0.01254	0.977	no	1525	19	1523	37	1523	64	0.2
NG043-125	683881	620	0.09492	0.00188	3.32990	0.16132	0.25444	0.01125	0.913	yes	1526	22	1488	37	1461	58	4.8
NG043-004	129890	0	0.09509	0.00114	3.58932	0.19532	0.27576	0.01453	0.975	no	1530	22	1547	42	1560	73	-2.2
NG043-083	147098	0	0.09521	0.00104	3.39139	0.14011	0.25835	0.01030	0.965	no	1532	20	1502	32	1481	53	3.7
NG043-077	1454764	972	0.09536	0.00145	3.38022	0.12477	0.25708	0.00865	0.911	yes	1535	28	1500	29	1475	44	4.4
NG043-129	236596	16	0.09554	0.00100	3.41401	0.15855	0.25918	0.01172	0.974	no	1539	20	1508	36	1486	60	3.9
NG043-048	644900	2124	0.09611	0.00358	3.50454	0.17349	0.26445	0.00862	0.658	yes	1550	68	1528	38	1513	44	2.7
NG043-081	373474	410	0.09761	0.00247	3.41909	0.16970	0.25406	0.01085	0.861	yes	1579	47	1509	38	1459	56	8.5
NG043-115	680642	59	0.09810	0.00116	3.80637	0.16852	0.28141	0.01201	0.964	no	1588	22	1594	35	1598	60	-0.7
NG043-049	1325621	10239	0.09885	0.00752	3.55290	0.31701	0.26068	0.01217	0.523	yes	1603	136	1594	68	1493	62	7.6
NG043-084	250231	1	0.09886	0.00109	3.57487	0.15904	0.26227	0.01130	0.969	no	1603	21	1544	35	1501	57	7.1
NG043-070	418642	11	0.09997	0.00109	3.54458	0.13333	0.25715	0.00926	0.957	no	1624	20	1537	29	1475	47	10.2
NG043-132	266994	35	0.10038	0.00155	3.92497	0.15645	0.28358	0.01042	0.922	no	1631	28	1528	32	1609	52	1.5
NG043-017	465644	2	0.10108	0.00135	4.07411	0.16999	0.29233	0.01156	0.948	no	1644	25	1649	33	1653	57	-0.6
NG043-001	163964	0	0.10203	0.00109	4.13479	0.19903	0.29392	0.01379	0.975	no	1661	20	1661	39	1661	68	0.0
NG043-119	438872	131	0.10321	0.00117	4.42135	0.20071	0.31069	0.01365	0.968	no	1683	21	1716	37	1744	67	-4.2
NG043-041	711574	334	0.10326	0.00106	3.93105	0.20012	0.27611	0.01377	0.979	no	1683	19	1620	40	1572	69	7.5
NG043-114	345375	39	0.10408	0.00129	4.20018	0.16568	0.29267	0.01096	0.949	no	1698	23	1674	32	1655	54	5.4
NG043-130	213768	19	0.10510	0.00137	4.34711	0.17982	0.29998	0.01177	0.949	no	1716	24	1702	34	1691	58	1.6
NG043-116	1139775	18	0.10694	0.00108	4.63768	0.17794	0.31452	0.01164	0.965	no	1748	18	1756	32	1756	57	-1.0
NG043-054	499191	1	0.10763	0.00114	4.65698	0.18859	0.31381	0.01227	0.965	no	1760	19	1760	33	1759	60	0.0
NG043-135	565632	24	0.10932	0.00142	4.82463	0.20943	0.32009	0.01326	0.954	no	1788	23	1789	36	1790	64	-0.1
NG043-099	377629	1	0.10934	0.00120	4.80938	0.19234	0.31904	0.01226	0.961	no	1788	20	1787	33	1785	60	0.2
NG043-066	226554	0	0.11037	0.00116	4.80381	0.20006	0.31567	0.01272	0.967	no	1806	19	1786	34	1769	62	2.3
NG043-078	1349339	2	0.11097	0.00121	5.16380	0.21817	0.33751	0.01378	0.966	no	1815	20	1847	35	1875	66	-3.8
NG043-019	526626	18	0.11283	0.00138	5.58640	0.29171	0.35908	0.01823	0.972	no	1846	22	1914	44	1978	86	-8.3

Apparent age summary

NG043 Charn Bank Formation																		
Isotopic ratios																		
sample name	²⁰⁶ Pb (cps)	²⁰⁴ Pb (cps)	²⁰⁶ Pb/ ²⁰⁶ Pb	2 s	²⁰⁷ Pb/ ²³⁵ U	2 s	²⁰⁶ Pb/ ²³⁸ U	2 s	f	Corr	Pb	age (Ma)	error (Ma)	age (Ma)	error (Ma)	age (Ma)	error (Ma)	discordance
										corrected	corrected	²⁰⁷ Pb/ ²⁰⁶ Pb	2 s	²⁰⁷ Pb/ ²³⁵ U	2 s	²⁰⁶ Pb/ ²³⁸ U	2 s	%
NG043-016	1194307	11	0.11592	0.00136	5.65097	0.24289	0.35357	0.01462	0.962	no	yes	1894	21	1924	36	1952	69	-3.5
NG043-101	367933	1517	0.11903	0.00475	5.42511	0.30837	0.33056	0.01337	0.712	yes	yes	1942	70	1889	48	1841	64	6.0
NG043-028	209457	0	0.12348	0.00131	6.39160	0.24075	0.37543	0.01357	0.959	no	no	2007	19	2031	33	2055	63	-2.8
NG043-061	235171	0	0.17374	0.00179	12.11442	0.46892	0.50571	0.01886	0.964	no	no	2594	17	2613	36	2638	80	-2.1
NG043-076	573937	10	0.17949	0.00198	12.69895	0.51091	0.51314	0.01985	0.961	no	no	2648	18	2658	37	2670	84	-1.0
NG043-059	1880810	74	0.18551	0.00188	13.27439	0.55307	0.51898	0.02097	0.970	no	no	2703	17	2699	39	2695	88	0.4
NG043-042	937591	301	0.18721	0.00206	13.80503	0.53465	0.53483	0.01986	0.959	no	no	2718	18	2736	36	2736	83	-2.0
NG043-045	560368	210	0.18755	0.00204	13.88241	0.58542	0.53684	0.02188	0.966	no	no	2721	18	2742	39	2770	91	-2.2
NG043-100	328250	1	0.19290	0.00206	14.83748	0.54307	0.53786	0.01953	0.956	no	no	2767	17	2805	34	2858	80	-4.1
NG043-012	946229	123	0.19517	0.00238	14.47527	0.59981	0.53791	0.02130	0.956	no	no	2786	20	2781	39	2775	89	0.5
NG043-112	405049	1022	0.20018	0.00407	15.09813	0.66350	0.54703	0.02132	0.887	yes	yes	2828	33	2821	41	2813	88	0.6
NG043-106	342759	9	0.22016	0.00227	17.81924	0.71868	0.58700	0.02289	0.967	no	no	2982	16	2980	38	2977	92	0.2
NG043-071	73295	7	0.07367	0.00114	1.57256	0.07817	0.15481	0.00731	0.950	no	no	1033	31	959	30	928	55	10.9
NG043-025	87723	0	0.09274	0.00194	2.92789	0.14901	0.22899	0.01063	0.912	no	no	1482	39	1389	38	1329	55	11.4
NG043-020	483808	1	0.07687	0.00121	1.76597	0.10483	0.16663	0.00954	0.964	no	no	1118	31	1033	38	994	52	12.0
NG043-097	26908	0	0.07563	0.00153	1.68225	0.06710	0.16132	0.00554	0.861	no	no	1085	40	1002	25	964	31	12.0
NG043-105	93128	90	0.07912	0.00161	1.91237	0.09319	0.17531	0.00777	0.909	no	no	1175	40	1085	32	1041	42	12.3
NG043-086	69368	34	0.08023	0.00332	1.97621	0.13354	0.17864	0.00954	0.790	no	no	1203	80	1107	45	1060	52	12.9
NG043-073	309012	94	0.10756	0.00258	4.01666	0.21558	0.27085	0.01300	0.894	no	no	1758	43	1545	46	1545	66	13.6
NG043-103	154094	19	0.07775	0.00123	1.80145	0.07154	0.16805	0.00612	0.917	no	no	1140	31	1046	26	1001	34	13.2
NG043-094	126100	41	0.07939	0.00303	1.89888	0.12422	0.17347	0.00921	0.812	no	no	1182	74	1081	43	1031	50	13.8
NG043-021	227722	20	0.07806	0.00247	1.80868	0.09216	0.16805	0.00670	0.783	no	no	1148	62	1049	33	1049	37	13.8
NG043-009	157979	0	0.09180	0.00196	2.76890	0.20174	0.21877	0.01524	0.956	no	no	1463	40	1347	53	1275	80	14.1
NG043-092	405640	595	0.11444	0.00280	4.37206	0.21353	0.27708	0.01171	0.865	yes	yes	1871	44	1707	40	1577	59	17.7
NG043-067	87743	2	0.08245	0.00131	2.02835	0.08813	0.17843	0.00722	0.931	no	no	1256	31	1125	29	1058	39	17.1
NG043-063	55160	5	0.05751	0.00138	0.53669	0.02220	0.06769	0.00228	0.815	no	no	511	52	456	15	422	44	18.0
NG043-056	760045	3183	0.20635	0.00440	12.64723	0.55955	0.44453	0.01723	0.876	yes	yes	2877	34	2654	41	2371	76	21.0
NG043-011	32920	20	0.07955	0.00349	1.77940	0.12464	0.16223	0.00885	0.779	no	no	1186	84	1038	45	969	49	19.7
NG043-085	103194	19	0.05792	0.00091	0.55045	0.02208	0.06893	0.00254	0.920	no	no	527	34	445	14	430	15	19.0
NG043-087	44725	30	0.08358	0.00339	1.98663	0.11303	0.17239	0.00687	0.700	no	no	1283	77	1111	38	1025	38	21.7
NG043-122	270256	578	0.08573	0.00369	2.08157	0.13086	0.17609	0.00807	0.729	yes	yes	1332	81	1143	42	1046	44	23.3
NG043-027	262650	458	0.10562	0.00331	3.32514	0.19355	0.22833	0.01135	0.846	yes	yes	1725	56	1487	45	1326	59	25.6
NG043-091	42946	44	0.08298	0.00781	0.19435	0.15435	0.16178	0.00754	0.444	no	no	1269	67	1064	67	967	52	25.6
NG043-006	415036	14	0.08585	0.00110	1.99794	0.11974	0.16879	0.00988	0.977	no	no	1335	24	1115	40	1005	54	4.2
NG043-075	2036031	16949	0.17640	0.00794	7.13775	0.59689	0.29346	0.02068	0.843	yes	yes	2619	73	2129	72	1659	102	41.5
NG043-098	37325	17	0.06232	0.00344	0.89851	0.04143	0.06860	0.00299	0.620	no	no	685	114	471	26	428	18	38.8
NG043-032	132033	4228	0.12462	0.00405	3.53369	0.16183	0.20565	0.01348	0.199	yes	yes	2023	482	1535	232	1206	72	44.2
NG043-128	44776	120	0.12820	0.01386	3.55413	0.40545	0.20107	0.00730	0.318	no	no	2073	179	1539	87	1181	39	47.0
NG043-095	46823	84	0.06474	0.00359	0.61453	0.04072	0.06884	0.00251	0.549	no	no	766	113	486	25	429	15	45.4
NG043-137	237096	1047	0.06803	0.00616	0.72794	0.07340	0.07071	0.00692	0.353	yes	yes	869	177	555	42	482	21	46.2
NG043-036	24370	201	0.15190	0.01412	4.13386	0.41059	0.19738	0.00692	0.353	no	no	2367	150	1661	78	1161	37	55.5
NG043-136	265588	98	0.07244	0.00255	0.73842	0.03894	0.07939	0.00290	0.744	no	no	998	70	561	22	460	17	55.9
NG043-065	47793	224	0.15824	0.01767	3.91924	0.47068	0.17963	0.00795	0.369	no	no	2437	178	1618	93	1065	60.9	60.9
NG043-064	215655	3376	0.09507	0.01743	0.99886	0.18714	0.07620	0.00293	0.205	yes	yes	1529	311	703	91	473	18	71.5

NP021A Red Island Road Formation

Isotopic ratios

Apparent age summary

sample name	²¹⁰ Pb (cps)	²¹⁰ Pb (cps)	²¹⁰ Pb/ ²¹⁰ Pb	2 s	²⁰⁷ Pb/ ²³⁵ U	2 s	²⁰⁶ Pb/ ²³⁸ U	2 s	Com Pb	age (Ma)	error (Ma)	age (Ma)	error (Ma)	age (Ma)	error (Ma)	age (Ma)	error (Ma)	discordance	
									corrected?	²⁰⁷ Pb/ ²¹⁰ Pb	2 s	²⁰⁷ Pb/ ²³⁵ U	2 s	²⁰⁶ Pb/ ²³⁸ U	2 s			%	
Better than ± 10% discordant																			
NP021A-087	5758	92	0.07078	0.00215	1.73483	0.09557	0.17776	0.00817	0.834	no	951	61	1022	35	1055	45	-11.8		
NP021A-047	313380	137	0.07175	0.00074	1.68331	0.05792	0.17016	0.00559	0.954	no	979	21	1002	22	1013	31	-3.8		
NP021A-097	55375	118	0.07297	0.00097	1.64819	0.06532	0.16382	0.00612	0.942	no	1013	27	989	25	978	34	3.7		
NP021A-078	32029	275	0.07394	0.00095	1.70780	0.07371	0.16751	0.00690	0.955	no	1040	26	1011	27	998	38	4.3		
NP021A-019	78818	56	0.07428	0.00086	1.66590	0.06660	0.16265	0.00623	0.957	no	1049	23	996	25	971	34	8.0		
NP021A-104	524570	165	0.07458	0.00117	1.76364	0.06468	0.17150	0.00568	0.903	no	1057	31	1032	23	1020	31	3.8		
NP021A-005	92150	63	0.07476	0.00081	1.70510	0.09539	0.16541	0.00908	0.981	no	1062	22	1010	35	987	50	7.7		
NP021A-058	37586	178	0.07479	0.00093	1.82670	0.07687	0.17713	0.00712	0.955	no	1063	25	1055	27	1051	39	1.2		
NP021A-060	154330	210	0.07483	0.00085	1.79607	0.06706	0.17408	0.00619	0.953	no	1064	23	1044	24	1035	34	3.0		
NP021A-012	131974	37	0.07483	0.00082	1.75717	0.06192	0.17030	0.00571	0.951	no	1064	22	1030	23	1014	31	5.1		
NP021A-045	178345	150	0.07489	0.00079	1.82788	0.06150	0.17702	0.00565	0.949	no	1066	21	1056	22	1051	31	1.5		
NP021A-027	55131	140	0.07492	0.00093	1.67235	0.06215	0.16189	0.00567	0.943	no	1066	25	998	23	967	31	10.0		
NP021A-061	26052	228	0.07493	0.00113	1.79382	0.07146	0.17362	0.00640	0.925	no	1067	30	1043	26	1032	35	3.5		
NP021A-044	172586	164	0.07494	0.00082	1.81470	0.06191	0.17563	0.00567	0.947	no	1067	22	1051	22	1043	31	2.4		
NP021A-042	34254	137	0.07501	0.00107	1.75602	0.06812	0.16979	0.00613	0.931	no	1069	28	1029	25	1011	34	5.8		
NP021A-081	165844	138	0.07514	0.00087	1.82147	0.08202	0.17581	0.00765	0.967	no	1072	23	1053	29	1044	42	2.9		
NP021A-098	38241	130	0.07520	0.00118	1.69924	0.06482	0.16389	0.00570	0.911	no	1074	31	1008	24	1011	31	9.6		
NP021A-059	33434	213	0.07525	0.00097	1.80703	0.07578	0.17416	0.00695	0.952	no	1075	26	1048	27	1035	38	4.1		
NP021A-014	53431	28	0.07527	0.00094	1.76157	0.06197	0.16974	0.00558	0.935	no	1076	25	1031	23	1011	31	6.5		
NP021A-096	124920	108	0.07566	0.00098	1.88018	0.08384	0.18023	0.00769	0.957	no	1086	26	1074	29	1068	42	1.8		
NP021A-006	42666	55	0.07571	0.00092	1.78000	0.09818	0.17051	0.00917	0.975	no	1087	24	1038	35	1015	50	7.2		
NP021A-064	8129	294	0.07578	0.00161	2.03148	0.09508	0.19442	0.00811	0.892	no	1089	42	1126	31	1145	44	-5.6		
NP021A-100	15583	128	0.07579	0.00176	1.83496	0.07698	0.17560	0.00614	0.833	no	1089	46	1058	27	1043	34	4.6		
NP021A-030	7143	164	0.07592	0.00153	1.77882	0.07968	0.16992	0.00680	0.893	no	1093	40	1038	29	1012	37	8.0		
NP021A-046	429220	126	0.07593	0.00080	2.00176	0.07472	0.19120	0.00684	0.959	no	1093	21	1116	25	1128	37	-3.5		
NP021A-068	74136	307	0.07626	0.00088	1.88764	0.07315	0.17953	0.00664	0.955	no	1102	23	1077	25	1064	36	3.7		
NP021A-020	115852	101	0.07654	0.00099	1.83963	0.09107	0.17432	0.00833	0.965	no	1109	26	1060	32	1036	46	7.2		
NP021A-048	34576	135	0.07656	0.00099	1.95897	0.07225	0.18483	0.00642	0.937	no	1110	26	1099	25	1093	35	1.6		
NP021A-092	31343	146	0.07664	0.00103	1.98001	0.07837	0.18738	0.00698	0.941	no	1112	27	1109	26	1107	38	0.4		
NP021A-101	108166	172	0.07700	0.00124	1.91439	0.07421	0.18032	0.00636	0.910	no	1121	32	1086	26	1069	35	5.1		
NP021A-083	37856	117	0.07708	0.00094	1.98455	0.07794	0.18673	0.00697	0.951	no	1123	24	1110	26	1104	38	1.9		
NP021A-049	628998	108	0.07709	0.00081	1.99186	0.07280	0.18740	0.00656	0.958	no	1123	21	1113	24	1107	36	1.6		
NP021A-023	46075	110	0.07711	0.00096	1.81263	0.06626	0.17048	0.00586	0.941	no	1124	25	1050	24	1015	32	10.5		
NP021A-102	66400	159	0.07727	0.00131	1.87167	0.07364	0.17569	0.00623	0.902	no	1128	33	1071	26	1043	34	8.1		
NP021A-002	139353	89	0.07730	0.00086	1.88146	0.10446	0.17653	0.00960	0.980	no	1129	22	1075	36	1048	52	7.8		
NP021A-093	338766	111	0.07731	0.00081	2.01606	0.07248	0.18913	0.00651	0.957	no	1129	21	1121	24	1117	35	3.5		
NP021A-091	167442	112	0.07735	0.00085	1.98282	0.07442	0.18891	0.00667	0.956	no	1130	22	1110	25	1099	36	3.0		
NP021A-111	100096	181	0.07737	0.00125	1.91218	0.06995	0.17925	0.00588	0.897	no	1131	32	1085	24	1063	32	6.5		
NP021A-095	74896	112	0.07752	0.00088	1.98470	0.07217	0.18570	0.00641	0.950	no	1134	23	1110	24	1098	35	3.5		
NP021A-021	81783	68	0.07759	0.00098	1.85424	0.08127	0.17332	0.00728	0.958	no	1136	25	1065	29	1030	40	10.1		
NP021A-086	69583	101	0.07761	0.00090	1.99686	0.07423	0.18660	0.00659	0.950	no	1137	23	1114	25	1103	36	3.3		

NP021A Red Island Road Formation

Isotopic ratios

sample name	²⁰⁶ Pb(cps)	²⁰⁴ Pb(cps)	²⁰⁷ Pb/ ²⁰⁶ Pb	2 s	²⁰⁷ Pb/ ²³⁵ U	2 s	²⁰⁶ Pb/ ²³⁸ U	2 s	f	f	Com Pb corrected?	age (Ma)	error (Ma)	2 s	age (Ma)	error (Ma)	2 s	age (Ma)	error (Ma)	2 s	discordance %
NP021A-090	82431	91	0.07768	0.00087	2.00609	0.07702	0.18729	0.00688	0.956	no	no	1139	22	1118	26	1107	37	3.1			
NP021A-105	86027	161	0.07769	0.00135	1.96528	0.07859	0.18347	0.00661	0.901	no	no	1139	34	1104	27	1086	36	5.1			
NP021A-082	89024	88	0.07773	0.00089	2.00563	0.07273	0.18713	0.00644	0.949	no	no	1140	23	1117	24	1106	35	3.3			
NP021A-109	68345	172	0.07780	0.00131	1.94279	0.07401	0.18112	0.00619	0.897	no	no	1142	33	1096	25	1073	34	6.5			
NP021A-026	28183	146	0.07780	0.00113	1.91963	0.07933	0.17895	0.00692	0.936	no	no	1142	29	1088	27	1061	38	7.6			
NP021A-084	78814	113	0.07784	0.00089	2.00659	0.07363	0.18696	0.00652	0.950	no	no	1143	23	1118	25	1105	35	3.6			
NP021A-013	19866	54	0.07788	0.00137	2.03301	0.08015	0.18932	0.00668	0.895	no	no	1144	35	1127	26	1118	33	2.5			
NP021A-080	262466	263	0.07790	0.00090	2.11425	0.07125	0.19685	0.00623	0.940	no	no	1144	23	1153	23	1158	33	-1.3			
NP021A-056	336500	144	0.07792	0.00081	2.07904	0.07155	0.19332	0.00635	0.953	no	no	1145	21	1142	23	1140	34	0.4			
NP021A-106	39086	168	0.07796	0.00136	1.98382	0.08236	0.18456	0.00695	0.907	no	no	1146	34	1110	28	1092	38	5.1			
NP021A-040	184871	205	0.07798	0.00083	1.99083	0.07052	0.18515	0.00625	0.953	no	no	1146	21	1112	24	1095	34	4.9			
NP021A-107	53575	165	0.07801	0.00130	1.99811	0.07945	0.18578	0.00671	0.909	no	no	1147	33	1115	27	1115	36	4.6			
NP021A-038	372730	205	0.07806	0.00082	2.02108	0.07795	0.18777	0.00697	0.962	no	no	1149	21	1123	26	1109	38	3.7			
NP021A-070	40605	303	0.07808	0.00104	1.98079	0.08840	0.18400	0.00784	0.955	no	no	1149	26	1109	30	1089	43	5.7			
NP021A-063	182329	287	0.07809	0.00082	2.12231	0.07604	0.19710	0.00675	0.956	no	no	1149	21	1156	24	1160	36	-1.0			
NP021A-062	147856	253	0.07811	0.00084	2.05576	0.07583	0.19089	0.00674	0.957	no	no	1150	21	1134	25	1126	36	2.2			
NP021A-103	107413	142	0.07812	0.00126	1.95010	0.07535	0.18104	0.00656	0.909	no	no	1150	32	1098	26	1073	35	7.3			
NP021A-108	117351	144	0.07814	0.00126	1.92688	0.07750	0.17885	0.00659	0.916	no	no	1150	32	1090	27	1061	36	8.4			
NP021A-024	158163	107	0.07817	0.00085	1.91700	0.07213	0.17787	0.00641	0.957	no	no	1151	21	1087	25	1055	35	9.0			
NP021A-054	35091	148	0.07818	0.00099	1.98540	0.07554	0.18418	0.00661	0.943	no	no	1151	25	1111	25	1111	36	5.8			
NP021A-074	157882	381	0.07821	0.00085	2.00967	0.08590	0.18636	0.00771	0.960	no	no	1152	21	1119	29	1102	42	4.8			
NP021A-016	282150	61	0.07823	0.00085	2.01488	0.07851	0.18679	0.00778	0.941	no	no	1153	21	1121	26	1104	38	4.6			
NP021A-072	20585	338	0.07826	0.00120	1.97317	0.08923	0.18285	0.00778	0.961	no	no	1154	30	1106	30	1083	42	6.7			
NP021A-039	105773	203	0.07833	0.00091	1.95640	0.07370	0.18115	0.00649	0.951	no	no	1155	23	1101	25	1101	35	7.7			
NP021A-011	78195	18	0.07834	0.00096	2.02719	0.07300	0.18768	0.00655	0.940	no	no	1155	24	1125	25	1107	34	4.4			
NP021A-075	32840	333	0.07841	0.00104	2.05544	0.08069	0.19012	0.00702	0.941	no	no	1157	26	1134	26	1122	38	3.3			
NP021A-099	82896	138	0.07841	0.00093	1.95970	0.07061	0.18126	0.00617	0.944	no	no	1157	23	1102	24	1074	34	7.8			
NP021A-066	100538	294	0.07842	0.00086	2.12171	0.08531	0.19622	0.00759	0.962	no	no	1158	22	1156	27	1155	41	0.2			
NP021A-065	96428	268	0.07853	0.00089	2.12838	0.08000	0.19658	0.00705	0.954	no	no	1160	22	1158	26	1157	38	0.3			
NP021A-077	146696	304	0.07857	0.00086	2.00142	0.07603	0.18474	0.00672	0.957	no	no	1161	22	1116	25	1093	36	6.4			
NP021A-034	46967	238	0.07861	0.00104	1.92202	0.07264	0.17733	0.00628	0.937	no	no	1162	26	1089	25	1052	34	10.2			
NP021A-069	25760	290	0.07867	0.00105	2.01453	0.07903	0.18572	0.00686	0.941	no	no	1164	26	1120	26	1098	37	6.1			
NP021A-017	121168	46	0.07869	0.00090	2.02632	0.07954	0.18677	0.00701	0.956	no	no	1164	23	1124	26	1104	38	5.6			
NP021A-029	44172	176	0.07870	0.00102	1.95133	0.07828	0.17982	0.00683	0.946	no	no	1165	25	1099	27	1066	37	9.2			
NP021A-004	68082	60	0.07871	0.00090	2.00196	0.11382	0.18447	0.01027	0.980	no	no	1165	23	1116	38	1091	56	6.9			
NP021A-043	52489	161	0.07876	0.00089	2.04692	0.07918	0.18849	0.00697	0.956	no	no	1166	22	1131	26	1131	38	4.9			
NP021A-018	76047	68	0.07881	0.00090	1.96104	0.07451	0.18048	0.00654	0.953	no	no	1167	23	1102	25	1070	36	9.1			
NP021A-022	206661	101	0.07883	0.00087	1.94186	0.07148	0.17867	0.00628	0.954	no	no	1168	22	1096	24	1060	34	10.0			
NP021A-055	63160	164	0.07884	0.00094	2.01997	0.07109	0.18582	0.00615	0.941	no	no	1168	22	1122	24	1099	33	6.5			
NP021A-007	82459	64	0.07910	0.00089	1.99835	0.11333	0.18323	0.01018	0.980	no	no	1175	22	1115	38	1085	55	8.3			
NP021A-015	39544	21	0.07916	0.00110	1.96788	0.07823	0.18030	0.00672	0.937	no	no	1176	27	1105	26	1069	37	9.9			
NP021A-110	24874	179	0.07917	0.00151	1.97288	0.08390	0.18073	0.00686	0.893	no	no	1176	37	1106	28	1071	37	9.7			
NP021A-053	55210	135	0.07934	0.00101	2.09233	0.08632	0.19127	0.00750	0.951	no	no	1181	25	1146	28	1128	40	4.8			
NP021A-052	14021	122	0.07973	0.00151	2.14244	0.09286	0.19489	0.00760	0.900	no	no	1190	37	1163	30	1148	41	3.9			
NP021A-076	28024	308	0.08012	0.00121	2.06481	0.08227	0.18690	0.00689	0.926	no	no	1200	29	1137	27	1105	37	8.7			

Apparent age summary

021A Red Island Road Formation																	
Isotopic ratios																	
file name	$^{206}\text{Pb}(\text{cps})$	$^{204}\text{Pb}(\text{cps})$	$^{207}\text{Pb}/^{206}\text{Pb}$	2 s	$^{207}\text{Pb}/^{235}\text{U}$	2 s	$^{206}\text{Pb}/^{238}\text{U}$	2 s	Γ	Com Pb corrected?	age (Ma) $^{207}\text{Pb}/^{206}\text{Pb}^*$	error (Ma) 2 s	age (Ma) $^{207}\text{Pb}/^{235}\text{U}$	error (Ma) 2 s	age (Ma) $^{206}\text{Pb}/^{238}\text{U}$	error (Ma) 2 s	discordance %
021A-003	30747	60	0.08020	0.00145	2.04537	0.11660	0.18497	0.01000	0.949	no	1202	35	1131	38	1094	54	9.7
021A-051	64374	114	0.08030	0.00121	2.05845	0.07482	0.18592	0.00615	0.910	no	1204	29	1135	25	1099	33	9.5
021A-067	17771	275	0.08051	0.00185	2.19469	0.09346	0.19771	0.00708	0.841	no	1209	45	1179	29	1163	38	4.2
021A-071	48475	315	0.08067	0.00099	2.08619	0.08355	0.18756	0.00715	0.952	no	1213	24	1144	27	1108	39	9.4
021A-050	277097	134	0.08174	0.00097	2.16609	0.07902	0.19219	0.00663	0.946	no	1239	23	1170	25	1133	36	9.3
021A-057	528704	186	0.08193	0.00085	2.46447	0.08753	0.21816	0.00741	0.957	no	1244	20	1262	25	1272	39	-2.5
021A-079	415392	286	0.08218	0.00086	2.48970	0.09584	0.21972	0.00814	0.962	no	1250	20	1269	28	1280	43	-2.7
021A-025	231552	149	0.09229	0.00103	3.04875	0.11556	0.23959	0.00868	0.956	no	1473	21	1420	29	1385	45	6.7
021A-009	369707	40	0.09761	0.00103	3.47481	0.19100	0.25818	0.01593	0.981	no	1579	20	1522	42	1481	71	7.0
021A-089	273009	86	0.10053	0.00107	3.84455	0.13474	0.27737	0.00926	0.953	no	1634	20	1602	28	1578	47	3.8
021A-088	59006	119	0.10358	0.00136	4.26713	0.17869	0.29878	0.01188	0.950	no	1689	24	1687	34	1685	59	0.3
021A-094	119456	100	0.11219	0.00121	4.94015	0.18422	0.31937	0.01140	0.958	no	1835	19	1809	31	1787	55	3.0
021A-041	205757	144	0.11294	0.00117	5.16602	0.19209	0.33175	0.01185	0.960	no	1847	19	1847	31	1847	57	0.0
021A-008	153471	46	0.11406	0.00122	4.91643	0.27977	0.31262	0.01747	0.982	no	1865	19	1805	47	1754	85	6.8
021A-032	68494	228	0.07930	0.00090	1.94509	0.06766	0.17789	0.00585	0.945	no	1180	22	1097	23	1055	32	11.4
021A-035	35104	225	0.07933	0.00108	1.93766	0.07469	0.17715	0.00639	0.935	no	1180	27	1094	25	1051	35	11.8
021A-037	32106	239	0.07958	0.00104	1.95425	0.07758	0.17810	0.00668	0.945	no	1187	25	1100	26	1057	36	11.9
021A-085	24244	120	0.08379	0.00264	2.24053	0.11355	0.19393	0.00770	0.783	no	1288	60	1194	35	1143	41	12.3
021A-001	92185	68	0.07931	0.00088	1.92699	0.10976	0.17622	0.00984	0.981	no	1180	22	1090	37	1046	54	12.3
021A-036	98830	263	0.07884	0.00106	1.89485	0.06754	0.17432	0.00576	0.926	no	1168	26	1079	23	1036	32	12.2
021A-028	23015	149	0.07991	0.00125	1.95564	0.06958	0.17750	0.00567	0.898	no	1195	31	1100	24	1053	31	12.8
021A-033	220136	212	0.07777	0.00087	1.80885	0.07097	0.16870	0.00634	0.958	no	1141	22	1049	25	1005	35	12.9
021A-010	156764	56	0.07641	0.00127	1.70826	0.10644	0.16215	0.00974	0.964	no	1106	33	1012	39	969	54	13.3
021A-073	60824	376	0.08191	0.00118	2.06629	0.07873	0.18295	0.00645	0.925	no	1243	28	1138	26	1083	35	14.0
021A-031	28174	197	0.08167	0.00226	1.98462	0.08912	0.17625	0.00623	0.787	no	1238	53	1110	30	1046	34	16.7

Apparent age summary